Expression and epigenetic regulation of imprinted genes in prostate cancer

Inaugural Dissertation

Presented to the Faculty of Natural Sciences,

Heinrich-Heine University Düsseldorf

in Partial Fulfillment
of the Requirements

for the Degree of

Doctor of Philosophy

by Teodora Ribarska

from Pleven, Bulgaria

Urologic Research Laboratory,

Heinrich-Heine-University, Düsseldorf

Düsseldorf, March 2013

Printed with the permission of the

Faculty of Natural Sciences,

Heinrich-Heine-University Düsseldorf

Supervisor: Prof. Dr. Wolfgang A. Schulz, Urologic Research Laboratory, Heinrich-Heine-University, Düsseldorf

Co-Supervisor: Prof. Dr. Martin Beye, Evolution Genetics Dept., Heinrich-Heine-University, Düsseldorf

Day of defense:

Publications:

Parts of this thesis have been published in the following articles:

“Specific changes in the expression of imprinted genes in prostate cancer- implications for cancer progression and epigenetic regulation.” Ribarska T., Bastian K.M., Koch A., Schulz W.A. Asian J Androl. 2012 May 14 (3): 436-50.

“Epigenetic inactivation of the placentally imprinted tumor suppressor gene TFPI2 in prostate carcinoma.” Ribarska T., Ingenwerth M., Goering W., Engers R., Schulz W.A. Cancer Genomics Proteomics 2010 Mar-Apr 7(2): 51-60.

Summary

Changed expression of imprinted genes is frequent in a large variety of human cancers and is often associated with disturbed epigenetic regulation. The aim of this thesis was to analyze which imprinted genes are differentially expressed between benign and cancerous prostate tissues and if their epigenetic status is affected. Following a pilot project on the imprinted gene *TFPI2* and its paralog *TFPI*, we analyzed the mRNA expression of 16 imprinted genes, whose deregulation in prostate cancer was suggested by an *in silico* analysis. By means of qRT-PCR, we found *PLAGL1/ZAC1* (6q24), *CDKN1C* (11p15), *NDN*, *MEG3* (14q32), *IGF2* and *H19* genes (both at 11p15) to be significantly downregulated in prostate cancer, compared to benign prostate tissues, while *PPP1R9A* and *PON2* genes (both at 7q21) and *KCNQ1OT1/LIT1* (11p15) were significantly upregulated. In the assessed cancer tissues, the expression of many analyzed imprinted genes correlated significantly pairwise and to the prostatic oncogenes *HOXC6* and *EZH2*. This suggests a coordinate deregulation of this group of imprinted genes. Interestingly, many of our candidates belong to an imprinted gene network (IGN) reported in the mouse. We further analyzed DNA methylation at the *PLAGL1* DMR, *MEG3* DMR, the 7q21 DMR, the KvDMR (11p15) and the *CDKN1C* promoter by bisulfite pyrosequencing. At all sites, the mean methylation levels were similar between benign and cancerous prostate tissues. Thus, altered DNA methylation is not responsible for the changed expression of imprinted genes in prostate cancers. Since Zac1 was shown to be a master regulator of the IGN in the mouse, we tested if this transcription factor was able to regulate other imprinted genes by overexpressing long and short ZAC1 protein isoforms in prostate cancer cell lines. Unexpectedly, the long isoform exhibited much lower protein and mRNA stability than the short ZAC1 isoform, which could be greatly alleviated by proteasome inhibition. Functionally, both ZAC1 isoforms induced *H19*, *IGF2*, *CDKN1C* and *LIT1* expression, while *PON2*, *SGCE*, *PEG3* and *HYMAI* were induced only by the short isoform. Furthermore, ZAC1 enhanced AR signaling and induced the cell cycle inhibitor *CDKN1A*/p21, supporting its function as a tumor suppressor in the prostate. In summary, the results of this study suggest that *PLAGL1*/*ZAC1* downregulation together with the activation of *EZH2* and *HOXC6* oncogenes may be involved in the deregulation of an imprinted gene network in prostate cancer which occurs without loss of imprinting and significant changes in DNA methylation.

Zusammenfassung

Veränderungen der Expression elterlich geprägter Gene treten häufig in verschiedenen menschlichen Krebserkrankungen auf und gehen oft mit einer gestörten epigenetischen Regulation einher. Ziel dieses Projekts war es, zu analysieren, welche geprägte Gene zwischen benignen und karzinomatösen Prostata-Geweben differentiell exprimiert sind und ob dies mit Veränderungen ihres epigenetischen Status einhergeht. Nach einer Pilotanalyse des elterlich geprägten Gens *TFPI2* und seines Paralogs *TFPI* wurde die mRNA Expression 16 geprägter Gene analysiert, deren Deregulierung in Prostatakarzinom eine *in silico* Analyse nahegelegt hatte. Mittels qRT-PCR wurde eine deutliche Verminderung von *PLAGL1/ZAC1* (6q24), *CDKN1C* (11p15), *NDN*, *MEG3* (14q32), *IGF2* und *H19* (beide 11p15) in Karzinomgeweben gegenüber gutartigen Prostatageweben gefunden, während *PPP1R9A* und *PON2* (beide 7q21) und *KCNQ1OT1/LIT1* (11p15) signifikant hochreguliert waren. Die Expression vieler analysierter geprägter Gene korrelierten signifikant paarweise und mit den in Prostatakarzinomen überexprimierten Onkogenen *HOXC6* und *EZH2*. Dies deutet auf eine koordinierte Deregulierung dieser Gruppe von geprägten Genen hin. Interessanterweise gehören viele unserer Kandidaten zu einem Netzwerk von geprägten Genen (auf Englisch- IGN), das in der Maus entdeckt wurde. Weiter wurde die DNA-Methylierung der *PLAGL1* DMR, *MEG3* DMR, 7q21 DMR, KvDMR (11p15) und des *CDKN1C* Promotors durch Bisulfit-Pyrosequenzierung gemessen. In allen Regionen war die Durchschnittsmethylierung in den benignen und Karzinomgeweben ähnlich. Somit ist veränderte DNA-Methylierung nicht ursächlich für die veränderte Expression von geprägten Genen im Prostatakarzinom. Da Zac1 als Master-Regulator des IGN in der Maus fungiert, testeten wir, ob dieser Transkriptionsfaktor auch in der Prostata andere geprägte Gene regulieren kann mittels Überexpression einer langen oder einer kurzen ZAC1 Isoform in verschiedenen Prostatakarzinom-Zelllinien. Dabei zeigte die lange Isoform eine deutlich niedrigere Protein- und mRNA-Stabilität, die beide durch Proteasom-Hemmung verbessert wurden. Die Expression von *H19*, *IGF2*, *CDKN1C* und *LIT1* wurde von beiden ZAC1 Isoformen induziert, während *PON2*, *SGCE*, *PEG3* und *HYMAI* nur durch die kurze Isoform induziert wurden. Neben der Regulierung dieser geprägten Gene verstärkte ZAC1 die Aktivität des Androgenrezeptors und induzierte die Expression des Zellzyklus-Inhibitors *CDKN1A*/p21. Diese Ergebnisse sprechen für eine Funktion von ZAC1 als Tumorsuppressor in der Prostata. Zusammenfassend deuten die Ergebnisse dieser Studie darauf hin, dass die Deregulierung eines Netzwerks geprägter Gene im Prostatakarzinom ohne Verlust der Prägung auftritt und eine Folge der PLAGL1/ZAC1 Herabregulation zusammen mit der Aktivierung der *EZH2* und *HOXC6* Onkogene darstellt.

Contents Page

List of Abbreviations

Abbreviation	Full Term
ARE	androgen responsive element
BIC	bicalutamide
bp	base pairs
BPH	benign prostatic hyperplasia
BSA	bovine serum albumin
BWS	Beckwith-Wiedemann-Syndrome
cAMP	cyclic adenosine monophosphate
cDNA	complementary DNA
cFCS	charcoal-stripped fetal calf serum
Chap.	chapter
ChIP	chromatin immunoprecipitation
CMV	human cytomegalovirus
CpG	cytosine-phosphate-guanine dinucleotide
DMR	differentially methylated region
DMSO	dimethyl sulphoxide
DNA	deoxyribonucleic acid
DNAse	desoxyribonuclease
dNTP	deoxynucleotide triphosphate
DTT	dithiothreitol
EDTA	ethylenediamine tetraacetic acid
ER	endoplasmic reticulum
FCS	fetal calf serum
Fig.	figure
HRP	horseradish peroxidase
ICR	imprinting control region
IGN	imprinted gene network
IRES	internal ribosome entry site
kDa	kilo Dalton
LB	Luria broth
LOI	loss of imprinting
Luc	luciferase
MCS	multiple cloning site
miRNA	micro RNA
mRNA	messenger RNA
ncRNA	non coding RNA
ORF	open reading frame
PB	processing body
PBS	phosphate-buffered saline
PCA	prostate cancer
PCR	polymerase chain reaction
PIN	prostatic intraepithelial neoplasia
PMSF	phenylmethylsulfonylfluoride
RLU	relative light units
RNA	ribonucleic acid
RNAse	ribonuclease

Abbreviation	Full Term
RT-PCR	reverse transcriptase-polymerase chain reaction
SAM	S-adenosylmethionine
SDS	sodium dodecyl sulfate
SG	stress granule
siRNA	small interfering RNA
snoRNA	small nucleolar RNA
SNP	single nucleotide polymorphism
SV40	Simian Virus 40
TBS	tris-buffered saline
TBST	tris-buffered saline plus 0.1 % Tween-20
TE	tris / EDTA
Tet	tetracycline
TNDM	transient neonatal Diabetes mellitus
TNM	tumor, lymph node, metastasis
TR	Tet repressor
TSS	translation start site
uORF	upstream open reading frame
UTR	untranslated region
vs.	versus

1. Introduction

1.1. Clinical aspects of prostate cancer progression

In most Western industrialized countries, prostate cancer is the most prevalent cancer in older men and the first or second most frequent cause of cancer mortality. An estimated 1 in 10 men will develop prostate cancer in their lifetime, with the likelihood increasing with age. Approximately 10-20% of newly diagnosed prostate cancer cases involve locally advanced disease; nonetheless, advanced disease is comparably less common, because more early stage cancer is discovered since the introduction of prostate-specific antigen (PSA) as a tumor serum biomarker.

Even more commonly in men over 50 a benign overgrowth of the prostate is present called benign prostate hyperplasia (BPH). An increased number of prostatic stromal and epithelial cells results in the formation of nodules in the periurethral region, leading to obstruction of the urethra. As the name indicates, BPH is a benign tumor but is commonly found associated with prostate cancer.

Prostate cancer is in most cases a slowly progressing disease. In the majority of cases the neoplasia arises from glandular epithelial cells to consequently form adenocarcinomas. A common precursor to prostate cancer, prostatic intraepithelial neoplasia (PIN), is characterized by hyperproliferation of morphologically aberrant luminar epithelial cells and a reduction in basal cells within the glandular epithelium. Microscopically the dysplastic changes include cell crowding, variation in nuclear size and shape, and irregular cell spacing. During its progression to cancer, the cellular hierarchy that normally maintains the glandular structure is permanently disturbed. Tumor growth can then extend into the stromal tissue surrounding the glands and beyond the organ to invade nearby tissues. Two classification systems, the TNM system for staging and the Gleason grading system, are commonly used to classify prostate cancers and predict their outcome, thereby providing crucial parameters for therapy decisions.

In the TNM (Tumor, Node, and Metastasis) system, pT1 to pT4 denotes the extension of the cancer within and beyond the organ of origin, whereas N and M stage indicate the presence of lymph node and distant metastases. Incidental T1 stage tumor are detected during transurethral resection for BPH, are not palpable and are present in less than 5% of the resected tissue. A T2 stage tumor can affect different parts of the prostate (as indicated by affixes a, b and c) but remains confined to the organ. In contrast, at stage T3 part of the tumor extends beyond the capsule of the prostate or into the seminal vesicles and in stage T4 the tumor invades the bladder, rectum or the pelvic wall.

Via microscopic examination a pathologist assigns microscopic tumor patterns a score between 1 and 5, called Gleason grade, to describe their degree of histological dedifferentiation and loss of the normal glandular tissue architecture. Tumor tissues with patterns 1-3 are considered low grade and have recognizable gland structures with cells that begin to invade the surrounding tissue. Patterns 4 and 5, considered high grade, are assigned to tissues with few or no recognizable glands with a higher degree of invasiveness. The grades of the two most common patterns are added to derive the Gleason Score. The Gleason score has been shown to correlate closely to clinical prognosis and therefore strongly informs the decisions on therapy options.

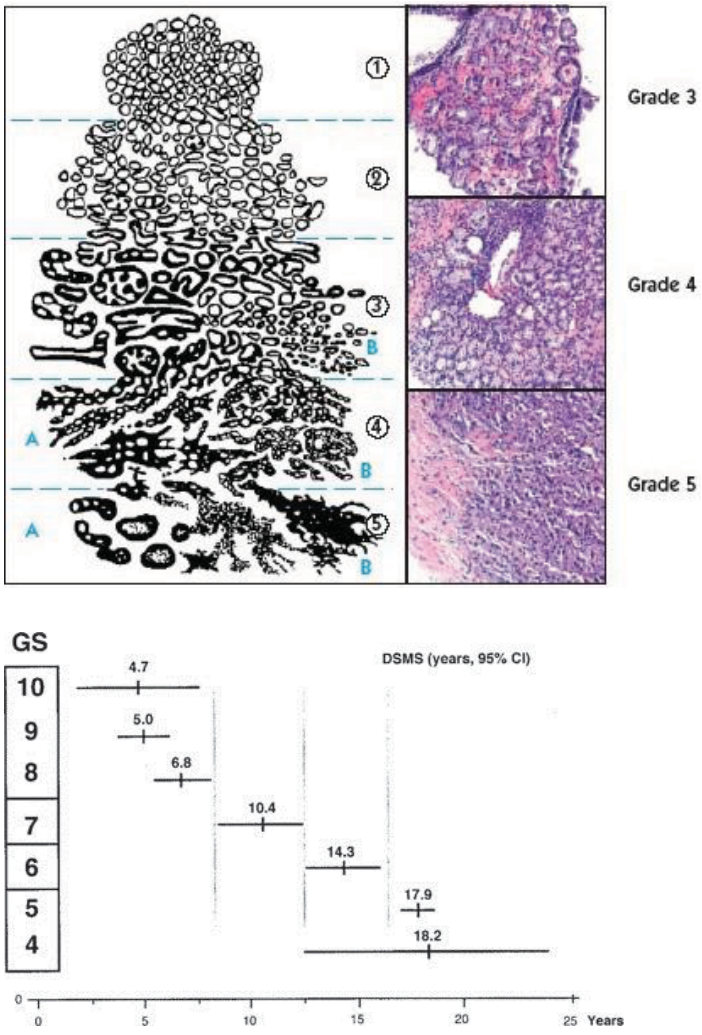

Fig. 1.1. Gleason grading diagram and disease specific mean survival of Gleason grade groups. Upper panel: schematic and photomicrograph examples of prostate cancers with different Gleason grades according to the Gleason grading system from its founding [1] until 2006 when it was modified [2, 3] (figure from www.prostate-cancer.org). The sum of the primary grade (representing the majority of tumor) and a secondary grade (assigned to the minority of the tumor) is called Gleason score (GS) and is a number ranging from 2 to 10. Lower panel: Confidence intervals of disease specific mean survival (years) of prostate cancer patients according to their GS [4]. The prostate cancer tissues used in this thesis project were graded according to the system used until 2006 as depicted here.

Prostate cancer growth can be detected by elevated levels in blood or urine of proteins normally secreted into the seminal fluid like the prostate-specific antigen (PSA), also known as gamma-seminoprotein or kallikrein 3, as well as prostatic acid phosphatase and human kallikrein 2 (hK2) [5, 6]. The PSA blood test is the most commonly used screening procedure as the risk of having prostate cancer rises with increasing PSA level(s). Most (older) healthy men have levels under 2 ng/mL blood.

The growth and maturation of the normal prostate as well as of prostate tumors until late stages is dependent, or at least responsive to male hormones (androgens). Androgens enter the prostate epithelial cells and bind to the androgen receptor (AR), which then translocates to the nucleus. Nuclear AR recruits a variety of co-factors including chromatin modifying enzymes and regulates the expression of genes involved in prostate growth, maintenance, and differentiation as well as prostate secretion products, like PSA [7].

Anti-androgenic therapy (androgen ablation), used as initial or adjuvant treatment, usually results in a significant decrease in tumor volume and serum PSA levels. However, after a period ranging from months to years, nearly all prostate cancers recur and grow independently of androgens ('androgen-resistant') or at their low residual levels (‘castration-resistant’). In these cancers, mutations and aberrations of the AR, its cofactors and their regulators result in the activation of AR independently of androgen ligands, further stimulating the growth and survival of prostate cancer cells [8, 9]. The emergence of AR-mediated castration-resistant tumor recurrence can be monitored by the increased serum levels of PSA, referred to as biochemical recurrence. Castration-resistant tumors are strongly associated with disseminated disease with metastases present in the lymph nodes and skeleton in nearly 100% of men who experience progressive disease.

1.2. Molecular aspects of prostate cancer progression

Distinct molecular pathologic processes are involved in the different stages of prostate cancer. While inflammation, oxidative DNA damage and telomere shortening are likely involved in its initiation, the progression to clinical adenocarcinoma is associated with the reactivation of developmental signaling pathways and the development of androgen-independent tumor cell proliferation (see Fig.1.2.1) [10]. These processes are directed by the various genetic and epigenetic changes occurring in cancer cells to alter the expression of particular genes.

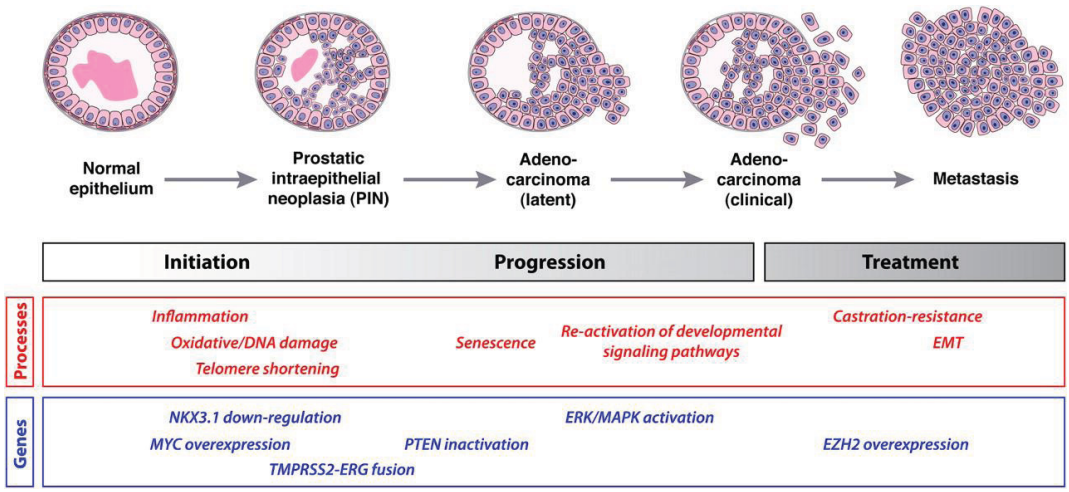

Fig. 1.2.1. Progression pathway for human prostate cancer. Stages of progressin are shown, together with molecular processes and genes/pathways likely to be significant at each stage [10].

Specific chromosomal lesions that are found in a substantial number of tumor samples provide important clues to the identity of oncogenes and tumor suppressor genes. Typical chromosomal aberrations in prostate cancer include losses of 3p, 8p, 5q, 6q, 10q, 13q and 17p and gains in 8q, 7q and 5p or smaller regions of these chromosomes [11-13]. Common deletions affect the inhibitor of the PI3K signallng pathway- *PTEN* (10q) as well as the cell cycle regulators *TP53* (17p), *RB1* (13q) and *CDKN1B*/p27 (12p) [13]. As a consequence, several signaling pathways that sustain cell proliferation and survival are overactivated. The heterozygous loss of the *NKX3.1* homeobox gene at 8p with prostate specific expression is thought to predispose to prostate epithelial dysplasia and hyperplasia [14].

The frequently amplified genes in prostate cancer include the proto-oncogenes *MYC* (8q) and less often *BRAF* (7q), the *AMACR* gene encoding an enzyme involved in peroxisomal fatty acid metabolism, the AR coactivator *NCOA2* (8q); the *SKP2* gene (5p) encoding S-phase kinase associated protein which promotes the degradation of the phosphorylated cell cycle inhibitor $p27^{KIP1}$ (encoded by *CDKN1B*); and *RICTOR* (5p), which as a part of mTORC2 promotes cell growth and survival in response to hormonal signals in part by phosphorylating AKT1 [13]. Focal amplifications of the *AR* gene (Xq12) and overexpression of its cofactor *FOXA1* occur mostly in metastatic cancers [15, 16]. Several HOXC genes have been found to be upregulated in prostate cancers [17]. Particularly, the overexpression of HOXC6 has been suggested to induce an undifferentiated and highly proliferative state and to parallel the clinical progression of prostate cancer [18, 19]. This transcription factor can both repress gene transcription and enhance activation by AR, playing an important role in the normal response of prostatic cells to hormonal signals [18].

More than half of all prostate cancers contain fusion genes in which androgen-dependent or prostate-specific promoters drive the expression of oncogenic transcription factors, usually of the ETS family [20, 21]. The most frequent fusion results from the interstitial deletion of a segment of chromosome 21q22.2-3 between the ETS family oncogene *ERG* and the AR target gene *TMPRSS2* [22]. TMPRSS2-ERG fusion protein inhibits AR expression, binds to and inhibits AR activity at specific loci, and induces repressive epigenetic programs via direct activation of the Polycomb Repressive Complex 2 (PRC2) component EZH2 [23]. The occurrence of *TMPRSS2-ERG* gene fusion as well as overexpression of *ERG* has been associated with earlier biochemical recurrence in some studies [24, 25], while in others- with a more favourable prognosis [26].
Amplifications in 7q may involve the *EZH2* gene. It encodes an H3K27 methyltransferase which as part of the PRC2 complex functions to repress genes involved in differentiation, thereby retaining stem and progenitor cells in an undifferentiated state [27-29]. EZH2 overexpression, which has been associated with highly proliferative and aggressive types of breast and prostate tumors with poor prognosis, may thus have global effects on gene expression [30-32]. However, increased expression of EZH2 does not necessarily correlate with increased general abundance of H3K27me3 [33, 34]. Rather, its effects in prostate cancer are gene-specific. It represses specific PcG proteins, transcription factors and cell-cycle regulators and especially AR-induced genes including cytoskeletal genes that promote epithelial differentiation and inhibit metastasis [28, 29, 32, 35]. ERG and EZH2 cooperate to mediate repression of AR-induced transcription, thereby impeding epithelial differentiation and promoting androgen-independent growth [23, 29, 36].

Castration-resistant growth of prostate cancers can also be induced by overactivation of growth and survival pathways like PI3K, JAK/STAT and MAPK signaling cascades [37, 38]. In the present context, PI3K signaling is particularly relevant.

The phosphatidylinositol-3 kinase (PI3K) is recruited and activated by many receptor tyrosine kinase proteins, like the IGF1R, EGF family receptors, and G protein-coupled receptors upon their activation. PI3K phosphorylates a phospholipid component of cell membranes, phosphatidylinositol 4,5-bisphosphate (PIP2), to form the second messenger phosphatidylinositol 3,4,5-trisphosphate (PIP3). Membrane PIP3 serves as a docking site for signaling proteins with pleckstrin homology domains like the Akt kinase (also known as PKB). Following recruitment to the cell membrane, Akt gets phosphorylated and activated by PDK1 and PDK2 kinases, upon which it mediates the activation and inhibition of various genes supporting cell proliferation, growth and survival. In prostate cancer, inactivation of its counteracting phosphatases PTEN, INPP4B and PHLPP1 leads to the overactivation of the PI3K/Akt pathway [39-41].

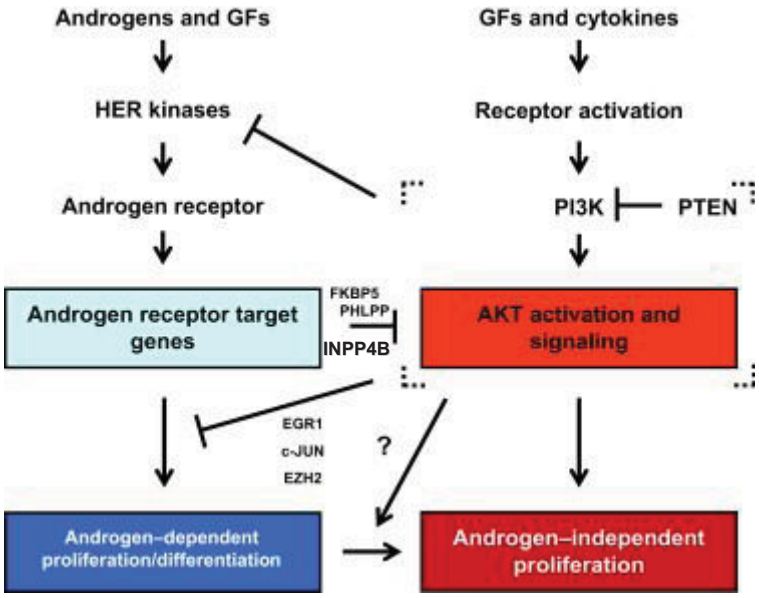

Fig. 1.2.2. Reciprocal inhibition feedback links AR- and PTEN loss/ PI3K-Akt signaling pathways in prostate cancer. As reported in [42, 43], reciprocal negative feedback underlies the oncogenic activities of *PTEN* loss/PI3K-AKT signaling (depicted as the area inside the dotted "corners"). Activation of PI3K-AKT leads to suppression/subversion of AR signaling through suppression of HER kinases; upregulation of EGR1 and c-JUN transcriptional coregulators; and upregulation of the Polycomb group protein EZH2. Reciprocal negative feedback is established, in part, through AR-stimulated, FKBP5-mediated activation of AKT phosphatase PHLPP. GFs: growth factors. Diagram and legend modified from [44].

The PI3K and AR signaling pathways exert reciprocal feedback regulatory on each other, in a way that inhibition of one activates the other (see Fig. 1.2.2). Blockade of AR impaired the phosphatase PHLPP1 and induced Akt signaling [42]. Similarly, AR was shown to induce INPP4B but not PTEN in prostate cancer cells, thereby negatively regulating Akt signaling [39]. On the other hand, overactive PI3K/Akt due to PTEN loss can lead to repression of AR signaling by suppression of HER kinases and upregulation of EGR1, c-JUN and EZH2 [43]. These events were collectively suggested to suppress androgen-responsive genes establishing a castrate genetic program [29, 42, 43, 45]. In concert, inhibition of PI3K/Akt signaling was reported to induce AR signaling in PTEN-negative cells, by relieving feedback inhibition of HER kinases on AR. This leads to a change of the AR transcriptional program of prostate cancers and a greater dependence of tumor cells on PI3K than on AR signaling, leading to androgen-independence [44].

Beside genetic changes, multiple epigenetic abnormalities affect key regulator and mediator proteins of the above mentioned signaling pathways thereby shaping the individual phenotype of each cancer [46, 47]. They comprise, among others, DNA hypermethylation, DNA hypomethylation, overexpression of the histone methyltransferase

EZH2 and several distinctive changes in histone modification patterns. At an early stage of prostate carcinogenesis, probably coinciding with the transition from pre-neoplastic stages to actual carcinoma, multiple genes become hypermethylated [47]. The best known of these are *GSTP1*, *RARB2*, *CDKN2A* and *RASSF1A* [48]. In contrast, genome-wide hypomethylation leading to a decrease in overall methylcytosine content occurs later during disease progression and is most pronounced in metastatic cases [49]. Hypomethylation is best studied for the repetitive LINE-1 elements which comprise about 18 % of the human genome. Although it is suspected that hypomethylation leads to reactivation of retroelements and thereby causes genetic instability, the functional contribution of LINE-1 hypomethylation to prostate progression is not really understood [50, 51].

The histone 3 K27 methyltransferase EZH2 is overexpressed in hormone-refractory and metastatic prostate cancer and has been shown to mediate neoplastic transformation of BPH1 in prostate cancer [32, 52, 53]. As part of the PRC2 complex, it participates in the silencing of particular developmental genes, thereby repressing undesirable differentiation and maintaining stemness in normal cells [35]. In cancer cells, overexpressed EZH2 is thought to recruit DNA methyltransferases to particular target genes leading to their *de novo* methylation [54]. Recent studies suggest that the oncogenic role of EZH2 in prostate cancer may involve the methylation of non-histone proteins like GATA4 and AR [55-58]. The phosphorylation of EZH2 by Akt was shown to convert it from transcriptional repressor to an activator [56]. Depending on the cellular context and particular protein interactions, EZH2 can enhance or repress gene transactivation by AR, ER, NFkB and TCF transcription factors [59, 60]. Thus, EZH2 may contribute to prostate cancer progression via many ways.

1.3. TFPI and TFPI2

In previous work done in this lab, a striking correlation between aberrations on chromosome 8 and hypomethylation of LINE-1 retroelements in prostate cancer samples was observed [49, 50]. These results led to the conclusion that DNA hypomethylation and alterations in chromosome 8 might together drive the progression of prostate carcinoma. Analysis of the expression changes associated with the combined presence of LINE-1 hypomethylation and chromosome 8 in prostate cancers identified markers of invasiveness as well as of an ongoing stress response [50]. Among the identified genes was a peculiar subgroup with functional association to coagulation, including the tissue factor pathway inhibitor *TFPI*. As the name suggest, TFPI inhibits the pro-coagulant tissue factor (TF) which is also an important cell-associated signaling receptor [61-63]. TF has been implicated in promoting angiogenesis and metastasis in a wide range of tumors

including prostate cancer [64-67]. It is a component of prostate secretions that can accumulate in the disorganized carcinoma interstitium and contribute to stroma remodeling. Importantly its expression levels have been shown to correlate significantly with Gleason score and the stage of the disease [68-70]. Therefore, by controlling TF signaling, TFPI may play an important tumor suppressor role in prostate cancer.

Interestingly, its paralogous *TFPI2* gene was also shown to exhibit tumor suppressive activity and to be downregulated in multiple cancers by epigenetic mechanisms including DNA hypermethylation [71-76]. The *TFPI2* gene belongs to a cluster of imprinted genes on chromosome 7q21, which are regulated by multiple epigenetic mechanisms. This raises the questions of whether *TFPI* and *TFPI2* might be silenced by epigenetic mechanisms in prostate cancer, and whether epigenetic changes affecting *TFPI2* might extend to other genes in the cluster as well. The *TFPI* and *TFPI2* genes might therefore represent new tumor suppressors in prostate cancer regulated by epigenetic mechanisms.

1.4. Genomic imprinting

Genomic imprinting involves a small group of genes (~80 in the human) whose expression is silenced on one of the two homologous chromosomes, thus resulting in monoallelic expression [77]. The 'imprints' are epigenetic modifications of regulatory regions around the affected loci and are established in the germ cells (gametic imprints) during fetal development (male) or in the early neonatal period (female) [78]. Typically, the establishment of imprints involves the *de novo* methylation of regulatory regions within imprinted gene clusters. These regulatory regions are termed imprinting control centers (ICR) or where marked by DNA methylation, differentially methylated regions (DMR) [79]. In maternal (oocyte) imprints the methylation marks are often found at the promoters of protein-coding genes or non-coding RNAs, while in paternal (spermatocyte) imprints methylation occurs rather in intergenic regions [80]. Upon fertilization, the oocyte and sperm cell transmit parental-origin-specific differential methylation to the new conceptus. These methylation marks are resistant to the epigenetic reprogramming that is initiated upon fertilization and are maintained throughout development, being only erased and reestablished in the cells of the germ lineage of the conceptus. A few additional DMRs are acquired in postimplantation embryos (somatic imprints) and are thought to emerge as a consequence of the *cis*-activity of a nearby gametic imprint [81]. Examples of imprinted gene clusters and their DMRs are depicted in Fig. 1.4.

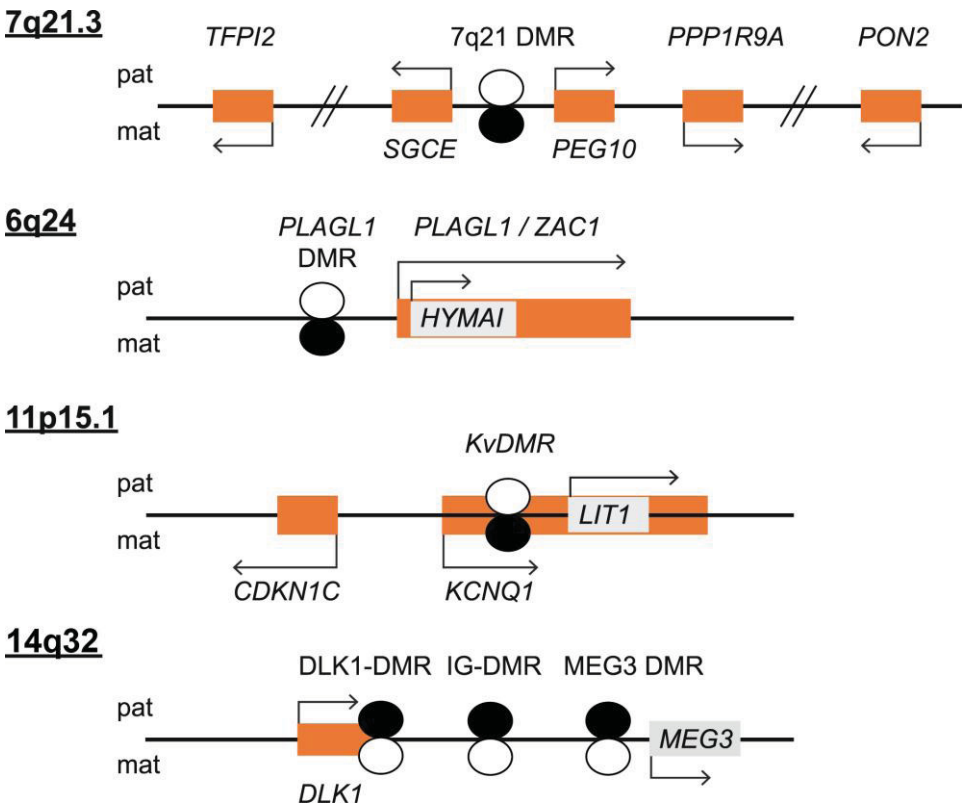

Fig.1.4. Schematic representation of the imprinted gene clusters on chromosomes 7q21, 6q24, 11p15 and 14q32. Imprinted protein-coding genes are shown as orange rectangles, while non-protein coding imprinted genes are shown in light grey rectangles. Differentially methylated regions are represented as black/white circles, whereby the methylated alleles are black filled circles and unmethylated ones- empty circles. The scheme is not to scale.

In addition to DNA methylation, imprinted genes are epigenetically regulated by reciprocal allelic association with non-histone proteins and histone modifications [82]. The silenced allele is usually marked by 'repressive' histone modifications including H3K9me3 and H3K20me3 or H3K27me3 put in place by histone methyltransferases like G9A, KMT5B and KMT5C, and the polycomb proteins EED and EZH2. In contrast, the actively transcribed allele, among others, is marked by the H3K4me3 modification established by enzymes of the trithorax MLL group [83-85].

Among the non-histone proteins associated with imprinted clusters, the transcriptional repressor protein CTCF binds to unmethylated CCCTC core sequences to act as a physical insulator, inducing chromatin structures (short-distance or long-distance looping) that block interactions between transcription activators and promoters on its two sides [86, 87]. The resulting chromatin barrier prevents the spread of heterochromatin structures and coordinates allele-specific histone modifications that facilitate marking of the parental origin of each allele. Of note, CTCF can also enable allele-specific inter-chromosomal interactions [88]. Other proteins associated with imprinted domains include ZFP57 and PGC7/Stella.

Integral to many imprinted clusters, non-coding RNAs, too, influence the epigenetic status and the expression of imprinted protein-coding genes in the respective gene cluster. The promoters of imprinted nc-RNAs are often located within or near DMRs. Their expression is thus directly dependent on the methylation status of the allele. With effects specific to each locus, the ncRNAs are thought to direct *in-cis* the silencing of multiple flanking genes e.g. by recruiting repressive polycomb proteins or by regulating higher order chromatin structures [89-91].

While also being present in plants, among animals the phenomenon of genomic imprinting is found only in placental mammals, where imprinting as a mechanism of gene regulation has evolved to balance the function of the placenta between the needs of the mother and those of the fetus [92-96]. Imprinting defects can lead to placental malformation and consequent to the limited transfer of nutritional resources to the fetus, to fetal intra-uterine growth retardation (IUGR) or spontaneous abortion [97-100]. Beyond the placenta, the expression levels of imprinted genes are also high in fetal and neonatal tissues, where they contribute to the specification of the musculoskeletal system and metabolism, thereby regulating fetal growth and development [101-109]. Furthermore, some postnatal processes including adaptation to feeding, social behavior and metabolism are also affected [109-112].

The expression of imprinted genes in the adult is tissue-specific but in general lower than in the placenta [113]. In some cases, particular genes may be biallelically expressed. A group of imprinted genes have been identified to be specifically expressed in adult stem cells or progenitor cells of various organs, namely kidney [114], liver [115], lung [116], adipose tissue [117], muscle tissue [118], blood [119, 120] and the brain [121, 122]. Furthermore, a group of imprinted genes was found to undergo a coordinate decline in mRNA expression with age in multiple organs [123]. These findings suggest that some imprinted genes in adults retain an importance for tissue renewal and regeneration.

1.5. Loss of imprinting (LOI)

While a failure to establish imprinting is a cause of pediatric diseases, secondary loss of imprinting (LOI) contributes to diseases of adults [124, 125]. In particular, it is a common epigenetic disturbance in cancers [126]. Aberrant regulation of several imprinted genes has been implicated in many rare congenital syndromes with higher predisposition to childhood cancer but also in common sporadic cancer types of adults [127, 128]. LOI as reflected by the convergence of epigenetic marks on both alleles leads to the transcriptional activation or silencing of both alleles. Since it is not always possible or practical to distinguish the expression of the two alleles, the DNA methylation state of DMRs is often analyzed as a surrogate marker of imprinted expression [129].

Among all imprinted genes and their products, in the context of cancer, the oncogenic function of IGF2 has been most widely studied. Like its non-imprinted homolog IGF1, it signals through IGF receptors, especially IGFR1, subsequently activating the Ras/Raf/MAPK and PI3K/Akt cascades, thereby stimulating cell proliferation, intermediary metabolism and/or differentiation in many tissues [130, 131]. PI3 kinase activation can lead to anti-apoptotic signals and components of this pathway are frequently mutated, deleted or amplified in cancers, including prostate cancer, as described above [132].

Commonly caused by epigenetic aberrations, LOI of *IGF2* is found in Beckwith-Wiedemann syndrome (BWS), Wilms' tumors (nephroblastoma) and other childhood cancers [133]. In adult cancers, loss of *IGF2* imprinting can be analyzed by means of sequencing of *IGF2* mRNA or sequence specific restriction digestion, covering a short nucleotide polymorphism in exon 9 [134]. Being found in a variety of primary cancers, mostly gastrointestinal, *IGF2* LOI has also been detected in non-tumorous tissues and may be a heritable rather than an acquired phenomenon [129, 135-140]. *IGF2* LOI is considered a predisposition factor for several cancers [139, 141, 142]. Often it was found associated with increased levels of *IGF2* in cancer [143]. However, studies investigating both normal and tumor tissues found that normal tissues with *IGF2* LOI expressed higher levels of *IGF2* than normal tissues without LOI [137, 144]. Also, tumor tissues with LOI exhibited lower *IGF2* expression than normally imprinted tumors [137]. In the prostate, LOI of *IGF2* was observed in the aging tissue, in normal tissues adjacent to the cancer and in BPH [144, 145]. Due to this 'field effect' the highest expression of *IGF2* in the prostate is actually found in benign tissues adjacent to cancer in comparison to fully normal tissues, but also to cancer tissues.

A study in mouse showed that *Igf2* LOI predisposes to cancer by increasing the sensitivity of Igf2 signaling and the downstream (PI3K/) Akt/PKB pathway to low doses of Igf2, thereby increasing the expression of proliferation-related genes in epithelial progenitor cells [146]. The enhanced IGF2 signaling of tissues may be maintained by higher levels of different components of the signaling pathway such as receptor and adaptor proteins. The effect of *IGF2* LOI might however not depend merely on IGF2 levels. The gene locus has been shown to interact with other loci, including many imprinted gene loci, through long-range chromatin interactions, which were abrogated when *IGF2* imprinting was lost [147]. Therefore, the correct imprinting of the *IGF2/H19* domain may be crucial for the regulation and expression of other imprinted genes.

Another imprinted gene, recognized for its tumor suppressor function- *CDKN1C*, codes for the protein $p57^{KIP2}$, a cyclin-dependent kinase inhibitor which cooperates with RB family proteins to inactivate E2F proteins and induce cell cycle arrest and/or differentiation [148].

In cultured human normal prostate epithelial cells, $p57^{KIP2}$ has been implicated in the acquisition of a senescent phenotype [149]. Loss of the protein may therefore be required for immortalization of prostate cells [150].

Loss of heterozygosity has been reported to affect the *CDKN1C*-containing 11p15 region in various cancer types [151, 152]. Promoter hypermethylation was also associated with *CDKN1C* repression in several malignancies, with one report including prostate cancer [153-158]. Imprinted maternal expression of *CDKN1C* is controlled by the nearby *KvDMR*. It serves as the promoter of the paternally expressed anti-sense non-coding RNA *LIT1* (*KCNQ1OT1*), which is thought to recruit repressive histone modifications and silence *CDKN1C* on the same allele [159]. LOI with loss of maternal methylation of *KvDMR*, but not necessarily *LIT1* overexpression, was found to correlate with *CDKN1C* silencing [160-162]. At least partial hypomethylation of the *KvDMR* has been observed in cancers of adults including hepatocellular carcinoma and bladder cancer, as an alternative mechanism to allelic loss [163, 164]. Repressive chromatin modifications have been suggested to associate with reduced *CDKN1C* expression in BWS patients, where neither *CDKN1C* promoter nor *KvDMR* were aberrantly methylated [165]. In breast cancer, low *CDKN1C* expression was shown to associate with a worse prognosis [166]. Furthermore, the authors of this study reported that its silencing involved the repressive histone H3K27me3 modifications, and that the gene could be reactivated by inhibition of EZH2 and treatment with a histone deacetylase inhibitor.

Interestingly, both *Cdkn1c* and *Igf2* have been found in mice to participate in a network of imprinted and other genes controlling embryonic growth which is likely regulated by the imprinted genes *Plagl1* (also known as *Zac1*) and *H19* [167, 168]. Characterized by remarkable co-expression across different organs and developmental stages and by functional association, the genes of the network are thought to control energy homeostasis at the levels of signal-sending (hypothalamus, pituitary and pancreas) and signal-receiving (liver, fat, muscle, cartilage and bone) organs to regulate body size, energy storage and expenditure during embryonic and postnatal development [101, 119, 169].

1.6. Deregulation of imprinted genes in prostate cancer

In the face of the severe and progressive disturbances of epigenetic regulation in prostate cancer, the question is imminent whether the correct maintenance of the epigenetic patterns of imprinted genes may be disturbed. Moreover, in addition to *IGF2* and *CDKN1C*, the expression of further imprinted genes may influence prostate cancer development and progression.

To investigate this hypothesis, an *in silico* analysis of microarray expression data available on the Oncomine website (www.oncomine.org) was performed by Klaus-Marius Bastian as a part of his medical doctoral thesis in our group [170]. The website www.geneimprint.com, which collects the most actual information on the `imprinted` status of genes in several species was used to select the genes with a definitively proved imprinted status in humans. Overall, 62 imprinted genes were proposed by the website, of which 52 had been investigated in at least two microarray studies comparing prostate cancer and benign tissues. Among them 12 genes showed consistent changes which at least approached statistical significance across multiple studies (Table 1.6). The 12 genes are *HYMAI*, *PLAGL1/ZAC1*, *SGCE*, *PEG10, PPP1R9A*, *INPP5F*, *CDKN1C*, *MEG3*, *NDN*, *SNRPN*, *PEG3,* and *GNAS*. A significant down-regulation in cancer was found for *HYMAI*, *PLAGL1/ZAC1*, *SGCE*, *PEG10, INPP5F*, *CDKN1C, MEG3*, *NDN,* and *PEG3*. Significant upregulation in the cancer tissues involved *PPP1R9A* and *GNAS*. An almost equal number of microarray sets manifested significant up- and downregulation of the *SNRPN* gene, which most likely could be accounted for by differences in the coverage of the many transcripts known for this gene.

Interestingly, most genes identified by this approach belong to the reported ZAC1-regulated imprinted gene network [168].

Table 1.6. Changes of imprinted gene expression in prostate benign vs. cancerous tissues.

Gene symbol	Gene product	Gene function	Location	Expression	Differential expression in PCA	Number of studies with		Total number of studies
						up-regulation	down-regulation	
HYMAI	Hydatidiform mole associated and imprinted	Non-coding RNA of unknown function	6q24.2	paternal	↓	0	3	4
PLAGL1/ ZAC1	Zinc finger protein PLAGL1	Potential tumor suppressor, transcription factor, nuclear receptor co-activator, inducer of apoptosis and cell cycle arrest	6q24	paternal	↓	1	12	16
SGCE	Epsilon-sarcoglycan	Transmembrane protein, part of dystrophin complex	7q21	paternal	↓	1	11	15
PEG10	Paternally expressed gene 10	Potential oncogene, inhibitor of apoptosis, inhibitor of TGF-β signalling	7q21	paternal	↓	1	6	14
PPP1R9A	Protein phosphatase 1, regulatory (inhibitor) subunit 9A	Potential tumor suppressor, protein phosphatase, regulator of adhesion-dependent signalling	7q21.3	maternal	↑	5	0	6
INPP5F	Inositol polyphosphate-5-phosphatase F	Inositol polyphosphate phosphatase, regulator of PI3K and PLC signalling	10q26.11	paternal	↓	0	10	15
CDKN1C	Cyclin-dependent kinase inhibitor 1C (p57,Kip2)	Tumor suppressor, inhibitor of CDKs, promoter of cell cycle arrest and differentiation	11p15.5	maternal	↓	0	12	12
MEG3	Maternally expressed 3	Non-coding RNA, regulator of imprinted gene cluster expression, potential regulator of p53 and Rb1 activities	14q32	maternal	↓	4	13	15
NDN	Necdin	Inhibitor of cell proliferation, transcription factor, activator of Wnt signalling, promoter of neuronal differentiation, inhibitor of adipocyte differentiation, pro-survival factor	15q11.2	paternal	↓	0	10	14
SNRPN/ SNURF	Small nuclear ribonucleoprotein-associated protein N/ SNRPN upstream reading frame protein	Regulator of pre-mRNA processing and tissue-specific splicing	15q11.2	paternal	↓ ↑	6	7	16
PEG3	Paternally expressed gene 3	Tumor suppressor, promoter of organism growth, pro-apoptotic, inhibitor of Wnt signalling	19q13.4	paternal	↓	2	10	16
GNAS	Guanine nucleotide binding protein (G protein), alpha stimulating activity polypeptide 1	Oncogene, G-protein α subunit, regulator of cAMP signalling	20q13.32	paternal	↑	11	6	15

Table 1.6. Changes of imprinted gene expression in prostate benign vs. cancerous tissues. Imprinted genes found to be frequently differentially expressed in prostate benign vs. cancerous tissues, as found by *in silico* analysis of changes in 16 microarray studies available in Oncomine. The arrows indicate over- or underexpression. Note: in cases when some studies measured no difference in expression between benign and cancerous tissues, the total number of studies is bigger than the sum of studies with up- and downregulation. The sum of studies reporting up- or downregulation can be bigger than the total number of studies due to differences between identifiers in complex genes such as *GNAS*. The table was published in [170].

1.7. PLAGL1/ZAC1

The *PLAGL1* gene is situated on chromosome 6q24, a region presumed to harbor a tumor suppressor gene and lost in some cancers [171-174]. Within the gene body of *PLAGL1* the small *HYMAI* gene is located, which encodes a non-protein-coding RNA of unknown function. *PLAGL1* encodes a C2H2 seven-zinc-finger protein with DNA-binding and transactivation activity, which is commonly designated as ZAC1 [171]. By binding to its GC-rich consensus binding site, singly or at tandem sites, ZAC1 can either activate or repress the expression of its target genes, depending on the orientation of the tandem sites to each other [175].

The role of ZAC1 was first recognized in the context of transient neonatal diabetes mellitus (TNDM), where *ZAC1* and *HYMAI* are overexpressed [176]. The symptoms include intrauterine growth retardation and hyperglycemia, due to impaired pancreas development, suggesting a function of ZAC1 in growth suppression and glucose homeostasis. Its role in embryonal growth and development was further confirmed in the knockout mouse model, in which *Zac1* deficient mice exhibited intrauterine growth restriction and impaired growth with altered development of bones and other organs [168].

During embryonal development, Zac1 was reported to be crucial for the induction of genes like *Pacap-R1*, which determines the insulin secretory function of the pancreas. Known Zac1 target genes include, in addition to *Pacap-R1*, *Pparg*, *Glut4* as well as the imprinted genes *Cdkn1c*, *Igf2*, *H19* and *Dlk1* that play important functions in many organs including development of the musculo-skeletal system, cardiac morphogenesis and others [168, 177, 178]. Together with its imprinted target genes, Zac1 belongs to and likely regulates an imprinted gene network which collectively controls embryonic growth and development [168].

Apart from its function as a DNA-binding transcriptional activator, ZAC1 acts as a powerful coactivator for p53 and the hormone-dependent activity of several nuclear receptors, including the androgen receptor [179-183]. In this role, it functions as a scaffolding protein recruiting chromatin activators (like the p160 family, CBP, p300 and PCAF), but also corepressors (like HDAC1 and mSin3a) to nuclear receptor target genes. Loss of ZAC1 may therefore promote castration-resistance in prostate cancer.

In vitro experiments in cancer cell lines have shown that ZAC1 can antagonize tumor cell proliferation directly by targeting and activating genes involved in cell cycle control and proliferation, like the cyclin-dependent kinase inhibitors $p21^{CIP1}$ and $p57^{KIP2}$, and indirectly by co-activating proteins like p53 and nuclear receptors. However, the protein was also able to induce cell cycle arrest and apoptosis independent of p53. Thereby, ZAC1 plays a role in cell fate decisions that regulate the homeostasis between cells with particular functions as well as overall organ growth and regeneration.

PLAGL1/ZAC1 expression is often diminished in various human cancers, suggesting its potential tumor suppressor function. Through its antiproliferative and AR-dependent effects, ZAC1 could be relevant as a tumor suppressor in prostate cancer too.

The monoallelic paternal expression of both *PLAGL1* and *HYMAI* is regulated by a maternally methylated DMR (here called *PLAGL1* DMR) present within the shared promoter (P1) of these genes (see Fig. 1.7 upper panel). A second upstream non-imprinted promoter (P2) has recently been reported to be utilized in parallel to the P1 promoter, resulting in biallelically expressed *PLAGL1* transcripts (P2 transcripts) [184]. In most adult tissues, including prostatic tissue, usage of the P1 promoter was shown to be predominant, indicating preserved monoallelic expression. In the liver, both promoters produced equal quantities of transcripts, while in peripheral blood lymphocytes P2 usage was dominant and *ZAC1* expression was biallelic [184]. Both kinds of transcripts starting from the P1 or the P2 promoters undergo alternative splicing, resulting in short and long transcript isoforms, encoding for respectively five- and seven zinc finger proteins. All transcripts encompass several non-protein-coding exons in the 5'-UTR. Isoform 1 is translated from two protein-coding exons, E7 and E8, and encodes a 463 amino acids protein with a predicted protein size of 51 kDa (uniprotKb database #Q9UM63). The alternatively spliced isoform 2, also called delta2, or just delta, results from transcripts with only one protein coding exon, E8, and represents a 411 amino acids protein with a predicted protein size of 45 kDa (Fig 1.7 lower panel). According to Valleley et al. the two mRNA isoforms are present in comparable amounts in most adult tissues tested, except the kidney, spleen and pancreas, where isoform 1 was more highly expressed than the delta isoform [184]. The seven-finger and five-finger ZAC1 proteins were reported to show functional differences [185]. While both isoforms antagonized proliferation to an equal extent, as tested in colony formation assays, delta ZAC1 was more efficient in the induction of cell cycle arrest, while isoform 1 ZAC1 could more efficiently induce apoptosis.

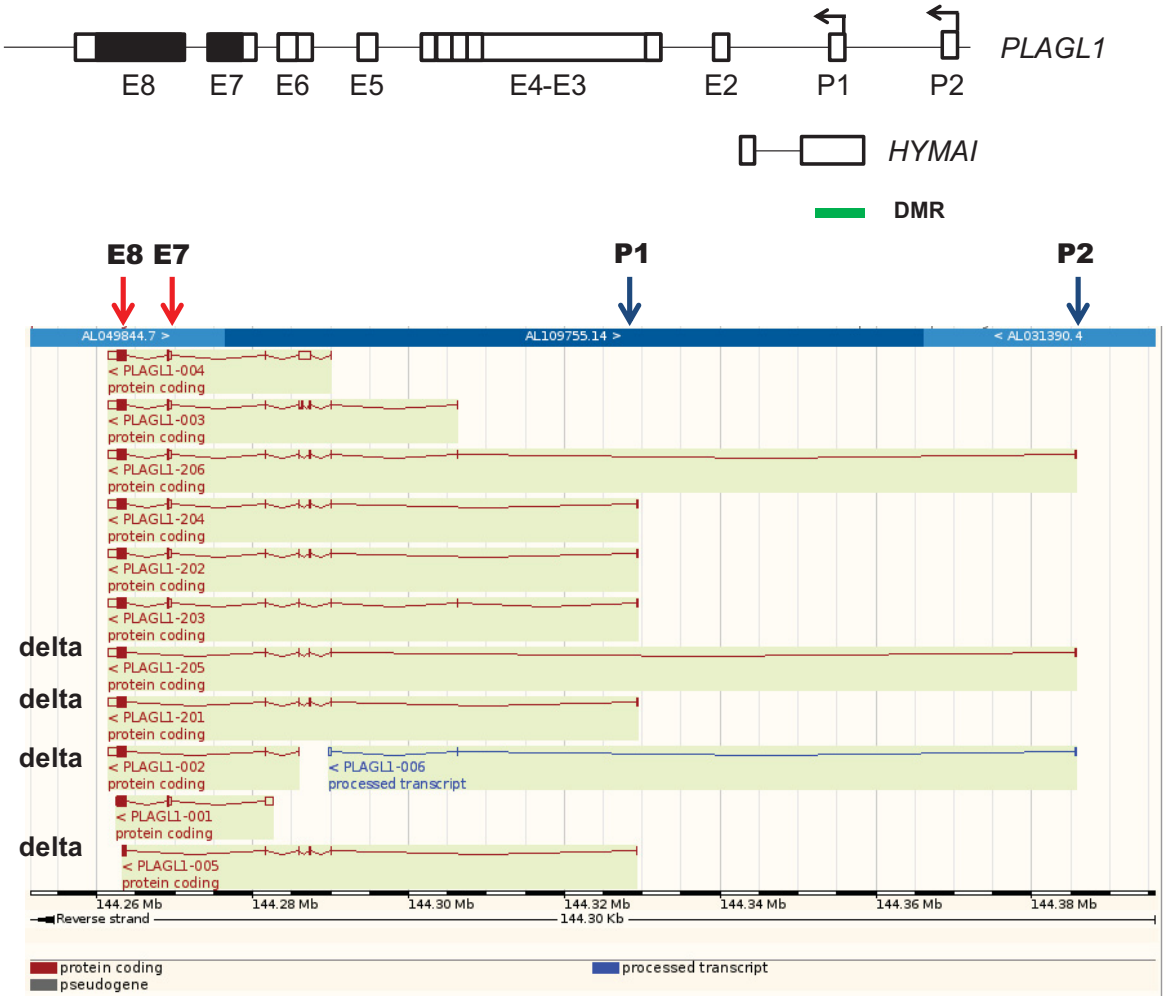

Fig. 1.7. PLAGL1/ZAC1 transcript variants included in the Ensembl database. PLAGL1/ZAC1 transcription can start from the imprinted P1 or the non-imprinted P2 promoter (blue arrows). Alternative splicing results in transcripts with two protein-coding exons (E7 and E8, red arrows), isoform 1, or only one (E8), delta isoform. The protein produced from isoform 1 transcripts is 463 amino acids long and has a predicted protein size of 51 kDa, whereas the delta isoform encoded protein is 411 amino acids long and has a predicted protein size of 45 kDa, according to UniprotKb database (#Q9UM63). The transcript variant corresponding to the ZAC1 cDNA in the pBS.hZAC1 plasmid obtained from A. Varrault is PLAGL1-001, transcript ID ENST00000367571, coding for a 463-amino acid- ZAC1 protein.

1.8. Aims of the study

Through their various functions in growth and development on the organism, organ and cellular levels, imprinted genes exert important functions in tissue homeostasis. The extensive epigenetic aberrations found generally in prostate cancer may disturb their complex regulatory patterns and thereby contribute to the disruption of important anti-tumor mechanisms in prostate cancer.

The initial aim of this study was to evaluate the expression of the presumed tumor suppressor genes *TFPI* and its imprinted homolog *TFPI2* in prostate cancer tissues and

cell lines and to elucidate if possible epigenetic aberrations of the 7q21 imprinted gene locus might influence *TFPI2* expression.

After an *in silico* analysis of microarray studies (performed by Klaus-Marius Bastian in our group) showed that changes in imprinted gene expression occur in a selective fashion in prostate cancer tissues, the next step was to validate these changes by qRT-PCR in the available tissue set and in prostate cancer cell lines. In order to understand the possible pathologic context in which the observed expression changes occur, their association with several clinical and molecular markers of prostate cancer progression, in particular the expression of the epigenetic modifier EZH2 and of the likely prostate oncogenes ERG and HOXC6 was statistically evaluated.

The assumption that epigenetic aberrations disturbing the imprinted gene clusters might affect the expression of the respective imprinted genes was tested by analysis of the DNA methylation status of ICRs and gene regulatory regions in several affected clusters.

Since the results of the expression and DNA methylation studies supported the idea that ZAC1 might function as a node in the imprinted gene network in the prostate, as reported in studies on various murine tissues, this study next addressed the question whether ZAC1 may act as an upstream regulator of the other imprinted genes with differential expression in prostate cancer. To answer this question, the expression of the potential ZAC1 targets was measured in transient, stable and inducible ZAC1 overexpression models.

In the course of these experiments, it was discovered that ZAC1 expression was strongly post-transcriptionally regulated. Several experiments in this thesis were conducted to elucidate the mechanisms involved in this unexpected phenomenon.

The final purpose of this study was evaluating prostate-relevant functional aspects of ZAC1. ZAC1 overexpression and downregulation experiments combined with reporter assays in prostate cancer cell lines were used to evaluate its influence on androgen signaling as well as on the activation of the p53-target gene *CDKN1A* (p21).

2. Materials & Methods

2.1. Materials

2.1.1. Prostate tissue samples (RNA and DNA)

High molecular RNA and DNA previously extracted from aliquots of powdered tissues of prostatic benign and cancer tissue specimens as described [49] were available for use. All tissues had been obtained by radical prostatectomy in the period 1997-2001 from patients treated at the Dept. of Urology with their informed consent. All investigations of these tissues have been authorized by the ethics committee of the Medical Faculty of the Heinrich-Heine University.

The tissue set from which RNA and DNA was used for analysis contained 47 tumor tissues and 13 benign tissues from cancer-carrying prostates. Benign tissues samples were collected from patients aged 55 -73 years, while cancer tissue samples were derived from patients aged between 59 and 76 (on average 67.5) years. The benign tissues were isolated from areas as distant as possible to the carcinomas and were histologically confirmed by eosin–haematoxylin staining. All tissue asservation had been performed by trained pathologists. Histologic diagnoses and Gleason grading of tumors was performed according to the TNM guidelines of the UICC from 1997.

Of the 47 postate cancer tissue samples, 20 were staged pT2, 25 as pT3, and 2 as pT4, respectively. Lymph node metastases were present in 12 of the patients at the time of prostatectomy, while no distant metastases had been found in any of the patients. The Gleason sum of the tumor samples was less than 7 in 13 cases, equaled 7 in 26 cases, and was higher than 7 in 8 cases. Patient outcome after the operation was further monitored for different periods with a median of 64 months. Follow-up data was available for 45 of the 47 patients, of which 18 experienced biochemical recurrence, as defined by a PSA value of > 0.2 ng/mL in two consecutive measurements.

Table 2.1.1. Clinical parameters of prostate cancer tissue samples

Sample	Age	T-Stage	Metastasis to Regional Lymph Nodes	Biochem. Relapse	Distant Metastasis	Gleason Score
pTu 36	72	pT3b	pN0	R1	M0	7
pTu 38	75	pT2b	pN0	R0	M0	7
pTu 50	67	pT3b	pN1	R1	M0	7
pTu 65	62	pT3b	pN0	R1	M0	7
pTu 83	76	pT3b	pN0	R0	M0	7
pTu 89	68	pT2b	pN0	R0	M0	3
pTu 93	73	pT3b	pN0	R1	M0	7
pTu 95	74	pT3b	pN1	R1	M0	10
pTu 97	71	pT3a	pN0	R0	M0	7
pTu 99	67	pT2b	pN0	R0	M0	5
pTu 101	68	pT3a	pN0	*NN*	M0	8
pTu 105	59	pT3a	pN0	R0	M0	5
pTu 107	59	pT3a	pN0	R1	M0	7
pTu 117	68	pT3b	pN0	R0	M0	5
pTu 119	63	pT3b	pN1	*NN*	M0	9
pTu 121	65	pT2b	pN0	R0	M0	6
pTu 127	71	pT2b	pN0	R0	M0	6
pTu 133	72	pT2b	pN1	R1	M0	7
pTu 137	73	pT2b	pN0	R0	M0	8
pTu 139	65	pT3b	pN1	R1	M0	9
pTu 141	69	pT2b	pN0	R0	M0	4
pTu 145	70	pT4	pN1	R0	M0	7
pTu 161	64	pT2b	pN0	R0	M0	5
pTu 163	65	pT3a	pN1	R0	M0	5
pTu 169	72	pT3a	pN0	R0	M0	7
pTu 171	61	pT2b	pN0	R1	M0	5
pTu 175	73	pT2b	pN0	R0	M0	8
pTu 183	67	pT3a	pN0	R0	M0	6
pTu 187	68	pT2b	pN0	R0	M0	8
pTu 189	63	pT2b	pN0	R0	M0	7
pTu 191	72	pT2b	pN0	R0	M0	7
pTu 205	73	pT3a	pN0	R0	M0	7
pTu 209	71	pT3a	pN0	R0	M0	7
pTu 213	59	pT2a	pN0	R0	M0	7
pTu 215	58	pT3a	pN0	R0	M0	7
pTu 217	62	pT2b	pN0	R0	M0	8
pTu 219	64	pT4	pN1	R0	M0	7
pTu 225	62	pT3b	pN0	R0	M0	6
pTu 227	72	pT2a	pN1	R0	M0	7
pTu 230	68	pT2a	pN0	R1	M0	7
pTu 232	70	pT2b	pN1	R1	M0	7
pTu 236	74	pT3a	pN0	R0	M0	7
pTu 238	62	pT2a	pN0	R0	M0	6
pTu 245	66	pT3a	pN0	R0	M0	7
pTu 247	55	pT3b	pN1	R1	M0	7
pTu 253	61	pT3a	pN1	R0	M0	7
pTu 256	71	pT3b	pN0	R0	M0	7

2.1.2. Prostate cancer cell lines

The LNCaP cell line has been isolated from the lymph node metastasis of a prostate cancer patient and its growth is dependent on steroids acting via an AR with a mutation in the ligand-binding domain. 22Rv1 is a human prostate carcinoma cell line derived from a xenograft that was serially propagated in mice after castration-induced regression and

relapse of the parental, androgen-dependent CWR22 xenograft. It expresses a wild type and a splice mutant AR, its growth being weakly stimulated by androgens. The PC3 and DU145 cell lines are androgen-independent and stem resp. from bone and brain metastases from two prostate cancer patients. The MDAPCa2b cell line was established from a bone metastasis of a patient with androgen-independent prostate cancer, but its growth is strongly dependent on androgens. VCaP is an androgen-sensitive cell line that was isolated from a bone metastasis of a patient with hormone refractory prostate cancer and was then passaged as xenografts in mice. The PNT2 cell line was established from normal adult prostatic epithelial cells by immortalization through transfection with a plasmid containing SV40 genome. Normal human prostate epithelial cells (PrEC) were purchased from Lonza as primary cells and contain predominantly cells with a basal phenotype.

2.1.3. Bacteria strains

Competent *E.coli* One Shot TOP10 cells or ultracompetent XL-2 blue cells were transformed with plasmids in cloning experiments. Bacterial stocks containing plasmids of interest were used for propagation and plasmid isolation.

2.1.4. Consumables, chemicals, reagents, and kits

Plastic consumables for molecular biology and cell culture experiments were purchased from Greiner, Sarstedt, and Eppendorf.

Chemicals, Reagents, Kits	Supplier
General chemicals	
NaCl	Merck
Tris	Merck
Glycine	Merck
NaOH	Merck
SDS	Merck
EDTA	Merck
NP-40	Merck
DOC	Sigma
Tween-20	Sigma
50x TAE Buffer	5-PRIME
Agarose	Sigma
Ethanol	Merck
Methanol	Merck
2-Propanol	Merck
HCl 25%	Merck
Chloroform	Merck
Formaldehyde 37%	Merck
β-Mercaptoethanol	Sigma
Giemsa's azur eosin methylene blue solution	Merck
RNA isolation, reverse transcription, PCR	
QIAzol	Qiagen
QIAshredder	Qiagen
RNeasy Mini Kit	Qiagen
RNase-Free DNase Set	Qiagen
RiboLock RNase Inhibitor	Thermo
SuperScript II Reverse Transcriptase	Invitrogen
Oligo(dT)$_{18}$ Primer	Fermentas
Random Hexamer Primer	Fermentas
0.1 M DTT	Invitrogen
5x First Strand Buffer	Invitrogen
QuantiTect Reverse Transcription Kit	Qiagen
dNTP Mix	Fermentas
HotStarTaq DNA Polymerase Kit	Qiagen
6x DNA Loading Dye	Thermo
GeneRuler DNA Ladder Mix	Thermo
QuantiTect SYBR Green PCR Kit	Qiagen

Chemicals, Reagents, Kits	Supplier
Cell Culture, Transfection, Treatments	
PBS Dulbecco	Biochrom
Fetal calf serum	Biowest
RPMI medium 1640 (1x) + GlutaMAX-I	Gibco
Trypsin-EDTA solution	Sigma
Penicillin, Streptomycin	Sigma
BRFF-HPC1 medium	AthenaES, Baltimore, MD
Insulin-Transferrin-Selenium	Gibco
Dimethyl sulfoxide (DMSO)	Sigma
Zeocin	InvivoGen
Blasticidin	PAA
Tetracycline	Sigma
R1881 C-III	Sigma
Bicalutamide (Casodex)	Sigma
5-Aza-2'-deoxycytidine	Sigma
Suberoylanilide Hydroxamic Acid (Saha)	Cayman Chem. Company
MG-132	Enzo
Optimem	Gibco
FuGENE 6 Transfection Reagent	Roche
X-tremeGENE 9 DNA transfection reagent	Roche
Lipofectamine RNAiMAX transfection reagent	Invitrogen
ZAC1 siRNA (h) (# sc-38183)	Santa Cruz
Control siRNA-A (# sc-37007)	Santa Cruz
Bacteria Culture	
Difco Luria Agar Base, Miller	BD
Luria Broth	Invitrogen
Ampicillin	Sigma
Kanamycin	Sigma
Fast Plasmid Mini Kit	5-PRIME
QIA Filter Plasmid Maxi Kit	Qiagen
One Shot TOP10 competent *E.coli* cells	Invitrogen
XL-2 Blue ultracompetent cells	Stratagene

Chemicals, Reagents, Kits	Supplier
Proteins, Western Blot	
Proteinase Inhibitor Cocktail	Sigma
Pierce BCA Protein Assay	Thermo
Albumin Standard	Thermo
Lämmli Sample Buffer	Biorad
PageRuler Prestained Protein Ladder	Thermo
Mini-PROTEAN TGX Gels (Any kD, 7%, 10%, 12%, 4-20%)	Biorad
10x Tris/Glycine/SDS Buffer	Biorad
Immobilon-P Transfer Membrane	Millipore
Whatman Paper	Whatman
Sucofin skimmed milk powder	TSI GmBH
Bovine Serum Albumin	Sigma
ECL Advance Western Blotting Detection Kit	GE Healthcare
High performance chemiluminescence film Amersham Hyperfilm ECL	GE Healthcare
Cloning, Reporter Assay	
Restriction digest buffers	New England Biolabs, Fermentas
100x BSA	New England Biolabs
S-Adenosyl-methionine	New England Biolabs
EcoRI	Fermentas
HindIII	Fermentas
NotI	Fermentas
BamHI	Fermentas
EcoRV	Fermentas
BsgI	New England Biolabs
BsaI	Fermentas
T4 DNA Ligase	Fermentas
PEG 4000	Fermentas
10x Ligation Buffer	Fermentas
Shrimp Alkaline Phosphatase (SAP)	Thermo
Klenow Fragment	Thermo

Chemicals, Reagents, Kits	Supplier
NucleoSpin Extract II	Macherey-Nagel
Dual-Luciferase Reporter Assay System	Promega
Bisulfite sequencing, and Pyrosequencing	
Blood and Cell Culture Midi Kit	Qiagen
Proteinase K	Qiagen
RNase A	Qiagen
EZ DNA Methylation-Gold Kit	Zymo Research
TOPO TA Cloning Kit For Sequencing (including pCR4- TOPO Vector)	Invitrogen
PyroMark PCR Kit	Qiagen
1x Coralload Concentrate	Qiagen
Streptavidin sepharose beads	Amersham
PyroMark Gold Q24 Reagents	Qiagen
ChIP	
ChIP-IT Express Kit	Active Motif
QIA Quick PCR Purification Kit	Qiagen
ChIP-IT Control Kit- Human	Active Motif

Table 2.1.4. Chemicals and reagents

2.1.5. Buffers and solutions

Table 2.1.5. Buffers and Solutions for Western blot analysis	End conc.	Quantity
Protein Lysis Buffer RIPA-type		
NaCl 5 M	150 mM	3 mL
NP-40	1%	1 mL
DOC	0.5 %	0.5 g
SDS 10 %	0.1 %	1 mL
EDTA 0.5 M	1 mM	200 µL
Tris pH 7,6 1 M	50 mM	5 mL
Aqua dest.		up to 100 mL
***add freshly Protease Inhibitor Cocktail 10 µl/1 mL RIPA**		
Transfer Buffer 5x Stock Solution		
Tris	0.28 M	34 g
Glycine	0.5 M	144 g
Aqua dest.		up to 2 L
***pH 8.3 adjust with NaOH**		
Electrophoresis Buffer		
10x Tris/Glycine/SDS Buffer (Biorad)	1x	100 mL
Aqua dest.		up to 1L
Transfer Buffer 1x		
Transfer Buffer 10x Stock Solution	1x	200 mL
Methanol	10%	100 mL
Aqua dest.		up to 1 L
TBS 10x		
Tris	0.5 M	24 g
NaCl	1.5 M	88 g
Aqua dest.		up to 1L
***pH 7.6 adjust with HCl**		
Washing Buffer (TBST)		
TBS Buffer 10x	1x	100 mL
Tween 20	0.1 %	0.5 mL
Aqua dest.		up to 1L
Blocking solution		
skimmed milk powder or BSA	5%	5 g
TBST 1x	1x	50 mL
Protein Stripping Solution		
Glycine	1.5 %	15 g
SDS 10% solution	0.1 %	1 mL
Tween 20	1%	1 mL
Aqua dest.		up to 100 mL
***pH 2, adjust with HCl**		

2.1.6. Antibodies

Table 2.1.6. Antibodies	Supplier
for Immunoblotting	
ZAC1 (H-253) rabbit polyclonal IgG (# sc-22811)	Santa Cruz Biotech.
Neurabin-I (H-300) rabbit polyclonal IgG (# sc-32932)	Santa Cruz Biotech.
Kip2 p57 (C-20) rabbit polyclonal IgG (# sc-1040)	Santa Cruz Biotech.
p21 mouse IgG (# 556430)	BD Biosc. Pharmingen
GAPDH (6C5) mouse monoclonal IgG (# ab8245)	Abcam
α-Tubulin mouse IgG (B-5-1-2) (# T5168)	Sigma
goat anti-mouse IgG-HRP (F1212) (# sc-2004)	Santa Cruz Biotech.
goat anti-rabbit IgG-HRP (C2309) (# sc-2005)	Santa Cruz Biotech.
for ChIP	
H3K4me3 rabbit polyclonal IgG (# ab8580)	Abcam
H3K9ac rabbit polyclonal IgG (# ab4441)	Abcam
H3K9me3 rabbit polyclonal IgG (#ab8898)	Abcam
H3K27me3 mouse monoclonal IgG (# 39535)	Active Motif

2.1.7. Oligonucleotide primers

DNA sequences, annealing temperatures, amplicon sizes and the software used for designing of the primers used in PCR, qRT-PCR, bisulfite sequencing and pyrosequencing are listed in the tables below.

Table 2.1.7.1. Primers for end point PCR and qRT-PCR

GENE (TRANSCRIPT)	PRI-MER	DNA SEQUENCE	ANN.T ° [°C]	PROD. LENGTH	DESIGN
TFPI	F+R	QuantiTect Primer Assay Hs_TFPI_1_SG #QT00086149 (Qiagen)	55°	121 bp	Qiagen
TFPI2	F+R	QuantiTect Primer Assay Hs_TFPI2_1_SG #QT00062804(Qiagen)	55°	136 bp	Qiagen
SGCE	F+R	QuantiTect Primer Assay Hs_SGCE_1_SG #QT00052507(Qiagen)	55°	134 bp	Qiagen
PON2	F+R	QuantiTect Primer Assay Hs_PON2_1_SG #QT00095690(Qiagen)	55°	101 bp	Qiagen
TBP	F+R	QuantiTect Primer Assay Hs_TBP_1_SG #QT00000721(Qiagen)	55°	132 bp	Qiagen
DLK1	F+R	QuantiTect Primer Assay Hs_DLK1_1_SG #QT00093128	55°	136 bp	Qiagen
PEG10	F	TCC ACC GAG CCT GGC GAA AG	62°	150 bp	Primer BLAST
	R	CCC GCT TAT TTC ACG CGA GG			
PPP1R9A	F	AGA GGC GCC AGA GAG AGC TGC	62°	70 bp	Primer BLAST
	R	ACA GTG TTC TCG TCA TCG TCG GCA			
HYMAI	F	GTG GAT CAC GAG GTC AGG A	62°	105 bp	Primer BLAST
	R	GTG TTC ACC CAC CAC TAT GC			

GENE (TRANSCRIPT)	PRI-MER	DNA SEQUENCE	ANN.T ° [°C]	PROD. LENGTH	DESIGN
PLAGL1 **(transcript variants 2-6) NM_006718.3 NM_001080951.1 NM_001080952.1 NM_001080953.1 NM_001080954.1)**	F1 R1	CTC ACC CTG GAG AAG TTC ACG GGG TAG CCA TAT GCC TCA TCA A	56°	127 bp	Primer BLAST
PLAGL1 **delta (for end- point PCR-all transcript variants)**	F1 R1	TGT TCC CTG TCA CTC AGT AG TGG TTT TTC AGG TGG TCT TTC	55°	107 bp; 583 bp	Primer BLAST
PLAGL1 **delta (transcript variants 1,7,8) NM_002656.3 NM_001080955.1 NM_001080956.1)**	F2 R2	ACA AAC TTC TGG GAG GAC TCG GT GGT AGC CAT ATG CCT ACT GAG TGA C	60°	73 bp	Primer BLAST
PLAGL1 **(transcript variants 1-8) all**	F2 R2	GGC ATA TGG CTA CCC ATT CTC CCC A TTC CGG TTG AAC GTC TTC TCA CAG T	60°	70 bp	Primer BLAST
CDKN1C	F3 R3	GCG GCG ATC AAG AAG CTG CGA CGA CTT CTC AGG CGC	60°	81 bp	Primer BLAST
LIT1 (KCNQ1OT1)	F1 R1	CCC TGC TGT GCC TTC AGC CC CCA GGC TGC CTC ACC CAA CG	62°	168 bp	Primer BLAST
MEG3	F2 R2	CCT CCT CTC CAT GCT GAG CTG C GCT CCT AGT GCC CTC GTG AGG T	62°	73 bp	Primer BLAST
INPP5F	F R	TCC CTC TGC CGC TGC TTC TCA GTA GCG GGT CGG AGC	60°	238 bp	PyroMark
INPP5Fv2	F R	GGG ATC ATG TTT GGC TGA TGT AA TGA GGG TGC ACT CTG AAA ATT GT	62°	156 bp	PyroMark
NDN	F1 R1	CTT GCC AGA CGG CGC AGA CA GGG GCC TCG GCT GCA AAG TT	60°	72 bp	Primer BLAST
SNRPN **(transcript variants 1-5 NM_003097.3 NM_0022805.2 NM_0022806.2 NM_0022807.2 NM_0022808.2)**	F R	TGG CCG AAT CTT CAT TGG CAC CT TCA CGC TCT GGT TGC TTC GCA	60°	117 bp	Primer BLAST
SNURF **(transcript variant 2 NM_0022804.2;** ***SNRPN*** **transcript variant 1 NM_003097.3)**	F R	CCG CCG GAG ATG CCT GAC G AAG CGA TCC CTT GCC CGC TC	60°	71 bp	Primer BLAST
GNAS **002 (transcript variant 4 NM_016592.2)**	F R	CAT CCC CAT CCG GCG TCA CT TGC AGG ATC CTC ATC TGC TTC ACA	62°	116 bp	Primer BLAST
GNAS **009 (transcript variant 2 NM_080425.2)**	F R	ACG CAG TAA GCT CAT CGA CAA ACA TGC AGG ATC CTC ATC TGC TTC ACA	60°	129 bp	Primer BLAST

GENE (TRANSCRIPT)	PRI-MER	DNA SEQUENCE	ANN.T° [°C]	PROD. LENGTH	DESIGN
***GNAS* 201 (transcript variants 1,3,6,7 NM_000516.4 NM_080426.2 NM_001077488.2 NM_001077489.2)**	F R	AGC AGC TGC AGA AGG ACA AGC A GAT TCT CCA GCA CCC AGC AGC A	60°	70 bp	Primer BLAST
PEG3	F3 R3	AGT GAC CGG GAC TGG GAC CG CGC GGA GGC ATC CTG CTT CT	62°	98 bp	Primer BLAST
IGF2	F2 R2	CAG TGA GAC CCT GTG CGG CG GCT TGC GGG CCT GCT GAA GT	62°	88 bp	Primer BLAST
H19	F1 R2	CAC CAG CTG CCG AAG GCC AA CCA GCC TAA GGT GTT CAG GAA GG	62°	122 bp	Primer BLAST
TBP	F R	ACA ACA GCC TGC CAC CTT A GAA TAG GCT GTG GGG TCA GT	56°	120 bp	PyroMark W.Göring
CDKN1A	F R	GGA AGA CCA TGT GGA CCT GT GGC GTT TGG AGT GGT AGA AA	56°	146 bp	P. Nikpour
PPARG	F1 R1	TCC GAG GGC CAA GGC TTC AT GCA AAC CTG GGC GGT CTC CA	62°	187 bp	Primer BLAST
GLUT4	F1 R1	CCG GGT CCT TGG CTT GTG GC GGG GGT TCC CCA TCT TCG GA	62°	213 bp	Primer BLAST

Table 2.1.7.2. Primers for bisulfite sequencing

GENETIC REGION	PRI-MER	SEQUENCE	ANN. T°	PROD. LENGTH	DESIGN
***TFPI2* promoter**	F R	GGT TAG ATA TTT GTT GGT TTT TGA G CTC TCC CTC TTA CAC AAT TTA C	54°	316 bp	[186]
7q21 DMR	F R	GTG TTA TGT TTT ATA AAT AGA TAA G AAC TCA TAT ACC TCT ACA ATT C	48°	375 bp	[186]

Table 2.1.7.3. Primers for ChIP

GENETIC REGION	PRIMER	SEQUENCE	ANN.T°	PROD. LENGTH	DESIGN
***TFPI2* promoter**	F R	CTC CGC CGG TTG GGG AGA GA GGG CCG CCT GGA GCA GAA AG	60°	219 bp	Primer BLAST
7q21 DMR	F R	AAT GTG CCA GTG GTC GCG GG GCC CGC CGC TAG AGG GAG TA	60°	229 bp	Primer BLAST
GAPDH	F R	TAC TAG CGG TTT TAC GGG CG TCG AAC AGG AGG AGC AGA GAG CGA	60°	166 bp	Active Motif Control Kit
CTCFL	F R	GAA CAG CCC ATG CTC TTG GAG CAG AGC CCA CAA GCC AAA GAC	60°	113 bp	PyroMark W.Göring

Table 2.1.7.4. Primers for bisulfite pyrosequencing

GENE	ASSAY	SEQUENCE	ANN.T°	PROD. LENGTH	DESIGN
7q21 DMR	7q21 DMR Pyro F	TTG GTT TTG GTT TTT GGA AAT AG	60°	185 bp	[200]
	7q21 DMR Pyro R	BIO-TTT CCC CCT CTT ACT AAA TAC ATT TCT			
	7q21 DMR Pyro S	TTG TTT AGT TTT TAG TAT TTT ATG A			
	Sequence to analyse	ttcCGcttccctgctcCGtaaaacCGaagaaaacCGagatttcCGtcacCG			
	Sequence to analyse bisulfit converted	TTTYGTTTTTTTGTTTTYGTAAAATYGAAGAAAATYGAGATTTTYGTTATYG			
	No. of CpG sites included	6			
	Chromosomal location (Sequenced strand)	Chr7: 94,284,600-94,284,784 (+)			
PLAGL1 DMR	PLAGL1 DMR Pyro F	GAG GAG GGT GTG TTT TTG T	50°	177 bp	[203]
	PLAGL1 DMR Pyro R	BIO- AAT CTA TAA ACC TCA TAC CAA ATA AAC			
	PLAGL1 DMR Pyro S	GTA ATT TAG GTA GTT TTA T			
	Sequence to analyse	CGCTGG**C**GCAGGTAGACC**C**GAGC**C**GG			
	Sequence to analyse bisulfit converted	YGTTGGYGTAGGTAGATTYGAGTYGGT			
	No. of CpG sites included	4			
	Chromosomal location (Sequenced strand)	Chr6: 144,371,328-144,371,508 (+)			
MEG3 DMR	MEG3 DMR Pyro F	BIO- AGT TAA TGA TTA GGG AGG TGA ATA TTG AT	57°	240 bp	A.Koch PyroMark
	MEG3 DMR Pyro R	TCC CAA ACT CTA ATC CCT AAA ACT CCT			
	MEG3 DMR Pyro S	TCT CTA TCT CCC CAA CAA TA			
	Sequence to analyse	CGcctgtttatgaaaaaaCGagccccccacaCGcCGtcccaaggctCGgCGcctctagtgacctgaCG			
	Sequence to analyse bisulfit converted	CRcctatttataaaaaaaCRaaccccccacaCRcCRtcccaaaactCRaCRcctctaataacctaaCR			
	No. of CpG sites included	7			
	Chromosomal location (Sequenced strand)	Chr14: 101,290,947- 101,291,130 (-)			
KvDMR	KvDMR Pyro F	TTA GTT TTT TGY GTG ATG TGT TTA TTA	60°	101 bp	[200]
	KvDMR Pyro R	BIO-CCC ACA AAC CTC CAC ACC			
	KvDMR Pyro S	TTG YGT GAT GTG TTT ATT A			
	Sequence to analyse	cccCGgggtgacCGCGtgaggacagCGgcCGcacccCGacactgctgtgggccctCG			
	Sequence to analyse bisulfit converted	TTTYGGGGTGATYGYGTGAGGATAGYGGTYGTATTTYGATATTGTTGTGGGTTTTTYG			
	No. of CpG sites included	7			
	Chromosomal location (Sequenced strand)	Chr 11: 2,721,588- 2,721,680 (+)			
CDKN1C promoter	CDKN1C Pyro F	BIO-AAA GAG TGG AGT TGA TT	56°	118 bp	[158]
	CDKN1C Pyro R	ACC TAC TAC TAC TAA ACT AAT ATC			
	CDKN1C Pyro S	TAC TAA ACT AAT ATC CCT T			
	Sequence to analyse	CGAGGGCTCCGCGCGCCTGGAGCCC			
	Sequence to analyse bisulfit converted	CRAAAACTCCRCRCRCCTAAAACCC			
	No. of CpG sites included	4			
	Chromosomal location (Sequenced strand)	Chr 11: 2,907,633- 2,907,750 (-)			

2.1.8. Plasmids

Table 2.1.8. Plasmids

Plasmid	Promoter	Insert	Bacterial/ mammalian resistance
T-Rex System Vectors [short]			
pcDNA 4/TO	CMV, 2x$TetO_2$	no insert	Ampicillin/Zeocin
pcDNA 4/TO/*lac*Z [lacZ]	CMV, 2x$TetO_2$	β-galactosidase	Ampicillin/Zeocin
pcDNA 6/TR	CMV, Rabbit ß-globin intron II	TetR	Ampicillin/Blasticidin
ZAC1 expression vectors			
pcDNA4.TO.ZAC1.VA [ZAC.VA]	CMV, 2xTetO2	ZAC1 cDNA isodform 1, 800 bp-long 5'-UTR ,140 bp 3'-UTR, corresponding to transcript variant PLAGL1-001 (ENST00000367571) (ensembl)	Ampicillin/Zeocin
pcDNA4/TO.ZAC.DS [ZAC.DS]	CMV, 2xTetO2	ZAC1 isoform 1 cDNA without UTRs, original ATG mutated, actual ATG at +24 bases from original ATG	Ampicillin/Zeocin
pcDNA4/TO.ZACdelta [ZACdelta]	CMV, 2xTetO2	ZAC1 cDNA from ZAC.VA lacking the 5'-UTR and the first protein-coding exons except the last isoform 2(delta),	Ampicillin/Zeocin
Luciferase reporter plasmids			
pGL3 Luciferase reporter vectors	no promoter	Luciferase	Ampicillin
pGL3-Basic vector	no promoter	Luciferase	Ampicillin
pARE-Luc	Androgen Responsive Elements	Luciferase	Ampicillin
p21-Luc (originally WWP-Luc, Addgene plasmid 16451)	CDKN1A promoter (1x p53 binding site)	Luciferase	Ampicillin
pPB-Luc	rat probasin promoter (AR-binding site)	Luciferase	Ampicillin
Other plasmids			
pSG5-AR	SV40	Androgen receptor	Ampicillin
pBS.hZAC1 [pBSIISK(-)]	T7	ZAC1 cDNA	Ampicillin
pBSK.hZAC1	T7	ZAC1 cDNA	Ampicillin
pEGFP-C1	CMV	EGFP	Kanamycin/Neomycin

2.1.9. Equipment

Table 2.1.9. Equipment

Instruments	Manufacturer
Mini spin centrifuge	Eppendorf
Thermomixer	Eppendorf
Vortexer	Neolab
Cooling centrifuge	Beckman Coulter
Shaker	Neolab
Trio thermoblock	Biometra
T3 Thermocycler	Biometra
Sonicator HTU SONI 130	Heinemann
Mini-PROTEAN Tetra System	Biorad
Nanodrop	Nanodrop technologies
LightCycler 2.0	Roche
ABI Prism 7900 HT	Applied Biosystems
Gel documentation system	Intas
ELISA Easy Reader	SLT Labinstruments Austria
Luminometer	
PyroMark Q24 Vacuum Workstation	Qiagen
PyroMark Q24 pyrosequencer	Biotage
Curix 60 (developing machine)	Agfa

2.1.10. Software list

The UCSC (http://genome.ucsc.edu/) and ensembl (http://www.ensembl.org/index.html) genome browsers with their applications and the protein database uniprotKb (http://www.uniprot.org/help/uniprotkb) were frequently used as references and for various analyses in this project. The Oncomine database (https://www.oncomine.org) was used to analyze gene expression in the available microarray studies. Tissue microarray datasets were downloaded from the NCBI GEO database (http://www.ncbi.nlm.nih.gov/gds). RegRNA (http://regrna.mbc.nctu.edu.tw/) and IRESite (http://iresite.org/) search tools were used to find regulatory RNA elements. PyroMark Assay Design software 2.0 (Qiagen) and the PrimerBLAST online tool (http://www.ncbi.nlm.nih.gov/tools/primer-blast/) were used for the design of primers for PCR, qRT-PCR and pyrosequencing as indicated. Real time RT-PCR data was analyzed with SDS 2.3 software (Applied Biosystems). The pyrosequencing data was analyzed with PyroMark Q24 software. IBM SPSS statistics version 20 and Excel 2010 were used for statistical analyses. Cytoscape software was used to visualize the interactions between imprinted gene products and other proteins. The network of 16 imprinted genes in the context of their biological intaractions (Fig. 4.2.3.8) was created by the CBio Cancer Genomics Portal (http://www.cbioportal.org/public-portal/index.do) using the MSKCC Prostate adenocarcinoma microarray expression set [13].

2.2. Methods

2.2.1. Growth and culture of prostate cell lines

The prostate carcinoma cell lines LNCaP, 22Rv1, PC-3 and DU145 were cultured in RPMI-1640 (Gibco), supplemented with 10% fetal calf serum (FCS) (Biowest), 100 µg/mL penicillin/streptomycin. The MDAPCa 2b cell line was cultured on collagen-coated dishes in BRFF-HPC1 (AthenaES), supplemented with 20% FCS, 2 mM L-glutamine, 100 mg/ml penicillin/streptomycin, 25 ng/ml cholera toxin, 10 ng/ml epidermal growth factor (Gibco), 0.005 nM phosphoethanolamine, 10 pg/ml hydrocortisone (Sigma), and Insulin-Transferrin-Selenium (Gibco). Normal prostate epithelial cells (PrEC) purchased from Lonza were cultured as recommended by the supplier.

2.2.2. DNA isolation from mammalian cells

High molecular weight genomic DNA was isolated using the Blood and Cell Culture Midi Kit (Qiagen). Concentration and purity were measured with a Nanodrop instrument using absorption at 260 nm or 260/280 nm and 230/260 nm ratios, respectively.

2.2.3. Bisulfite conversion

Genomic DNA (1 µg) was treated with sodium bisulfite to convert unmethylated cytosines to uracils, leaving methylated cytosines unchanged, with the EZ DNA Methylation Gold Kit (Zymo Research) according to the manufacturer´s instructions. The final elution volume was 20-25 µl.

2.2.4. Bisulfite sequencing

Bisulfite converted DNA was used to amplify the gene regions of interest (*TFPI2* promoter and 7q21 DMR) by PCR. The used primers (see Table 2.1.7.2) do not cover CpG residues in order to avoid amplification bias for methylated or unmethylated DNA. Each 50 µl PCR reaction contained: 1x HotStarTaq buffer (including 1.5 mM $MgCl_2$); 0.2 mM of each dNTP; 10 pmol of each primer, 1 U HotStarTaq DNA Poylmerase, and 2 µl bisulfite-converted DNA. Thermocycling conditions included: an initial denaturation step at 95°C for 15 min, followed by 40 cycles of each denaturation at 95°C for 30 sec, annealing at the specific for each primer set temperature (see Table 2.1.7.2) for 30 sec, and 45 sec extension at 72°C, followed by a final extension step at 72°C for 10 min. After confirmation of product sizes on a 2 % agarose gel, PCR products were cloned into the pCR4-TOPO vector using the TOPO TA Cloning Kit for Sequencing (Invitrogen) and transformed into competent *E. coli* cells (One Shot TOP10 Competent Cells, Invitrogen) according to the manufacturer's protocol. After selection on LB ampicillin plates single bacterial clones were picked and cultured overnight at 37°C in LB medium containing ampicillin. Plasmid DNA was isolated using the 5 Prime plasmid DNA isolation kit (5 Prime) and the correct

size of the inserted fragment was controlled by *EcoRI* digestion. Four to eight plasmid clones per gene and sample were then Sanger sequenced at the central sequencing facility (BMFZ) of the Heinrich Heine University.

2.2.5. Pyrosequencing

Semi-quantitative measurement of the level of methylation at specific CpG sites in the *PLAGL1* DMR, the 7q21 DMR, the *MEG3* DMR, the *KvDMR* and the *CDKN1C* promoter (for chromosomal location and sequence details see Appendix 2 and Table 2.1.7.4) was performed by pyrosequencing on a Biotage PyroMark Q24 instrument using PyroMark Gold Q24 reagents (Qiagen). The data was analyzed with PyroMark Q24 version 2.0 software.

To generate the products to be sequenced, bisulfite-converted DNA was amplified by PCR as follows. Each 50 µl PCR reaction contained 1x Coralload Concentrate (including 1.5 mM $MgCl_2$), 10 µmol dNTPs, 20 pmol of each amplification primer (one of which was biotinylated)(for primer sequences see Table 2.1.7.4), 4 U HotStarTaq DNA Poylmerase, and 2.5 µl bisulfite-converted DNA. Thermocycling conditions included: initial denaturation at 95°C for 15 min, 45 cycles of: denaturation at 95°C for 30 sec, annealing at specific for each primer set temperature for 30 sec, extension at 72°C for 30 sec; and a final extension at 72°C for 10 min. After confirmation of product size on a 2%-agarose gel, PCR products were prepared for pyrosequencing.

The biotinylated PCR product (20-30 µl) was bound to 2 µl streptavidin sepharose beads (Amersham Biosciences) in 40 µl binding buffer by rigorous agitation on a shaking (96-well) platform for 15 min. The DNA-bound beads were then aspirated, washed in 70% ethanol, denatured in 0.2 M NaOH and neutralized in washing buffer (Qiagen) on the PyroMark Q24 Vacuum Workstation. Finally, the DNA-bound beads were released in the wells of a 24-well pyrosequencing plate (Qiagen), which contained 0.33 mM sequencing primer (Table 2.1.7.4) in 25 µl annealing buffer (Qiagen). The mix was denatured at 80°C for 2 min and allowed to cool down for 15 min. In the meanwhile, the reagent cartridge was loaded with substrate, enzyme and dNTPs (Qiagen) according to the pre-run information suggested by the software. The plate was loaded into the pyrosequencer and the reaction was performed. The data was analyzed and the average methylation across the assessed CpG sites for each region was used for quantitation. For *MEG3* CpG2 the single CpG methylation values were additionally considered specifically.

2.2.6. Chromatin Immunoprecipitation (ChIP) and qPCR analysis of immunoprecipitated DNA

To study histone modifications enriched at the *TFPI2* promoter and the 7q21 DMR, ChIP was performed using the ChIP-IT Express Kit (Active Motif) according to the manufacturer's protocol. In brief, intact cells were treated with 1% formaldehyde to fix protein/DNA interactions. The cells were lysed to free the nuclei, which were sheared by sonication to obtain DNA/protein fragments corresponding to DNA with sizes in the range 200 - 1500 bp. In order to determine the concentration of DNA in the chromatin, it was isolated from 10 µl chromatin with the QIAquick PCR Purification Kit (Qiagen) and the concentration was determined on a Nanodrop instrument. The fragmentation was controlled on a 1% agarose gel. Estimated quantity of 7 µg of sheared chromatin per reaction was immunoprecipitated overnight with protein-G coated magnetic beads, anti-sera against H3K4me3 (Abcam #ab8580), H3K9ac (Abcam #ab4441), H3K9me3 (Abcam #ab8898), H3K27me3 (Active Motif #39535) or positive (RNA Pol II antibody) or negative (IgG antibody) control antibodies (CHIP-IT Control Kit, Active Motif), in the presence of proteinase inhibitor cocktail (Sigma). After washing out unbound proteins from the beads, the bound chromatin was eluted, cross-links were reversed, and DNA was recovered after treatment with proteinase K (ChIP-IT Express Kit, Active Motif). Before DNA was used for PCR analysis, it was treated with a proteinase K inhibitor. Parallel to the ChIP reactions, a DNA sample (called 'input DNA') of the non-precipitated sheared chromatin was purified and used for the standard curve in the qPCR analysis.

Quantitation of the eluted DNA was performed by qPCR using SYBR Green PCR mix (Qiagen) and amplification primers for the *TFPI2* promoter and 7q21 DMR DNA, and as references for open and closed chromatin, respectively the housekeeping *GAPDH* gene and the testis-specific *CTCFL* gene (Table 2.1.7.3). Input DNA was used for the standard curve. The qPCR was performed with the following conditions: denaturation at 95°C for 15 minutes, followed by 45 cycles of PCR (94°C for 15 s, 60°C for 30 s, and 72°C for 30 s), followed by a dissociation step (95°C for 15 sec, 60°C for 15 seconds, 95°C for 15 seconds). The relative quantities of the measured active histone modifications (H3K4me3 and H3K9ac) at the *TFPI2* and DMR genomic regions were normalized versus the enrichment of these modifications at the *GAPDH* promoter. Analogously, repressive histone modifications (H3K9me3 and H3K27me3) enrichment on the regions of interest was normalized to the respective enrichment at the *CTCFL* gene.

2.2.7. RNA isolation and cDNA synthesis

Total RNA of all samples from the experiments, with exception of the tissue set, was isolated using the RNeasy Mini Kit (Qiagen). Synthesis of cDNA was performed using the

QuantiTect Reverse Transcription Kit (Qiagen), according to the manufacturer's protocol including an extra DNA removal step by DNase as recommended by the supplier. Synthesis of complementary DNA (cDNA) for the tissue set was performed according to the manufacturer's protocol using the SuperScript II Reverse Transcriptase (Invitrogen) using mixture of random hexamer primers and oligo$(dT)_{18}$ primers (Fermentas).

2.2.8. Real time quantitative RT-PCR (qRT-PCR)

Each 25 µl qRT-PCR reaction contained 2 µl cDNA sample (1:10 diluted), 1x QuantiTect SybrGreen PCR Kit (Qiagen) and 10 pmol oligonucleotide primers (Table 2.1.7.1). Each sample was measured as a duplicate. Real time RT-PCR was performed on an ABI 7900 HT PCR System (Applied Biosystems). Primers designed using the online tool Primer-BLAST or the PyroMark Assay Design Software 2.0. (Qiagen), were ordered from MWG Operon. QuantiTect primer assays were purchased from Qiagen. The PCR conditions were as follows: polymerase activation step at 95°C for 15 min, followed by 35 amplification cycles consisting of denaturation at 94°C for 15 s, annealing at the specific for each primer set temperature for 30 s, and extension at 72°C for 30 s, upon which a gradient melting of the products was performed at 0.2 °C/sec from 50°C to 95°C (melting curve analysis). Experimental variation for the quantity of PCR product in each sample was below 10%. Relative expression was calculated by the standard curve method using a cDNA dilution series of a cell line or normal tissue, which strongly expressed the gene of interest. The mRNA expression was normalized to that of the housekeeping *TBP* gene, which was measured in the same sample. Therefore the mRNA (cDNA) quantity of the measured genes was presented as relative to that of *TBP*.

2.2.9. Immunoblot analysis (Western blot)

Whole cell protein lysates were prepared by lysing the cells with RIPA-type buffer (Table 2.1.5) and centrifuging at 15,000 g for 10 min to pellet the cell debris. The supernatant was collected and the protein concentration was determined with the Pierce BCA Protein assay (Thermo) according to the manufacturer's instructions.

The protein lysates (5-15 µg) were mixed with Laemmli Sample buffer (Biorad) and after denaturing at 95°C for 3 min were loaded on Any kD Mini-PROTEAN TGX precast gels (Biorad). Electrophoresis was performed in Mini-PROTEAN Tetra Cell chambers (Biorad) at 120 V and the separated proteins were subsequently transferred to Immobilon-P polyvinylidene fluoride membrane (Millipore) by blotting in transfer buffer (Table 2.1.5) at 180 mA for 90 min. Membranes were blocked in blocking solution (Table 2.1.5) for 1 h and then incubated overnight at 4°C with the primary antibody against the protein of interest. Generally, after every incubation with antibodies, the membranes were washed 4x10 min with washing buffer (Table 2.1.5). Incubation with the respective HRP-conjugated

secondary antibodies was performed for 1 h at room temperature. The ECL Advance Western blotting detection kit (GE Healthcare) was used to visualize the activity of the HRP enzyme. Chemiluminescence was detected by exposure of the blots to photosensitive films (Amersham Bioscience) and their development in the dark. To control for loading of equal protein amounts, the abundant and 'housekeeping' proteins α-tubulin or GAPDH were detected on the same blots.

2.2.10. Standard end point PCR

Amplification of DNA or cDNA was performed using the enzyme and reagents from the HotStarTaq DNA polymerase Kit (Qiagen). The reactions were carried out in 50 µl volume and contained 1x PCR buffer, 5-10 pmol of each oligonucleotide primer, 2.5-10 nmol dNTPs, 1 U Taq polymerase, water and 2 µl DNA (1:10 or 1:20 cDNA or 50 ng genomic DNA). The PCR reactions were performed on a Biometra thermocyler with the following PCR program: DNA denaturation and enzyme activation at 95°C for 15 min, followed by 35-45 cycles of: denaturation 94°C 30 sec, annealing at temperature dependent on the primers used for 30 sec, and extension at 72°C for 30 sec; and in the end a final extension at 72°C for 10 min. PCR products were visualized on agarose gels using 6x DNA Loading dye (Thermo) and GeneRuler DNA Ladder mix (Thermo).

The specific conditions of PCR reactions used in bisulfite sequencing and pyrosequencing reactions are additionally described in the corresponding sections.

2.2.11. Transformation, bacterial culture and plasmid DNA isolation

Transformation of competent *E.coli* One Shot TOP10 or ultracompetent XL-2 blue cells was performed according to producer's instructions. The transformed bacteria were spread on agar plates, containing Difco agar and 100 µg/mL ampicillin or kanamycin, and cultured overnight in an 37°C incubator. Overnight mini cultures were prepared from single clones. Bacteria were cultured in LB medium containing 50 µg/mL ampicillin or kanamycin, depending on the contained plasmids. Maxi cultures were prepared from fresh mini cultures, and were used for Maxi prep isolation of plasmids after bacterial growth for 12 h. Bacterial stocks were prepared by freezing at – 70°C 1 mL fresh bacterial Maxi culture in 20% glycerol. The rest of the Maxi culture was used for plasmid isolation. Growing of bacteria from a glycerol stock involved spreading a small quantity of frozen bacteria glycerol stock on a selection agar plate and its incubation at 37°C overnight.

Plasmid DNA from mini cultures was isolated with the Fast plasmid mini kit (5 Prime), while for maxi cultures the QIA Filter Plasmid Maxi Kit (Qiagen) was used. The correct insertion of the desired DNA in the plasmids was controlled by target-specific restriction digestion and sequencing of the plasmids.

2.2.12. Restriction digestion and purification of DNA fragments from agarose gels

Restriction digests were performed with restriction enzymes and their corresponding optimal reaction buffers and additives, purchased from Fermentas and New England Biolabs. Reactions were typically performed in a volume of 50 µL, using at least 1 U of each enzyme per µg plasmid DNA. The temperature and duration of incubation, as well as the conditions of its inactivation were reaction-specific. The digested fragments were visualized by agarose gel electrophoresis, and when necessary purified using the NucleoSpin Extract II gel extraction kit (Macherey-Nagel) according to manufacturer's instructions.

2.2.13. Agarose gel electrophoresis

Electrophoresis of PCR products or digested and undigested plasmids was performed in 0.7 – 2 % (in 1x TAE buffer) agarose gels, depending on the expected fragment sizes. Electrophoresis was performed at 120 V in 1x TAE buffer. Upon fragment separation, the gels were stained in an ethidium bromide-containing water bath and photographed with a gel documentation system.

2.2.14. Ligations

In bisulfite sequencing experiments, PCR products were ligated in the pCR4-TO vector, using the vector and reagents from the TOPO TA Cloning Kit for Sequencing (Invitrogen) according to the manufacturer's protocol.

For cloning experiments, DNA fragments (insert) and vectors were ligated using the T4 DNA ligase enzyme in general at 1:3 (vector:insert) molar ratios. The reactions were performed in the corresponding buffer overnight at 16 °C.

In both cases only freshly ligated vectors were used for transformation of bacteria.

2.2.15. Cloning of ZAC1 expression plasmids

2.2.15.1. T-REx™ System for tetracycline regulated gene overexpression

The T-Rex System (Invitrogen) is comprised of the commercially available plasmid vectors pcDNA4/TO, pcDNA4/TO/lacZ, and pcDNA6/TR (see Table 2.1.8) for the tetracycline-regulated expression of transfected genes. The backbone vector pcDNA4/TO contains two tetracycline operator sites (2x $TetO_2$) upstream of the MCS (Fig. 2.2.15.1) in which the gene of interest can be cloned. The control (and reporter) pcDNA4/TO/lacZ vector contains the lacZ gene coding for β-galactosidase. The pcDNA6/TR vector (containing a blasticidin resistance gene for selection in mammalian cells) codes for the Tet-repressor (TR) protein. Its function is to block the expression of the gene, cloned in the pcDNA4/TO vector, in the absence of tetracycline. Addition of tetracycline relieves this repression and the cloned gene of interest is transcribed (inducible expression). The LNCaP6TR cell line

which expresses stably the tet-repressor has been created in our lab and was available to use. The pcDNA4/TO vector contains the strong CMV minimal promoter and a resistance gene to zeocin for selection of mammalian cells. This also enables the use of this vector for gene overexpression in cells that do not stably express the TR protein, as has been done in this study in either transient or stable fashion (see below).

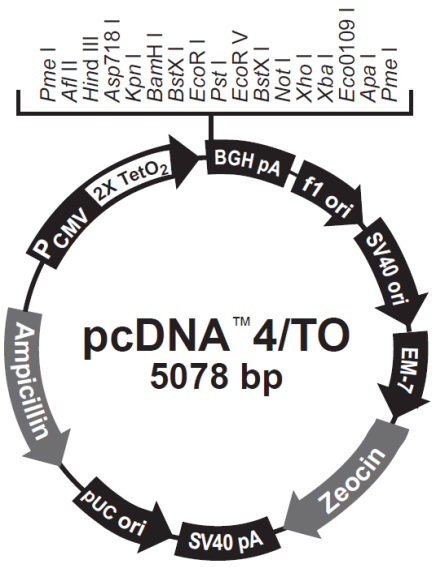

Fig. 2.2.15.1. Scheme of the pcDNA4/TO vector. Expression of the vector is driven by the human cytomegalovirus (CMV) immediate early promoter allows for high level expression of the cloned gene of interest. Two tandem tetracycline operator sequences ($TetO_2$), which serve as binding sites for Tet repressor (TR) homodimers, allow the induction of gene expression upon tetracycline treatment. The multiple cloning site (MCS) allows insertion of the gene of interest. The zeocin resistance gene allows selection in mammalian cells, while the ampicillin resistance gene- for selection in bacteria.

2.2.15.2. Cloning of pcDNA4/TO.ZAC1.VA (ZAC.VA)

The pBS.hZAC1 plasmid obtained from Dr. A. Varrault, Montpellier, contains the full protein-coding cDNA sequence of human ZAC1 together with a ~800 bp-long 5'-UTR and ~140 bp of the 3'-UTR, corresponding to transcript variant PLAGL1-001 (ENST00000367571) from the Ensembl database (Appendix 4 Fig.1). ZAC1 cDNA was excised with *HindIII* and *NotI* and was inserted into the pcDNA4/TO vector digested with the same enzymes to obtain the pcDNA4/TO.ZAC1.VA vector. An excerpt of the ZAC.VA sequence containing the insert and the used cloning sites is shown in Appendix 4 Fig. 2.

2.2.15.3. Cloning of pcDNA4/TO.ZAC1.DS (ZAC.DS)

Another plasmid containing human ZAC1 cDNA, pBSK.hZAC1, was obtained from Dr. D. Spengler, Munich. The insert contains ZAC1 cDNA without the UTRs and with a mutated original first ATG codon. As a consequence, the first functional start codon is located at

position -24 resulting in the obliteration of the first 8 amino acids of the original ZAC1 protein. The ZAC1 insert was excised using *BamHI* and *EcoRV* and inserted into the pcDNA4/TO vector digested with the same enzymes. The resulting vector was named pcDNA4/TO.ZAC.DS. An excerpt of the ZAC.DS sequence containing the insert and the used cloning sites is shown in Appendix 4 Fig. 3.

2.2.15.4. Cloning of pcDNA4/TO.ZACdelta (ZACdelta)

The 5'-UTR and a large part of the first coding exon of ZAC1 gene were excised from the pcDNA4/TO.ZAC.VA plasmid using the restriction nucleases *HindIII* and *BsgI*. Following digestion and loading on an agarose gel, the excised part of the ZAC1 sequence appeared as a short band. The DNA from the larger band (vector + remainder of the ZAC1 sequence) was purified from the gel, blunted by Klenow enzyme and religated, resulting in the pcDNA4/TO.ZACdelta plasmid. An excerpt of the ZACdelta sequence containing the insert and the used cloning sites is shown in Appendix 4 Fig. 4.

2.2.16. Treatment with inhibitors of DNA methylation and histone deacetylation

Cells were treated with 2 μM of the DNMT1 inhibitor 5-aza-2'-deoxycytidine (Sigma) (here named 5-Aza) with daily medium changes for 72 h. The histone deacetylase inhibitor suberoylanilide hydroxamic acid (Saha) (Cayman Chem. Company) was added to cells at 5 μM only for the last 24 h of culture.

2.2.17. Treatment with proteasome inhibitor

The proteasome inhibitor MG-132 (Enzo) was added to culture medium at a concentration of 1 μM for 24 h.

2.2.18. Androgen stimulation and ablation

22Rv1 cells were treated for 24 h with or without 10 nM of the synthetic androgen R1881 (Sigma) in RPMI-1640 with 10% charcoal-stripped (steroid-free) fetal bovine serum (cFBS) (Biowest). MDAPCa2b cells were treated for 24 h with or without 10 μM of the AR antagonist bicalutamide (BIC) (Casodex) (Sigma) in RPMI-1640 with 10 % charcoal-stripped cFBS.

2.2.19. Transient, stable and inducible transfections of ZAC1 expression plasmids

LNCaP, 22Rv1 and PC3 cells at 60-70% confluence were transfected in 6-well plates with 1 μg plasmid using the X-tremeGENE 9 DNA transfection reagent (Roche) at a ratio 3:1 (reagent:DNA) according to the manufaturer's instructions. Untransfected cells and cells transfected with the control lacZ plasmid were always included as controls. For transient transfection, the cells were harvested after 24-72 h. To create stably transfected clones, after reaching confluence (2-4 days) the transfected cells were re-seeded at 1:2-1:3 ratio

in 10 cm culture plates and cultured in the presence of the selection antibiotic zeocin (600 µg/ml for LNCaP, 800 µg/ml for 22Rv1 and 120 µg/ml for PC3) for 2-5 weeks until the surviving colonies became well discernible with the naked eye.
For isolation of single clones, the plates were treated with trypsin and small filter pieces were carefully placed on each colony. Then, the filter pieces, to which the single colonies stick, were picked and transferred one each to a new well of a 24-well plate with selection medium. By and by the selected survival clones were expanded into bigger plates until enough cells were present for further studies. Positivity of each clone for expression of the transfected gene was tested by real time RT-PCR analysis with primers for ZAC1. Most of the isolated clones were positive for ZAC1. Several stable clones for the lacZ gene were also created.
Additionally, polyclonal populations were obtained by pooling and lysing all surviving clones from one plate for further RNA or protein preparation.

To create clones with tetracycline-inducible expression, the ZAC1-plasmids were stably transfected into LNCaP6TR cells, which express stably the Tet-repressor protein. In addition to zeocin (600 µg/ml), the selection media included blasticidin (5 µg/ml) for ensuring pcDNA6/TR plasmid retention as well. Single stable clones were created and their positivity for ZAC1 was tested in a tetracycline induction experiment. For the purpose, cells from each clone were seeded in 6-well plates and treated with or without tetracycline (1 µg/ml) for 24 h, after which RNA and proteins were isolated. Inducibility of ZAC1 in 'positive' clones was confirmed by qRT-PCR.

2.2.20. Clonogenicity assay

22Rv1 cells at 60% confluence were transfected in 6-well plates with 1 µg/well ZAC.VA, ZAC.DS or ZACdelta plasmids. Upon reaching of ~100% confluence, the cells were split into two 10 cm plates and selection with zeocin was commenced. For 22Rv1 cells a zeocin concentration of 800 µg/ml was determined as optimal for selection of transfected cells. Cells were grown with regular change of medium for 3-4 weeks until visible colonies formed. Then the plates were fixed with methanol and stained with Giemsa. Pictures from the plates were taken with a non-professional digital camera and the light reflection was removed using the photocopy artistic effect feature of Microsoft PowerPoint.

2.2.21. Transfection of siRNA

Transfection of cells with 25 pmol siRNA against ZAC1 (Santa Cruz Biotechnology, #sc-38183) or an irrelevant target (IR) siRNA (Control siRNA-A Santa Cruz Biotechnology, #sc-37007) was performed in 6-well plates using 5 µl/well Lipofectamine RNAiMAX transfection reagent (Invitrogen) according to the manufacturer's protocol. The reactions

were performed in triplicates and mean values with standard deviation values were calclulated for each condition.

2.2.22. Luciferase reporter assays

Reporter assays were performed using luciferase reporter vectors and the Luciferase Reporter Assay System from Promega according to the manufacturer's protocol. In general, 22Rv1 and PC3 cells were transiently co-transfected with reporter plasmids and ZAC1-expression plasmids. At the end of the desired incubation period (48-72 h), protein lysates were prepared and used for detection of luciferase activity. Autoluminescence of the measuring tubes was registered and in the end subtracted from the sample measurements. Each sample was measured twice and the average for the relative light units (RLU) in each measurement was used for data analysis. As transfections were performed in triplicates, mean values and standard deviation values were calculated for each condition.

2.2.22.1. Androgen response

Luciferase reporter plasmids driven by a probasin promoter (here called pPb-Luc, originally 'pGL3Eprob') or an androgen response element (ARE)-containing promoter (here called pARE-Luc, originally pGL3-ARE-Luc) were used to measure the androgen receptor AR-mediated response of prostate cancer cells upon stimulation with the synthetic ligand R1881 (Sigma).

The hormone-resistant PC3 cells are reported to express low levels of endogenous AR which does not activate androgen-responsive reporters upon androgen stimulation. Having practically no basal AR activity, this cell line is considered to be a good model for studying the androgen-response upon transfection with exogenous AR.

In order to estimate the influence of ZAC1 on the androgen response, PC3 cells (which endogenously express high ZAC1 protein levels) were co-transfected with 200 ng of either pPb-Luc or pARE-Luc reporter plasmid and the same amount of the AR expression plasmid pSG5-AR. Control transfections without the AR plasmid were replenished with lacZ plasmid in order to reach equal amounts of DNA transfected in each condition. All transfection conditions were performed in triplicates. R1881 was added to the cells at a concentration of 10 nM 24 h after plasmid transfection, when transfection with an siRNA against ZAC1, or control siRNA was performed. Protein lysates were prepared from the cells after another 24 h (in total 48 h) and used to measure the luciferase activity.

2.2.22.2. CDKN1A promoter activity

The *CDKN1A* gene, containing in its promoter two p53-binding sites is a prototypic target gene of p53, which ZAC1 can coactivate. In order to explore the transcriptional activity of

transfected ZAC1 on *CDKN1A* as a target gene, the *CDKN1A* promoter-driven reporter plasmid p21-Luc (originally WWP-Luc, Addgene plasmid 16451) containing one of the p53-binding sites was used. 22Rv1 cells (with relatively low to moderate endogenous ZAC1 expression) were co-transfected with 200 ng of the p21-Luc plasmid and 500 ng of each of the three ZAC1 expression plasmids. A control transfection without a ZAC1 plasmid was replenished with lacZ plasmid in order to reach equal amounts of DNA transfected in each condition. Cells were lysed 48 h upon transfection and the lysates were used to detect reporter activity.

2.2.23. Statistical methods

All statistical analyses were conducted with IBM SPSS 20 software.

2.2.23.1. Non-parametric tests

The Mann-Whitney-U test, also called Wilcoxon rank-sum test, was used to evaluate whether gene expression of the samples from the prostatic tissue set was different within the following groups: benign vs. tumor, pT2 vs. pT3+pT4 T-stage, GS <7 vs. 7 and 7 vs. >7 Gleason sum, N0 vs. N1 local lymph node metastasis, no vs. yes biochemical recurrence, and low vs. high expression of each *EZH2*, *ERG* and *HOXC6* genes. For a more detailed description of the clinical parameters see Section 2.2.1. The stratification into low and high oncogene expression groups was according to the following expression cut-off values: for *EZH2* gene: the maximum expression of benign tissues, for *ERG*: the median expression of the tumor tissues, and for *HOXC6*: the first quartile of the expression of tumor tissues. Boxplot diagrams of *EZH2*, *HOXC6* and *ERG* expression groups are shown in Fig. 2.2.23.1. The sizes of the sample groups are shown in Table 2.2.23.1.

Variable	Groups	n (total 45)
Gleason score	<7	13
	7	26
	>7	6
Tumor stage		
	T2	20
	T3 + T4	25
Lymph node metastasis		
	yes	11
	no	34
Biochemical recurrence		
	yes	18
	no	27
EZH2 expression		
	low	16
	high	29
HOXC6 expression		
	low	12
	high	33
ERG expression		
	low	23
	high	22

Table 2.2.23.1. Size of sample group pairs according to clinical parameters and oncogene expression. 45 prostatic cancer tissues for which patient follow-up information was available were grouped in pairs according to the indicated parameters for the purpose of statistical tests.

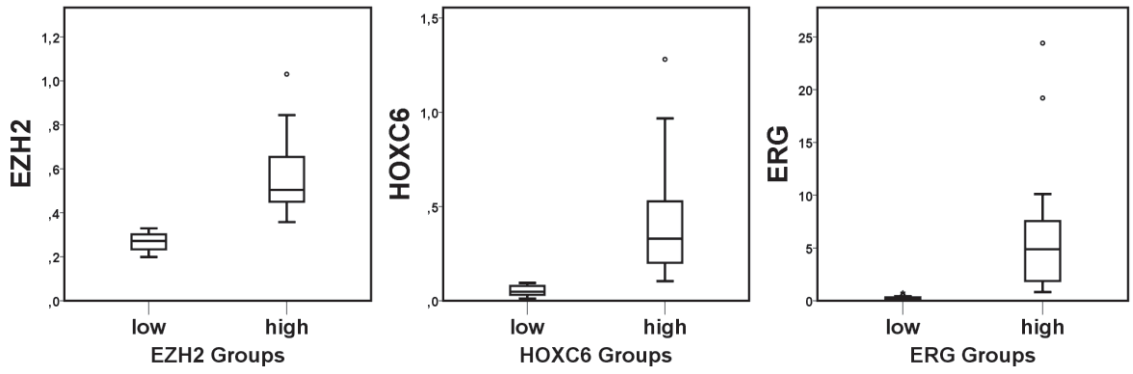

Fig. 2.2.23.1. Boxplot diagram of oncogene expression groups. 45 prostatic cancer tissues for which patient follow-up information was available were grouped in pairs (low vs. high) according to *EZH2*, *HOXC6* and *ERG* gene expression for the purpose of statistical tests.

2.2.23.2. Correlation analysis

The Spearman´s rank correlation coefficient (ρ) measures the statistical dependence between two variables. It was used to estimate the dependence among the analyzed imprinted genes (as based on mRNA expression relative to *TBP*) and between them and the *EZH2*, *HOXC6* and *ERG* oncogenes. Furthermore, the Spearman

correlation was applied to study the relation of expression of the assessed genes and the methylation levels of *PLAGL1* DMR, 7q21 DMR, *MEG3* DMR, *KvDMR* and *CDKN1C* promoter in the prostatic tumor tissues.

2.2.23.3. Survival analysis

Kaplan-Meier analysis was performed to monitor how well a low or high expression of the analyzed imprinted genes (and as control also the oncogenes) in the prostatic cancer tissue set can predict the occurrence of biochemical recurrence after tissue removal by radical prostatectomy. Recurrence was defined as a PSA value of at least 0.2 ng/mL found in two consecutive measurements. Of the 45 tumor patients, 18 patients experienced biochemical recurrence, while 27 did not (censored). The time to biochemical recurrence [months] was used as time variable and the gene expression (below vs. above threshold) as grouping variable. Threshold values of gene expression that divided the samples in relative to each other lower and higher risk groups were determined by testing multiple levels with the logrank test. The optimal threshold values where significance was found corresponded to the following parameters: for *PLAGL1* and *MEG3* - mean value of tumors, for *PLAGL1delta*- median value of tumors, for *PPP1R9A*- the 3rd quartile of tumors, and for *H19* the minimum value of benign tissues. The maximum expression of *EZH2* in benign tissues (also used to divide tissues in groups of low vs. high *EZH2* expression in 2.2.23.1) was also used here in the Kaplan-Meier analysis as a threshold value.

Cox regression analysis was used to evaluate the impact of gene expression levels (as continuous variable) of imprinted genes in the prostatic cancer tissue set on the risk of biochemical recurrence of the prostate cancer patients.

3. Results

3.1. Epigenetic inactivation of the placentally imprinted tumor suppressor gene TFPI2 in prostate carcinoma.

The potential tumor suppressor *TFPI2* gene has been proposed to be silenced by DNA hypermethylation in several cancer types. The first goal in this project was to find out whether *TFPI2* and its homolog *TFPI* are epigenetically silenced in prostate cancer. For this purpose the expression of these genes was assessed in a set of prostate benign and cancer tissues and cell lines, upon which the epigenetic status of the *TFPI2* promoter and the proximal DMR were analyzed in detail in several exemplary cases.

3.1.1. Expression of TFPI, TFPI2, SGCE and PON2 genes in prostate cancer tissues and cell lines

TFPI and *TFPI2* mRNA levels were assessed by means of qRT-PCR in 47 prostate carcinoma tissue samples and 13 benign prostate tissues (Fig. 3.1.1.1). Full *TFPI* and *TFPI2* expression profiles are shown in Appendix 1. *TFPI* mRNA levels were found to be relatively more stable in both carcinoma and normal samples (see Appendix 1 A) than *TFPI2* mRNA expression, which was highly divergent in cancerous as well as in benign tissues (see Appendix 1 B). Mann-Whitney U statistical tests were performed to evaluate the differences in expression in carcinoma versus benign tissues. None of the two genes was significantly differentially expressed between the two tissue groups (Fig. 3.1.1.1). However, among the cancer tissues, there was a considerable and significant negative correlation ($\rho = -0.450$, $p < 0.01$) between *TFPI* and *TFPI2* expression.

A discernible trend toward higher expression of *TFPI2* in the tumor tissues in the boxplot representation (Fig. 3.1.1.1) is due to upregulation in individual tumor samples (see Appendix 1) In general, the high rate of expression variation may suggest a higher susceptibility of *TFPI2* to epigenetic or microenvironmental factors.

Such factors would then likely also affect other genes in the imprinted gene cluster at 7q21 to which *TFPI2* gene belongs. For that reason, the expression of two further genes, *SGCE* and *PON2,* was measured in the prostate tissue cohort. Spearman´s rank correlation coefficient was used to find statistical dependences between the expression of the analyzed imprinted genes among tumor tissues. The expression of *TFPI2* correlated significantly with that of *SGCE* ($\rho = 0.439$, $p < 0.01$) and *PON2* ($\rho = 0.312$, $p < 0.05$) genes (Fig. 3.1.1.2). Interestingly, while *SGCE* expression did not differ significantly between the normal samples and the carcinomas, *PON2* was highly significantly overexpressed in the cancer tissues ($p = 0.003$) (Fig. 3.1.1.1). Statistical tests of *PON2* expression correlation with clinical prostate cancer parameters are presented in Chap. 3.2 together with those of other imprinted genes subsequently analyzed.

TFPI2 and *SGCE* mRNA levels were also measured by qRT-PCR in several prostate cancer cell lines in order to chose two of them for detailed epigenetic analysis. PC3 and DU145 cells expressed *TFPI2* at higher levels than LNCaP, 22Rv1 and MDAPCa2b (Fig. 3.1.1.2 right panel). Therefore PC3 and LNCaP were selected for use in further experiments as examples of high and low *TFPI2* expression. The *SGCE* gene was expressed at a similar level in DU145, PC3 and 22Rv1, but was almost undetectable in LNCaP and MDaPCa2b (Fig. 3.1.1.2 left panel). Based on this observation, the expressions of the two genes did not seem to significantly correlate with each other in the assessed prostate cancer cell lines, unlike in prostate cancer tissues.

The high variability of *TFPI2* expression among the tissue samples hints at the presence of differential mechanisms that may cause its up- or down-regulation in individual tumors. In order to explore these mechanisms, the epigenetic status of the locus was investigated in more detail in selected prostate cancer cell lines and prostate carcinoma tissues with low and high *TFPI2* expression.

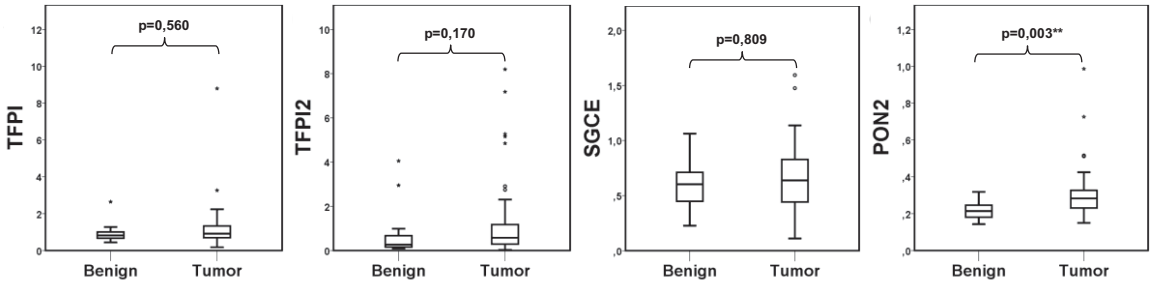

Fig. 3.1.1.1. Boxplot representation of TFPI, TFPI2, SGCE and PON2 expression in prostatic benign vs. tumor tissues. The mRNA levels of the indicated genes relative to *TBP* were measured by qRT-PCR in 47 prostate carcinoma and 13 benign prostate tissue samples. The expression differences between benign and tumor tissues groups were statistically evaluated with Mann-Whitney-U test (p-values are shown above the brackets in each panel, *p<0.05, **p>0.01).

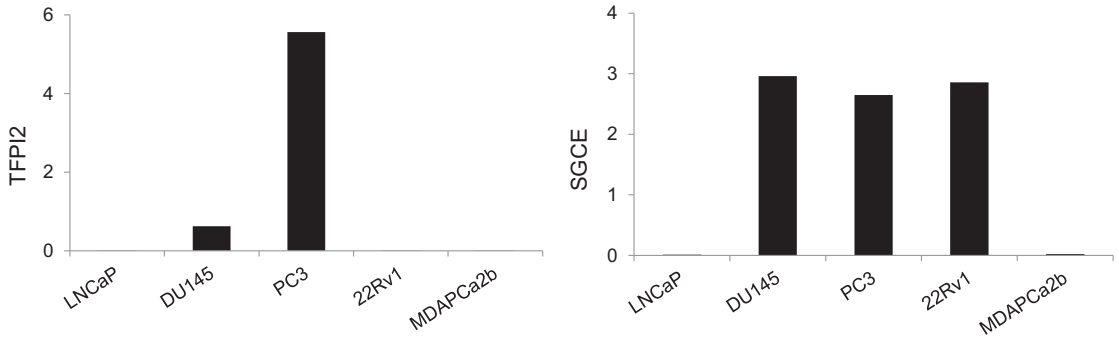

Fig. 3.1.1.2. TFPI2 and SGCE expression in prostate cancer cell lines. The mRNA levels of *TFPI2* (left panel) and *SGCE* (right panel), relative to *TBP* were measured by qRT-PCR in the indicated prostate cancer cell lines. The measurements were performed in duplicate and the average was used, whereby less than 10% variation between duplicates was accepted.

3.1.2. Analysis of CpG methylation of TFPI2 promoter and DMR in selected prostate cancer tissues and cell lines

Bisulfite sequencing of individual alleles was applied to study whether aberrations of DNA methylation at the *TFPI2* promoter or the near DMR (located on chromosome 7q21 between the *SGCE* and *PEG10* genes) may account for the changes in gene expression. Methylation patterns of these regions were investigated in cultured normal prostate epithelial cells, normal urothelial cells, each two high (pTu 89 and pTu 145) and low (pTu 209 and pTu 232) *TFPI2* expressing prostate carcinoma tissues, as well as the PC3 and LNCaP cell lines.

Normal tissues and highly *TFPI2*-expressing cells (PC3) and cancer tissues (pTu 89 and pTu 145) harbored an essentially unmethylated *TFPI2* promoter (Fig. 3.1.2). In contrast, the low *TFPI2*-expressing carcinoma samples (pTu 209 and pTu 232) and LNCaP cells exhibited increased CpG methylation on individual alleles. In pTu 209 the promoter methylation pattern resembled the typical pattern of the DMR, where half of the alleles are fully methylated, and the other half were fully unmethylated. In the DMR, this pattern was correctly preserved in all high- and low- expressing carcinoma and normal tissues, as well as in the PC3 cell line and normal cells from prostate and bladder urothelium. However, the DMR methylation pattern was severely disturbed in LNCaP cells, whose alleles exhibited DNA partial methylation clustering in the 5' end of the assessed region with no fully methylated alleles detected.

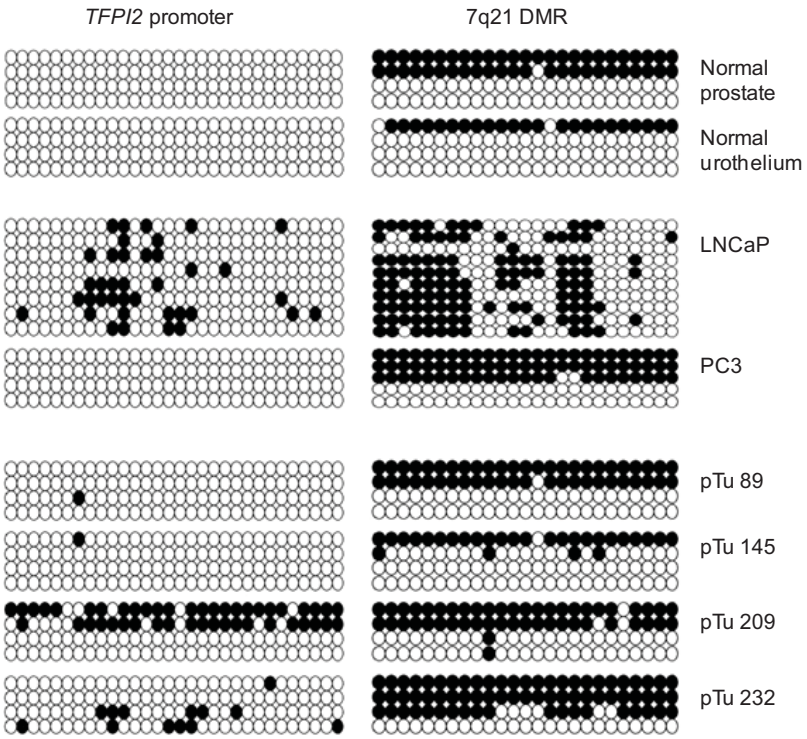

Fig. 3.1.2. Methylation status of TFPI2 promoter and chromosome 7q21 DMR. CpG methylation was assessed by sequencing of bisulfite-converted DNA from normal prostate epithelial cells, normal urothelial cells, the prostate cancer cell lines LNCaP and PC3, two highly *TFPI2*-expressing (pTu 89 and pTu 145) and two low *TFPI2*-expressing (pTu 209 and pTu 232) prostate carcinoma tissues. Each line corresponds to one cloned PCR product; white circles represent unmethylated and black circles methylated CpG sites.

3.1.3. Enrichment of histone modifications at the TFPI2 promoter and DMR in LNCaP and PC3 cells

The balance of histone tail modifications affects the structure of chromatin and its accessibility to the transcription machinery. H3K4me3 and H3K9ac modifications associate with open chromatin and respectively with active transcription, whereas predominance of H3K9me3 and H3K27me3 modifications is a sign of compact and transcriptionally inactive chromatin.

Chromatin immunoprecipitation (ChIP) was applied to test for the enrichment of these histone modifications around the *TFPI2* promoter and the 7q21 DMR in LNCaP and PC3 cells.

As expected, the promoter of *TFPI2* was more enriched with active histone marks in high *TFPI2*-expressing PC3 cells, while repressive histone modifications were more strongly represented in the low *TFPI2* expressing LNCaP cells (Fig. 3.1.3 left panel). In contrast,

the DMR was more enriched with active than with repressive histone modifications in both LNCaP and PC3 cell lines, suggesting accessible chromatin states (Fig. 3.1.3 right panel).

The stable DMR methylation in tissues with low and high *TFPI2* expression, as in normal bladder urothelial and prostate cells indicates that this region is not likely to be involved in the silencing of *TFPI2* in cancer tissues. Rather, the partial hypermethylation that was found at the *TFPI2* promoter in prostate cancer tissues may play a role for its reduced expression. Accordingly, in the LNCaP cell line, where the methylation of both the *TFPI2* promoter and the DMR were disturbed, repressive histone modifications were found to associate only with the *TFPI2* promoter but not with the DMR.

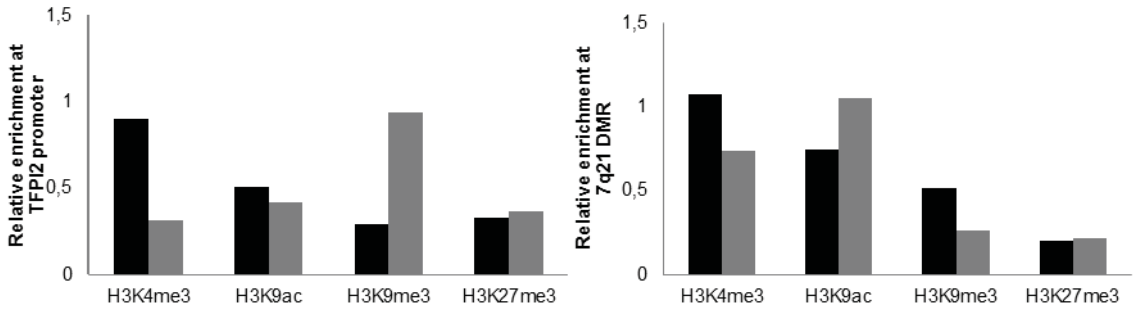

Fig. 3.1.3. Enrichment of selected histone modifications associated at TFPI2 promoter and 7q21 DMR. Chromatin immunoprecipitation analysis of H3K4me3, H3K9ac, H3K9me3 and H3K27me3 histone modifications at the *TFPI2* promoter (left panel) and the 7q21 DMR (right panel) in PC3 cells (black bars) and LNCaP cells (grey bars). Data represent qPCR results normalized as described in 2.2.6. The qPCR measurements were performed in duplicate and the average was used, whereby less than 10% variation between duplicates was accepted.

3.2. Expression of imprinted genes in prostate cancer

3.2.1. Selection of imprinted genes to be studied

The group of imprinted genes found by the *in silico* study (Table 1.6) to be differentially regulated in prostate benign vs. cancer tissues was used as the basis for further molecular studies. For this study, the group was extended by several additional imprinted genes or alternative transcripts on grounds of affiliation to the same locus or in order to test for likely regulatory associations.

In particular, several of the selected genes belong to imprinted gene clusters. Often the epigenetic status of the cluster (mostly of the Imprinting Control (IC) regulatory regions) determines the coordinate expression of maternally or paternally expressed genes. Therefore, by measuring the expression of additional neighboring genes to those selected via the *in silico* study, it becomes possible to draw conclusions of epigenetic determinants of their regulation. For example, several differentially expressed imprinted genes in the 7q21 imprinted gene cluster appeared in the list generated by the *in silico* study suggesting an involvement of the whole cluster, or an interdependency between the affected genes. In order to monitor such connections, the *PON2* and *TFPI2* genes from this cluster were additionally considered (see also 3.1).

The *CDKN1C* gene is situated on chromosome 11p15 where two imprinted gene clusters are found very close to each other, namely the *CDKN1C- LIT1-KCNQ1* cluster and the *IGF2-H19* cluster. The *IGF2* and *H19* imprinted genes are often reported to be epigenetically deregulated in cancer (see Chap.1.5). Therefore, those genes were also included among the analyzed imprinted genes, even though they were not significant in the *in silico* analysis.

The *LIT1* gene codes for a non-coding RNA, whose expression is thought to be determined by the methylation status of the DMR situated upstream of the gene. This non-coding RNA can influence the epigenetic status of the locus in which *CDKN1C* is situated. Therefore, *LIT1* expression was measured too.

The *PLAGL1* gene encodes an mRNA which is alternatively spliced. As shown below (Chap. 3.4 and 3.5), alternative splicing may affect the translational regulation of its RNA and produces protein isoforms with potentially different properties. As it is conceivable that the differential *PLAGL1/ZAC1* expression observed in the *in silico* study was specific for one of the isoforms, additional primers were designed that differentiate between *PLAGL1/ZAC1* and *ZAC1delta* (for transcript details see Chap.3.4.1 and Appendix 4).

The *SNRPN* gene is more precisely called *SNURF-SNRPN* gene, as it encodes two bicistronic transcripts- the *SNRPN* and the *SNURF* transcripts. Although only *SNRPN* was significantly differentially expressed in prostate cancer according to the *in silico* study, *SNURF* transcript mRNA levels were also analysed.

The *GNAS* gene is in fact a complex gene locus, which includes many different alternative promoters and transcription starting sites. In addition, the transcripts can also be alternatively spliced. Several primer pairs were designed to assess the expression of several of its major transcripts. However, only one of them was expressed in prostate tissues, and thus only primers for this transcript were chosen to assess *GNAS* expression quantitatively in further experiments.

For comparison, expression measurements for the prostate cancer oncogenes *EZH2*, *ERG* and *HOXC6* were included.

3.2.2. Expression of imprinted genes in benign and cancer prostate tissues

Based on the arguments above, the mRNA expression of the imprinted genes (transcripts) *PLAGL1/ZAC1*, *PLAGL1/ZAC1delta*, *TFPI2*, *SGCE*, *PEG10, PPP1R9A*, *PON2*, *INPP5F*, *INPP5Fv2*, *CDKN1C*, *LIT1*, *IGF2*, *H19*, *MEG3*, *NDN*, *SNRPN*, *SNURF*, *PEG3*, and *GNAS* was measured by real time RT-PCR in our prostate tissue series of benign and cancer samples (see 2.1.1). *HYMAI* expression was too low in the prostatic tissues to be quantitatively assessed. Boxplot representations of the aggregate results for benign vs. tumor sample groups are presented in Fig. 3.2.2.1. Values for individual samples depicted in Excel graphs can be found in Appendix 1. The differences in expression of imprinted genes and the prostatic oncogenes in the benign vs. tumor sample groups were tested by the non-parametric Mann-Whitney-U test using SPSS. A significance level of 0.05 was utilized as a threshold value (Table 3.2.2.1).

The expression of *PLAGL1*, *PLAGL1delta*, *CDKN1C*, *IGF2*, *H19*, *MEG3* and *NDN* was significantly ($p<0.01$) lower in carcinomas than in benign prostate tissues (Fig. 3.2.2.1 A, B, J, L, M, N, and O). The *PEG3* gene exhibited similarly strong downregulation in carcinomas, which was however only close to significance ($p=0.071$) (Fig. 3.2.2.1 R). A trend towards lower expression in the tumor was also observed for the genes *PEG10* ($p=0.149$) and *INPP5Fv2* ($p=0.121$) (Fig. 3.2.2.1 E and I). Significantly ($p<0.01$) higher expression in the carcinoma tissues than in the benign ones was observed for *PPP1R9A*, *PON2*, *LIT1* (Fig. 3.2.2.1 F, G, and K), and as expected for the oncogenes *EZH2*, *ERG* and *HOXC6* (Fig. 3.2.2.1 T, U, and V). Note that as expected *ERG* expression was increased in a large subgroup of the cases rather than throughout. The *TFPI2* gene

exhibited a trend towards higher expression in the tumors, although this was not significant (p=0.170) (Fig. 3.2.2.1 C).

Gene	Significance
PLAGL1	**0,000****
***PLAGL1* delta**	**0,000****
TFPI2	0,170
SGCE	0,809
PEG10	0,149
PPP1R9A	**0,000****
PON2	**0,003****
INPP5F	0,240
INPP5Fv2	0,121
CDKN1C	**0,000****
LIT1	**0,029***
IGF2	**0,000****
H19	**0,000****
MEG3	**0,000****
NDN	**0,000****
SNRPN	0,394
SNURF	0,513
PEG3	0,071
GNAS	0,490
ERG	**0,029***
EZH2	**0,000****
HOXC6	**0,000****

Table 3.2.2.1. Significance values for differential gene expression in benign vs. tumor sample groups. The distributions of the mRNA expression for the indicated genes relative to *TBP* in benign vs. tumor sample groups was analyzed by the non-parametric Mann-Whitney-U test using SPSS *p<0.05; **p<0.01.

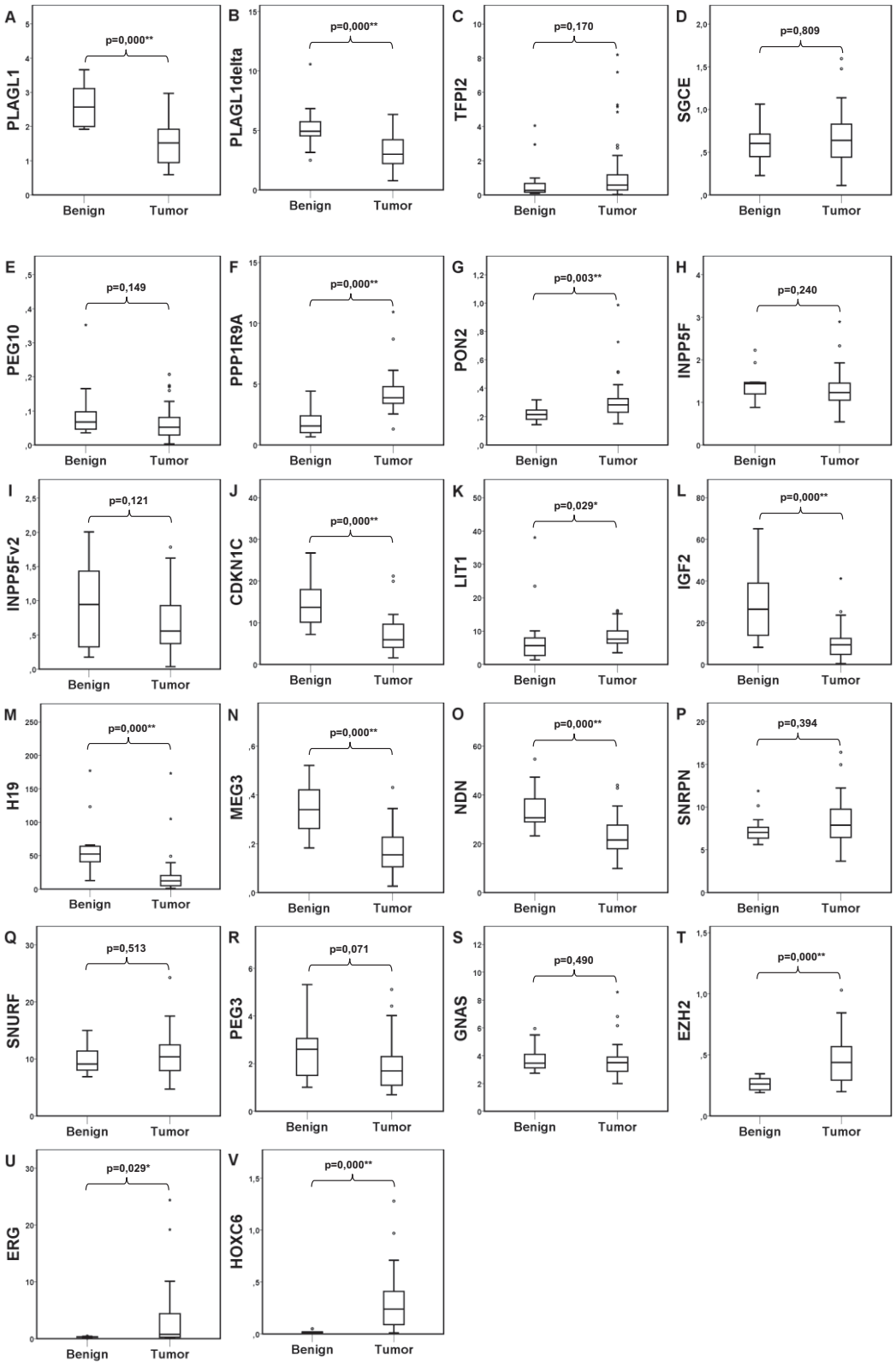

Fig. 3.2.2.1. Boxplot representations of the distribution of gene expression in benign vs. tumor tissue groups. Significance of the differences (p) was calculated with the Kruskal-Walis test and is shown above the brackets in each panel.

3.2.3. Correlations among imprinted genes

Spearman rank-order correlation was used measure the association between imprinted genes expression, as well as between each one and the oncogenes *ERG*, *EZH2* and *HOXC6*. Data for all genes is included in Table 3.2.3.

Among the genes belonging to the 7q21 cluster, there was a significant positive correlation between *SGCE* and *PEG10*, while *TFPI2* correlated only with *SGCE* and *PON2*. In contrast, the expression of *PPP1R9A* correlated negatively to *SGCE* and *PEG10*.

A significant positive correlation was also found between the clustered *H19* and *IGF2* genes, as well as between the *SNURF* and *SNRPN* transcripts, and the transcripts amplified by the *PLAGL1* and *PLAGL1delta* primers, that originate from the same loci.

Among all imprinted genes, significant positive correlations were observed between any two of the *PLAGL1*, *CDKN1C*, *MEG3*, *NDN*, *PEG3*, *INPP5Fv2*, *H19* and *IGF2* genes. This observation suggests their co-regulation in prostate cancer tissues. In contrast, the expression of the *PPP1R9A* gene was negatively correlated to that of most genes in this group.

Spearman rho	PLAGL1	PLAGL1 delta	SGCE	PEG10	PPP1R9A	PON2	INPP5F	INPP5Fv2	CDKN1C	LIT1	MEG3	NDN	PEG3	SNRPN	SNURF	GNAS	TFPI2	H19	IGF2	ERG	EZH2	HOXC6
PLAGL1	1,000																					
PLAGL1 delta	,638**	1,000																				
SGCE	,244	,214	1,000																			
PEG10	,367*	,258	,600**	1,000																		
PPP1R9A	-,377*	-,227	-,436**	-,575**	1,000																	
PON2	,116	-,222	,214	-,216	,226	1,000																
INPP5F	,324*	,285	,223	,148	,069	,174	1,000															
INPP5Fv2	,636**	,361*	,553**	,476**	-,383**	,192	,209	1,000														
CDKN1C	,551**	,457**	,566**	,651**	-,448**	-,130	,470**	,584**	1,000													
LIT1	,019	,112	,163	,025	,175	-,080	,096	,123	,362*	1,000												
MEG3	,544**	,614**	,288	,493**	-,311*	-,131	,335*	,520**	,589**	,307*	1,000											
NDN	,554**	,493**	,558**	,477**	-,416**	,090	,226	,648**	,618**	,290	,620**	1,000										
PEG3	,483**	,457**	,260	,358*	-,053	-,074	,517**	,471**	,623**	,429**	,564**	,572**	1,000									
SNRPN	-,050	-,330*	-,120	-,215	,336*	,339*	-,094	,103	-,161	,034	-,025	,086	,007	1,000								
SNURF	-,190	-,459**	,054	-,216	,272	,479**	-,075	,097	-,140	,111	-,155	,139	,034	,878**	1,000							
GNAS	-,045	-,028	-,026	-,206	,211	,205	,045	-,021	-,040	,202	,023	,266	,219	,414**	,562**	1,000						
TFPI2	,077	,167	,439**	,025	,091	,312*	-,018	,199	,037	-,029	,007	,175	-,183	,072	,080	-,179	1,000					
H19	,519**	,438**	,433**	,430**	-,424**	-,097	,251	,448**	,479**	,120	,407**	,669**	,326*	-,107	-,109	,071	,199	1,000				
IGF2	,506**	,532**	,362*	,471**	-,458**	-,182	,219	,512**	,552**	,074	,602**	,735**	,368*	-,008	-,107	-,016	,149	,700**	1,000			
ERG	-,303*	-,192	-,275	-,426**	,489**	,046	,277	-,217	-,250	,019	-,164	-,334*	,090	,138	,119	,091	-,071	-,362*	-,297*	1,000		
EZH2	-,314*	-,218	-,434**	-,518**	,638**	,068	-,059	-,507**	-,566**	-,022	-,466**	-,463**	-,348*	,121	,053	,139	-,063	-,305*	-,371*	,207	1,000	
HOXC6	-,658**	-,471**	-,389**	-,555**	,541**	-,025	-,385**	-,644**	-,587**	,013	-,599**	-,636**	-,476**	,062	,095	-,005	-,017	-,488**	-,548**	,218	,611**	1,000

Table 3.2.3. Spearman Correlation coefficient of the expression among imprinted genes and with oncogenes was calculated by SPSS using data for 45 prostate cancer tissues. **p<0.05, *p< 0.01

3.2.4. Correlation of imprinted gene expression with clinical prostate cancer progression markers

To find out how the levels of mRNA expression of the assessed imprinted genes relate to the clinical parameters of the respective patients, the samples were stratified in groups according to tumor stage (pT2 vs. pT3+pT4), presence of lymph node metastasis (yes vs. no, i.e. pN0 vs. pN1+pN2), Gleason score (GS, <7 vs. 7 and 7 vs. >7) and biochemical recurrence (yes vs. no) (for details see Chap. 2.2.23.1). The expression levels of *ERG*, *EZH2* and *HOXC6* genes, which often correlate with clinical parameters of prostate cancer progression, were included in the analysis for comparison.

Non-parametric Mann-Whitney-U test was used to evaluate the distributions of gene expression as a categorical variable between the tumor groups. The significance values are listed in Table 3.2.5.1. Boxplots of the significantly different distributions are presented in Fig. 3.2.5.1.

PLAGL1 expression correlated significantly with tumor stage, being lower in higher stage tumors (T3+T4 vs. T2). Among the oncogenes, *ERG* expression correlated marginally significantly with tumor stage. *PLAGL1* and *PLAGL1delta* mRNA expression levels were significantly lower in tumors with biochemical recurrence than in those without. Among the oncogenes, only *HOXC6* overexpression could significantly predict biochemical recurrence. The expression of *PEG10* was lower in cancers with local lymph node metastasis, in contrast to *EZH2* and *HOXC6* that were higher expressed in those cancers. The mRNA levels of *PON2* and *NDN* were significantly higher in tumors with GS <7 than tumors with GS =7. Interestingly, *ERG* overexpression was found to be specific for tumors with GS =7, but was much less frequent in cancers with lower and higher Gleason scores.

Gene	Tumor Stage	Lymph node metastasis	Gleason groups <7 vs. 7	Gleason groups 7 vs. >7	Bioch. recur-rence
PLAGL1	**0,038***	0,327	0,071	0,832	**0,041***
***PLAGL1* delta**	0,171	0,948	0,268	0,408	**0,031***
TFPI2	0,964	0,948	0,586	0,588	0,982
SGCE	0,648	0,473	**0,054**	0,189	0,594
PEG10	0,157	**0,034***	0,105	0,308	0,266
PPP1R9A	0,349	0,213	0,076	0,189	0,247
PON2	0,349	0,105	**0,027***	0,724	0,799
INPP5F	0,891	0,575	0,803	0,087	0,144
INPP5Fv2	0,337	0,070	0,087	0,689	0,203
CDKN1C	0,171	0,706	0,081	0,724	0,391
LIT1	0,982	0,558	0,187	0,524	0,297
IGF2	0,337	0,523	0,076	1,000	0,228
H19	0,465	0,706	0,081	0,906	0,487
MEG3	0,193	0,079	0,368	0,381	0,144
NDN	0,537	0,649	**0,003****	0,655	0,203
SNRPN	0,253	0,805	0,826	**0,055**	0,487
SNURF	0,105	0,785	0,566	0,131	0,228
PEG3	0,599	0,649	0,255	0,494	0,297
GNAS	0,451	0,382	0,872	0,464	0,132
ERG	0,068	0,745	**0,004****	**0,006****	0,404
EZH2	0,235	**0,009****	0,062	0,524	0,132
HOXC6	0,537	**0,048***	0,087	0,796	**0,026***

Table 3.2.4.1. Significance values for the distribution of imprinted genes expression in prostate cancer tissues in groups according to clinical parameters. The distributions of mRNA expression for the indicated genes relative to TBP in groups according to tumor stage, lymph node metastasis, Gleason score and biochemical recurrence was analyzed with SPSS using the non-parametric Mann-Whitney-U test. (For grouping details see Chap. 2.2.23.1) *p<0.05; **p<0.01

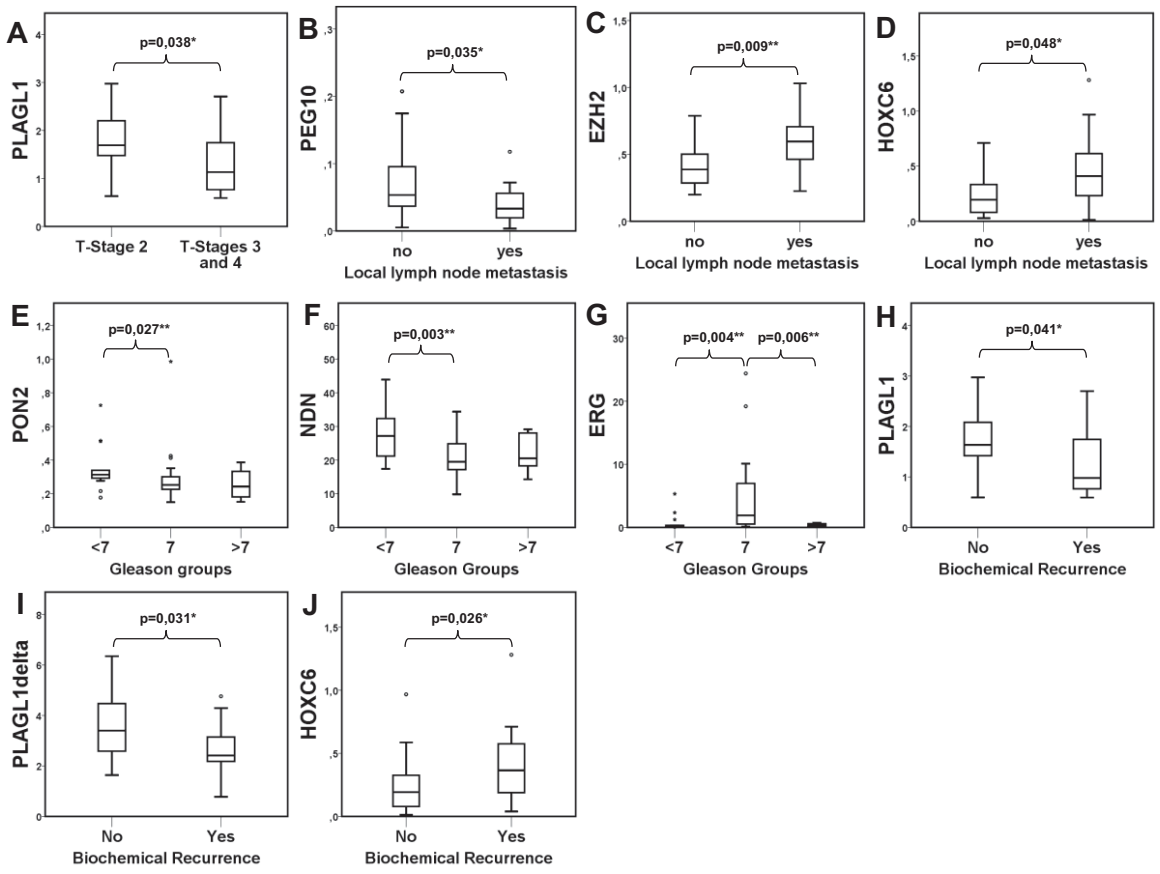

Fig. 3.2.4.1. Boxplot representation of significant distributions of gene expression in prostate cancer tissues grouped according to clinical parameters. Significance of the distribution of the expression of the indicated genes in groups according to the Gleason score, tumor stage and lymph node metastasis was calculated with Mann-Whitney-U test in SPSS software (for grouping details see Chap. 2.2.23.1). Significance values are shown above the brackets in each panel *p<0.05; **p<0.01.

3.2.5. Correlation of imprinted gene expression with *ERG*, *HOXC6* and *EZH2* expression in prostate tumor tissues

The *HOXC6*, *ERG* and *EZH2* genes, which are overexpressed in advanced prostate cancers, act as transcription factors and chromatin modulators, and thereby can influence the transcriptional program of these tumors. Spearman correlation analysis was performed to test the expression of imprinted genes against the expression of these oncogenes.

Initially, *ERG*, *HOXC6* and *EZH2* expressions were used as continuous variables and correlated to the expressions of imprinted genes by means of Spearman correlation analysis. The resulting correlation coefficients are listed in Table 3.2.6.1. Unlike all other analyzed imprinted genes, the expression of *PPP1R9A* strongly correlated positively to the expressions of *ERG*, *EZH2* and *HOXC6* genes. The expression of *HOXC6* and *EZH2* correlated negatively in a statistically significant fashion with that of several imprinted

genes, i.e. *PLAGL1*, *SGCE*, *PEG10*, *INPP5Fv2*, *CDKN1C*, *IGF2*, *H19*, *MEG3*, *NDN*, and *PEG3*. Notably there was also a strong statistically significant positive correlation between the expressions of these two oncogenes. In comparison, the expression of *ERG* correlated negatively with fewer imprinted genes, i.e. most strongly with *PEG10*, and more weakly with *PLAGL1*, *NDN*, *H19* and *IGF2* genes.

In a second analysis, the tumor samples were stratified in two groups each (low- vs. high-expressing) according to the mRNA levels of *EZH2*, *HOXC6* and *ERG*. Mann-Whitney-U test was applied to test the distribution of imprinted gene expression in the *ERG*, *HOXC6* and *EZH2* expression groups. Significance values are given in Table 3.2.6.2. Boxplot graphs of the significant results, created with SPSS, are presented in Figs. 3.2.6.1 - 3.2.6.3. The imprinted genes which highly correlated with *EZH2* and *HOXC6* expression as continuous variables were also very significantly differentially distributed between the *EZH2* and *HOXC6* categorical expression groups (Table 3.2.6.2). The two *PLAGL1* variants, *PEG10*, *PPP1R9A* and *NDN* were differentially distributed but with a slightly lower significance between the *ERG* expression groups.

Gene	*ERG* expression	*HOXC6* expression	*EZH2* expression
PLAGL1	**- 0,303***	**- 0,658****	**- 0,314***
PLAGL1delta	-0,192	**- 0,471****	-0,218
TFPI2	-0,071	-0,017	-0,063
SGCE	-0,275	**- 0,389****	**- 0,434****
PEG10	**- 0,426****	**- 0,555****	**- 0,518****
PPP1R9A	0,236	**0,309***	0,018
PON2	0,046	-0,025	0,068
INPP5F	0,277	**- 0,385****	-0,059
INPP5Fv2	-0,217	**- 0,644****	**- 0,507****
CDKN1C	-0,250	**- 0,587****	**- 0,566****
LIT1	0,019	0,013	-0,022
IGF2	**- 0,297***	**- 0,548****	**- 0,371***
H19	**- 0,362***	**- 0,488****	**- 0,305***
MEG3	-0,164	**- 0,599****	**- 0,466****
NDN	**- 0,334***	**- 0,636****	**- 0,463****
SNRPN	0,138	0,062	0,121
SNURF	0,119	0,095	0,053
PEG3	0,090	**- 0,476****	**- 0,348***
GNAS	0,091	-0,005	0,139
EZH2	0,207	**0,611****	-
HOXC6	0,218	-	**0,611****
ERG	-	0,218	0,207

Table 3.2.5.1. Correlation of imprinted gene expression with EZH2, HOXC6 and EZH2 genes expression as continuous variables. Spearman's correlation coefficient values of the correlation of imprinted gene expression with the expression of *EZH2*, *HOXC6* and *ERG* genes as continuous variables *<0.05; **<0.01

Gene	*ERG* groups	*HOXC6* groups	*EZH2* groups
PLAGL1	**0,037***	**0,000*****	**0,012***
PLAGL1delta	**0,039***	0,065	0,075
TFPI2	0,716	0,441	0,704
SGCE	0,146	0,068	**0,035***
PEG10	**0,041***	**0,003****	**0,001****
PPP1R9A	**0,037***	0,663	0,569
PON2	0,751	0,778	0,492
INPP5F	0,196	0,137	0,265
INPP5Fv2	0,140	**0,000*****	**0,004****
CDKN1C	0,112	**0,001****	**0,000*****
LIT1	0,510	0,626	0,670
IGF2	0,173	**0,003****	**0,006****
H19	0,107	**0,017****	0,079
MEG3	0,180	**0,013****	**0,000*****
NDN	**0,029***	**0,000****	**0,003****
SNRPN	0,196	0,441	0,981
SNURF	0,204	0,959	0,831
PEG3	1,000	**0,009****	**0,029***
GNAS	0,540	0,817	0,522
EZH2	0,440	**0,002****	-
HOXC6	0,180	-	**0,000*****
ERG	-	0,572	0,107

Table 3.2.5.2. Correlation of imprinted gene expression with EZH2, HOXC6 and EZH2 genes expression groups. The distributions of the relative to TBP mRNA expression for the indicated genes by group according to *EZH2*, *HOXC6* and *EZH2* expression were analyzed with SPSS using the non-parametric Mann-Whitney-U resp. Kruskal-Wallis test. (For grouping details, see Chap. 2.2.23.1) *p<0.05; **p<0.01.

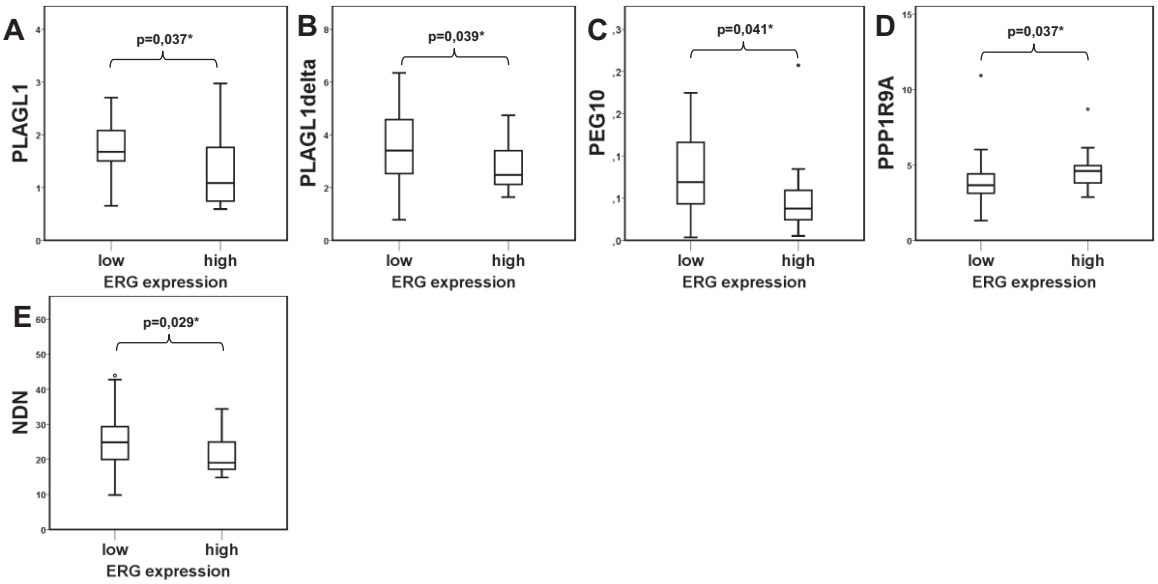

Fig. 3.2.5.1. Boxplot representation of significantly distributed expression of imprinted genes in ERG expression groups. *PLAGL1* (A), *PLAGL1* delta (B), *PEG10* (C), *PPP1R9A* (D), and *NDN* (E) gene expression distribution in high and low *ERG* expression groups. Significance of the distribution (p) was calculated with the Mann-Whitney-U test and is shown above the brackets in each panel, *p<0.05; **p<0.01.

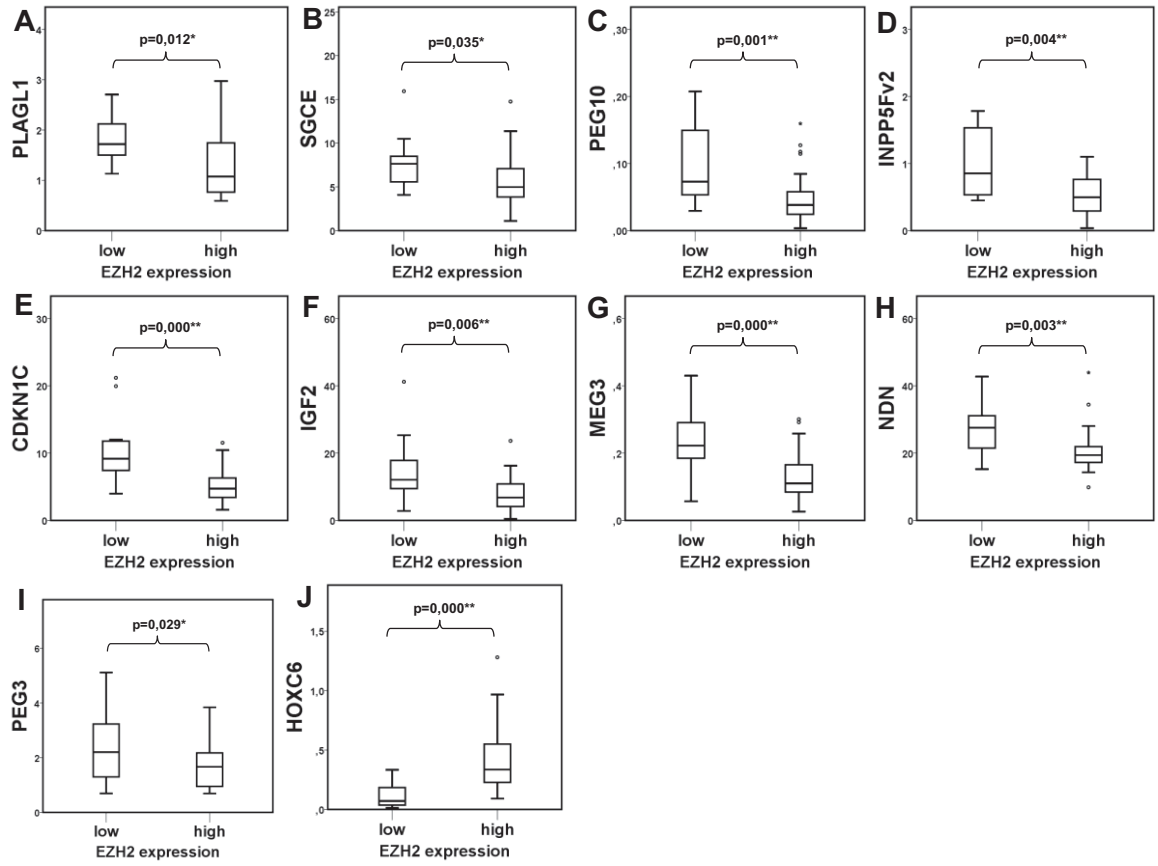

Fig. 3.2.5.2. Boxplot representation of significantly distributed expression of imprinted genes by EZH2 groups. *PLAGL1* (A), *SGCE* (B), *PEG10* (C), *INPP5Fv2* (D), *CDKN1C* (E), *IGF2* (F), *MEG3* (G), *NDN* (H), *PEG3* (I), and *HOXC6* (J) gene expression distribution in high and low *EZH2* expression groups. Significance of the distribution (p) was calculated with the Mann-Whitney-U test and is shown above the bracket in each panel *p<0.05; **p<0.01.

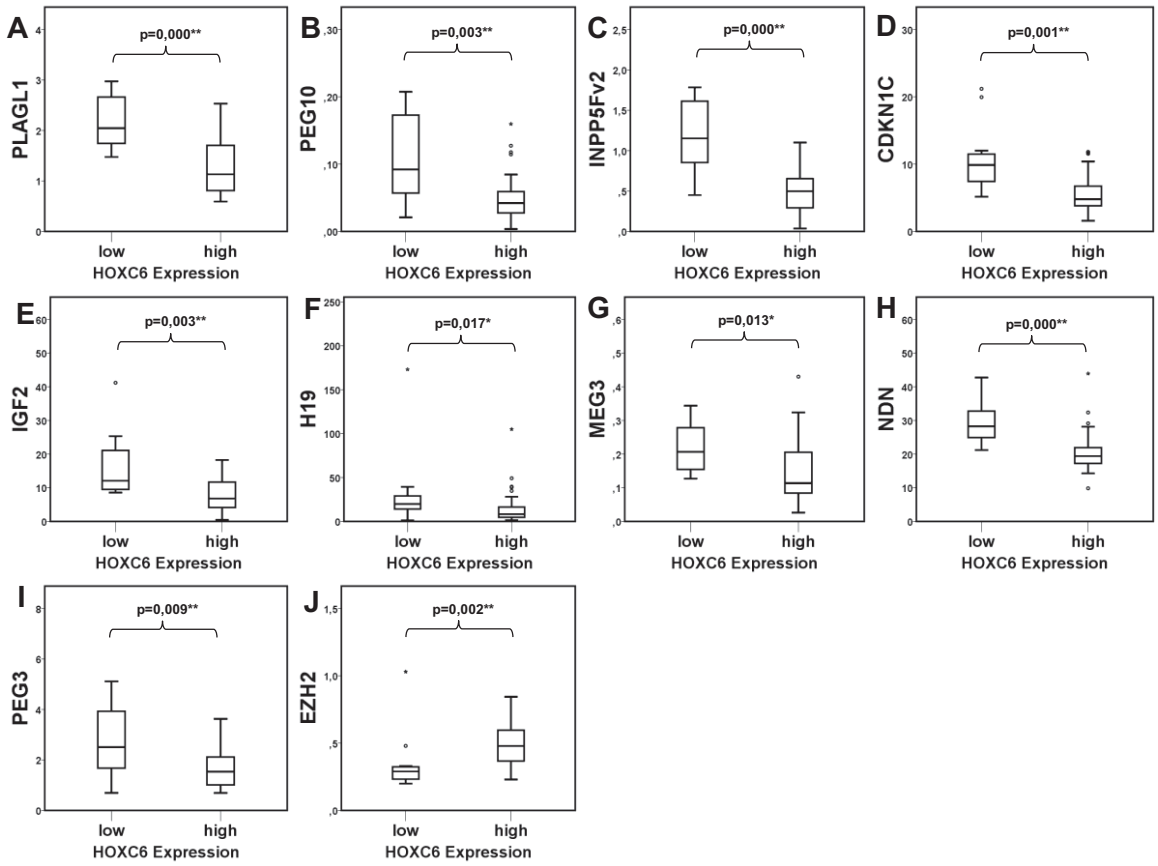

Fig. 3.2.5.3. Boxplot representation of significantly distributed expression of imprinted genes by HOXC6 groups. *PLAGL1* (A), *PEG10* (B), *INPP5Fv2* (C), *CDKN1C* (D), *IGF2* (E), *H19* (F), *MEG3* (G), *NDN* (H), *PEG3* (I), and *EZH2* (J) gene expression distribution in high and low *HOXC6* expression groups. Significance of the distribution (p) was calculated with the Mann-Whitney-U test and is shown above the bracket in each panel *p<0.05; **p<0.01.

3.2.6. Prognostic values of imprinted genes

According to the results from the statistical analysis of the correlation of imprinted genes with clinical parameters and oncogene expression in prostate cancer, the observed expression changes of a group of imprinted genes may functionally associate with disease progression. In order to estimate their prognostic value, survival analysis based on imprinted gene expression was performed. Follow-up data, i.e. time to biochemical recurrence (months) after prostatectomy, was available for the patient cohort tissue series and was used as the time variable in proportional hazards Cox regression analysis and Kaplan-Meier analysis.

3.2.6.1. Cox regression analysis

By means of the Cox regression analysis, the relative hazard rates of imprinted gene expression as continuous variable were related to the time to biochemical recurrence (relapse). Significant prognostic values for the risk to biochemical recurrence were found for *PLAGL1* (p=0.019), *PLAGL1delta* (p=0.030), *GNAS* (p=0.053), and as expected for *HOXC6* (p=0.009). Borderline significance was found for *PPP1R9A* (p=0.076) and *INPP5Fv2* (p=0.077) (Table 3.2.6.1).

Variable	B	SE	Wald	df	Signifi-cance	Exp(B)	95% CI for Exp(B) lower	upper
PLAGL1	-0,984	0,420	5,490	1	**0,019***	0,374	0,164	0,851
PLAGL1delta	-0,500	0,230	4,720	1	**0,030***	0,606	0,386	0,952
TFPI2	0,017	0,152	0,013	1	0,910	1,017	0,755	1,371
SGCE	0,008	0,081	0,010	1	0,921	1,008	0,861	1,181
PEG10	-5,386	5,435	0,982	1	0,322	0,005	0,000	193,659
PPP1R9A	0,211	0,119	3,138	1	**0,076**	1,235	0,978	1,559
PON2	0,160	1,449	0,012	1	0,912	1,173	0,069	20,067
INPP5F	-0,226	0,587	0,148	1	0,700	0,798	0,253	2,519
INPP5Fv2	-1,202	0,679	3,131	1	0,077	0,300	0,079	1,138
CDKN1C	-0,098	0,075	1,736	1	0,188	0,906	0,783	1,049
LIT1	-0,037	0,072	0,367	1	0,605	0,963	0,836	1,110
IGF2	-0,074	0,046	2,606	1	0,106	0,929	0,850	1,016
H19	-0,021	0,017	1,594	1	0,207	0,979	0,947	1,012
MEG3	-4,745	2,994	2,512	1	0,113	0,009	0,000	3,074
NDN	-0,058	0,041	2,048	1	0,152	0,944	0,872	1,022
SNRPN	0,032	0,085	0,141	1	0,708	1,032	0,874	1,219
SNURF	0,042	0,056	0,566	1	0,452	1,043	0,935	1,163
PEG3	-0,302	0,277	1,188	1	0,276	0,740	0,430	1,272
GNAS	0,277	0,143	3,740	1	**0,053***	1,319	0,996	1,747
EZH2	1,642	1,074	2,338	1	0,126	5,164	0,630	42,352
ERG	0,051	0,034	2,273	1	0,132	1,053	0,985	1,125
HOXC6	1,752	0,721	5,904	1	**0,015***	5,767	1,403	23,699

Table 3.2.6.1. Univariate Cox regression analysis of the influence of imprinted gene expression on the risk for biochemical recurrence in prostate cancer. Gene expression data as continuous variable was used as regressor. The expression of *EZH2*, *ERG*, and *HOXC6* genes was included in the analysis as reference. B- coefficient, SE- standard error of B, Wald-statistics of Wald test [=(B/S.E.)*2], df-degree of freedom, Significance of hazard ratio, Exp(B)- hazard ratio, 95% CI- 95% confidence interval for hazard ratio.

2.2.23.4. 3.2.6.2. Kaplan-Meier analysis

The prognostic value of imprinted gene expression to predict patient survival as defined by the time to reach biochemical recurrence was also analyzed by means of the log-rank test and visualized by Kaplan-Meier curves (Fig. 3.2.6.2). For this test the gene expression of the tumors was dichotomized into groups of „high“and „low“ (for details see 2.2.23.1).

According to the log-rank test, the expression of *PLAGL1delta* (p=0.012), *PPP1R9A* (p=0.012) and *H19* (p=0.012) exhibited significant high associations with the time to biochemical recurrence in prostate cancer patients. As may be expected *EZH2* expression was also significantly associated (p=0.012). The predictive values of *PLAGL1* (p=0.060) and *MEG3* (p=0.058) expression groups were very close to significance (Table 3.2.6.2).

Logrank test (Mantel-Cox)	Chi-Square	df	Significance
PLAGL1	3,529	1	0,060
PLAGL1delta	6,255	1	**0,012****
PPP1R9A	4,771	1	**0,029***
H19	5,510	1	**0,019***
MEG3	3,584	1	0,058
EZH2	4,318	1	**0,038***

Table 3.2.6.2. Statistics of Logrank test (Mantel-Cox) for the influence of gene expression on the risk of biochemical recurrence. df-degree of freedom, *p<0.05; **p<0.01.

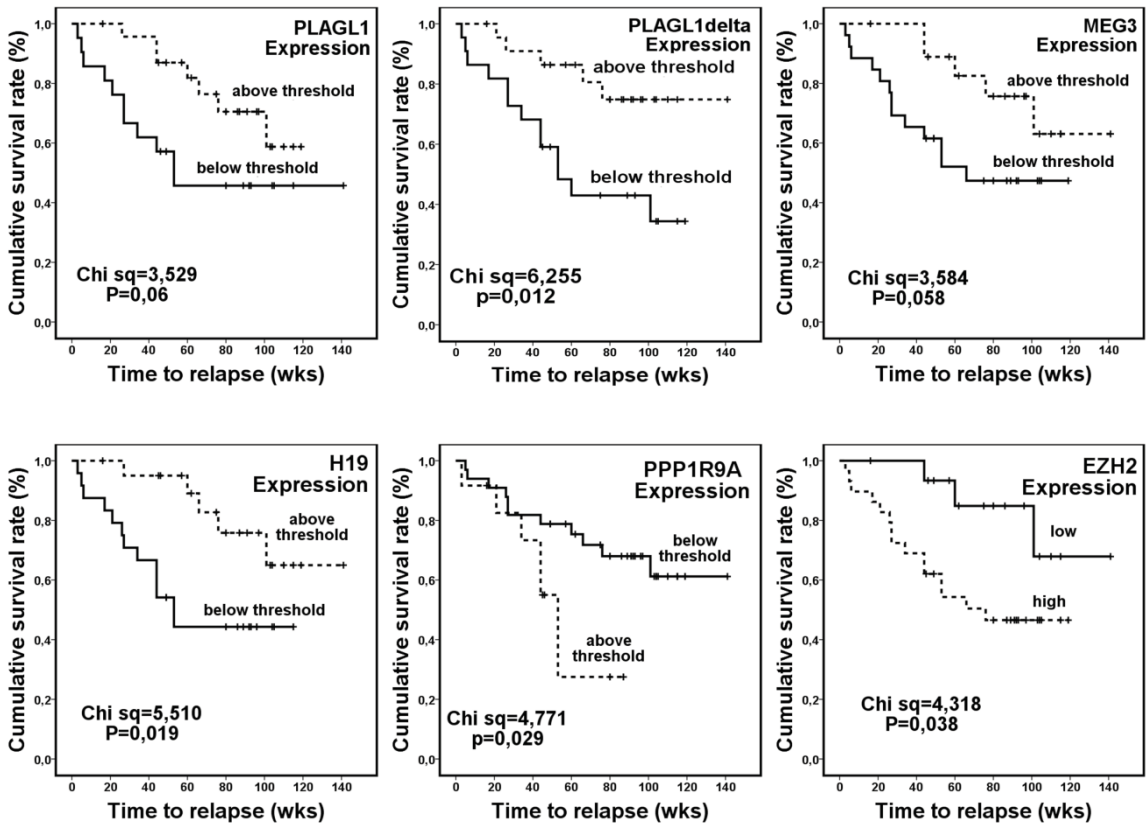

Fig. 3.2.6.2. Imprinted genes with significant prognostic value for the time to biochemical recurrence. Kaplan-Meier plots of *PLAGL1*, *PLAGL1delta*, *MEG3*, *H19*, *PPP1R9A* and *EZH2* expression groups as a descriptive variable to cumulative survival rate (%) as defined by the detection of biochemical relapse. Chi sq- Chi square of the log-rank test, p-significance.

3.2.7. Influence of androgens on expression of imprinted genes

Changes in the androgen response are central to the development and progression of prostate cancer. Since many observed changes in imprinted gene expression also tend to occur in advanced cancers, it was interesting to find whether androgens could influence their expression. For the purpose, androgen-dependent LNCaP cells were treated for 24 h with the synthetic androgen R1881. The MDAPCa2b cells, which are also androgen-dependent, are normally cultured in the presence of androgens. Therefore, they were used as a model for androgen ablation by 24 h treatment with the androgen receptor antagonist bicalutamide.

Real-time RT-PCR analysis of *PLAGL1*, *CDKN1C*, *SGCE*, *PEG10*, *PON2*, *PPP1R9A*, *NDN*, *GNAS*, *SNRPN,* and *INPP5F* genes detected only minor expression changes upon androgen treatment or ablation in LNCaP and MDaPCa2b cells (Fig. 3.2.7). These results suggest the relative stability of the assessed imprinted genes in androgen-enriched or androgen-depleted conditions.

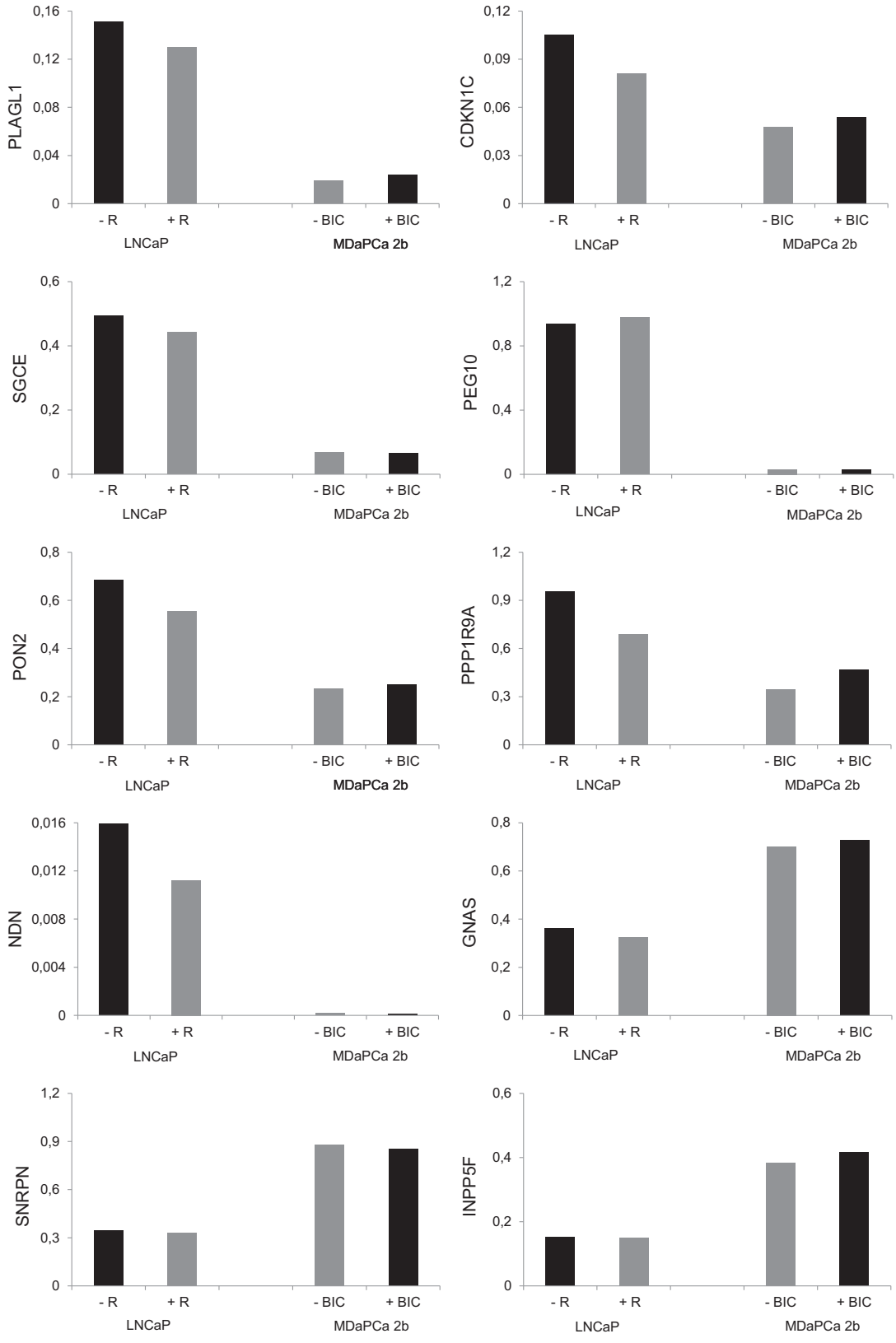

Fig. 3.2.7. Influence of androgens on imprinted genes expression. Relative to TBP mRNA expression of the indicated imprinted genes in LNCaP cells treated for 24 h with the androgen R1881 (abb. R) (10 nM) and MDaPCa2b cells treated for 24 h with the androgen receptor antagonist bicalutamide (abb. BIC) (10 μM). Androgen supplemented conditions are indicated as grey bars, while androgen-depleted conditions as black bars. The measurements were performed in duplicate and the average was used, whereby less than 10% variation between duplicates was accepted.

3.2.8. ZAC1 protein expression in prostate cancer tissues

Since downregulation of *ZAC1* at the mRNA level was significant in prostate tumor tissues compared to benign tissues, a downregulation on the protein level would further support its possible tumor suppressor function. To detect ZAC1 protein in the tissues, protein lysates made directly from four frozen prostate tissue benign and tumor pairs from the same patients were used. Depending on the translated mRNA transcript and the utilized translation start site, ZAC1 protein products of the following sizes might be expected: ~51, 45, 40, 38 or 27 KDa [185]. Interestingly, the major ZAC1 protein band detected in the prostatic tissue samples was ~27 kDa of size, in comparison to the ~40-45 kDa size of the ZAC1 protein detected in the PC3 (Fig. 3.2.8) and 22Rv1 or LNCaP cells (data not shown). These proteins likely correspond to isoforms resulting from translation starts at ATG6 or ATG2/3 (see Fig. 3.4.1). In the three tissue pairs that were evaluable (N/Tu 2-4) ZAC1 protein appeared to be decreased in the tumor compared to the benign tissue.

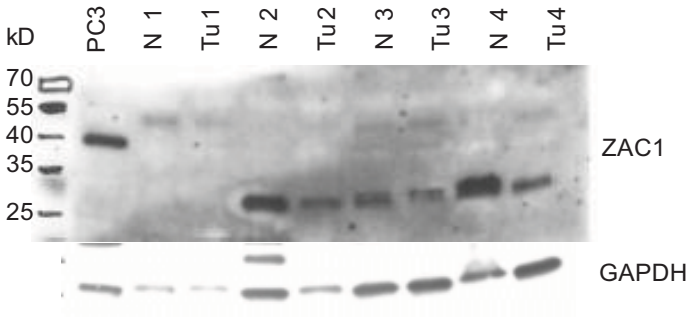

Fig. 3.2.8. Protein expression of ZAC1 in prostate benign and tumor tissues. ZAC1 and GAPDH proteins as detected by immunoblot analysis of benign (N) and tumor (Tu) tissue sample pairs from four patients (1-4). A protein lysate from the PC3 cell line was loaded as a reference. The expected protein sizes of the protein products of different ZAC1 transcripts according to Bilanges et al. [185] are ~51, 45, 40, 38 or 27 kDa (see Fig. 3.4.1). Proteins in pair N1/Tu1 were likely degraded and not evaluable.

3.2.9. Expression of *PLAGL1*, *CDKN1C*, *PPP1R9A* and *EZH2* in prostate cancer cell lines

Among the differentially expressed imprinted genes in prostate cancer, further studies were focused on the downregulated potential tumor suppressors *PLAGL1* and *CDKN1C* and the upregulated potential oncogene *PPP1R9A*. In order to monitor the expression of these genes in prostate cancer cell lines and thereby chose suitable models for further experiments, real time RT-PCR analysis was applied. Since it was hypothesized that the *EZH2* oncogene may have a functional impact on imprinted genes, its expression was analyzed in search of a possible correlation.

The levels of *PLAGL1* and *CDKN1C* were relatively low in the androgen-dependent cell lines (VCaP, MDAPca2b, LNCaP and 22Rv1) compared to the androgen-independent PC3 cell line, but also relatively low in androgen-independent DU145 cells (Fig. 3.2.9.1). In further experiments, LNCaP and 22Rv1 were used as models with low *PLAGL1* expression, while PC3 cells were used as a model with high expression.

The normal human epithelial cells (PrEC) expressed relatively high *PLAGL1* level, while it was already downregulated in immportalized benign prostate hyperplasia (BPH1) cells. CDKN1C gene expression was low in all normal or benign prostate cells (PrEC, BPH1, and PNT2) while it was higher expressed in the prostate cancer cell lines.

As high *EZH2* expression was detected in cell lines with both high and low expression of *CDKN1C* and *PLAGL1* genes, *EZH2* levels do not seem to straightforwardly correlate to their downregulation in the cell line models of prostate cancer (Fig. 3.2.9.1).

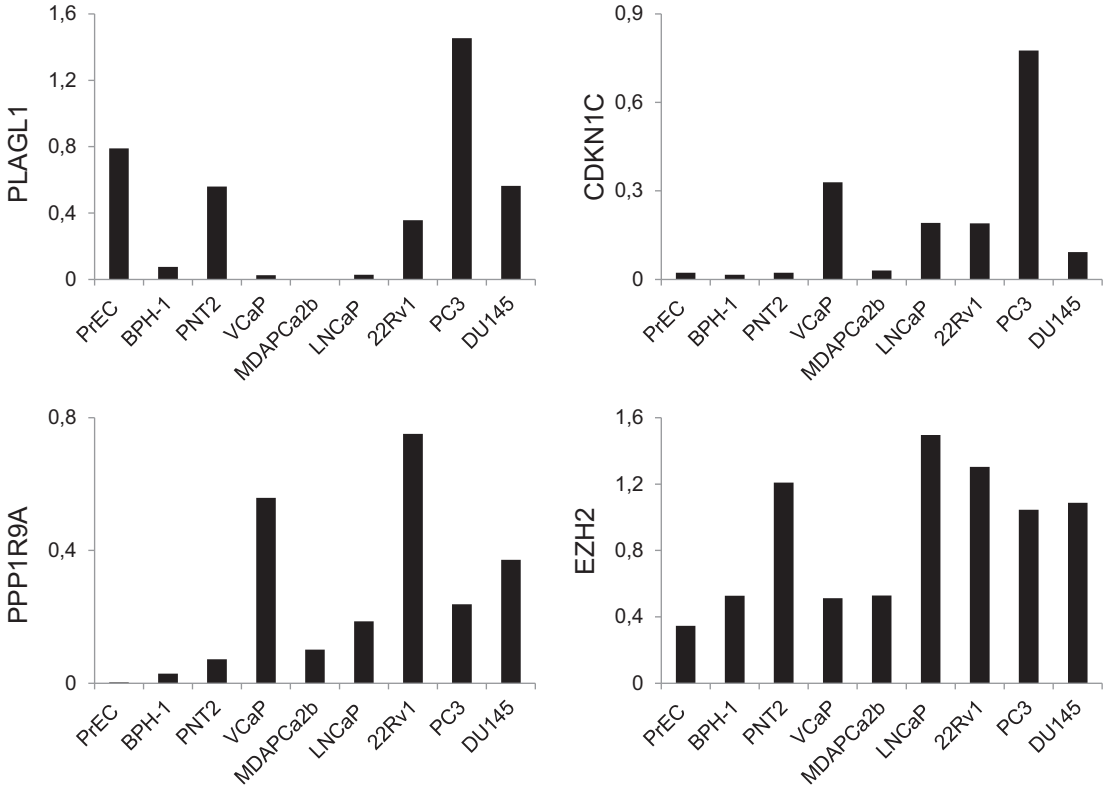

Fig. 3.2.9.1. Expression of PLAGL1, CDKN1C, PPP1R9A and EZH2 in prostate cancer cell lines. Expression of *PLAGL1*, *CDKN1C*, *PPP1R9A*, and *EZH2* genes relative to *TBP* mRNA as measured by qRT-PCR in normal prostate primary cells (PrEC) and the indicated prostate cancer cell lines. The measurements were performed in duplicate and the average was used, whereby less than 10% variation between duplicates was accepted.

While the expression of *PPP1R9A* was low in PrEC, BPH1 and PNT2 cells, it was upregulated in the prostate cancer cell lines, with highest values in VCaP and 22Rv1 cells. Immunoblot analysis was applied to monitor whether the levels of *PPP1R9A* mRNA in the

cell lines corresponded to the protein levels of the encoded neurabin I. Although the antibody used detected several protein bands, the expected 180 kDa band was more prominent in the lysates of LNCaP and 22Rv1 cells than in the other cell lines (Fig. 3.2.9.2). Due to the low specificity of the antibody, one cannot make a firm conclusion about the protein levels of neurabin I in prostate cancer cell lines, though.

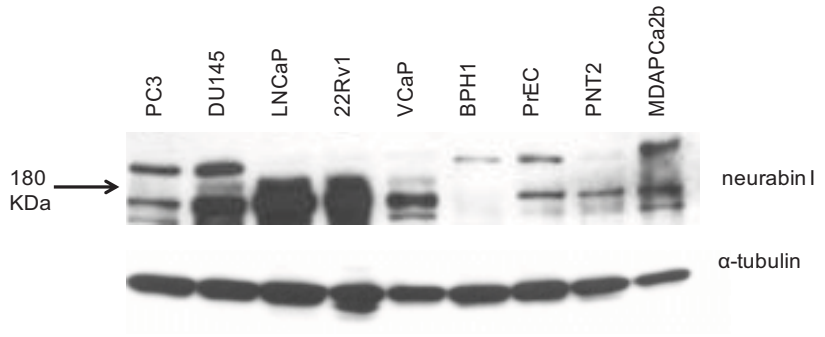

Fig. 3.2.9.2. Protein expression of neurabin I in normal prostate epithelial cells (PrEC) and prostate cancer cell lines. Neurabin I and α-tubulin proteins as detected by immunoblot analysis of the indicated prostate cancer cell lines and normal prostate epithelial cells (PrEC). The expected protein sizes of neurabin I is ~180 kDa (arrow). The anti-neurabin I antibody also detected several more bands at lower molecular weights (not shown).

3.3. Epigenetic regulation of imprinted genes

The correct expression of imprinted genes depends on the appropriate epigenetic modifications of the local ICR and DMR. DNA methylation was assessed in selected regions in the DMRs of several imprinted gene clusters of interest in this study, as well as the promoter region of the *CDKN1C* gene in the prostatic benign and cancer tissue set. The potential influence of DMR methylation on the expression of the associated imprinted genes was evaluated using bivariate Spearman correlation analysis.

3.3.1. Methylation of 6q24/*PLAGL1* DMR, 7q21 DMR, *MEG3* DMR, *KvDMR* and *CDKN1C* promoter

Pyrosequencing analysis of DNA methylation was performed for the 7q21 DMR, the 6q24/*PLAGL1* DMR, the 14q32.2/*MEG3* DMR and the 11p15 *KvDMR* as well as in the promoter region of the *CDKN1C* gene. The chromosomal locations of the regions evaluated by pyrosequencing analysis are schematically displayed in Appendix 2. The mean methylation of several (4-7) CpG positions from each region was quantitatively determined and used for further analysis. Additionally, in the *MEG3* DMR analysis, the methylation of one specific CpG site was also considered for reasons explained below. Boxplot analysis using the SPSS software was applied to compare the distribution of

methylation in benign vs. tumor tissues (Fig. 3.3.1.1). Graphs depicting the mean methylation percentages of the assessed regions for each individual sample of the benign and cancer prostate tissue set are shown in Appendix 3.

The methylation of the 6q24/*PLAGL1* DMR was relatively stable among the benign (mean 35%, n=11) and tumor tissues (mean 40%, n=42), with exception of single cases where diminished methylation (less than 20%) was found in either sample group (Appendix 3). No case of substantial hypermethylation was observed. The difference between the distributions of the methylation of benign vs. tumor tissues was not statistically significant (Fig. 3.3.1.1 A).

The mean amount of methylation of the 7q21 DMR was much lower than the 50% expected for DMR, reaching about 10% in the whole sample set, with minor differences between the tumor group (11%, n=44) and the benign group (7%, n=11) (Table 3.3.1 and Fig. 3.3.1.1 B). Moreover, the methylation levels between the individual tissues were quite variable, mostly in the tumor group where exceptional tissues exhibited more than 20% methylation (Appendix 3).

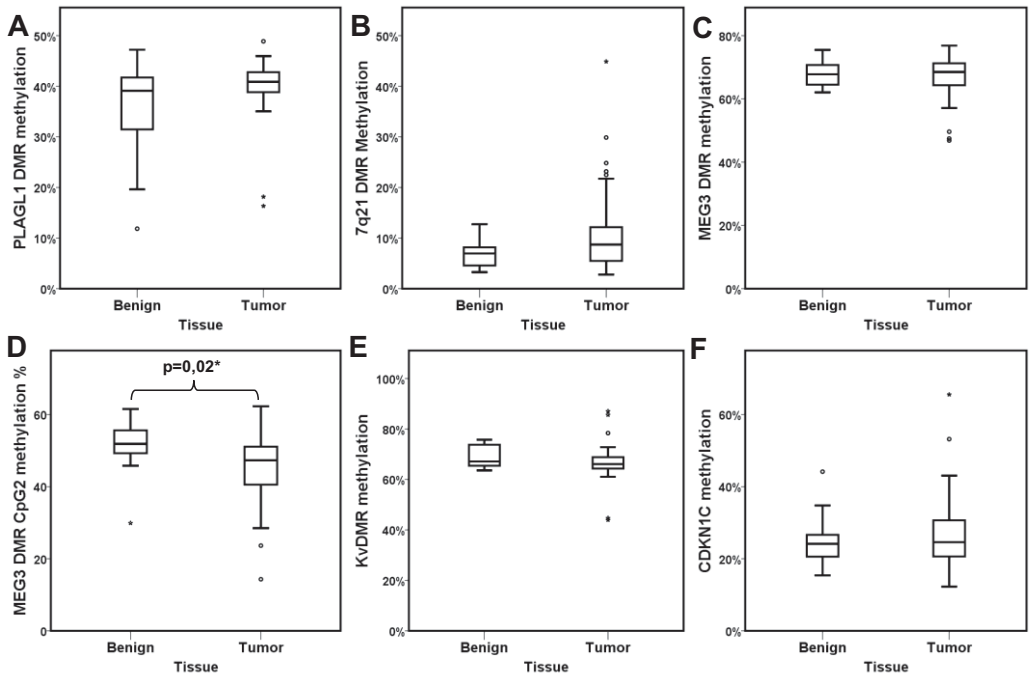

Fig. 3.3.1.1. Boxplot comparison of the mean DNA methylation [%] of the assessed DMRs and the CDKN1C promoter in prostate benign and tumor tissue samples. Mean methylation of benign and tumor prostate tissues was quantified by bisulfite pyrosequencing for the following regions: (**A**) *PLAGL1* DMR, (**B**) 7q21 DMR, (**C**) *MEG3* DMR, (**D**) CpG2 of *MEG3* DMR region, (**E**) *KvDMR*, and (**F**) *CDKN1C* promoter. Boxplots were created with SPSS software. Mann-Whitney-U test was performed to calculate the significance in distributions between the groups. Only the methylation of CpG2 of *MEG3* DMR was found to be significantly different in benign compared to tumor tissues (p=0.02) *p<0.05.

Tissues	Mean methylation				
	PLAGL1 DMR	**7q21 DMR**	**MEG3 DMR**	**KvDMR**	**CDKN1C**
tumor + benign	39 ± 7% (n=53)	10 ± 8% (n=55)	67 ± 6% (n=60)	67 ± 7% (n=60)	26 ±10% (n=57)
tumor	40 ± 6% (n=42)	11 ± 8% (n=44)	67 ± 7% (n=47)	67 ± 7% (n=47)	27 ±10% (n=44)
benign	35 ± 11% (n=11)	7 ± 3% (n=11)	68 ± 4% (n=13)	69 ± 4% (n=13)	25 ± 8% (n=13)

Table 3.3.1. Summary of mean DNA methylation values of the assessed regions. Methylation values of benign and tumor prostate tissues were obtained by bisulfite pyrosequencing of *PLAGL1* DMR, 7q21 DMR, *MEG3* DMR, *KvDMR* and *CDKN1C* promoter. Mean values with standard deviation were calculated using Excel, n=number of samples for which high quality data was obtained.

The *MEG3* DMR region was uniformly methylated in most of the analyzed prostate tissues (mean of 67%) with very similar methylation between the benign and tumor tissue groups revealing methylation stability (Table 3.3.1 and Fig. 3.3.1.1 C). Oddly, among the six CpG positions tested in the pyrosequencing analysis, position 2 exhibited consistently lower methylation (around 50%) than the other positions (around 70%)(Fig. 3.3.1.2). Benign tissues were slightly more methylated at this position than tumor tissues. Statistical analysis by Mann-Whitney-U test showed that this difference was significant (p=0.02) (Fig. 3.3.1.1 D).

Like at the *MEG3* DMR, DNA methylation was overall stable in prostate tissues at the *KvDMR* with a total mean of 67% and similar means in the benign and tumor groups (Table 3.3.1 and Fig. 3.3.1.1 E).

The pyrosequencing assay for the *CDKN1C* promoter applied here was previously published by Pateras et al [158]. The assessed region contains four CpG positions situated between -714 and -701 relative to the transcription start site. This region was shown by Pateras et al. to be hypermethylated in some non-small cell lung cancers, which according to their findings negatively correlated with *CDKN1C* mRNA expression [158]. In the prostate tissues the average methylation was found to be around 25% with similar levels in the benign and tumor groups (Table 3.3.1. and Fig. 3.3.1.1 F). The methylation was higher than 40% only in a few single cases, one of which belonged to the benign group (Appendix 3).

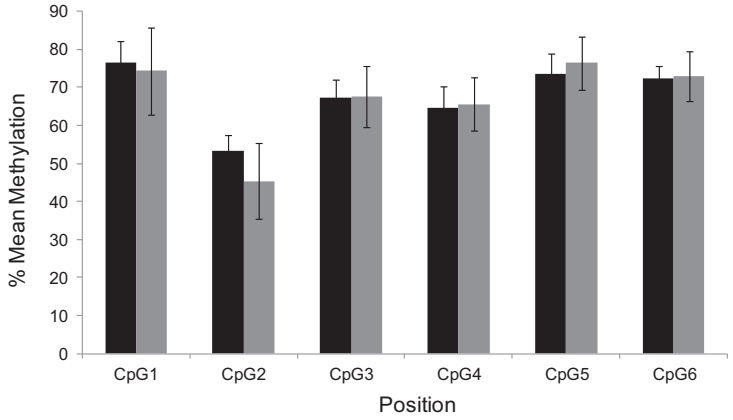

Fig. 3.3.1.2. Methylation of MEG3 DMR region in detail. Methylation values of the six CpG positions in the assessed *MEG3* DMR region in 13 benign (black bars) and 47 cancerous (grey bars) prostatic tissues were obtained by pyrosequencing analysis. Mean values with standard deviation (error bars) were calculated using Excel.

3.3.2. Correlation of DNA methylation with imprinted gene expression

As imprinted gene expression was found to be altered in prostate tumors, changes in the methylation of several associated DMRs and promoter regions could represent a responsible mechanism. In search of such an association, bivariate Spearman correlation analysis was applied. The coefficients of correlation (ρ) between the assessed imprinted genes and the DNA methylation of the analyzed regulatory regions are listed in Table 3.3.2.

To visualize the interdependence between methylation and gene expression for each sample, the relative mRNA gene expression was plotted on the x axis and the percentage of methylation of the corresponding tissue sample was plotted on the y axis (Fig. 3.3.2).

While the expression of *PLAGL1* was significantly different between benign and tumor samples, the methylation of the 6q24 *PLAGL1* DMR was very similar among the two groups, except for few outliers. This difference fits with the observed low correlation (ρ= -0.175) between DMR methylation and *PLAGL1* expression in the tumor samples, suggesting that the observed *PLAGL1* mRNA downregulation is unrelated to the methylation state of this region. Analogously, the observed stable methylation of *KvDMR* results in its low correlation with the significantly changed *CDKN1C* (ρ= 0.009) and *LIT1* (ρ= -0.035) mRNA expressions in the tumor group. Although *CDKN1C* promoter methylation was relatively variable in the tumor group, it showed only a relatively small negative and not statistically significant correlation with the expressions of *CDKN1C* (ρ= -0.274) and *LIT1* (ρ= -0.216) mRNA. Although *MEG3 DMR* methylation was relatively stable among the tumors, the slight differences in the samples seem to positively but weakly correlate with *MEG3* mRNA expression (ρ= 0.255).

Gene	*PLAGL1* methylation	*CDKN1C* methylation	*MEG3* DMR methylation	7q21 DMR methylation	*KvDMR* methylation
PLAGL1	-0,175	-0,089	-0,005	-0,260	0,088
PLAGL1 delta	-0,170	**-0,331***	-0,110	-0,197	0,058
SGCE	-0,043	**-0,440***	0,109	**-0,441****	-0,133
PEG10	0,109	-0,088	0,240	**-0,408****	-0,030
PPP1R9A	-0,230	0,015	-0,148	0,187	-0,026
PON2	-0,043	-0,204	0,082	0,252	-0,004
CDKN1C	-0,091	-0,274	0,140	**-0,588****	0,009
MEG3	-0,100	**-0,303***	0,255	-0,237	0,071
NDN	-0,183	**-0,457****	0,123	**-0,413****	-0,070
PEG3	-0,037	-0,266	0,215	-0,245	-0,026
SNRPN	-0,211	-0,061	0,273	0,196	-0,172
SNURF	-0,159	-0,081	**0,295***	0,116	**-0,295***
GNAS	-0,043	-0,101	0,160	0,047	**-0,378***
INPP5F	-0,077	-0,202	0,193	0,046	0,016
INPP5Fv2	-0,197	**-0,377***	0,217	**-0,487****	-0,179
LIT1	0,022	-0,216	-0,060	-0,152	-0,035
H19	-0,127	-0,111	0,055	-0,299	-0,066
IGF2	**-0,363***	**-0,369***	0,176	**-0,483****	-0,029
TFPI2	-0,017	**-0,419****	-0,021	-0,126	0,117

Table 3.3.2. Correlation of DNA methylation and imprinted gene expression. Spearman ρ correlation coefficient (with 2-tailed test of significance (p)) of the mean DNA methylation of the indicated DMRs with the expression of the listed imprinted genes in prostate cancer tissues was calculated with the SPSS software, *p <0.05; **p <0.01.

Since CpG2 in the analyzed region of the *MEG3 DMR* was significantly less methylated in the cancerous than in the benign tissues, it was tested for correlation to *MEG3* mRNA expression in the tumor group. Astonishingly, CpG2 methylation correlated strongly and positively (ρ= 0.559) to *MEG3* mRNA expression with high statistical significance (p<0.001). This finding suggests an important role for this CpG position for *MEG3* expression.

Although the 7q21 region investigated by pyrosequencing is probably slightly outside the actual DMR, its methylation was found to correlate well, with high statistical significance (p<0.001), with the expression of the *SGCE* (ρ= -0.441) and *PEG10* (ρ= -0.408) genes, which are located most proximally in the cluster. In contrast, it correlated only weakly with the expression of the more distal *PPP1R9A* (ρ= 0.187), *PON2* (ρ= 0.252) and *TFPI2* (ρ= -0.126) genes.

Strong and statistically significant correlations were found between the methylation of several of the analyzed regions and the expression of imprinted genes located on different chromosomes (Table 3.3.2). These correlations are at first glance unexpected, but may be explained by three-dimensional trans-regulatory effects of certain DNA regions on non-local genes (addressed in more detail in Chap. 4.2).

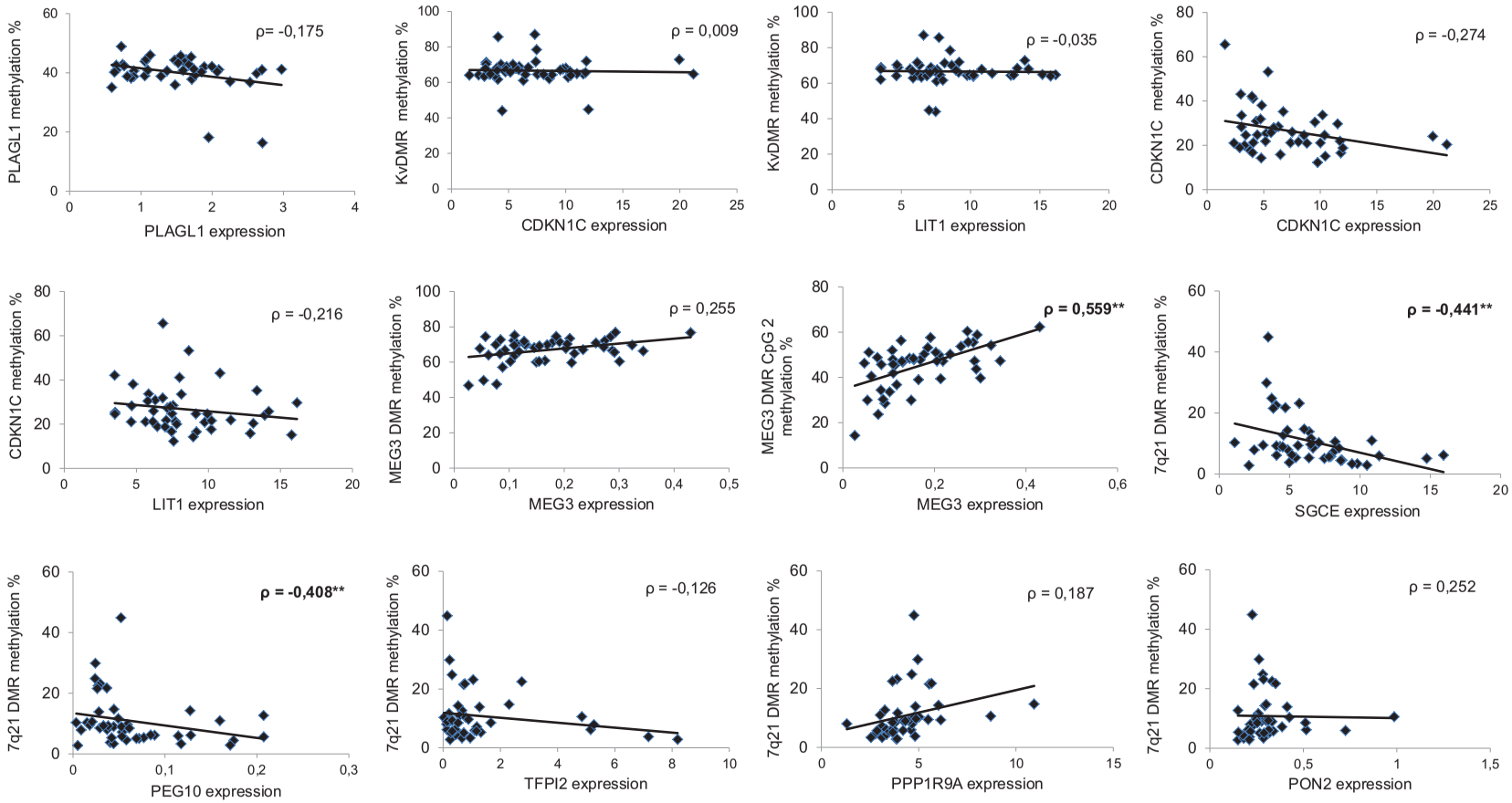

Fig. 3.3.2. Correlation between DMR methylation and imprinted gene expression. Each diamond represents the indicated mRNA expression (relative to TBP) and DNA methylation value (determined by bisulfite pyrosequencing) of a prostate cancer sample The trendline was drawn by Excel. The Spearman correlation coefficient (ρ) of the correlation of the two variables for all tumor tissues was determined using the SPSS software, *p <0.05; **p <0.01.

3.3.3. Effect of pharmacological inhibition of DNA methylation and histone acetylation on imprinted gene expression

LNCaP, 22Rv1 and PC3 cells were treated with the DNMT inhibitor 5-aza-2'-deoxycytidine (5-aza) and with the pan-histone deacetylase inhibitor suberoylanilide hydroxamic acid (Saha) in order to analyze the effect of these agents on the expression of imprinted genes. In general, only moderate changes were detected (Fig. 3.3.3.1).

Consistent, albeit in some cases slight induction of gene expression by 5-aza treatment could be observed for *PLAGL1*, *PEG3*, *MEG3* and *H19* genes in all three cell lines. This may be expected since DMRs are part of the promoters of these genes. While *PEG3* expression was distinctively enhanced by 5-aza in all cell lines, the most distinctive induction was observed for *PLAGL1*, *MEG3* and *H19* in PC3. *CDKN1C* expression, which is influenced by the methylation status of the near *KvDMR*, was also induced by 5-aza in 22Rv1 and PC3 cells. The effect of 5-aza treatment seemed to be more pronounced in PC3 than in the other two cell lines.

Moderate 5-aza-induced expression of *SNRPN* and *SNURF* genes was observed in LNCaP, while in 22Rv1 and PC3 the expression of the two genes decreased slightly.

Robust induction of *NDN*, *MEG3* and *PEG10* by Saha was observed in LNCaP and 22Rv1 cells. This may indicate an involvement of histone deacetylation in the repression of these genes in prostate cancer.

Saha treatment resulted in the downregulation of *SNRPN*, *SNURF* and *SGCE* genes expression in all three cell lines. Notably, Saha treatment of PC3 lowered the expression of all assessed imprinted genes. One might deduce that PC3 cells may be more susceptible to Saha toxicity than LNCaP and 22Rv1 cells.

As may be expected, the patterns of expression of *SNRPN* and *SNURF*, which are two products of the same gene, were very similar in this experiment. Expression patterns silimar to each other were also noticed for the adjacent *SGCE* and *PPP1R9A* genes, whose levels were consistently reduced upon 5-aza treatment and Saha treatment in all three cell lines.

Protein lysates of the 5-aza- and Saha-treated cells were used to detect the protein product of the *PPP1R9A* gene- neurabin I by Western blot analysis. Although the primary anti-neurabin I antibody detects several bands, the prominent band at 180 kDa seen in the untreated control lane was diminished in the 5-aza- and Saha-treatment lanes in all three cell lines, whereas the GAPDH protein levels were equal in all lanes (Fig. 3.3.3.1).

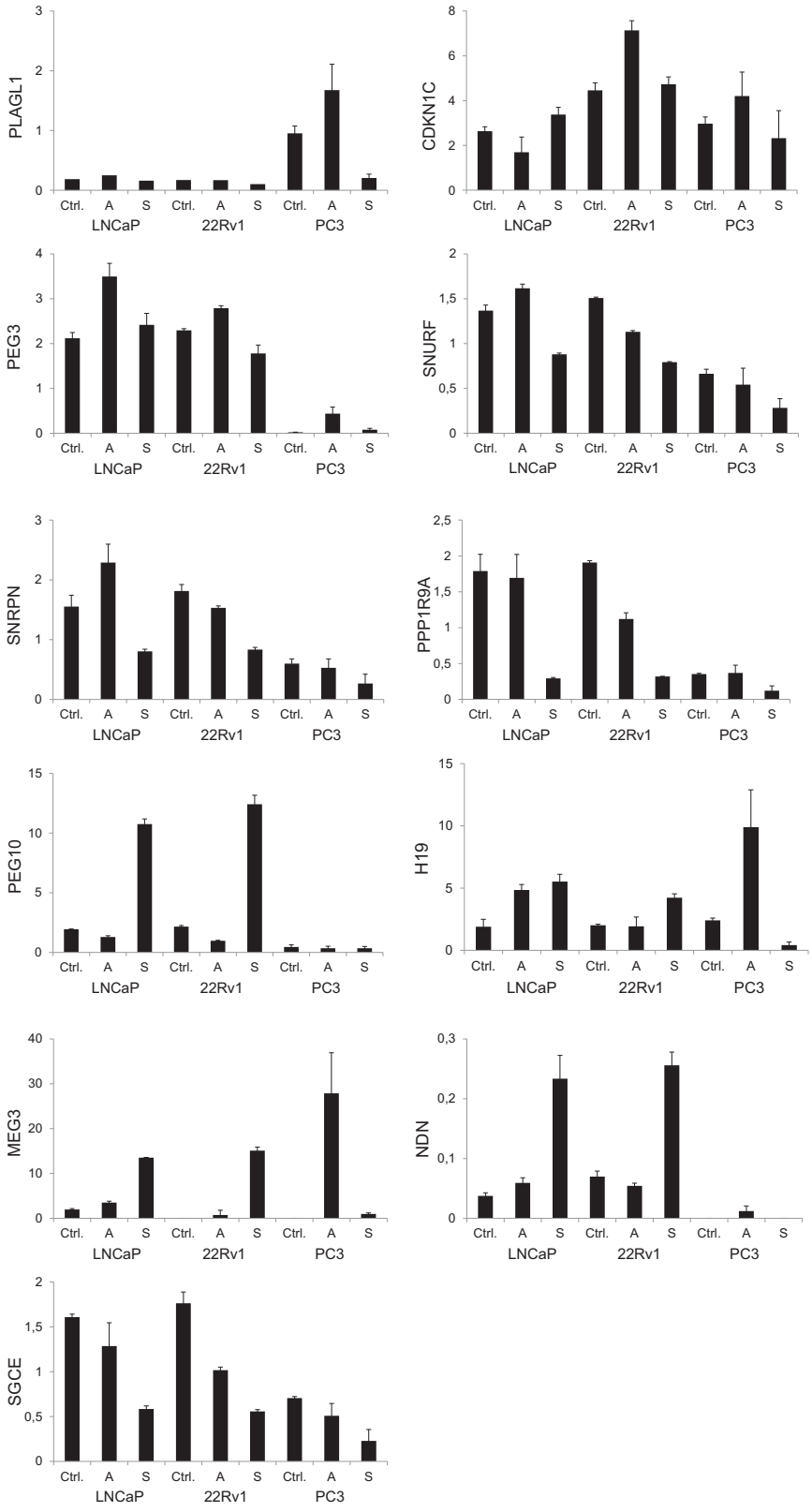

Fig. 3.3.3.1. Effect of inhibitors of DNA methylation and histone deacetylation on imprinted gene expression. Expression of the indicated imprinted genes relative to TBP mRNA was assessed by qRT-PCR analysis of LNCaP, 22Rv1 and PC3 cells treated with 2 µM 5-aza ("A") for 48 h, with 5 µM Saha ("S") for 24 h or untreated ("Ctrl."). The treatments were performed in biological triplicates and PCR was performed in duplicates, standard deviation is given as error bars. The measurements were performed in duplicate and the average was used, whereby less than 10% variation between duplicates was accepted.

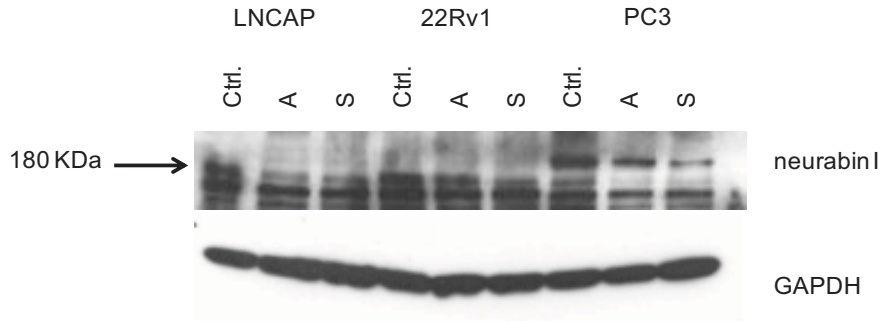

Fig. 3.3.3.2. Effect of inhibitors of DNA methylation and histone deacetylation on neurabin I protein levels. Neurabin I and GAPDH proteins as detected by immunoblot analysis of LNCaP, 22Rv1 and PC3 cells treated with 2 µM 5-aza ("A") for 48 h, with 5 µM Saha ("S") for 24 h or untreated ("Ctrl."). The expected protein size of neurabin I is 180 kDa. GAPDH was detected at 35 kDa as expected.

3.4. ZAC1 overexpression models

3.4.1. Subcloning of ZAC1 expression plasmids

The *PLAGL1/ZAC1* gene contains next to its two protein-coding exons several non-protein coding exons, resulting in long 5' and short 3' untranslated regions (UTRs) (see Fig. 3.4.1 A). As the UTRs can play important roles in regulation of gene function, initially two variants of *ZAC1* cDNA, a long one with 5' and 3' UTRs and a short one without UTRs, were subcloned into the expression vector pcDNA4/TO (see Fig. 3.4.1.B). The subcloning procedure is described in Chap. 2.2.15.2-3.

The long *ZAC1* cDNA, containing a 790 bp 5'-UTR, corresponding to sequences from *PLAGL1/ZAC1* exons 6 and 7, and a small 140 bp-long 3'-UTR, was named after the donator (Dr. Varrault) pcDNA4/TO.ZAC.VA (VA from VArault). The short *ZAC1* cDNA form, without UTRs and with an exon 1 shortened by 24 bases (coding for the initial 8 amino acids), was named pcDNA4/TO.ZAC.DS (DS for D. Spengler). For convenience, these vectors are shortly called ZAC.VA and ZAC.DS in the following descriptions. Depending on the translation starting site used, the two vectors may encode proteins of various predicted sizes ranging from 51 kDa to 27 kDa. The longest protein that can be produced by the ZAC.VA plasmid is ~ 51 kDa of size, while the ZAC.DS plasmid may produce a by 3 amino acids shorter protein, which should not visibly affect its protein size on gels.

At a later point in the study when the instability of the overexpressed ZAC1 protein became obvious (see below), the alternatively spliced ZAC1 transcript isoform (called ZAC1delta) came to our attention. We therefore decided to investigate this isoform and

particularly its stability as well. The ZACdelta isoform has only one protein-coding exon (coding for 5 zinc fingers) as compared to the two exons (coding for 7 zinc fingers) of regularly spliced transcripts. As suggested in the literature, the ZACdelta isoform may have different functions from that of the other isoforms [185]. Therefore, a third expression vector containing the short "delta" isoform, namely the pcDNA4/TO.ZACdelta plasmid (shortly ZACdelta) was constructed (for cloning procedure see Chap. 2.2.15.4) and compared with the ZAC.VA and ZAC.DS vectors. Subcloned from the ZAC.VA plasmid, the ZACdelta plasmid contains a short stretch of bases from exon 7, potentially coding for 3 amino acids if the first ATG (ATG2) is used, and the same region sequence from exon 8 (including the 3'-UTR) as ZAC.VA (Fig. 3.4.1.B bottom). The protein encoded by the ZACdelta plasmid should have an approximate size of 45 kDa.

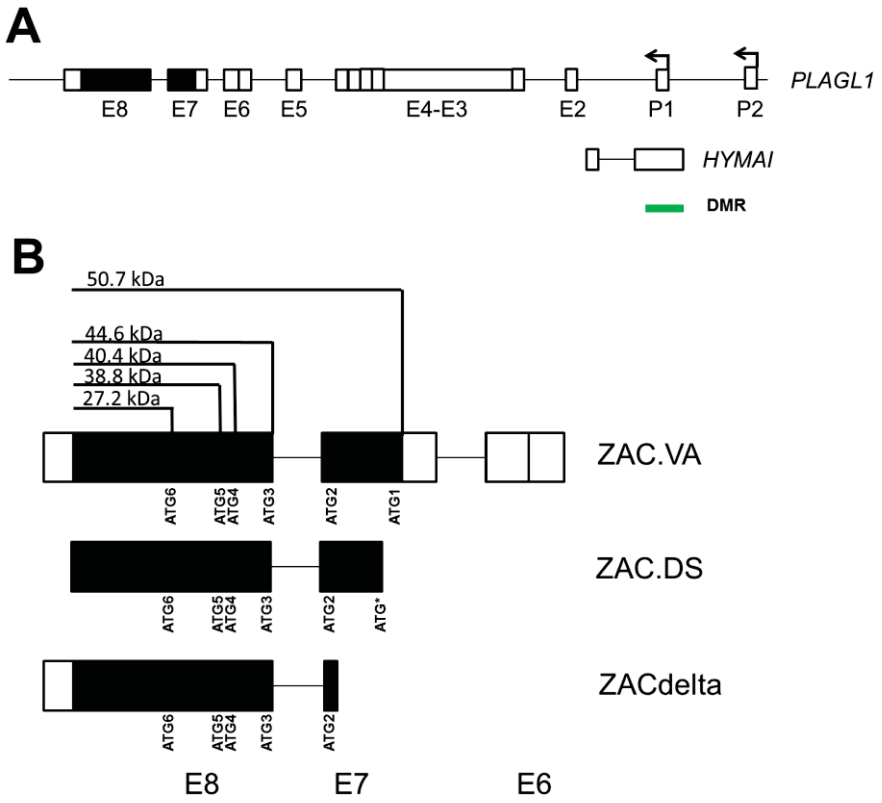

Fig. 3.4.1. Schematic diagram showing the PLAGL1/ZAC1 gene on human chromosome 6q24 and the regions cloned into ZAC1 expression vectors. (Not to scale) (**A**) The *PLAGL1* gene contains several 5' untranslated exons (open bars) and transcripts can contain one or two protein coding exons (filled bars) (adapted from [184]) (**B**) Different cDNA regions from *PLAGL1/ZAC1* gene were subcloned in pcDNA4/TO vectors, shortly named ZAC.VA, ZAC.DS and ZACdelta. The ZAC.VA plasmid contains cDNA with sequences of both exons E7 and E8 protein coding exons (filled bars), a 5'-UTR from exons E6 and E7 and a short 3'-UTR from the end of exon E8 (open bars). The ZAC.DS plasmid contains the protein-coding sequences from E7 and E8 exons, except for 23 bases missing at the 5'-end of E7. The ZACdelta plasmid contains a small stretch of bases from E7, potentially coding for 3 amino acids if ATG2 is used, and the same E8 sequence (including the 3'-UTR) as ZAC.VA. Depending on the translation starting codon used (depicted as several in frame ATG codons), the plasmids can encode protein products of variable size as indicated (predicted molecular weight in kDa as adapted from [185]).

In order to study the function of ZAC1 (encoded by the ZAC.VA, ZAC.DS and ZACdelta plasmids) in prostate cancer cells, transient, stable, and inducible overexpression approaches were applied in LNCaP, 22Rv1 and PC3 cell lines.

3.4.2. Stable ZAC1 overexpression

ZAC1 is known to be a potential tumor suppressor gene having pro-apoptotic functions. At first, a stable transfection approach was chosen to judge the clonogenic potential of the transfected cells and in order to isolate stable overexpressing cell clones.

Initially the LNCaP and 22Rv1 cell lines, which endogenously express low *ZAC1* mRNA and protein levels, were stably transfected with ZAC.VA and ZAC.DS plasmids, in addition to the non-specific control lacZ plasmid. The number of cell colonies that survived the antibiotic selection upon transfection was visibly much lower in the ZAC.VA and ZAC.DS transfected cell plates than the lacZ-transfected cell plate (data not shown). This observation hinted at a potential anti-proliferative effect of ZAC1 in the LNCaP and 22Rv1 cell lines.

In a formal analysis, we wanted to compare the tumor suppressive potential of ZAC1 as encoded by the three plasmids ZAC.VA, ZAC.DS and ZACdelta by a clonogenicity assay. Their stable transfection into 22Rv1 cells resulted in the formation of many colonies by the cells transfected with the ZAC.VA plasmid, while ZAC.DS-stable clones were significantly fewer in number and only few colonies formed from the ZACdelta-transfected cells (Fig. 3.5.3.1). Thus one can conclude that the different ZAC1 plasmids influence cell survival and clonogenic potential to very different extents.

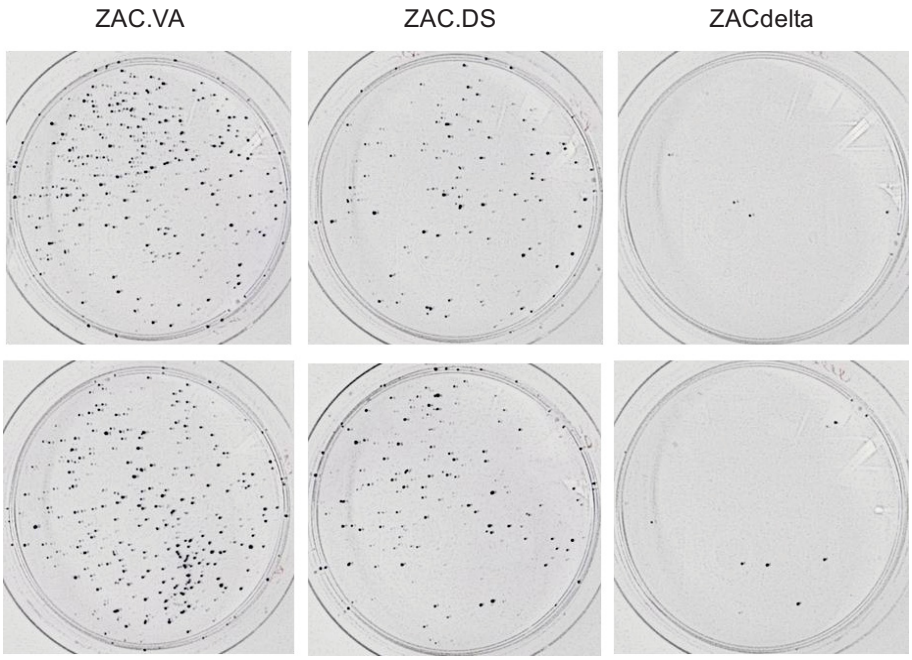

Fig. 3.4.2.1. Clonogenicity of stable ZAC1 clones. 22Rv1 cells were stably transfected with ZAC.VA (left panel), ZAC.DS (middle panel) and ZACdelta (right panel) plasmids and selected for the resistance gene contained in each plasmid by zeocin for four weeks. Plates were then stained with Giemsa.

Single *ZAC1*-expressing clones were isolated from LNCaP, 22Rv1 and PC3 cells, stably transfected with the ZAC.VA, ZAC.DS plasmids or control lacZ plasmids. The mRNA and protein expression levels of *ZAC1* in each clone were analyzed by means of qRT-PCR and immunoblotting analyses, respectively. As ZACdelta evidently prevented clone formation, no stable ZACdelta clones have been isolated.

As judged by qRT-PCR, true positive cell clones from all three cell lines expressed *ZAC1* mRNA several fold higher than control LacZ clones. The difference of *ZAC1* mRNA expression between the positive clones and the control clones was much higher in LNCaP and 22Rv1 cells than in PC3 cells, which have endogenously high *ZAC1* expression (Fig. 3.4.2.2 left panels). Subsequently, ZAC1 protein levels of the positive clones were analyzed by immunoblotting. Unexpectedly, *ZAC1* mRNA positive clones from all three cell lines exhibited very similar ZAC1 protein levels to the LacZ control cell clones (Fig. 3.4.2.2 right panels). As a positive control, a protein lysate from PC3 cells transiently transfected with *ZAC1* for 48 h exhibited much higher ZAC1 protein.

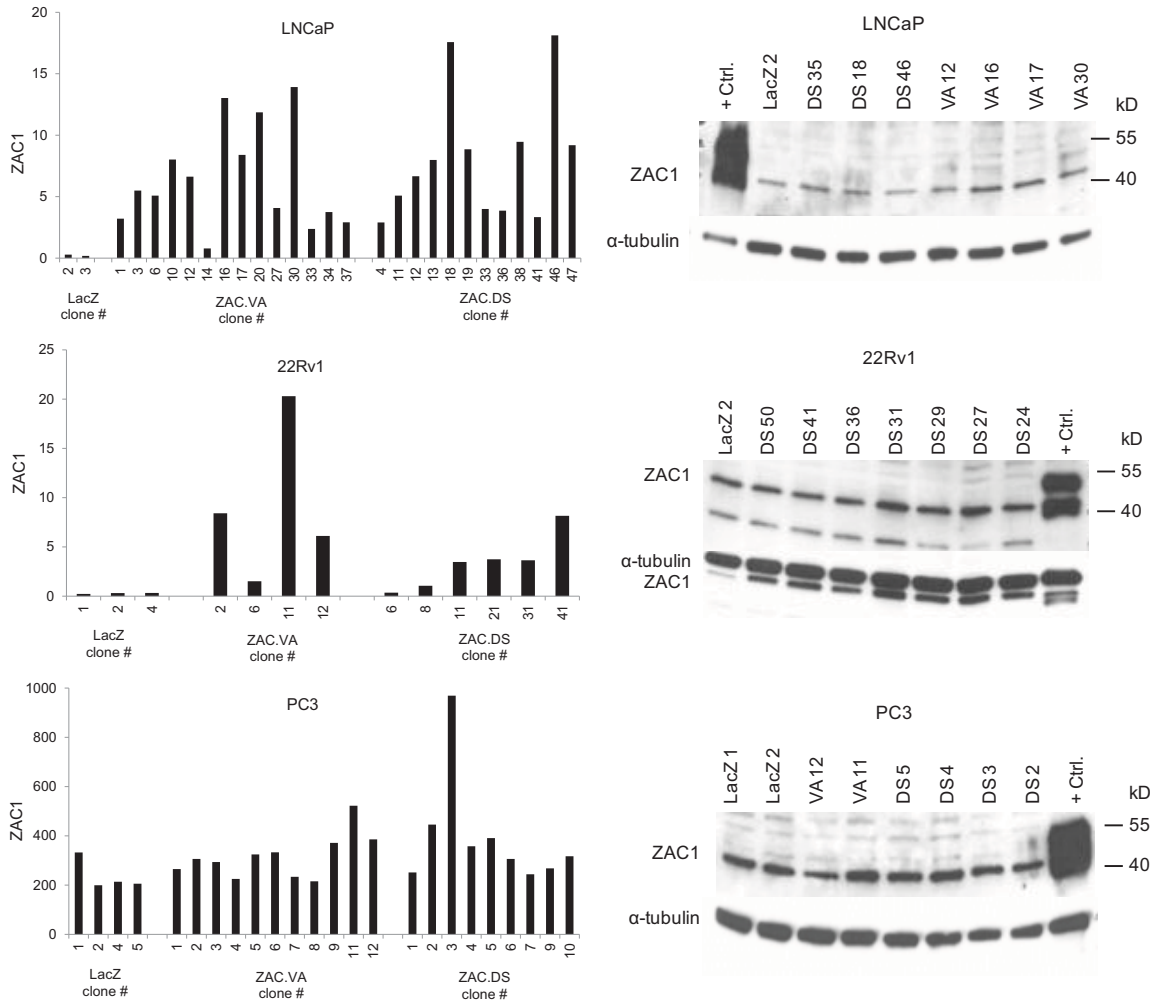

Fig. 3.4.2.2. ZAC1 expression in stably transfected clones. LNCaP, 22Rv1 and PC3 cells were stably transfected with ZAC.VA, ZAC.DS and as control lacZ plasmids. Relative mRNA expression of *ZAC1* was assessed by qRT-PCR (left panels). Protein levels were determined by immunoblotting using protein lysates from several *ZAC1*-positive (as judged by mRNA) and control (lacZ) clones (right panels). As a positive control for ZAC1 protein, lysates from transiently transfected PC3 cells with ZAC.VA (for LNCaP clones blot) or ZAC.DS (for 22Rv1 and PC3 clones blot) were used. The qRT-PCR measurements were performed in duplicate and the average was used, whereby less than 10% variation between duplicates was accepted.

In order to determine the general level of ZAC1 overexpression in the stable transfections, the stable colonies of each plate of 22Rv1 and LNCaP cells transfected with either lacZ, ZAC.VA or ZAC.DS-tranfected 22Rv1 and LNCaP cells were pooled after 4-5 weeks of selection and RNA was isolated. The resulting polyclonal populations exhibited increased ZAC1 mRNA levels following ZAC.VA or ZAC.DS transfection as compared to the lacZ-stable transfected cells (Fig. 3.4.2.3), similar to the single clones. Unfortunately, no protein lysates were prepared from these polyclonal populations, and therefore their expression of ZAC1 on the protein level was not determined. Taken together, the above

experiments show that *ZAC1* mRNA can be overexpressed after transfection of ZAC.VA or ZAC.DS, but protein overexpression does not necessarily follow.

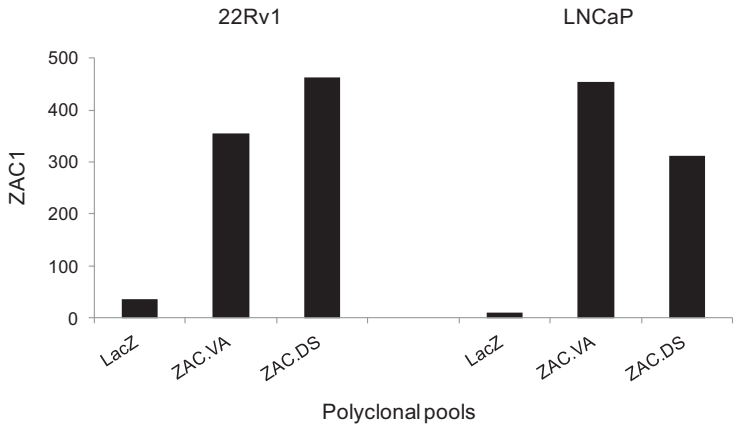

Fig. 3.4.2.3. Overexpression of ZAC1 mRNA in stably transfected polyclonal pools. *ZAC1* mRNA expression was measured relative to *TBP* by qRT-PCR in polyclonal pools from 22Rv1 and LNCaP cells stably transfected with ZAC.VA, ZAC.DS or lacZ (control) harvested 4 weeks after transfection. The measurements were performed in duplicate and the average was used, whereby less than 10% variation between duplicates was accepted.

3.4.3. Inducible ZAC1 overexpression

In a second series of experiments, pcDNA4/TO-ZAC1 (zeocin resistance) expression plasmids were stably transfected into LNCaP cells. Different from the above experiments, however, the host cells (called LNCaP 6TR) in this case stably express the Tet-repressor protein whose expression is ensured by addition of the antibiotic blasticidin, thereby selecting for the 6TR expression vector which contains an according resistance gene. Eventually upon transfection and selection with zeocin and blasticidin, surviving cell clones have stably integrated the *ZAC1* plasmid and maintained the integrated Tet-repressor cassette. In the absence of tetracyline the expression from the transgene *ZAC1* is ideally constantly repressed. The inducibility of presumable ZAC1-positive clones was tested by qRT-PCR analysis of cDNA from cell clones incubated with or without tetracycline for 48 h (Fig. 3.4.3 upper panel).

In many of the clones *ZAC1* overexpression could be induced by tetracycline. However, several clones exhibited relatively high *ZAC1* expression also without tetracycline. This variation may be attributed to the integration site of the *ZAC1* plasmid, multiple integrated ZAC1 plasmids per cell or to insufficient repression by the Tet-repressor protein. The inducibility of several positive clones was also tested on the protein level by means of

immunoblotting. However, no significant differences in the induced vs. uninduced cells were observed for any of the tested clones (Fig. 3.4.3 lower panel).

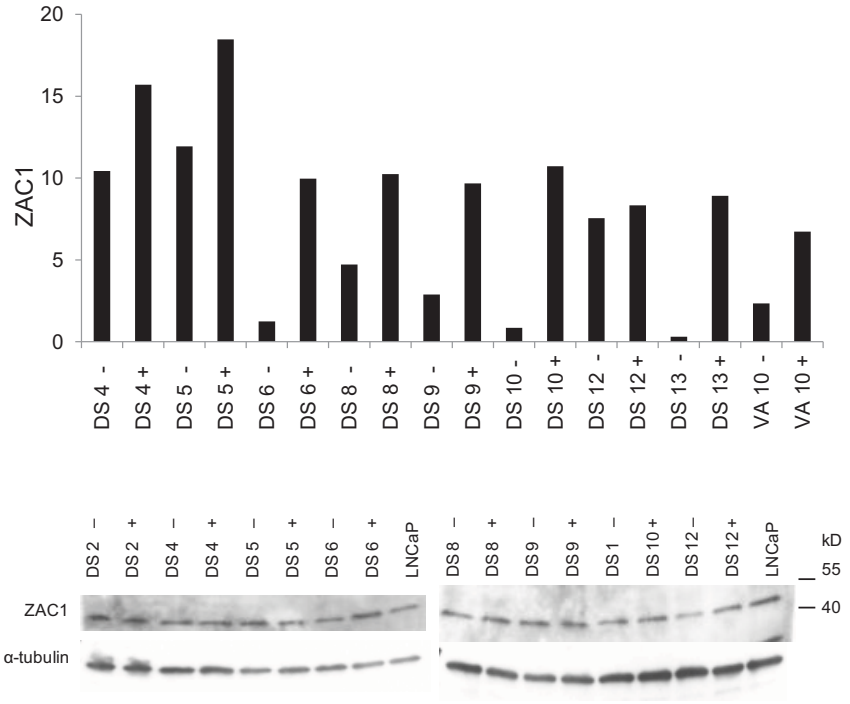

Fig. 3.4.3. ZAC1 mRNA and protein levels of stably transfected inducible ZAC1 clones in the LNCaP6TR cell line. Expression of *ZAC1* was measured relative to *TBP* mRNA by qRT-PCR (upper panel) and ZAC1 protein levels were analysed by immunoblotting (lower panel) in LNCaP6TR cell clones stably transfected with ZAC.VA or ZAC.DS and treated (+) or untreated (-) with tetracycline for ZAC1 induction. Non-transfected protein lysate presenting the endogenous ZAC1 protein level in LNCaP was included for comparison in the immunoblotting assay. The qRT-PCR measurements were performed in duplicate and the average was used, whereby less than 10% variation between duplicates was accepted.

3.4.4. Transient ZAC1 overexpression

The ZAC.VA and ZAC.DS plasmids and as a control the lacZ plasmid were transfected for 24 - 72 h into the LNCaP, 22Rv1 or PC3 cell lines. Transient transfection of both *ZAC1* expression plasmids resulted in increased *ZAC1* mRNA levels in all three cell lines as compared to the levels in control-transfected cells as assessed by qRT-PCR. The increase in *ZAC1* mRNA was highest (several hundred-fold) in PC3 cells (Fig. 3.4.4 left side), which express also the highest endogenous levels of *ZAC1*. Similarly the increases in ZAC1 protein levels were much stronger in PC3 than in 22Rv1 and LNCaP cells (Fig. 3.4.4 right side). The ZAC1 protein level of transfected LNCaP cells was only very slightly higher than that of control cells, in which it is very low. In 22Rv1 *ZAC1* mRNA and protein overexpression were stronger than in LNCaP, but significantly lower than in PC3 cells.

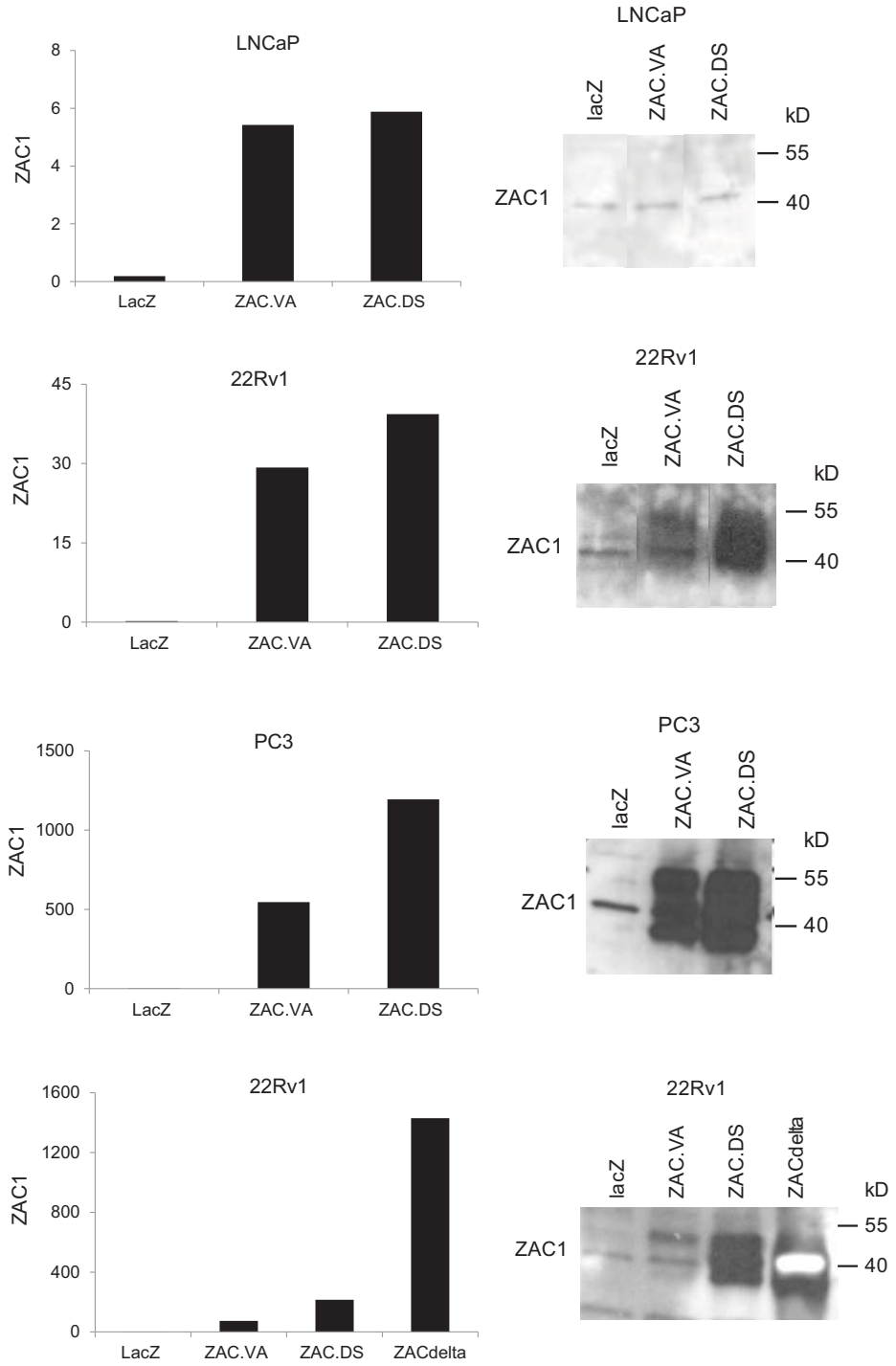

Fig. 3.4.4. ZAC1 expression in transiently transfected cells. LNCaP, 22Rv1 and PC3 cells (as indicated) were transiently transfected with ZAC.VA, ZAC.DS and lacZ plasmids as a control. Additionally, 22Rv1 was transfected with the ZACdelta plasmid (bottom panel). The expression of *ZAC1* relative to *TBP* mRNA was measured using qRT-PCR (left panels). ZAC1 protein levels were analyzed by immunoblotting. Approximate protein sizes are indicated. The qRT-PCR measurements were performed in duplicate and the average was used, whereby less than 10% variation between duplicates was accepted.

Different transfection efficiencies of the three cell lines may be one factor that could explain these observations, as it is known that LNCaP cells are more difficult to transfect than PC3 and 22Rv1 cells. This is evident from the mRNA measurements revealing levels of *ZAC1* mRNA that are orders of magnitude lower in LNCaP than in the other cell lines. However, since the latter two cell lines have similar transfection efficiencies, other reasons must be involved such as cell-specific differences in translation efficiency and protein stability. Furthermore, there were clear differences in the degree of protein overexpression from the ZAC.VA and ZAC.DS plasmids, the latter producing higher mRNA and protein levels. Therefore, one can hypothesize that differences in the *ZAC1* cDNA used might influence transcription and translation and stability of the mRNA and protein products. Since the difference between ZAC.VA and ZAC.DS resides mainly in the presence of a 5'-UTR and since untranslated regions of the cDNA can regulate mRNA stability and translational efficiency, one may suppose that the 5'-UTR might be involved in the observed lower *ZAC1* levels upon transient transfection. As it was described in the literature that the natural *ZAC1* splice isoforms, one containing two protein-coding exons and the other- only one, have different functions [185], we hypothesized that they could also be differently regulated. To examine this issue, the pcDNA4/TO.ZACdelta plasmid containing the short *ZAC1* isoform with only one protein-coding exon (see Chap. 3.4.1 for details) was created and transfected into the 22Rv1 cell line in parallel with the two other ZAC1-coding transcripts. Remarkably, the resulting amounts of ZACdelta mRNA and protein were much higher than the levels achieved by ZAC.VA and ZAC.DS (Fig. 3.4.4).

3.5. Regulation of ZAC1 protein/RNA stability

In order to find out whether protein degradation might underlie the differences in ZAC1 protein levels in cells transfected with the different ZAC expression plasmids, the proteasome was inhibited by MG-132 in transfected cells.

3.5.1. Influence of proteasome inhibition on ZAC1 levels in transiently transfected cells.

Treatment with the proteasome inhibitor stabilized ZAC1 protein levels in cells transiently transfected with ZAC1 expression plasmids but did not affect the level of endogenous ZAC1 in either control-transfected cells or untransfected cells (Fig. 3.5.1 left panels). Unexpectedly, a similar effect was also observed for the mRNA levels of the transfected cells (Fig. 3.5.1 right panels). Thus, inhibition of the proteasome either stabilizes the mRNA of the exogenous *ZAC1* or it enhances its rates of transcription or translation into protein. This effect was most clearly observed with the transfected ZAC.VA and ZAC.DS plasmids. Due to the extremely high ZAC1 protein level produced by the ZACdelta plasmid, it was difficult to discern whether it was enhanced by MG-132 treatment.

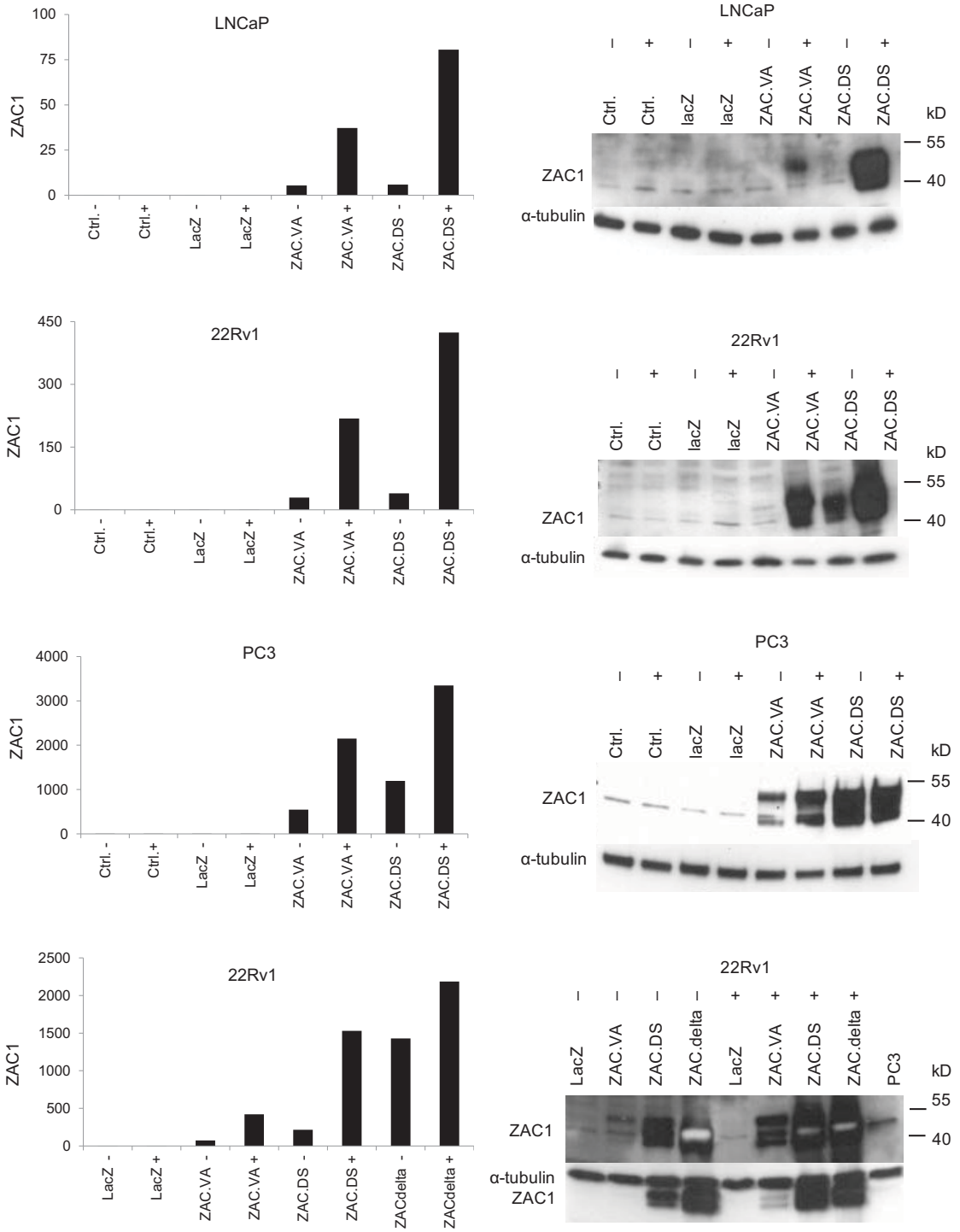

Fig. 3.5.1. Effect of proteasomal inhibition on ZAC1 expression in transiently transfected cells. LNCaP, 22Rv1 and PC3 cells (as indicated) were transiently transfected with ZAC.VA, ZAC.DS or lacZ plasmids as a control. Additionally, 22Rv1 was transfected with the ZACdelta plasmid. 24 h after transfection the cells were treated with the proteasome inhibitor MG-132 at a final concentration of 1 μM for 24 h, after which RNA and protein lysates were prepared. The expression of *ZAC1* relative to *TBP* mRNA was measured by qRT-PCR (left panels). ZAC1 protein levels were analyzed by immunoblotting (right panels). The qRT-PCR measurements were performed in duplicate and the average was used, whereby less than 10% variation between duplicates was accepted.

3.5.2. Influence of proteasome inhibition on ZAC1 levels in stable and inducible ZAC1 clones

As proteasome inhibition resulted in increased *ZAC1* mRNA and protein levels in transiently transfected cells, it was tested whether it had an analogous effect in stable ZAC1-overexpressing clones. Constitutive 22Rv1 and inducible LNCaP6TR ZAC1-overexpressing cell clones were treated for 24 h with MG-132 and compared to non-treated cells for their ZAC1 protein and RNA levels. Similar to its effect on the transiently overexpressed ZAC1, the proteasome inhibitor increased both mRNA and protein levels in the stably expressing and inducible ZAC1 clones, but not in lacZ-transfected controls or in uninduced ZAC1 clones (Figs. 3.5.2.1 and 3.5.2.2). Importantly, the ZAC1 protein level of the induced clone 22Rv1 DS2 was only slightly higher than in uninduced cells, increasing dramatically after MG-132 treatment (Fig. 3.5.2.2 right panel) As in previous experiments, proteasome inhibition also enhanced *ZAC1* mRNA levels (Fig. 3.5.2.2 left panel). These results suggest that a process that can be inhibited by the MG132 reagent may be involved in the regulation of *ZAC1* translation efficiency and mRNA and protein stability.

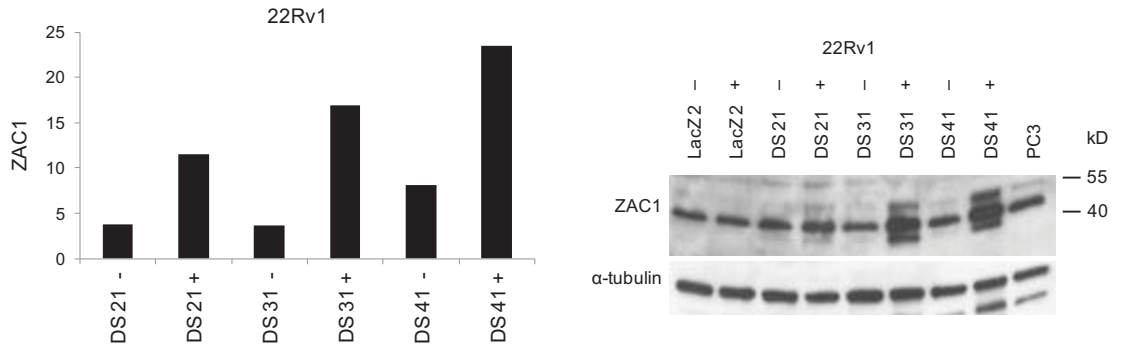

Fig. 3.5.2.1. Induction of ZAC1 mRNA and protein levels by proteasomal inhibition. *ZAC1* mRNA levels relative to *TBP*, assessed by qRT-PCR (left panel) and ZAC1 and α-tubulin (as control) protein levels, assessed by immunoblotting (right panel) of stable ZAC1-overexpressing 22Rv1 clones, and, in the immunoblot, control lacZ clones, treated (+) or untreated (-) with the proteasome inhibitor MG-132 at 1 μM. A protein lysate of untreated PC3 cells was included in the immunoblot analysis as a reference for protein size and relative quantity. The qRT-PCR measurements were performed in duplicate and the average was used, whereby less than 10% variation between duplicates was accepted.

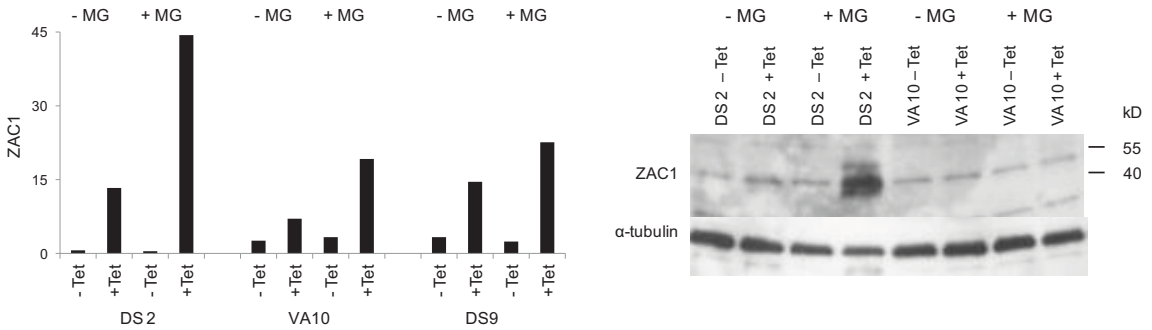

Fig. 3.5.2.2. Induction of ZAC1 mRNA and protein levels by proteasomal inhibition. *ZAC1* mRNA levels relative to *TBP*, measured by qRT-PCR (left panel) and ZAC1 protein levels, assessed by immunoblotting (right panel) of tetracycline-induced (+Tet) or uninduced (-Tet) ZAC1-overexpressing LNCaP6TR clones being treated (+MG) or untreated (-MG) with the proteasome inhibitor MG-132 at 1 μM. The qRT-PCR measurements were performed in duplicate and the average was used, whereby less than 10% variation between duplicates was accepted.

3.6. ZAC1 target genes

ZAC1 protein acts as a transcription factor and transcriptional co-activator of p53 and nuclear receptors, like the AR, and has been shown to exert tumor suppressive functions in cancer cells. ZAC1 has been proposed to be the single protein, apart from p53, able to induce both cell cycle arrest and apoptosis. However, the mechanism of their induction by ZAC1, especially human ZAC1, is less well studied. It was therefore important to investigate the ZAC1-induced transcriptional program.

Zac1 was proposed to be a major regulator of a transcriptional network of genes regulating mouse embryonic development and growth, including the imprinted genes *Cdkn1c*, *Dlk1*, *Gtl2* (homolog of human *MEG3*), *H19* and *Igf2*. Since we found the mRNA levels of many of these genes, including *ZAC1/PLAGL1* itself, to be significantly differentially expressed in prostate cancer (see Chap. 3.2), we hypothesized that ZAC1 downregulation may be related or even functionally responsible.

Furthermore, the *CDKN1A* gene, a known p53 target gene, has been proposed to be induced by mouse Zac1 in p53-dependent and –independent ways. The encoded p21 protein can induce cell cycle arrest and cellular senescence. Thus its induction by human ZAC1 in cancer cells may contribute to the reported anti-proliferative activity of ZAC1.

In order to study the potential tumor suppressive function of ZAC1 in prostate cancer, and especially its ability to induce the differentially expressed imprinted genes from the imprinted gene network and *CDKN1A*, we employed different *ZAC1* overexpression approaches and a reporter assay.

3.6.1. Induction of imprinted genes by ZAC1

To test if ZAC1 can induce the expression of the imprinted genes found to be deregulated in prostate cancer, their expression was measured in transiently *ZAC1*-overexpressing 22Rv1 cells, transfected with either of the three ZAC1 expression plasmids (Fig. 3.6.1.1), and in polyclonal ZAC1-overexpressing pools of LNCaP and 22Rv1 cells, 4 weeks after transfection with ZAC.VA or ZAC.DS plasmids (Fig. 3.6.1.2).

Among the assessed imprinted genes, *H19* and *CDKN1C* were induced by more than 200-fold following transient ZAC1 overexpression in 22Rv1 cells (Fig. 3.6.1.1). The observed effect was most pronounced when ZAC.DS and ZACdelta plasmids were transfected, while ZAC.VA plasmid had a comparatively slight effect. A modest induction was observed for *IGF2*, *LIT1* and *PEG10* genes. Similar to *H19* and *CDKN1C*, the induction of *IGF2* was greater in ZAC.DS and ZACdelta-transfected cells than in ZAC.VA-transfectants. Specific upregulation by the ZACdelta form, in contrast to slight effects by the other two ZAC1 forms, involved *SGCE*, *PON2*, *PEG3* and *HYMAI* genes. Expression

of the putative ZAC1 target genes *MEG3* and *DLK1* was hardly detectable in the analyzed prostate tissues and cell lines and was not induced in any of the overexpression experiments (data not shown).

To confirm *CDKN1C*, *IGF2,* and *LIT1* as ZAC1 targets, their expression was also measured in stable polyclonal pools of LNCaP and 22Rv1 cells transfected with ZAC.VA and ZAC.DS (Fig. 3.6.1.2). In contrast to the strong induction of *CDKN1C* expression by transient ZAC1 overexpression, the expression of this gene was rather unchanged in the stable pools. The reason might be downregulation of this gene or selection against its expression in the stable clones as its function is detrimental to cell survival. Like in the transient ZAC1-overexpression, *LIT1* and *IGF2* genes were also induced in the stably transfected cell pools.

The different ZAC1 forms encoded by the ZAC.VA, ZAC.DS and ZACdelta expression plasmids exerted differential influences on the induction of the assessed target genes. These differences could be based on different stability of the mRNA products and/or may reveal different functional properties of the respective encoded ZAC1 protein forms.

In order to determine whether the robust induction of *CDKN1C* observed after transient ZAC1 overexpression in 22Rv1 cells resulted also in an increase of the protein product $p57^{KIP2}$, a protein immunoblot was conducted using protein lysates from the same transient ZAC1 overexpression experiment. Protein levels of $p57^{KIP2}$ were substantially induced by ZAC.DS and even more strongly by ZACdelta plasmid, but only weakly by the ZAC.VA plasmid, as compared to the almost undetectable $p57^{KIP2}$ level in lacZ-transfected 22Rv1 cells (Fig. 3.6.1.3). The housekeeping GAPDH protein level, used here as a loading control, was similar in all samples.

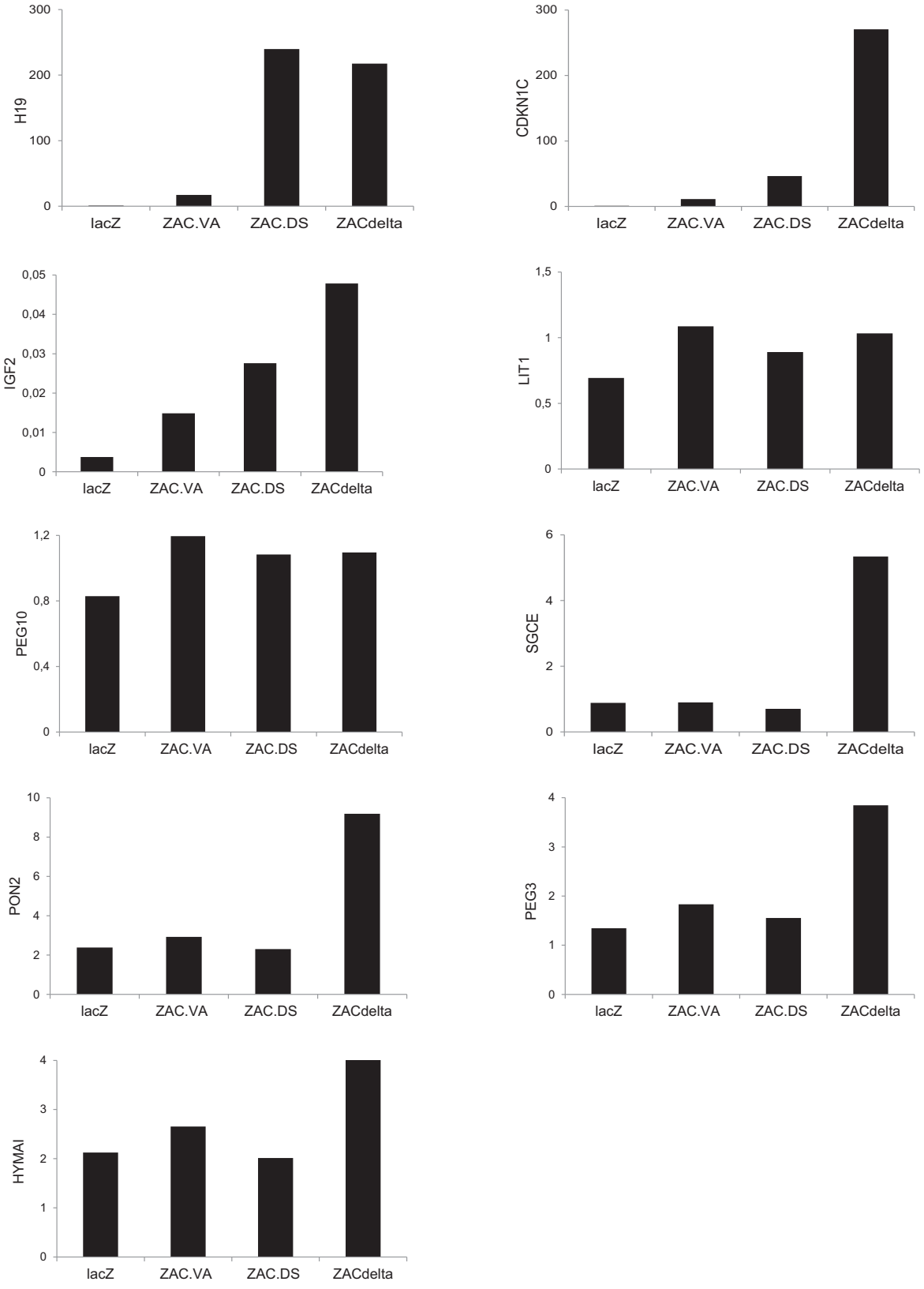

Fig. 3.6.1.1. Induction of imprinted genes by ZAC1 transient overexpression. Expression of the indicated imprinted genes relative to *TBP* mRNA was measured by qRT-PCR in 22Rv1 cells transiently transfected with ZAC.VA, ZAC.DS, ZACdelta or lacZ (control) plasmids. The measurements were performed in duplicate and the average was used, whereby less than 10% variation between duplicates was accepted.

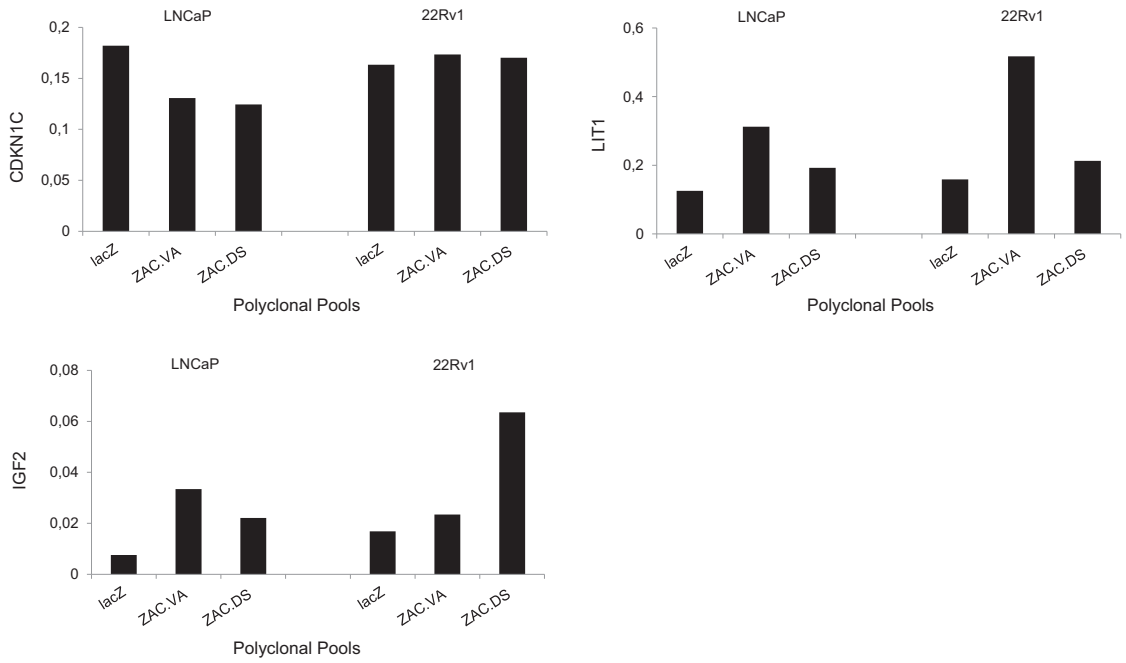

Fig. 3.6.1.2. Induction of CDKN1C, LIT1 and IGF2 genes by ZAC1 in polyclonal pools. mRNA expression of the indicated genes relative to *TBP* mRNA was measured by qRT-PCR in polyclonal pools of LNCaP and 22Rv1 cells stably transfected with ZAC.VA, ZAC.DS and lacZ (control) plasmids. The measurements were performed in duplicate and the average was used, whereby less than 10% variation between duplicates was accepted.

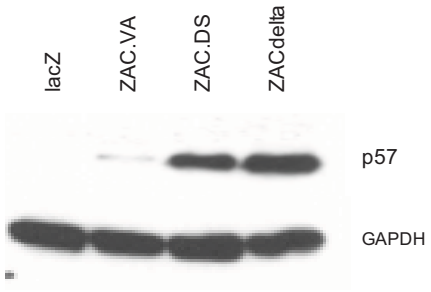

Fig. 3.6.1.3. Induction of p57 protein by ZAC1 transient overexpression. p57 and GAPDH proteins were detected by immunoblot analysis of 22Rv1 cells transiently transfected with ZAC.VA, ZAC.DS, ZACdelta or lacZ (control) plasmids. The expected protein size of p57 is indeed 57 kDa. GAPDH was detected at 35 kDa as expected.

3.6.2. Induction of CDKN1A expression and promoter-driven reporter activity by ZAC1

The ability of ZAC1 to induce the expression of the *CDKN1A* gene was assessed by transient ZAC1-overexpression in 22Rv1 cells (Fig. 3.6.2.1 A) and in polyclonal ZAC1-overexpressing pools of LNCaP and 22Rv1 cells, transfected with ZAC.VA or ZAC.DS plasmids (Fig. 3.6.2.1 B).

CDKN1A mRNA expression was only moderately induced by the transient transfection of the ZAC.VA and ZAC.DS vectors, while it was downregulated by the ZACdelta plasmid.

Similarly, the induction of *CDKN1A* gene was relatively moderate in the stable polyclonal ZAC1-overexpressing cell pools and was higher in cells transfected with ZAC.VA than ZAC.DS in both 22Rv1 and LNCaP cell lines.

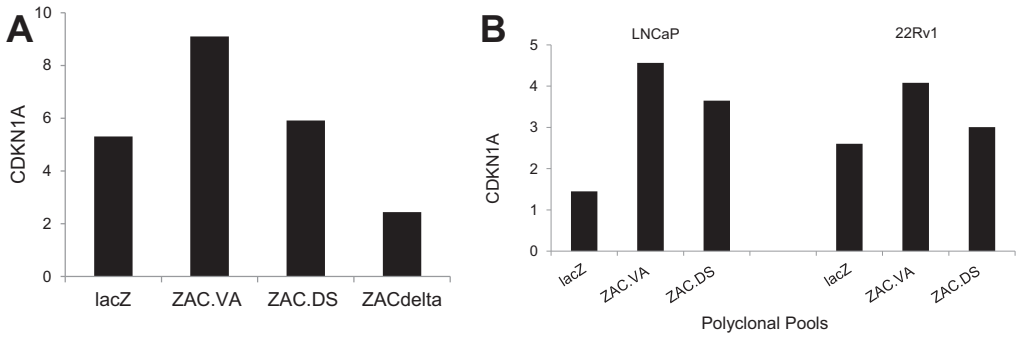

Fig. 3.6.2.1. Induction of CDKN1A expression by ZAC1. mRNA expression of CDKN1A relative to *TBP* mRNA was measured by qRT-PCR in A) 22Rv1 cells transiently transfected with ZAC.VA, ZAC.DS, ZACdelta or lacZ (control) plasmids; or B) polyclonal pools of LNCaP and 22Rv1 cells stably transfected with ZAC.VA, ZAC.DS and lacZ (control) plasmids. The qRT-PCR measurements were performed in duplicate and the average was used, whereby less than 10% variation between duplicates was accepted.

The *CDKN1A* gene, encoding the $p21^{CIP1}$ protein, contains two p53-binding sites and six SP1-response elements in its promoter. Zac1 has been demonstrated to be able to interact directly with the Sp1-responsive element in the p21 promoter and enhance the transactivation activity of Sp1.

In order to test the functional ability of transfected ZAC1 to enhance transcription from a p21 promoter-driven reporter, 22Rv1 cells were transiently cotransfected with the ZAC1-expression plasmids and a p21-Luc reporter plasmid (see Chap. 2.2.22.2). All ZAC1-expression plasmids enhanced the luciferase activity by ~2 fold in comparison to the control lacZ plasmid. Thus, ZAC1 can transactivate the *CDKN1A* promoter in 22Rv1 cells.

This result confirms the upregulation of *CDKN1A* detected in ZAC.VA and ZAC.DS-transfected 22Rv1 cells but does not match with the *CDKN1A* downregulation in ZACdelta-transfected cells (compare Fig. 3.6.2.1 A with Fig. 3.6.2.2).

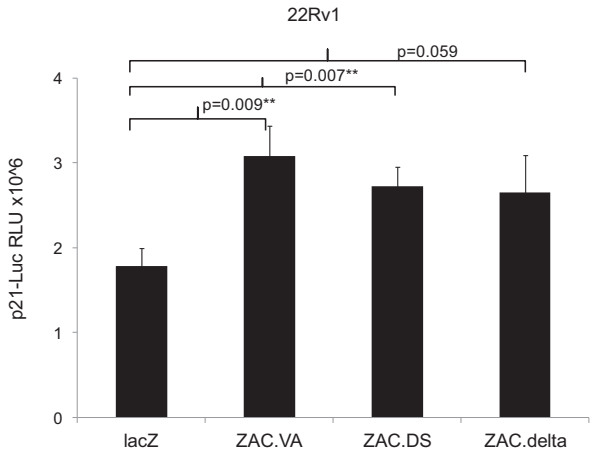

Fig. 3.6.2.2. Induction of p21-Luc reporter gene by ZAC1. Luficerase activity driven by the p21-Luc reporter gene was measured by luminometry in 22Rv1 cells transiently transfected with ZAC1 expression plasmids. The data is shown as mean values of biological triplicates with standard deviation presented as error bars. T-test in Excel was used to calculate significance levels, **p<0.01.

3.7. Influence of ZAC1 on AR signaling

Luciferase reporter assays analyzing the androgen response were performed in combination with ZAC1 siRNA downregulation in order to assess its influence on AR signaling.

The response of prostate cells to androgens involves translocation of the AR upon ligand binding to the nucleus, where it binds to hormone response elements of androgen-responsive genes, subsequently stimulating their transcription. A useful approach to analyze AR function or new target genes is an in vitro reporter assay using plasmids in which androgen responsive elements drive luciferase reporter gene expression. Here the probasin promoter luciferase reporter plasmid (Pb-Luc), containing a fragment from the rat probasin gene promoter, and a reporter driven by three tandem repeats of the androgen response element (ARE-Luc) were used to study the influence of ZAC1 on the androgen response in PC3 cells.

Since AR expression in PC3 cells is very low, exogenous AR was co-transfected. PC3 cells have comparatively high amounts of ZAC1 mRNA and protein, and one approach was to silence it with siRNA upon androgen stimulation. *ZAC1* mRNA levels could be diminished by several cycles of siRNA treatment against ZAC1 compared to siRNA

against an irrelevant target in PC3 cells (data not shown). SiRNA treatment also resulted in diminished ZAC1 protein levels in PC3 cells in comparison to control siRNA (Fig. 3.7.1).

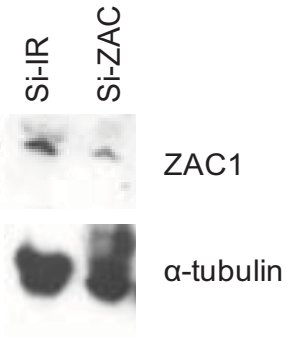

Fig. 3.7.1. ZAC1 protein downregulation by siRNA. ZAC1 and α-tubulin proteins were detected by immunoblotting in PC3 cells transfected with 10 nM siRNA against ZAC1 (si-ZAC) or an irrelevant target (si-IR).

Cells in which no AR had been transfected exhibited low activity of Pb-Luc and ARE-Luc even in the presence of the synthetic androgen R1881 (Fig. 3.7.2). In contrast, transfection of AR led to a moderate increase of the basal Pb-Luc activity but not of ARE-Luc. One can conclude that the AR can induce Pb-Luc activity to a certain degree in an androgen-independent fashion. Both reporters were induced by stimulation with R1881 which was more significant with the ARE-Luc reporter. Silencing of ZAC1 by siRNA, as compared to the effect of irrelevant (IR) siRNA, significantly reduced androgen-induced Pb-Luc and ARE-Luc reporter activation, but affected reporter gene activity only weakly in the absence of R1881. The results of these experiments suggest that ZAC1 may function as a co-activator of the AR.

Alternatively, the influence of ZAC1 on AR function was assessed upon co-transfection of the ARE-Luc reporter with the AR and ZAC1 expression vectors (Fig. 3.7.3). In the absence of the AR, androgen stimulation of the ZAC1-transfected PC3 cells induced ARE-Luc activity only weakly in comparison to lacZ-transfected cells. The presence of AR led to an increase in ARE-Luc activity in all transfectants, even in the absence of R1881. The increase was notably higher in the ZAC.VA and ZACdelta-transfected cells than in the ZAC.DS- and lacZ-transfectants (Fig. 3.7.3 left panel). Nevertheless, the total reporter activity in these controls was about 100-fold lower (Fig. 3.7.3 left panel, notice the difference in the ordinate scale) than upon induction with R1881 in the presence of transfected AR. All three ZAC1 isoforms significantly enhanced R1881-stimulated ARE-Luc activity by about 2-fold in PC3 cells, as compared to lacZ-transfected cells (Fig. 3.7.3 right panel).

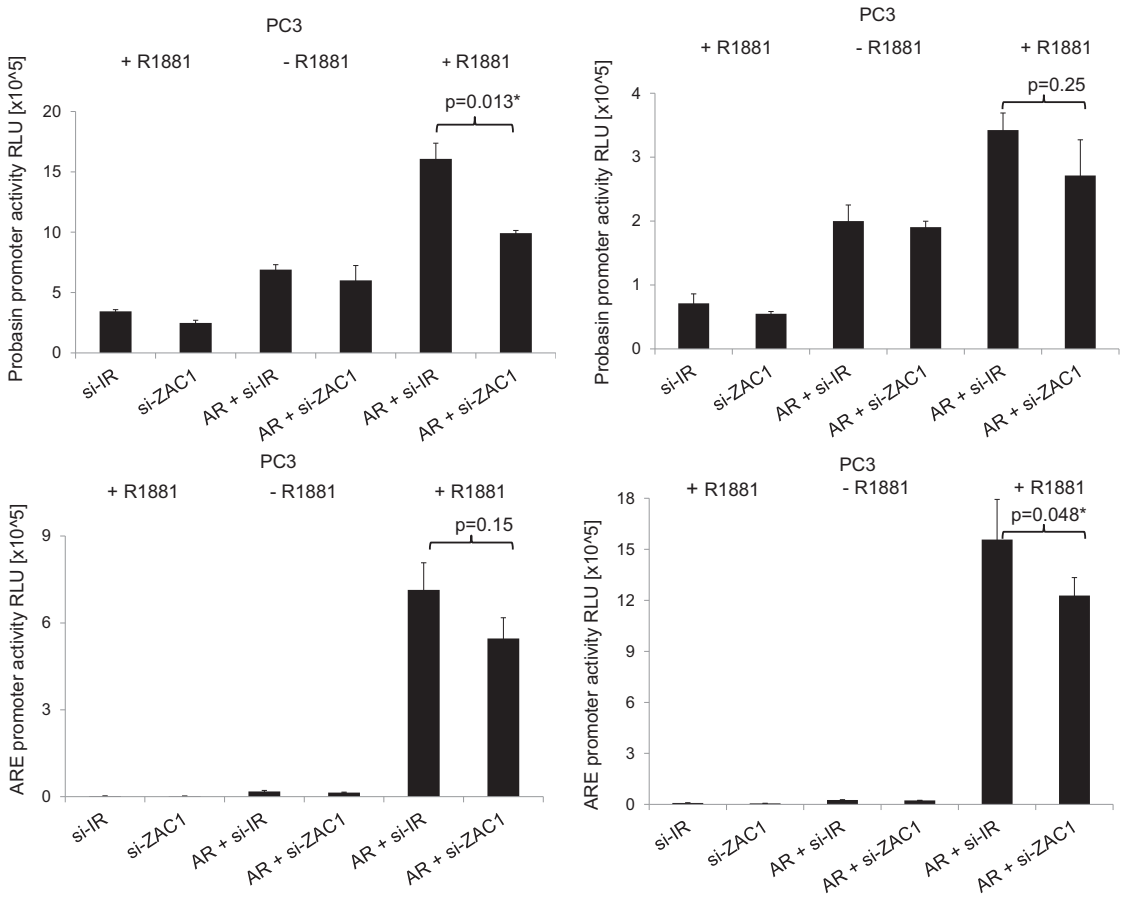

Fig. 3.7.2. Effect of ZAC1 siRNA-mediated downregulation on the androgen response of AR-transfected PC3 cells. Activity of Pb-Luc (upper panels) and ARE-Luc (lower panels) was measured by luminometry in PC3 cells transfected with AR (or not) and with or without R1881 stimulation, upon downregulation of ZAC1 with siRNA (siZAC) or treatment with control siRNA (si-IR). The data is shown as mean values of biological triplicates with standard deviation presented as error bars. T-test in Excel was used to calculate significance levels, **p<0.01.

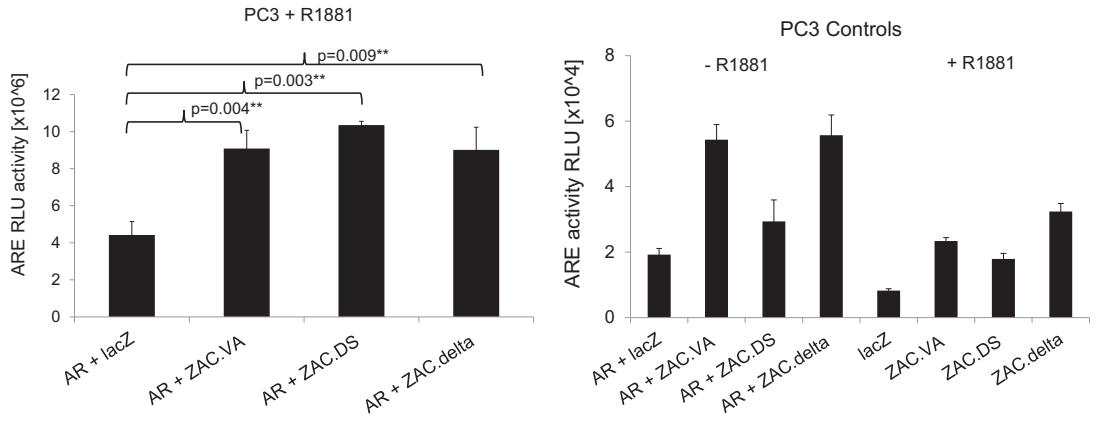

Fig. 3.7.3. Effect of ZAC1 on the androgen response of AR-transfected PC3 cells. Activity of ARE-Luc was measured by luminometry in PC3 cells transfected with AR, ZAC1 and lacZ as control upon stimulation with R1881 (left panel). Control transfections without R1881 stimulation (right panel, left side) and without AR expression plasmid but treated with R1881 (right panel, right side) exhibited low ARE activity. The data is shown as mean values of biological triplicates with standard deviation presented as error bars. T-test in Excel was used to calculate significance levels, **p<0.01.

4. Discussion

4.1. Expression and regulation of TFPI and TFPI2 in prostate cancer

Although the expression of the potential tumor suppressor genes *TFPI* and *TFPI2* was not significantly different between benign and cancerous prostate tissues, *TFPI2* was very heterogeneously expressed among the single tissue samples. Interestingly, a significant negative correlation was observed between the expression values of *TFPI* and *TFPI2* in the prostate cancer tissues, hinting at the presence of reciprocal feedback regulatory mechanisms that may adjust their expression in order to control their protein function.

As it was reported that CpG hypermethylation and repressive histone modifications are involved in the silencing of *TFPI2* in many cancer types [72-76, 187], bisulfite sequencing and chromatin immunoprecipitation were applied to study the epigenetic status of the *TFPI2* promoter in prostate cancer. While unmethylated in normal prostate and urothelium tissues, as well as in the PC3 cell line and two prostate cancer tissues with high *TFPI2* expression, the *TFPI2* promoter was partially methylated in the LNCaP cell line and two prostate cancer tissues with low *TFPI2* expression. These results suggest that promoter CpG hypermethylation associates with a decreased *TFPI2* expression in some cases of prostate cancer, similar to the observations in other cancer types [72-76].

Being part of an imprinted gene locus, the maternally expressed *TFPI2* gene could be regulated by epigenetic mechanisms affecting the whole locus or parts of it [72-74, 186, 188].

In order to monitor if a mechanism affecting the imprinted gene cluster at 7q21 was involved in the regulation of *TFPI2* expression and of the neighboring PON2 and SGCE imprinted genes in prostate tissues, the epigenetic status of the ICR/DMR was studied. The expression of *TFPI2* correlated well with that of *SGCE* and less strongly with that of *PON2* in prostate tumor tissues. Thus it can be suspected that a locus-specific co-regulatory mechanism might be present, more strongly affecting adjacent genes than more distant genes in the cluster. The close proximity of *TFPI2* and SGCE to the DMR may explain the stronger dependence of their expression on the epigenetic status of the DMR expression than the more remote imprinted genes in the locus like *PON2*. Indeed, in LNCaP cells, where *SCGE* and *TFPI2* genes were feebly expressed, the DNA methylation pattern of the DMR was severely disturbed, presenting no fully methylated or fully unmethylated alleles, but alleles with a mixture of methylated and unmethylated CpG sites. In comparison, in PC3 cells, where *TFPI2* and *SGCE* were more strongly expressed than in LNCaP, the methylation pattern of the DMR was intact. In both PC3 and LNCaP cell lines, however, the histone modifications associated with the DMR suggested a relatively open chromatin state. In contrast, the *TFPI2* promoter exhibited a more closed

chromatin state in the low *TFPI2*-expressing LNCaP cells. One may thus conclude that DNA hypermethylation and repressive histone modifications specifically associated with the *TFPI2* promoter rather than the DMR are likely to play a role in the downregulation of *TFPI2* in prostate cancer.

The disturbance in the DNA methylation of the DMR, observed only in LNCaP, may affect the expression of the nearby *SGCE* and *TFPI2* genes, and likely extend to silence *TFPI2* transcription, although DMR chromatin remains accessible.

As our later studies of the 7q21 imprinted gene locus showed, the expression levels of *TFPI2* and of the nearby *SGCE* and *PEG10* genes, situated around the 7q21 DMR, correlated positively in prostate cancer tissues too. However, there was a strong negative correlation between the expressions of the paternally expressed *SGCE* and *PEG10* genes with that of the maternally expressed and more distant *PPP1R9A* gene, which was overexpressed in prostate cancer. We thus hypothesized that the expression of certain paternally and maternally expressed imprinted genes in the 7q21 locus may be reciprocally regulated. In our later experiments we showed that the reciprocal expression affected only specific genes from the locus and could not be attributed to changes of the 7q21 DMR methylation status (see Chap. 4.2.3.1).

4.2. Expression, regulation and potential function of imprinted genes in prostate cancer

4.2.1. Hypotheses

In a pilot project on the expression and regulation of the *TFPI2*, *SGCE*, and *PON2* genes from the 7q21 cluster of imprinted genes (See Chap. 3.1 and 4.1), we found that the expression of *TFPI2* and *PON2* is unstable in prostate cancer tissues and cell lines and was accompanied by epigenetic disturbances at the 7q21 DMR and *TFPI2* promoter regulatory regions. Specifically, the increased methylation at *TFPI2* promoter associated with its decreased expression in exemplary samples. This observation hinted at a possible impact of disturbed epigenetic mechanisms in prostate cancer that may selectively affect particular imprinted genes.

In order to analyze which imprinted genes may be deregulated in prostate cancer, KM Bastian performed a database survey on the expression of imprinted genes in prostate cancer [170]. He found 12 imprinted genes to be significantly differentially expressed between prostate benign and cancerous tissues across up to 14 microarray studies (see Chap. 1.6 and Table 1.6.1). Peculiarly, many of these genes were reported to belong to an imprinted gene network active in the mouse embryo [168]. The imprinted *Plagl1/Zac1* and *H19* genes are thought to exert a central role in the transcriptional and epigenetic

regulation of the network *in vitro* and *in vivo* in the mouse. Many of these imprinted genes have been reported to have potential tumor suppressor functions (*PLAGL1*, *CDKN1C*, *MEG3*, *NDN*, *PEG3*, *INPP5F*, and *PPP1R9A),* or to be potential oncogenes (*PEG10* and *GNAS*). Thus we hypothesized that a deregulation of imprinted genes expression in the prostate could functionally contribute to prostate carcinogenesis and may occur during the progression of prostate cancer.

We analyzed by RT-PCR whether this group of imprinted genes is differentially expressed in prostate benign and cancerous tissues using our well characterized tissue set. Indeed, from the 12 candidate genes of the *in silico* study, we found *PLAGL1*, its splice variant *PLAGL1delta*, *CDKN1C*, *MEG3* and *NDN* genes to be significantly downregulated, while *PPP1R9A* was significantly upregulated in prostate cancer tissues in comparison to benign tissues in our set. Furthermore, three other imprinted genes were significantly differentially expressed in prostate cancer tissues, namely *IGF2* and *H19* were downregulated, while *LIT1* was significantly overexpressed in cancer samples. No significant difference between benign and tumor prostate tissues was found in the expressions of *PEG3, SGCE*, *GNAS*, *SNRPN*, *SNURF*, *INPP5F* and *INPP5Fv2*. Nevertheless, they tended to follow the predicted trends and might be altered only in smaller groups of the prostate cancer tissues from our set. Therefore, these genes may likely be found deregulated in prostate cancer, if their expression would be studied in a larger set of prostate cancer tissues, as indicated by the microarray results in the *in silico* study.

Altogether, we confirmed the differential expression between benign and cancerous prostate tissues of several of the imprinted gene candidates from the *in silico* study and several additional imprinted genes belonging to the published imprinted gene network (IGN) (Fig. 4.2.2 A and B). This raised the questions if such an IGN is detectable in the prostate (discussed in 4.2.2); if yes, what are the mechanisms that cause its deregulation in cancer (discussed in 4.2.3); whether ZAC1 functions as a regulator of the IGN in the prostate, as reported in the mouse (discussed in 4.4.2); and whether the deregulation functionally contributes to cancer progression (discussed in 4.2.4).

4.2.2. Imprinted gene network

Meta-analysis studies of mouse embryonic tissue microarray data revealed the presence of a network of imprinted and other genes, whose expression was co-regulated to that of *Zac1* (Fig. 4.2.2 A) [168]. This coordinate expression is similar to that of genes coordinately transcribed from one cluster; however the reported imprinted genes are situated on different chromosomes. Thus genetic linkage cannot cause their co-expression. Experiments using a *Zac1* knockout mouse model and a mouse cell line

indicated that *Zac1* acts as a transcriptional trans-regulator of the network by inducing other imprinted genes from the network. Furthermore, the overexpression of *H19* in *H19*-null mice also led to the deregulation of several imprinted genes from the network, suggesting that some imprinted genes may exert regulatory effects on the other members of the network (Fig. 4.2.2 B) [167]. Since the database analysis indicated that many of these genes are aberrantly expressed in prostate cancer, we hypothesized that an imprinted gene network, similar to that found in the mouse, was deregulated in prostate cancer. In this context, we predicted that the expression changes of these imprinted genes occur in a coordinated manner and that a common mechanism may act upon them as a group.

Indeed, the expressions of *PLAGL1/ZAC1*, *SGCE*, *PEG10*, *INPP5Fv2*, *NDN*, *PEG3*, *MEG3*, *CDKN1C*, *IGF2* and *H19* correlated positively to each other with high significance, while most of them were negatively correlated to *PPP1R9A* expression (Table 3.2.3 and Fig. 4.2.2 C). The result of this analysis provides a strong indication for the simultaneous deregulation of this group of imprinted genes and suggests the presence of an imprinted gene network in the normal prostate and its aberrant expression in prostate cancer.

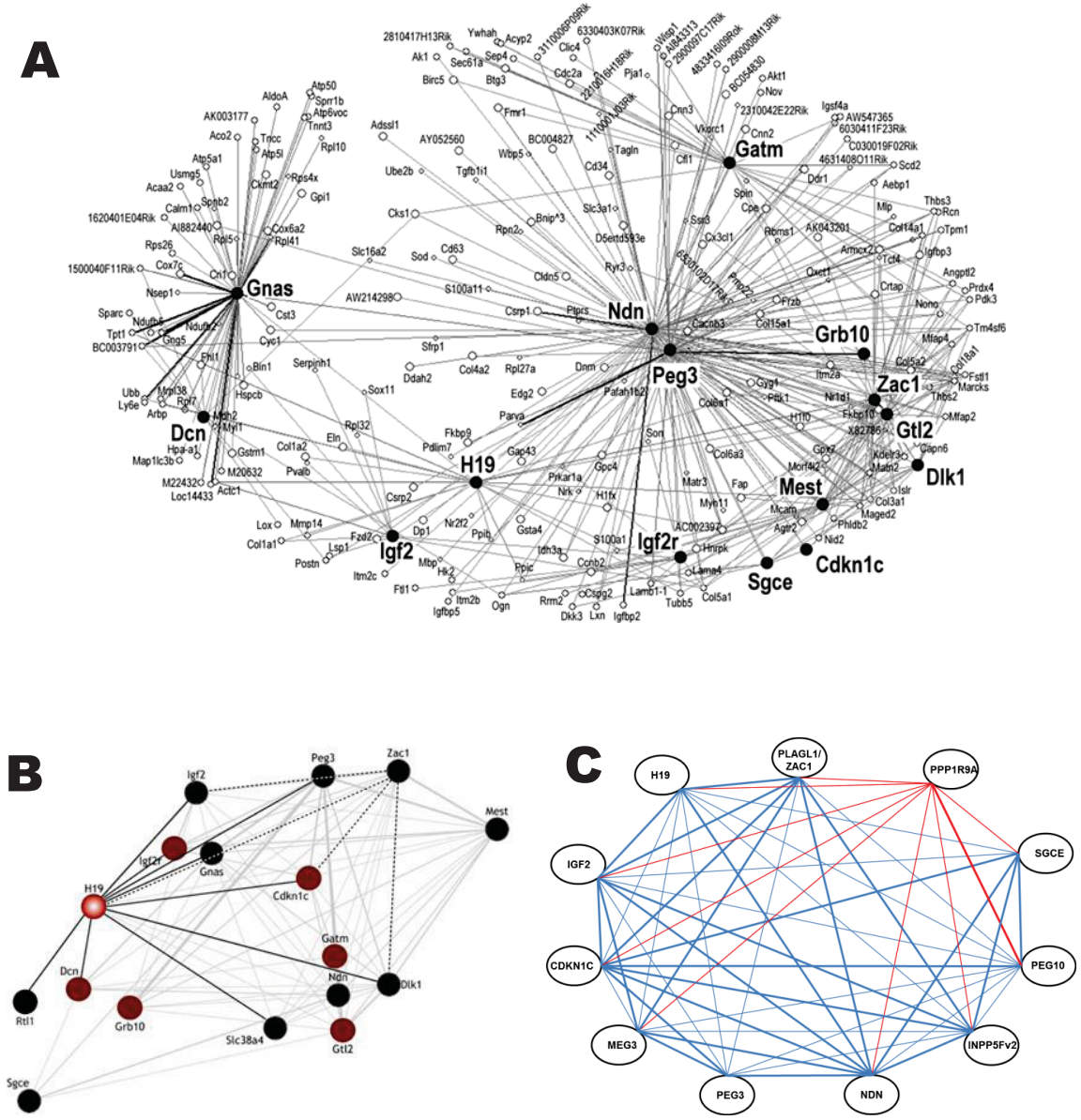

Fig. 4.2.2. Evidence for an imprinted genes network. A) Network of Zac1-coregulated genes found in the mouse [168]: B) Links of imprinted genes with H19 (black lines) found by A.Gabory [189], based on the network in A), maternally expressed genes are shown in red, and paternally expressed genes in black; C) Network of significantly ($p<0.05$) correlated imprinted genes in prostate cancer tissues as evident from a Spearman correlation analysis performed in SPSS software using imprinted genes expression data for 45 prostate cancer tissues. Thicker links represent correlations with $\rho > 0.5$, thinner lines - significant correlations with $\rho < 0.5$, positive ρ values are shown in blue and negative ρ values- in red. Exact values are given in Table 3.2.3.

4.2.3. Regulation of imprinted genes in prostate cancer

The overactivation of oncogenes in prostate cancer is known to drive its dedifferentiation and proliferation. The expression of each *HOXC6*, *ERG*, and *EZH2* oncogenes in prostate cancer associates frequently with advanced tumor stage and recurrence. Thus, their expression carries prognostic value for the patient and may go along with particular pathogenic molecular programmes that drive cancer progression. In our sample set *EZH2* and *HOXC6* expressions, which correlated highly positively with each other, were significantly associated with lymph node metastasis (Fig. 3.2.4.1). *HOXC6* was overexpressed in recurrent cancers and was a risk factor for relapse. Similarly, *EZH2* overexpression was associated with a shorter time to recurrence. (See Fig. 3.2.4.1). In our series *ERG over*expression was specific for cancers with GS 7, but infrequent in the GS groups <7 and >7 and did not significantly associate with other clinical parameters. In acord with our results, *ERG* overexpression has been reported to correlate with adverse prognosis in some, but not all studies [24, 190-192]. The expression of most imprinted genes that were co-expressed in prostate cancer correlated highly significantly in a reciprocal manner to *HOXC6* and *EZH2* expression (only *PPP1R9A* was positively correlated), but only a few imprinted genes correlated significantly to *ERG* expression (Table 3.2.3). One might therefore conclude that the aberrant expression of a group of coexpressed imprinted genes is most pronounced in advanced cancers with high *HOXC6* and *EZH2* expression. Furthermore, these associations may indicate a potential tumor suppressor role for the silenced imprinted genes, and may implicate *HOXC6* and *EZH2* oncogenes or their downstream signaling pathways as regulators of imprinted genes expression. HOXC6 has been suggested in the literature to promote a less differentiated cancer phenotype [17, 19]. The high correlation of imprinted genes expression to that of the histone H3K27 methyltransferase *EZH2* may suggest a role for role of repressive histone modifications in their altered expression. EZH2 has been reported to silence particular genes in cancer which is in some cases followed by DNA hypermethylation [54, 193, 194]. Thus, a functional role of EZH2 in imprinted gene silencing is possible.

Alternatively, independently of its function in the histone repressive PCR2 complex, but likely in combination with the AR, EZH2 was recently shown to be able to activate a set of genes through directly binding to cis-regulatory elements near their TSS. This function of EZH2 was required for the growth of castration-resistant prostate cancer [56]. In this context, EZH2 could also contribute to the silencing of imprinted genes by activating genes with negative influence on the network. As the imprinted *PPP1R9A* gene was significantly overexpressed and negatively correlated to the silenced imprinted genes, it may be a candidate target gene of EZH2 oncogenic function as a transactivator.

The expression of imprinted genes is known to be highly dependent on the epigenetic status of their promoters and local DMR regions. The correct imprinted methylation pattern of regulatory regions is important for allele-specific interaction between DMRs that may coordinate the expression of imprinted genes [195].

We studied the DNA methylation of *PLAGL1* DMR, KvDMR, 7q21 DMR, *MEG3* DMR and *CDKN1C* promoter regions in the imprinted gene clusters in prostate tissues and inhibited the DNA methylation and histone acetylation in prostate cancer cell lines. Since many of the genes are located in imprinted gene clusters, we hypothesized that the regulatory mechanisms that cause their altered expression in prostate cancer may function through the clusters. Thus the results from our analysis are discussed in the context of each cluster, where applicable.

4.2.3.1. Imprinted genes from the 7q21 cluster

Among the genes in the 7q21 imprinted gene cluster, the maternally expressed genes *PPP1R9A* and *PON2* were found to be significantly overexpressed in prostate cancer tissues, while the expression of the paternally expressed *SGCE* and *PEG10* genes was not significantly changed. Gain or amplification of 7q21 is frequent in several cancer types including prostate cancer [196-199]. Therefore, preferential chromosomal gain of the maternally inherited chromosome could be a reason for the increased expression of maternally expressed genes. Since the 7q21 DMR is normally maternally methylated, amplification of the maternal allele should result in an increase in its methylation. Indeed, this was observed for several tumor tissues but there was no correlation between methylation and the expression of the *PPP1R9A* and *PON2* genes (Fig. 3.3.1.2). 7q21 gain was present in six tumor tissues [50], while *PPP1R9A* and *PON2* were homogenously overexpressed in most analyzed prostate tissues. Therefore, if the increased methylation indeed reflects gain of the maternal allele, this genetic aberration does not underlie the observed overexpression of *PPP1R9A* and *PON2* genes.

The region assessed by bisulfite pyrosequencing and recommended by others [200] did not show the ~50% methylation level expected for a DMR, in either benign or cancer tissues, but rather about 10% methylation. Therefore, this region is likely only adjacent to the actual DMR (see Appendix 2). Nevertheless, the methylation of this region correlated significantly negatively with the expression of *PEG10* and *SGCE* genes (Fig. 3.3.1.2). As the DMR is located in the first intron of *SGCE* and in close proximity to *PEG10*, it is plausible that its epigenetic status may closely relate to the transcriptional activity of these two genes specifically. Silencing of *SGCE* and *PEG10* may be caused by or followed by hypermethylation of the DMR in single tumors. Peculiarly, it was also found to correlate negatively in a significant fashion with the expression of *CDKN1C*, *NDN*, *INPP5Fv2*, and

IGF2 genes, which are located on other chromosomes. Since the expression levels of those genes highly correlated with those of *SGCE*, *PEG10*, *H19, MEG3* and *PLAGL1*, one may suspect that the epigenetic status of the 7q21 DMR, despite being largely unchanged, may have an influence on the expression of a group of imprinted genes, similar to the reported *in-trans* influence of the *H19* maternal DMR [195, 201]. The fact that *PPP1R9A* expression was found to significantly correlate negatively to the expression levels of this group of genes, but was itself not influenced by the methylation status of the 7q21 DMR, could indicate that *PPP1R9A* may be functionally involved in the silencing of the imprinted genes.

4.2.3.2. PLAGL1 and HYMAI

The gene body of the non-coding RNA *HYMAI* encompasses the first exon of the imprinted *PLAGL1* gene if promoter P1 is used (see Fig. 1.7 upper panel) and parts of its intronic sequence. Since P1, which is maternally methylated, serves as a promoter of *HYMAI* at the same time, the expression of both imprinted *PLAGL1* and *HYMAI* genes occurs from the paternal chromosome and therefore ought to be concurrent. One may therefore hypothesize that the transcription of *PLAGL1* from the P1 promoter may inhibit the transcription of *HYMAI*, and vice versa. However, since *HYMAI* expression could not be detected in either normal or cancerous prostatic tissues, it is conceivable that *PLAGL1* is preferentially expressed over *HYMAI*. Both *HYMAI* and *PLAGL1* were reported to be overexpressed in the pediatric disease transient neonatal diabetes mellitus (TNDM), where the imprinting of the domain was found to be relaxed with two unmethylated alleles present [202, 203].

The methylation level of the DMR in the promoter region of *PLAGL1* was found to be stable in benign and tumor prostate tissues except for a small number of samples with low methylation, which may have lost the maternal allele. Therefore *PLAGL1* mRNA downregulation in most tumor samples cannot have been caused by aberrant DMR methylation. In the PC3 cell line, which expresses *PLAGL1* strongly, inhibition of DNA methylation induced its mRNA, while this treatment had no effect in the LNCaP and 22Rv1 cell lines, where *PLAGL1* is expressed very weakly. Thus, *PLAGL1* is not silenced by DNA methylation in LNCaP and 22Rv1 cells and DNA demethylation can have a positive effect on *PLAGL1* expression in the context of a transcriptionally active *PLAGL1*. Inhibition of histone deacetylation, which relaxes ‘silent’ chromatin, did not affect *PLAGL1* expression either. Therefore, its deregulated expression in prostate cancer does not seem to depend on the epigenetic status of its DMR/promoter.

The *PLAGL1* mRNA is alternatively spliced to create two mRNAs- one containing 2 coding exons and the other, the delta isoform, containing one coding exon only (Fig. 1.7). Since

the proteins encoded by the two splice forms were shown to have differences in their function [185], we wondered whether the mRNA forms may be differentially regulated. However, using primer pairs specific for the isoforms, we found that the expression of the *PLAGL1*delta isoform like *PLAGL1* isoform 1 was significantly reduced in prostate cancer tissues. Among the tumors, the mRNA expression levels of both forms positively correlated with each other, likely reflecting their origin from a common pre-mRNA. Therefore, the low levels of *PLAGL1* mRNA in the tumor tissues affect both splice forms and occur while its promoter methylation remains unchanged. One possibility may be that the imprinted domain at 6q24 is uncoupled from a potential transcriptional factory that brings together the genes from the network. Alternatively, *PLAGL1* mRNA may be actively destabilized in tumor cells. Evidence for such a mechanism was gained from our experimental models of *ZAC1* overexpression (see Chap. 4.3).

PLAGL1 correlated significantly negatively with the expression of *ERG*, *HOXC6* and *EZH2* oncogenes. A similar result was obtained for *PLAGL1delta*. One can thus conclude that downregulation of both *PLAGL1* splice variants is most pronounced in tumors with overactive prostatic oncogenes. This association may implicate these oncogenes in *PLAGL1* silencing.

Similar to HOXC6, the expression of HOXC8 gene has been reported to inhibit cellular differentiation, modulate AR target gene expression and correlate with Gleason score in prostate cancer [17, 19, 204]. While *ZAC1* was not among the genes shown to be targets of HOXC6 in prostate cancer [205], it was found to be directly inhibited by Hoxc8 in MEFs [206]. Therefore, the effect of HOXC6 on ZAC1 may be indirect or HOXC8 may be the actual repressor.

Since ZAC1 functions as a transcriptional co-activator of the AR its expression may be induced by AR through a positive feedback mechanism. Thus, through modulating AR target gene activation, the two HOXC factors may indirectly affect *ZAC1* expression. However, our in vitro androgen treatment and ablation experiments in LNCaP and MDAPCa2b cell lines, respectively, did not reveal any considerable influence on the expression of *PLAGL1* or other analyzed imprinted genes (Fig. 3.2.7).

4.2.3.3. CDKN1C and LIT1

Confirming a previous report [157], we found the mRNA expression of *CDKN1C*, encoding the CDK inhibitor and tumor suppressor protein $p57^{KIP2}$ to be significantly downregulated in prostate cancer tissues. *CDKN1C* silencing also occurs in many other tumor types [148, 152]. The involved mechanisms include allelic loss, aberrations in DNA methylation and in H3K4 and H3K9 histone modifications at the *CDKN1C* promoter and the *KvDMR*, often in

a reciprocal fashion [153, 155, 158, 165, 166, 207, 208]. Likewise, simultaneous inhibition of EZH2 and histone deacetylases was reported to reinduce *CDKN1C* expression [166]. In breast cancer cells, estrogen signaling was reported to confer repressive histone modifications at the *KvDMR* and the *CDKN1C* promoter, with a concomitant increase of *LIT1* expression [209]. The authors proposed a model in which estrogen induces the transcription of *LIT1* and the recruitment of CTCF to mediate KvDMR silencing activity, leading in turn to the repression of *CDKN1C*.

LIT1 expression was indeed significantly overexpressed in prostate cancers, but peculiarly, it correlated positively with *CDKN1C* expression. This finding does not fit with a decisive negative effect of *LIT1* expression on *CDKN1C* in prostate cancer.

The methylation of the *KvDMR* that contains the *LIT1* promoter remained largely stable in benign and tumor tissues and did not correlate to either *LIT1* or *CDKN1C* expression in tumor tissues. Similarly, the analyzed region in the *CDKN1C* promoter, containing a CTCF-binding site, was found to be equally methylated (about 26 %) in benign and tumor tissues and its methylation did not correlate to either *CDKN1C* downregulation or *LIT1* upregulation in tumor tissues. The similar DNA methylation levels in benign and cancerous prostatic tissues clearly argue against a role for DNA methylation in the aberrant *CDKN1C* and *LIT1* expressions in cancer tissues. In the 22Rv1 and PC3 prostate cancer cell lines treatment with an inhibitor of DNA methylation induced *CDKN1C* expression. Thus, in contrast to prostate cancer tissues, where the methylation of the *CDKN1C* promoter and *KvDMR* are stable, DNA hypermethylation may have a certain repressive influence on *CDKN1C* expression in prostate cancer cell lines.

While DNA methylation does not seem to be involved in the aberrant expression of *CDKN1C* in prostate cancer tissues, altered histone modifications may be involved, as *CDKN1C* but peculiarly not *LIT1* mRNA expression correlated strongly negatively to the expression of *EZH2* gene. Although inhibition of histone deacetylation was not sufficient to induce CDKN1C expression in cell lines, repressive histone modifications may play a role in *CDKN1C* repression in prostate cancer tissues and should be further analyzed by chromatin immunoprecipitation experiments and treatment with recently published specific inhibitors of EZH2 [210-212].

4.2.3.4. MEG3

The *MEG3* gene that was significantly downregulated in prostate cancer is situated in an imprinted gene cluster on chromosome14q32.2. The region contains a.o. the paternally expressed protein-coding *DLK1* gene and many maternally expressed genes encoding regulatory RNAs like micro-RNAs, small nucleolar RNAs, and several long non-coding

RNAs like *MEG3* itself. The imprinted expression of the genes is epigenetically regulated by three DMRs -*DLK1* DMR and IG-DMR, situated upstream of *MEG3*, and *MEG3*-DMR which spans its promoter and first exon (see Fig. 1.4). Methylation aberrations of the IG-DMR and *MEG3* DMR have been implicated in the silencing of *MEG3* in cancer [213, 214]. According to our findings, the DNA methylation level of the *MEG3*-DMR was relatively high (~ 67%) but stable in both benign and tumor prostate tissues and did not significantly correlate to *MEG3* expression. One CpG site from the analyzed region, CpG2, however, exhibited consistently lower methylation (~ 50%) than the neighboring CpG sites. Furthermore, the methylation level of this CpG was significantly lower in prostate tumor tissues than in benign tissues and strongly correlated to the expression of *MEG3*. Since the methylation status of *MEG3*-DMR as such was largely stable, one can conclude that it does not contribute to *MEG3* silencing. Instead, hypomethylation of a single CpG position was associated with silencing. The mechanism underlying this association is unknown. Conceivably, this site may be a methylation-sensitive binding site for a transcriptional repressor protein, but other mechanisms can be envisioned.

As evidenced from the in vitro experiments, either inhibition of DNA methylation (in PC3 cells) or of histone deacetylation (in LNCaP and 22Rv1 cells) could substantially induce *MEG3* expression depending on the cell line. Therefore, either of these epigenetic mechanisms may be involved in the regulation of *MEG3*, likely depending on the cell context.

4.2.3.5. NDN

NDN is a paternally expressed gene belonging to an imprinted gene cluster on chromosome 15q11, which together with other paternally expressed imprinted genes is deficient in Prader-Willi syndrome. In our cohort of prostate cancer tissues *NDN* expression was significantly downregulated. Silencing of *NDN* in prostate tumors seems to occur concurrently to that of the other genes of the imprinted gene group. We did not assess the methylation status of *NDN* or the associated DMR. However, it could be silenced by repressive histone modifications as it was strongly induced by treatment of 22Rv1 and LNCaP cells with the histone deacetylase inhibitor Saha.

4.2.3.6. IGF2 and H19

We found both *IGF2* and *H19* genes to be significantly downregulated in prostate cancer tissues, in accord with previous reports [144]. Increased *IGF2* expression in benign tissues of older men seems to represent an early phenomenon often associated with *IGF2* LOI [144, 215], while the observed concomitant downregulation of *IGF2* and H19 genes occurs in advanced prostate cancer and is likely tumor-specific. The mechanisms underlying this downregulation are unknown. In our set of prostate cancer tissues the

repression of *IGF2* and *H19* was significantly associated with a higher expression of *ERG*, *EZH2* and *HOXC6* oncogenes. Of note, this positive correlation should not be observed, if the expression changes were due to LOI.

4.2.3.7. INPP5F and INPP5Fv2

The *INPP5F_v2* gene uses an alternative transcriptional start site within an intron of *INPP5F*, which contains a CpG-island differentially methylated in an allele-specific manner in some tissues [216, 217]. While neither *INPP5F* nor *INPP5Fv2* were significantly differentially expressed in prostate cancers, the *INPP5Fv2* variant showed a clear tendency towards lower expression in the tumors. Tumor tissues with low *INPP5Fv2* expression exhibited high *EZH2* and *HOXC6* expression.

A homolog of *INPP5F- INPP4B* was shown to be induced by AR in prostate cells [39]. Thus one could suspect that *INPP5F* may be regulated in a similar fashion in prostate cancer. However, our androgen supplementation and ablation experiments showed that its expression is not responsive to androgens. Additional experiments in non-tumor prostate cells and other prostate cancer cell lines should be performed to validate this result.

4.2.3.8. Regulation summary

The concomitant deregulation of several imprinted genes has been reported to occur in congenital imprinting disorders like BWS, SRS and WT. In these diseases, aberrant imprinted gene expression is caused by a failure to establish imprinting in the germ cells of the parents, which is inherited by the embryo. These events exert effects on embryonic and placental development as such but also predispose to certain childhood tumors. In germ cells, mostly deletions and other chromosomal aberrations or epimutations disturb the correct establishment of imprints.

The mechanisms underlying aberrant imprinted gene expression in adult cancers are not as well characterized. Deregulation of single imprinted genes like *IGF2*, *CDKN1C* and *TFPI2* has been ascribed to LOI and promoter hypermethylation [72, 76, 137, 141, 153, 160, 208]. Moreover, LOI at some imprinted domains is occasionally observed in preneoplastic tissues as well, suggesting that it could predispose to cancer [140, 144, 215]. We found here that a group of imprinted genes belonging to an imprinted gene network is coordinately deregulated during prostate cancer progression.

Quantitative DNA methylation assessment of the regulatory regions *PLAGL1* DMR (6q24), KvDMR (11p15), 7q21 DMR, *MEG3* DMR (14q32) and *CDKN1C* promoter (11p15) revealed no significant differences between benign and cancer tissues. Thus the observed gene expression changes in prostate cancer tissues occur in the presence of intact imprints i.e. in the absence of LOI. In accord, a recent study which extensively studied the

methylation of DMRs in many imprinted loci in adult somatic tissues, reported their stable CpG methylation levels with little variation [216]. Several of these DMRs are situated in the imprinted gene promoters of *PLAGL1* and *HYMAI*, *LIT1*, *SGCE* and *PEG10*, *MEG3* and *CDKN1C* genes. Being equally methylated in benign and cancerous tissues, misexpression can therefore not be attributed to aberrant promoter methylation either.

Thus in contrast to the mechanisms that have been associated with aberrations of single imprinted genes in cancer tissues, the mechanisms that cause the observed coordinate expression changes of a group of imprinted genes in prostate cancer tissues do not seem to involve LOI or promoter hypermethylation at the studied domains.

We have not studied the methylation status of the several DMRs in the *H19*/*IGF2* cluster, as it has been reported to be disturbed in both benign and cancerous prostate tissues [145]. This region could be very important for the coordinate regulation and expression of the imprinted genes group, since the *H19* DMR has been reported to interact with regions of multiple imprinted domains on other chromosomes [147, 195]. In this fashion, this locus could directly or indirectly influence the epigenetic states and coordinate the expression of many imprinted genes.

In contrast to primary prostate cancers, in the prostate cancer cell lines LNCaP, 22Rv1 and PC3 DNA methylation at imprinted domains appears to contribute more strongly to the aberrations of particular imprinted genes, which could be induced, albeit moderately, by inhibition of DNMTs. *PLAGL1*, *H19* and *MEG3* genes, whose promoters are DMRs, were most strongly inducible by 5-aza-dC treatment in the PC3 cell line. This may be attributed to its higher proliferation rate than 22Rv1 and LNCaP cells or to its general higher susceptibility to this agent. In general, cell lines exhibit many more chromosomal and epigenetic aberrations than primary tissues and can only serve as hints for molecular mechanisms that occur in advanced cancers. As the *in vitro* culture of primary prostate cancers is extremely difficult, we cannot test the effect of DNA methylation inhibition on tissues.

Similar to developmental genes, imprinted ICRs (particular DMRs) have been shown to be marked by bivalent chromatin domains, containing overlapping active H3K4me3 and repressive H3K9me3 or H3K27me3 histone modifications [218, 219]. Since H3K4me3 is thought to protect the unmethylated allele from methylation and H3K27me3 - to pre-mark genes for de novo methylation in cancer, aberrations in the enzymes modulating these marks may disturb the imprints [54]. Overexpression of the H3K27me3 methyltransferase EZH2 in prostate cancer tissues correlated to the diminished expression of most imprinted genes. Thus it could functionally contribute to their silencing by increasing repressive histone modifications at these genes. As cancer cell lines appear not fully representative

for these changes according to our results, chromatin immunoprecipitation analysis of prostate tissue samples should be performed in order to prove such a mechanism.

Recent publications, interestingly, report that the oncogenic function of EZH2 in prostate cancer is independent of the Polycomb complex [56]. Instead, EZH2 is post-translationally modified by PI3K/Akt signaling to become a transcriptional activator. In our tissue set, *EZH2* overexpression was highly positively correlated with the expression of the imprinted *PPP1R9A* gene, but significantly inversely associated with the co-regulated silencing of the other imprinted genes of the group. This association may hint at a potential activatory effect of EZH2 on *PPP1R9A*, which could in turn affect the expression of the imprinted gene network.

The histone deacetylase inhibitor Saha induced markedly the expression of *MEG3* and *NDN* in the LNCaP and 22Rv1 cell lines, while it had no effect or even reduced the expression of the other assessed imprinted genes in all three cell lines treated. This may result from effects on both active and inactive alleles that eventually cancel each other out. The influence on imprinted gene expression of other histone modifying proteins, like Trithorax, (other) Polycomb, and Jumonji familiy proteins needs to be investigated in the future.

Almost all imprinted gene clusters contain non-coding RNAs. These are thought to contribute to allelic silencing by physical association of the RNA with the imprinted domain DNA on one chromosome *in cis*. NcRNAs are proposed to induce repressive histone modifications by recruitment of the Polycomb complex [220, 221]. Several imprinted genes aberrantly expressed in our prostate cancer tissue samples are indeed ncRNAs- the downregulated *H19* and *MEG3* and the overexpressed *LIT1*. Correlation analyses, however, showed that the change in expression of these ncRNAs was not reciprocal to the expression of their oppositely imprinted and neighboring imprinted genes. For instance, the assessed ncRNA/protein-coding gene pairs *H19*/*IGF2* and *MEG3*/*DLK1* were both silenced. Only *LIT1* ncRNA was overexpressed in prostate cancer, but its levels did not correlate to the silencing of the neighboring *CDKN1C* gene or the more distant *H19* and *IGF2* genes. Thus, the aberrant expression of particular imprinted ncRNAs is unlikely to account for the expression changes of the neighboring reciprocally imprinted protein-coding genes.

One similar mechanism for coordinated gene expression involves so called transcriptional factories, in which many actively transcribed genes bound by a common transcriptional factor are dynamically localized into a shared nuclear subcompartment [222]. This mechanism may be involved in the co-regulation of the imprinted genes network and may be mediated a.o. by ncRNAs like *H19* [167]. In that case, the diminished expression of the imprinted gene group could be caused by the loss of a common transcriptional activator.

ZAC1 has been reported to be a master transcriptional regulator of the imprinted genes network in mice [168]. We showed that it is significantly downregulated in prostate cancer and its expression is strongly significantly correlated to the expressions of several other aberrantly expressed imprinted genes in prostate cancer tissues. One may thus speculate that the lack of *PLAGL1*/ZAC1 expression in prostate cancer may cause the coordinate aberrant expression of the other imprinted genes. The ability of ZAC1 to induce the other imprinted genes from the group in prostate cancer was therefore studied using several different experimental models and is discussed in Chap. 4.3.4.

Next to ZAC1, several of its target genes can regulate the expression of imprinted genes from the network. For example, the *H19* non-coding RNA has been proposed to exert a fine-tuning regulatory effect on the expression of several genes from the imprinted gene network including *Igf2*, *Cdkn1c*, *Dlk1*, *Gnas*, and others in the mouse [167]. In a similar fashion, the ncRNA *LIT1* may also exert regulatory effects on the expression of imprinted genes, especially on *CDKN1C* [223]. Furthermore, Igf2 treatment was reported to lead to the downregulation of *Cdkn1c* on mRNA and protein levels in mouse embryonic fibroblasts [224]. The reported interactions point to potential feedback regulatory roles among the imprinted genes from the network.

The silencing of the imprinted genes prostate cancer may also be caused by a transcriptional repressor like HOXC6 or HOXC8 (see also 4.2.5), which have been shown to suppress the expression of AR-target genes in prostate cancer. While several of the assessed imprinted genes are reported to be AR target genes or may functionally be involved in AR signaling, our *in vitro* androgen supplementation or ablation experiments did not support an influence of androgens on the expression of these imprinted genes. *HOXC6* expression, however, significantly negatively correlated to the expressions of the silenced imprinted genes in our cancer tissues sample set. Thus it may be involved in the repression of imprinted genes, independent of androgens or specifically in the context of castration-resistant prostate cancer.

An online functional association analysis (Fig. 4.2.3.8) hinted that most of the aberrantly expressed in prostate cancer imprinted genes from the network are functionally related to p53. It may act as a transcriptional activator of the network but also influence it on the protein level as the products of several of the aberantly expressed imprinted genes interact or functionally associate with p53 [182, 225-228]. *TP53* is infrequently mutated in prostate cancer [13, 229, 230], but its function is likely to be compromised by other mechanisms [231]. It should be investigated to what extent loss of its imprinted interaction partners, e.g. *MEG3* RNA, might contribute to this inhibition.

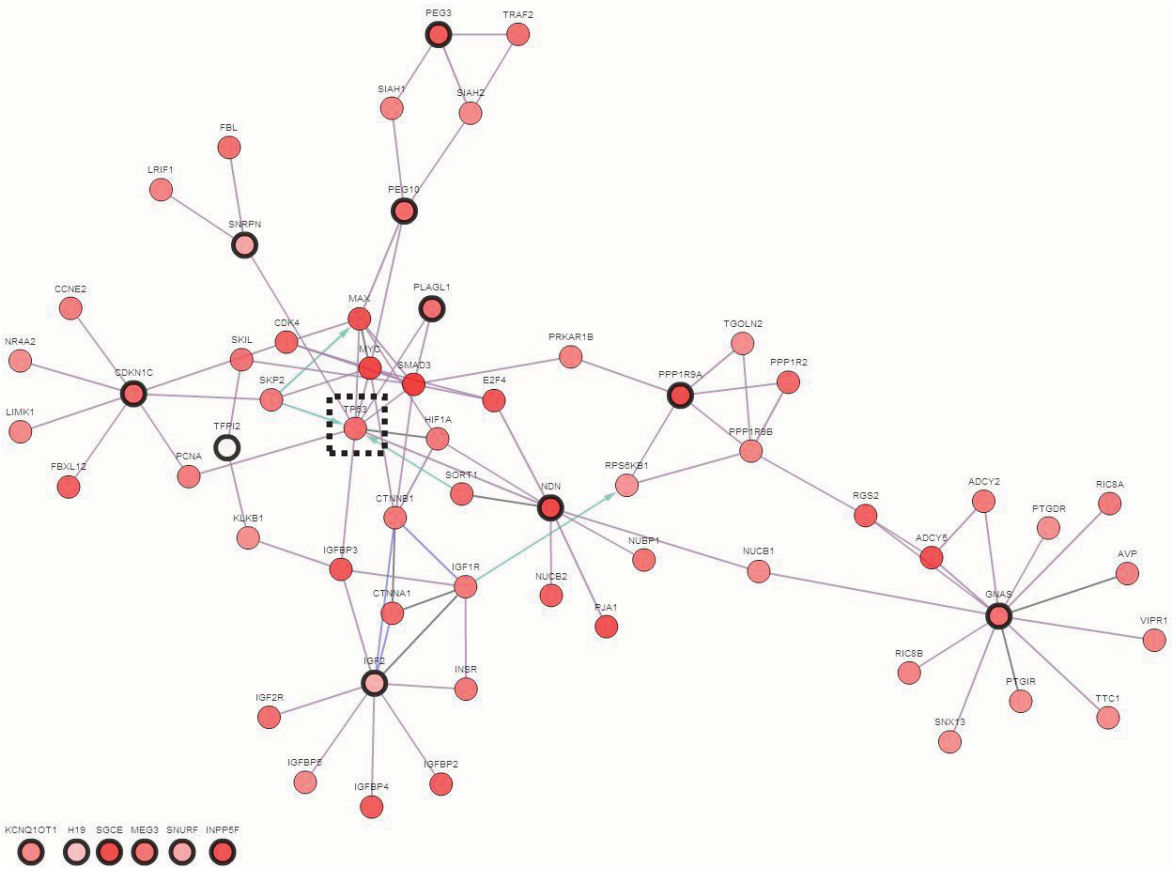

Fig. 4.2.3.8. Network of the 16 assessed imprinted genes in the context of biological interactions derived from public pathway databases. Note that most of the analyzed imprinted genes interact directly or indirectly with p53 (squared in dotted lines). Seed nodes (thick lines) are the entered 16 genes; linker nodes (thin lines) are genes that connect to one or more of the seed genes. The intensity of the white-to-red gradient colour in the nodes indicates the total frequency of alterations in the cancer tissues across the online available MSKCC prostate cancer tissue set [13]. The network was created with the CBio Cancer Genomics Portal and is based on pathway and interaction data derived from multiple databases.

Altered signal-transduction pathways during tumor development can induce epigenetic silencing of particular genes in cancer. Specifically, overactive PI3K/Akt signaling has been shown to modulate the activity of the epigenetic regulators EZH2 and BMI1, which may in turn modulate epigenetic regulation of imprinted genes [56, 232, 233]. The loss of a particular signaling pathway could also lead to the (epigenetic) silencing of its downstream targets [234, 235]. It is not known which pathway might regulate the imprinted gene network, but its prominent expression in stem-like cells points to pathways regulating cell stemness like Notch, Wnt, Smad and Hedgehog pathways. While we do not know at which stage of prostate carcinogenesis imprinted genes deregulation occurs, our statistical association analysis suggests that advanced stage cancers with overexpression of *EZH2* and *HOXC6* tend to carry these changes.

4.2.4. Potential function of imprinted genes and the IGN in prostate cancer

Our findings of the coordinately deregulated expression in prostate cancer of the group of imprinted genes, likely belonging to a gene network, open the question on the function of the network in the normal prostate and the consequences of its silencing for prostate carcinogenesis.

The potential function of such a network in the normal prostate can be studied using mouse models, but it is a difficult task in humans. Nevertheless, statistical analyses of the available expression data of our well characterized set of prostate cancer tissues allowed us to make indirect associations between imprinted genes and some clinical and molecular parameters of prostate cancer progression. These associations are discussed below together with reports for the function of the respective imprinted genes in cancer.

4.2.4.1. PPP1R9A

In hepatocellular carcinoma higher *PPP1R9A* expression levels have been shown associated with disease progression and poor prognostic outcomes [197, 236-238]. Similarly, in the prostate tissue cohort studied here, *PPP1R9A* overexpression was found to significantly associate with shorter time to biochemical recurrence. These associations suggest a tumor-promoting role in prostate cancer. Unfortunately, very little is known about the function of neurabin I, the product of the *PPP1R9A* gene. It is an F-actin-binding protein that was proposed to enhance p70 S6 kinase activity. This kinase is activated downstream of PI3K/mTOR signaling and enhances protein synthesis, thereby promoting cell survival. Neurabin-I could therefore contribute to the overactivity pf PI3K/mTOR signaling, which is a general feature of prostate cancer. The significant negative correlation of *PPP1R9A* expression with all silenced imprinted genes may imply its involvement in their silencing, or its concomitant upregulation. Our findings indicate that *PPP1R9A* is a potential new oncogene in prostate cancer, whose functions, especially in respect to the regulation of the imprinted genes group may reveal a new molecular mechanism of prostate cancer progression and should be further investigated.

4.2.4.2. PLAGL1/ZAC1

According to the results from our statistical analysis, low *PLAGL1* expression significantly correlated with advanced tumor stage, as well as higher incidence and shorter time to biochemical recurrence. These associations together with the insights from our functional experiments suggest that PLAGL1/ZAC1 plays a tumor suppressor role in prostate cancer in part by inhibiting the proliferation of prostate cancer (discussed in Chap. 4.3).

The high correlation of *PLAGL1* expression to a group of aberrantly expressed imprinted genes in prostate cancer together with its ability to induce several of them likely reflect

another important aspect of its tumor suppressive function (discussed in more detail in Chap. 4.3)

4.2.4.3. MEG3

Multiple studies provide evidence for *MEG3* being a potential tumor suppressor gene, as it is downregulated in many cancers and its ectopic expression suppresses tumor cell proliferation [239-243]. Although the exact mechanisms involved are not clear, *MEG3* was reported to induce *TP53* expression and protein accumulation, to physically interact with p53 and to be able to stimulate transcription in p53-dependent and independent manners [242].

In prostate cancers from our cohort, low *MEG3* expression associated, albeit not significantly (p=0.058), with an increased risk for biochemical recurrence, suggesting its tumor suppressor role in prostate cancer.

4.2.4.4. NDN

Functionally, necdin was reported to control the proliferation of preadipocyte and hematopoietic progenitor cells [120, 244-246] but also to exert a pro-survival effect on myocytes and neurons upon stress or DNA damage [247-252].

The expression of *NDN* was reported to be downregulated in several primary cancers and cancer cell lines, suggesting its potential tumor suppressor function [253]. Acordingly, we found downregulated *NDN* expression in dedifferentiated prostate tumors with Gleason score 7 rather than more differentiated ones with lower GS. This observation may point to a role of *NDN* in differentiation of prostate cancer.

4.2.4.5. CDKN1C

The product of *CDKN1C*, $p57^{KIP2}$ is a cell cycle inhibitor and its expression can induce differentiation or cellular senescence [148]. Its loss in cancer is considered to contribute to cellular immortalization [149]. Furthermore, $p57^{KIP2}$ can influence actin cytoskeleton dynamics and thereby affect the cellular migratory potential [254, 255].

In prostate cancers CDKN1C may act as an important brake to the mitogenic activity of oncogenes or increased pro-survival signaling and its loss may contribute to tumorigenesis [39, 151, 152, 256].

4.2.4.6. H19

The ncRNA *H19* can interact with chromatin modifying enzymes, RNA-binding proteins and p53. It has been proposed to play a regulatory role in the imprinted gene network [167]. Although its function in cancer is controversial, it is reported to be upregulated and

to promote cell cycle progression in many cancer types [225, 257-259]. In other cancers, however, it was downregulated and proposed to act as a tumor suppressor [260, 261].

Acording to our findings, low *H19* expression in prostate cancers was significantly associated with a shorter time to biochemical recurrence. Interestingly, steroid hormones have been suggested to downregulate *H19* expression. Thus, while *H19* overexpression in benign tissues may predispose to transformation, its silencing at later stages, potentially as a result of increased AR signaling, may characterize aggressive cancer.

4.2.4.7. IGF2

The insulin-like growth factor 2 (IGF2) plays an essential role in growth and development before birth. IGF2 acts as a paracrine growth factor in the prostate and its overactivation likely promotes the onset of prostate cancer [135, 144, 146]. While it enhances the activity of the PI3K and Ras-MAPK pathways stimulating tumor cell survival, it may not be oncogenic on its own [128, 147]. LOI of IGF2 has been shown to disrupt long-range chromatin interactions, which may affect the expression of interacting genes, among which are many imprinted genes [147]. The downregulation of *IGF2* that we and others have observed in prostate cancers may disturb the epigenetic interactions between imprinted genes and thereby diminish the differentiation capacity of prostate cancer.

4.2.4.8. Section summary

In this study we found aberrant expression of several imprinted genes which significantly associated with clinical and molecular markers of prostate carcinogenesis. Particularly, *PLAGL1* downregulation occured in high stage tumors, while *NDN* expression was specifically lower in tumors with intermediate prognosis (with Gleason score 7) than good prognosis ones (with lower GS). Furthermore, lower expression of each *PLAGL1*, *MEG3* and *H19* and overexpression of *PPP1R9A* was preferrentially found in patient with shorter time to biochemical recurrence. Hence our findings suggest the functional importance of imprinted genes for prostate cancer and ought to be investigated in larger patient cohorts as prognostic determinants.

A group of imprinted genes, several of which we found to be deregulated in prostate cancer, have been reported to be more highly expressed in progenitor cells in several adult tissues in comparison to their more differentiated cellular counterparts [119]. Imprinted gene expression was suggested to contribute to a poised state of growth control permitting the rapid response to growth stimulatory signals in this special cell population [119]. In concert, some paternally expressed imprinted genes were reported to be involved in the development and organ regeneration of the kidney and muscle [114, 118]. Furthermore, imprinted genes have been proposed to contribute to the pluripotency potential of stem and progenitor cells [116, 117, 121, 122] which may explain the reported

decline in expression of *Plagl1*, *Meg3*, *Peg3*, *Ndn*, *Cdkn1c*, *H19* and *Igf2* genes in multiple mouse organs during aging [123]. This decline may reflect an age-dependent extinction of progenitor cells or to their loss of potential to regenerate the tissue, due to loss of differentiation capacity and/or proliferation arrest. Given these observations, aberrant expression of imprinted genes in prostate cancer may disconnect particular developmental signals that conduct lineage specification and maintain the hierarchy among the different functional cellular layers.

4.3. ZAC1 regulation

4.3.1. ZAC1 overexpression models

ZAC1 has been reported to function as a tumor suppressor in various models of cancer [171, 172, 185, 262]. In order to test whether it has a similar role in prostate cancer, we used three different ZAC1 expression plasmids in stable, inducible and transient transfection experiments. Transient and inducible transfection models are usually utilized to study the short-term (24-96 h) impact of altered gene or protein expression. In comparison, stable overexpression ensures the permanent expression of the introduced gene and allows its manipulation and study in long term experiments (longer than 96 h). In order to avoid the potential negative effect of long term exogenous ZAC1 protein expression, we also created stable clones with tetracycline-inducible *ZAC1* overexpression.

Stable ZAC1-overexpressing clones were created by transfection of the ZAC.VA and ZAC.DS plasmids in parallel to lacZ plasmids in two prostate cancer cell lines with endogenously low *ZAC1* expression- LNCaP and 22Rv1, and one with high expression - PC3. Many positive clones exhibiting several-fold higher *ZAC1* mRNA expression than control lacZ-transfected stable clones were selected. Unexpectedly, the ZAC1 protein levels as determined by immunoblotting in positive clones from all three cell lines were not much different from those of control lacZ clones. In all analyzed stable ZAC1- and lacZ-clones clones, however, only the endogenous ZAC1 proteins with a size of ~45 kDa were detected. The protein encoded by ZAC.VA and ZAC.DS, however, is expected to have the size of ~50 kDa. As the α-tubulin protein levels were comparable in all samples, one could rule out differences in the total protein amounts loaded. Used as a positive control, a protein sample of transiently *ZAC1*-transfected PC3 cells produced three strong protein bands with sizes of ~50 kDa, ~45 kDa, and another one at ~38-40 kDa. We assumed that the ~38-40 kDa and ~45 kDa bands likely represent ZAC1 protein variants differing at their N-terminus which may result from the parallel usage of translation starting sites (TSS) downstream of the annotated TSS (ATG1) respectively- ATG3, and ATG4 or ATG5 (see Fig. 3.4.1). Thus, while the used plasmids lead to overexpression of the expected 50

kDa protein in the transient transfection, the stable clones exhibited no increases in the exogenous ZAC1 protein. These results suggest an active downregulation of ZAC1 in the stable clones, possibly during cell adaption to the activity of the potential tumor suppressor protein. Since the selection and expansion of positive clones until definitive protein analysis takes ~7 weeks, there is sufficient time for 'positive' cells to downregulate ZAC1 protein.

In the *ZAC1*-inducible clones of LNCaP6TR cells, the uninduced *ZAC1* mRNA level was initially low and became maximally increased by 5-10-fold after tetracycline treatment for 24 h. However, despite the increased *ZAC1* mRNA levels, its protein levels remained relatively low with no discernible differences between induced and uninduced cells, similar to the control α-tubulin protein levels.

Since no ZAC1 protein overexpression could be achieved in either stable LNCaP, 22Rv1 and PC3 cells, or inducible LNCaP6TR clones, the observed effect is not likely to occur by adaptation during long term selection and is more pronounced in stable clones than in transiently transfected cells. In stable clones, the DNA of a single expression plasmid is integrated and can be constitutively or inducibly transcribed for long periods of time. In comparison, in transient transfections - many plasmid DNA molecules enter one cell and can be transcribed for short periods of time producing in effect much higher mRNA amounts than stable constitutive or induced transfection. Thus, we assumed that the extremely high amounts of ZAC1 plasmids achieved upon transient transfection may temporarily overcome the resistance of a cellular regulatory mechanism controlling ZAC1 levels and preventing its protein overexpression. The mechanism underlying this phenomenon may involve the active degradation of ZAC1 protein and/or mRNA as well as inefficient translation.

Similar to our observations, Varrault et al. experienced difficulties to overexpress human ZAC1 protein, but not mouse Zac1 protein or another tumor suppressor protein -human p53 [171]. In their transient transfection experiments, human ZAC1 could be overexpressed by transfecting at least 1 µg of the pRK-hZAC plasmid in order to get the equal amount of protein that was produced by transfecting as much as 50 ng of pRK-mZac plasmid (countaining mouse *Zac1* cDNA) or 100 ng of pRK-p53. The mouse Zac1 protein shares 69% identity with the human ZAC1 and has additional sequences downstream of the region coding for the seven zinc fingers, giving rise to a bigger *Zac1* protein (~112 kDa) (see Fig. 4.3.1).

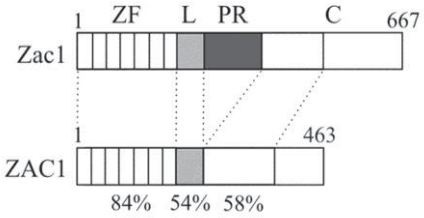

Fig. 4.3.1. Scheme of mouse Zac1 and human ZAC1 proteins. The mouse Zac1 and human ZAC1 proteins are composed of 693 and 463 amino acids respectively with a calculated weight of ~75 kDa and ~51 kDa. Amino acid identity (%) between the corresponding domains of mice and humans is indicated.The N-terminal DNA-binding domain comprises of seven classical C2H2-type zinc fingers (ZF) that are highly conserved between mouse and human ZAC1. The central Pro-repeat domain (PR) is exclusively present in mice. (L)-linker domain, (C)- coactivator-binding domain [179].

The greater efficiency of mouse Zac1 expression in comparison to the smaller human protein is at first glance contraintuitive. However, the C-terminal and central proline-rich sequences in m*Zac1*, missing in h*ZAC1*, may function to stabilize the mRNA or protein. These differences suggest a more complex regulation of human *ZAC1* and may explain why most functional studies with *ZAC1* employ the mouse homolog instead of the human gene.

4.3.2. ZAC1 translation efficiency

With the hope of increasing the stability of the overexpressed ZAC1 protein, we excised the first protein coding exon from the ZAC.VA plasmid, resulting in cDNA that codes for the shorter *ZAC1* alternatively spliced transcript isoform *ZAC1 delta*. Instead of 7 zinc fingers (protein size ~51-54 kDa), this isoform codes for 5 zinc fingers (protein size ~45 kDa). As suggested in the literature, the protein products of the two isoforms both induce cell cycle arrest and apoptosis but with different efficiency [185]. Our observations sugest that the reported functional differences may reflect to some extent the different stability of the various gene products.

Indeed, the short protein-coding plasmid - ZACdelta produced much higher *ZAC1* mRNA and protein levels than the two long protein-coding plasmids (ZAC.VA and ZAC.DS) upon transient transfection in 22Rv1cells. Among the latter two, the plasmid containing parts of the 5'- and 3'-UTRs (ZAC.VA) was much less efficient than the plasmid without UTRs (ZAC.DS) (for details see Fig. 3.4.1 B). These differences occurred consistently and are not likely to result from different transcription efficiencies, as all ZAC1 plasmids have the same vector backbone and thus the same promoter. Instead, the different regulatory and protein-coding elements contained in their gene sequences may influence the stability of the encoded mRNAs or the efficiency of their translation. Upon a closer examination of the protein coding sequence of the long isoform we observed the presence of several alternative translation starting sites (ATG codon) downstream of the first one (see

Appendix 4). This may lead to leaky ribosome scanning, producing several small ORFs that strongly diminish the efficiency of translation. Without the bias of multiple downstream ATGs, present in the long isoform plasmids, ZACdelta cDNA may allow for more efficient translation. Indeed, the long isoform plasmids produced 45 kDa and 38-40 kDa protein bands additional to the expected 51 kDa band demonstrating the parallel usage of several ATGs. In contrast, the ZACdelta plasmid produced a much stronger single 45 kDa protein band. Thus we may conclude that the first protein coding exon strongly inhibits ZAC1 translation, likely through a bias from multiple downstream translation start sites. Alternatively, the secondary structure of the shorter mRNA may allow more optimal translation than that of the longer mRNA.

An unusually high number ATG sites were additionally present in the non-coding 5'-UTR in ZAC.VA plasmid (see Appendix 4 Fig.2). These constitute 5-6 short untranslated open reading frames (uORFs), that may produce short peptides stalling the ribosome and diminishing the translation efficiency of the main ORF [263-265]. This may explain why ZAC.VA produced much less protein than ZAC.DS plasmid, which lacks the 5'-UTR. However, ZAC.VA produced also much less *ZAC1* mRNA. Thus the presence of the 5'-UTR sequence may also affect the stability of the mRNA, possibly by affecting its secondary structure and thereby its stability. Furthermore, the pre-mature stop codons in this UTR may trigger nonsense mediated decay of the mRNA. This may be a new potential mechanism regulating ZAC1 expression and should be studied in detail.

4.3.3. ZAC1 protein stability

Many transcription factors and proteins involved in the regulation of cell proliferation and apoptosis get polyubiquitinated and quickly targeted for degradation by the proteasome-resulting in a short half-life. Since ZAC1 is reported to exert similar functions, we hypothesized that it follows this pattern. To prove this hypothesis, we treated stable, inducible or transiently transfected *ZAC1*-expressing cells and control transfected cells with the proteasome inhibitor MG132.

Indeed, MG132 treatment induced ZAC1 protein expression in positive stable 22Rv1 cell clones, but not in control lacZ clones. Most prominently increased was the ~45 kDa protein band, but two additional protein bands at ~50 kDa and ~40 kDa became visible. Furthermore, treatment of the tetracycline-induced ZAC.DS clone 2 with MG132 also markedly increased the ZAC1 protein level, while it had no effect on the uninduced cells. Similarly to the stable clones treated with MG132, an intensifying protein band of 45 kDa and two smaller protein bands at ~50 and ~40 kDa were also present in the induced MG132-treated clone. These results suggest that the exogenously-encoded ZAC1 is subjected to proteasomal degradation in stable and inducible clones.

Notably, treatment with MG132 of another inducible clone (ZAC.VA clone 10) did not result in any significant enhancement of ZAC1 protein. Since ZAC.VA plasmid was less efficient in ZAC1 protein production than ZAC.DS plasmid (discussed in 4.2.3), we suspected that the lack of visible MG132-effect may be due to generally low *ZAC1* mRNA production by ZAC.VA.

Collectively, these results suggest that a proteasome-dependent degradation process is involved in the down-regulation of ZAC1 protein levels in stable positive clones and inducible clones. Evidently, this process affected only the protein expressed from the transfected plasmids but not the endogenous ZAC1 protein.

The fact that only short (30 kDa and 45 kDa) endogenous ZAC1 protein forms (but not the 51 KDa form) were detected in untransfected LNCaP, 22Rv1 and PC3 cells despite equal amounts of the two spliced ZAC1 transcripts (not shown), suggests that the shorter mRNA/protein is more stable. Similarly, in prostate tissues, only a ~27 KDa ZAC1 protein was detected. Thus, our observations with the exogenous ZAC1 from the expression plasmids seem to be valid also for the endogenous ZAC1 in tissues.

4.3.4. ZAC1 mRNA stability

Interestingly, the protein induction by MG132 was always accompanied by a strong increase of *ZAC1* mRNA. This effect was present in all ZAC1 transfection models and affected only the exogenous mRNA, but had no effect on the endogenous ZAC1 in control lacZ transfections or uninduced clones.This effect may result from the inhibition of ZAC1 mRNA degradation by MG132 (Fig. 3.5.1).

MG132 induces a cellular stress response similar to ER stress [266-268].This means that several cellular processes like mRNA synthesis and translation are generally halted until the stress is relieved. Exceptions to this rule are mRNAs that contain internal ribosome entry site (IRES) sequences [269]. Such mRNAs are typically long, GC-rich, highly structured and may contain several upstream initiation codons. Under normal physiological conditions when cap-dependent translation is fully active, their highly structured 5'-UTR strongly inhibits their translation. However, under certain conditions like ER stress, when cap-dependent translation initiation is inhibited, cellular IRES-mediated translation is substantially increased. Online analysis using the IRESite database (http://iresite.org/IRESite_web.php) and the RegRNA tool (http://regrna.mbc.nctu.edu.tw/) revealed that the 5'-UTR of *ZAC1* contained in the ZAC.VA plasmid contains several potential IRES sequences (see Appendix 5). These sequences may contribute to the inefficient translation of ZAC.VA under normal conditions, and explain its enhancement under MG132 treatment.

Furthermore, certain mRNAs, which under normal conditions undergo a rapid decay in processing bodies (PBs), can be stabilized during the stress response/MG132 treatment [270-272]. The mechanism likely involves the sequestering of common protein components from PBs to other temporary organelles called stress granules (SG) [273]. This inhibits the mRNA degradatory function of PBs resulting in the accumulation of certain short-lived mRNAs.

Such a mechanism is known to regulate the stability of *CDKN1A* mRNA [267, 271]. The AU-rich motifs present in its 3‘-UTR are recognized by the CUGBP1 protein, that under normal growth conditions sequesters it to PBs for rapid degradation. Upon cell stress or treatment with proteasome inhibitors, *CDKN1A* mRNA is sequestered in SGs instead, which correlates with its stabilization.

Analogously, a similar mechanism may underly the stabilization of *ZAC1* mRNA upon proteasomal inhibition observed in our transfection experiments. Since the mRNAs produced from ZAC.VA and ZAC.DS were more strongly stabilized than that from ZACdelta plasmid, we suspected that particular motifs present mostly in the long ZAC1 mRNA isoform may be important for its degradation. Such motifs may be present in the UTRs as well as in the protein-coding sequences. As discussed in 4.4.2, the clustered upstream and downstream short ORFs in in the long ZAC1 isoform plasmids may be involved. Except interfering with the translation of mRNAs, uORFs have also been shown to enhance their degradation [274]. Using TargetScan online tool, we searched for miRNA binding sites or for motifs recognized by RNA-binding proteins in the 3’-UTR sequence contained in the ZAC.VA and ZACdelta plasmids but found no such elements (not shown). Nevertheless, yet unidentified RNA elements or secondary structures in the protein-coding sequence may be recognized by RNA-binding proteins which potentially regulate its localization, stability and availability for translation. In this respect, the differences in the 5‘-UTR and the protein-coding sequence between mouse and human ZAC1 can provide clues for the motifs involved in their regulation.

The localization of mouse *Zac1* mRNA to structures near nucleolus in mouse embryonic fibroblast cells has been suggested to be involved in its physical retention away from the translation machinery [275, 276]. Upon disruption of the nucleolus (and any adjacent structures) by Actinomycin D or DNA damage (through etoposide), *Zac1* mRNA was released, resulting in the strong induction of Zac1 protein. The authors suggested that this mechanism may enable rapid Zac1 protein synthesis upon stress. Importantly, in this study, both the *Zac1* gene and mRNA accumulated in close proximity to the nucleoli within the cell nucleus. The reports of Zac1 sequestration combined with our observations may

indicate the presence of an mRNA sequestration and degradation mechanism, inhibiting ZAC1 protein synthesis in many conditions.

4.4. ZAC1 function

4.4.1. Clonogenicity assay

We performed a clonogenicity assay to monitor the influence of stably transfected ZAC1 on the ability of cells to survive and form colonies. ZAC1-transfected cells could form visibly less colonies than lacZ-transfected cells. Thereby, the clonogenicity potentials of the cancer cells transfected with the three ZAC1 expression plasmids were different. While ZAC.VA-expressing cells could form more colonies than ZAC.DS, on the ZACdelta-transfected plates only very few clones survived. This is likely in part due to their different potency to overexpress ZAC1 proteins (discussed in 4.3.1 and 4.3.3). These results demonstrate the anti-proliferative and tumor suppressive function of ZAC1 in prostate cancer in principle. Our further experiments suggest that these effects may be mediated in particular through induction of cell cycle inhibitors such as $p57^{KIP2}$ and $p21^{CIP1}$.

4.4.2. ZAC1 –regulator of an imprinted gene network

Zac1 consensus binding sites were also found in the promoters or enhancers of several imprinted genes like *Lit1*, *Cdkn1c*, *Igf2* and *H19* [168, 277]. Based on bioinformatic analysis of a large amount of mouse RNA microarray expression data and confirmed by functional assays, Varrault et al. suggested that Zac1 is a master regulator of an imprinted gene network by activating the expression of the imprinted *Igf2*, *H19*, *Cdkn1c*, *Dlk1* and *Gtl2/Meg3* genes [168].

Several of these genes including ZAC1 were found to be deregulated in prostate cancer by the *in silico* analysis of KM Bastian and my experiments. Thus we wanted to find whether ZAC1 can induce these genes in prostate cancer. For the purpose we assessed ZAC1-transiently transfected cells and stable polyclonal cell pools. Indeed, transient overexpression of *ZAC1* in 22Rv1 resulted in significant increases in the expression of *CDKN1C*, *H19*, and *IGF2*, and more modestly of *LIT1* and *PEG10* genes. The strong induction of *H19* and *IGF2* may likely be caused by the previously reported ZAC1 direct binding to G_4C_4 sequences in their endodermal enhancers and thereby transactivation of their promoters [168]. *IGF2* and *LIT1* were also induced in the polyclonal pools from both 22Rv1 and LNCaP cell lines. *LIT1* has been reported to be a direct target gene of ZAC1 [277]. However, the long term effect of *ZAC1* overexpression on *LIT1* induction, exemplified by polyclonal stable pools, was relatively stronger than the short term effect of the transient *ZAC1* transfection. It might thus be modulated by a ZAC1-induced target. In contrast, the expression of *CDKN1C* was not increased in 22Rv1 and even slightly decreased in LNCaP, compared to lacZ-transfected stable polyclonal pools. As the

expression of *CDKN1C* can induce cell cycle arrest in prostatic cells [149], it is likely that during the polyclonal selection, $p57^{KIP2}$ expressing cells may stop dividing and ultimately die, leading to its downregulation in surviving clones. Indeed, 22Rv1 cells transiently transfected with ZAC.DS or ZACdelta exhibited strongly increased $p57^{KIP2}$ protein levels. Therefore, *CDKN1C* levels of polyclonal stable cells may have been strongly downregulated by feedback regulatory mechanisms or as a consequence of negative selection.

In transient transfection experiments, the expression of *SGCE*, *PON2*, *PEG3* and *HYMAI* genes was also induced, but peculiarly only by the ZACdelta plasmid, and not as much by the other two ZAC1-coding plasmids. This effect may be due to the higher ZAC1 protein amount produced by ZACdelta in comparison to the ZAC.VA and ZAC.DS plasmids. Similarly, ZACdelta overexpression had a much more potent inducing effect on *CDKN1C* and *IGF2*. Alternatively, these results may reflect an improved DNA binding and transcriptional regulatory activity of the 5-finger ZAC1 delta protein isoform over the 7-finger form. Clearly the findings open the question whether the two isoforms exert differential effects on the imprinted gene network.

4.4.3. Induction of CDKN1A by ZAC1 isoforms

The short ZAC1delta isoform has been shown to induce more efficiently G0/G1 cell cycle arrest than the long ZAC1 protein form [185]. We hypothesized that this effect may be in part mediated by the induction of the *CDKN1A* gene coding for the $p21^{CIP1}$ protein. It is a known target gene of p53 and was shown to be transactivated by Zac1 in conjunction with p53 or independently of it [278]. During the neuronal differentiation of embryonic stem cells Zac1 is recruited to the p21 promoter by the p73 protein, where it acts as a scaffolding protein stabilizing the association of the histone acetyltransferases PCAF and p300 [179]. In order to monitor if ZAC1 isoforms may exhibit different potentials for inducing *CDKN1A*, we measured its expression in *ZAC1*-overexpressing cells and assessed the influence of transient *ZAC1* overexpression on the activity of a *CDKN1A* promoter-luciferase reporter assay.

Indeed, the *CDKN1A* gene was induced in stably polyclonal cells transfected with the ZAC.VA and ZAC.DS plasmids. In this experiment, ZAC.VA was slightly more potent in the induction of *CDKN1A* than ZAC.DS. Unfortunately, we could not generate ZACdelta-transfected stable polyclonal cells and cannot compare the effect of the short ZAC1 isoform in this model. Nevertheless, in the transient transfection experiment where all plasmids were applied, the long ZAC1 isoforms encoded by ZAC.VA induced the expression of *CDKN1A*, ZAC.DS had no significant influence on it, and the short isoform ZACdelta repressed it. In fact, ZAC1 has been reported to posseses repressive activity on

some promoters, depending on the orientation of its consensus binding sites when several of them are present in tandem [175]. Thereby the structure of ZAC1 dimers can determine its interactions with histone modifying- and other partner proteins, influencing its transactivation or repression activity [279]. Our results suggest that the long ZAC1 isoforms activate, while the short isoform represses *CDKN1A* expression. This may, however, be also a dosage-dependent effect of ZAC1 protein, being more highly produced by ZACdelta plasmid.

Luciferase reporter assay using a segment of the *CDKN1A* promoter upstream of the luciferase gene was used to prove these differences. However, the activity of the reporter gene was increased by transfection of all three *ZAC1* expressing plasmids. This discrepancy with the results from the experiments discussed above may be due to the different contexts of the wild type *CDKN1A* promoter and the short sequence present in the reporter gene. The former is very long and contains binding sites for many proteins, which may modulate each others activity resulting in either activated or repressed transcription. It is therefore possible that differential co-modulatory proteins of the long and short ZAC1 isoforms at the wild type *CDKN1A* promoter may be absent at the shorter reporter gene promoter. This may explain the observed different transcriptional activity of ZAC1 in the two promoter contexts.

Notably, the regulation of *CDKN1A*/p21 is very complex. Apart from transcriptional activation it includes posttranscriptional mechanisms at the mRNA and protein levels that may also influence the amount of *CDKN1A* mRNA via feedback regulation [280-284]. The differences between reporter gene and mRNA expression measurements could also arise at this level of regulation.

4.4.4. Influence of ZAC1 on androgen response

The PC3 prostate cancer cell line, derived from metastatic androgen-insensitive lesions in the bone, endogenously expresses AR at a very low level and grows independently of androgens [285]. However, when transfected with wild type AR, PC3 cells can actively respond to androgens and activate reporter constructs containing AR-responsive elements. This model is often used to study the effect of different treatments or exogenous proteins on the androgen response in prostate cancer [285].

In order to examine the role of endogenous and exogenous ZAC1 in AR signaling, we combined the AR response PC3 cell line model with siRNA-mediated downregulation of *ZAC1* or transfection of *ZAC1*-expression plasmids. Thereby, the activity of two AR-responsive reporter genes -one containing the rat probasin promoter- Pb-luc and the other one containing several androgen responsive elements- ARE-luc were assessed.

In the absence of AR ligand, the synthetic androgen R1881, Pb-luc activity was slightly higher in PC3 cells transfected with the AR than without it. The activatory role of AR on this reporter gene is therefore not exclusively dependent on androgen ligands. In contrast, the activity of ARE-luc was androgen-specific, being only increased in the presence of both AR and androgens. When ZAC1 was downregulated with siRNA the response of both reporters to R1881 was diminished. Thus, the endogenous human ZAC1 seems to assist the activation of the AR-sensitive reporters, confirming its role as an AR co-activator in the prostate. This function has been previously reported in experiments using mouse *Zac1* in human cancer cell lines [183]. Further supporting evidence for a stimulatory role of ZAC1 on androgen signaling was gained by the transient ZAC1 overexpression experiments in PC3 cells where ZAC1 significantly stimulated the AR response.

As androgen signaling supports growth and survival of prostate cancer, the stimulatory activity of ZAC1 would appear to contradict its presumable tumor suppressor function. In order to explain this apparent paradox, it is important to consider that the androgen response in prostate cancer is different from that in normal prostate tissue, in being distorted towards supporting proliferation rather than differentiation [23, 286, 287]. Among others, the AR has been reported to exert anti-proliferative effects on PC3 cells, by activating genes with functions in cell proliferation and programmed cell death [288]. One may therefore speculate that loss of ZAC1 expression during cancer progression may affect the induction of certain AR- and ZAC1-co-targeted genes that limit proliferation and stimulate differentiation. This hypothesis could be tested by gene expression profiles of PC3 cells with different levels of ZAC1 and AR activity.

List of References

1. Mellinger GT, Gleason D, and Bailar J, 3rd. **The histology and prognosis of prostatic cancer**. *J Urol* 1967; 97(2): p. 331-7.
2. Epstein JI. **An update of the Gleason grading system**. *J Urol* 2010; 183(2): p. 433-40.
3. Epstein JI, Allsbrook WC, Jr., Amin MB, and Egevad LL. **Update on the Gleason grading system for prostate cancer: results of an international consensus conference of urologic pathologists**. *Adv Anat Pathol* 2006; 13(1): p. 57-9.
4. Egevad L, Granfors T, Karlberg L, Bergh A, and Stattin P. **Percent Gleason grade 4/5 as prognostic factor in prostate cancer diagnosed at transurethral resection**. *J Urol* 2002; 168(2): p. 509-13.
5. De Angelis G, Rittenhouse HG, Mikolajczyk SD, Blair Shamel L, and Semjonow A. **Twenty Years of PSA: From Prostate Antigen to Tumor Marker**. *Rev Urol* 2007; 9(3): p. 113-23.
6. Potter SR and Partin AW. **Tumor markers: an update on human kallikrein 2**. *Rev Urol* 2000; 2(4): p. 221-2.
7. Heemers HV and Tindall DJ. **Androgen receptor (AR) coregulators: a diversity of functions converging on and regulating the AR transcriptional complex**. *Endocr Rev* 2007; 28(7): p. 778-808.
8. Feldman BJ and Feldman D. **The development of androgen-independent prostate cancer**. *Nat Rev Cancer* 2001; 1(1): p. 34-45.
9. Chmelar R, Buchanan G, Need EF, Tilley W, and Greenberg NM. **Androgen receptor coregulators and their involvement in the development and progression of prostate cancer**. *Int J Cancer* 2007; 120(4): p. 719-33.
10. Shen MM and Abate-Shen C. **Molecular genetics of prostate cancer: new prospects for old challenges**. *Genes Dev* 2010; 24(18): p. 1967-2000.
11. Lapointe J, Li C, Giacomini CP, Salari K, Huang S, Wang P, Ferrari M, Hernandez-Boussard T, Brooks JD, and Pollack JR. **Genomic profiling reveals alternative genetic pathways of prostate tumorigenesis**. *Cancer Res* 2007; 67(18): p. 8504-10.
12. Dong JT. **Chromosomal deletions and tumor suppressor genes in prostate cancer**. *Cancer Metastasis Rev* 2001; 20(3-4): p. 173-93.
13. Taylor BS, Schultz N, Hieronymus H, Gopalan A, Xiao Y, Carver BS, Arora VK, Kaushik P, Cerami E, Reva B, Antipin Y, Mitsiades N, Landers T, Dolgalev I, Major JE, Wilson M, Socci ND, Lash AE, Heguy A, Eastham JA, Scher HI, Reuter VE, Scardino PT, Sander C, Sawyers CL, and Gerald WL. **Integrative genomic profiling of human prostate cancer**. *Cancer Cell* 2010; 18(1): p. 11-22.
14. Bhatia-Gaur R, Donjacour AA, Sciavolino PJ, Kim M, Desai N, Young P, Norton CR, Gridley T, Cardiff RD, Cunha GR, Abate-Shen C, and Shen MM. **Roles for Nkx3.1 in prostate development and cancer**. *Genes Dev* 1999; 13(8): p. 966-77.
15. Edwards J, Krishna NS, Grigor KM, and Bartlett JM. **Androgen receptor gene amplification and protein expression in hormone refractory prostate cancer**. *Br J Cancer* 2003; 89(3): p. 552-6.
16. Gerhardt J, Montani M, Wild P, Beer M, Huber F, Hermanns T, Muntener M, and Kristiansen G. **FOXA1 promotes tumor progression in prostate cancer and represents a novel hallmark of castration-resistant prostate cancer**. *Am J Pathol* 2012; 180(2): p. 848-61.
17. Miller GJ, Miller HL, van Bokhoven A, Lambert JR, Werahera PN, Schirripa O, Lucia MS, and Nordeen SK. **Aberrant HOXC expression accompanies the malignant phenotype in human prostate**. *Cancer Res* 2003; 63(18): p. 5879-88.
18. Ramachandran S, Liu P, Young AN, Yin-Goen Q, Lim SD, Laycock N, Amin MB, Carney JK, Marshall FF, Petros JA, and Moreno CS. **Loss of HOXC6 expression induces apoptosis in prostate cancer cells**. *Oncogene* 2005; 24(1): p. 188-98.

19. Bibikova M, Chudin E, Arsanjani A, Zhou L, Garcia EW, Modder J, Kostelec M, Barker D, Downs T, Fan JB, and Wang-Rodriguez J. **Expression signatures that correlated with Gleason score and relapse in prostate cancer**. *Genomics* 2007; 89(6): p. 666-72.
20. Tomlins SA, Rhodes DR, Perner S, Dhanasekaran SM, Mehra R, Sun XW, Varambally S, Cao X, Tchinda J, Kuefer R, Lee C, Montie JE, Shah RB, Pienta KJ, Rubin MA, and Chinnaiyan AM. **Recurrent fusion of TMPRSS2 and ETS transcription factor genes in prostate cancer**. *Science* 2005; 310(5748): p. 644-8.
21. Tomlins SA, Laxman B, Dhanasekaran SM, Helgeson BE, Cao X, Morris DS, Menon A, Jing X, Cao Q, Han B, Yu J, Wang L, Montie JE, Rubin MA, Pienta KJ, Roulston D, Shah RB, Varambally S, Mehra R, and Chinnaiyan AM. **Distinct classes of chromosomal rearrangements create oncogenic ETS gene fusions in prostate cancer**. *Nature* 2007; 448(7153): p. 595-9.
22. Hermans KG, van Marion R, van Dekken H, Jenster G, van Weerden WM, and Trapman J. **TMPRSS2:ERG fusion by translocation or interstitial deletion is highly relevant in androgen-dependent prostate cancer, but is bypassed in late-stage androgen receptor-negative prostate cancer**. *Cancer Res* 2006; 66(22): p. 10658-63.
23. Yu J, Mani RS, Cao Q, Brenner CJ, Cao X, Wang X, Wu L, Li J, Hu M, Gong Y, Cheng H, Laxman B, Vellaichamy A, Shankar S, Li Y, Dhanasekaran SM, Morey R, Barrette T, Lonigro RJ, Tomlins SA, Varambally S, Qin ZS, and Chinnaiyan AM. **An integrated network of androgen receptor, polycomb, and TMPRSS2-ERG gene fusions in prostate cancer progression**. *Cancer Cell* 2010; 17(5): p. 443-54.
24. Barwick BG, Abramovitz M, Kodani M, Moreno CS, Nam R, Tang W, Bouzyk M, Seth A, and Leyland-Jones B. **Prostate cancer genes associated with TMPRSS2-ERG gene fusion and prognostic of biochemical recurrence in multiple cohorts**. *Br J Cancer* 2010; 102(3): p. 570-6.
25. Attard G, Clark J, Ambroisine L, Fisher G, Kovacs G, Flohr P, Berney D, Foster CS, Fletcher A, Gerald WL, Moller H, Reuter V, De Bono JS, Scardino P, Cuzick J, Cooper CS, and Transatlantic Prostate G. **Duplication of the fusion of TMPRSS2 to ERG sequences identifies fatal human prostate cancer**. *Oncogene* 2008; 27(3): p. 253-63.
26. Saramaki OR, Harjula AE, Martikainen PM, Vessella RL, Tammela TL, and Visakorpi T. **TMPRSS2:ERG fusion identifies a subgroup of prostate cancers with a favorable prognosis**. *Clin Cancer Res* 2008; 14(11): p. 3395-400.
27. Bryant RJ, Cross NA, Eaton CL, Hamdy FC, and Cunliffe VT. **EZH2 promotes proliferation and invasiveness of prostate cancer cells**. *Prostate* 2007; 67(5): p. 547-56.
28. Cao Q, Yu J, Dhanasekaran SM, Kim JH, Mani RS, Tomlins SA, Mehra R, Laxman B, Cao X, Kleer CG, Varambally S, and Chinnaiyan AM. **Repression of E-cadherin by the polycomb group protein EZH2 in cancer**. *Oncogene* 2008; 27(58): p. 7274-84.
29. Chng KR, Chang CW, Tan SK, Yang C, Hong SZ, Sng NY, and Cheung E. **A transcriptional repressor co-regulatory network governing androgen response in prostate cancers**. *EMBO J* 2012; 31(12): p. 2810-23.
30. Bachmann IM, Halvorsen OJ, Collett K, Stefansson IM, Straume O, Haukaas SA, Salvesen HB, Otte AP, and Akslen LA. **EZH2 expression is associated with high proliferation rate and aggressive tumor subgroups in cutaneous melanoma and cancers of the endometrium, prostate, and breast**. *J Clin Oncol* 2006; 24(2): p. 268-73.
31. Pietersen AM, Horlings HM, Hauptmann M, Langerod A, Ajouaou A, Cornelissen-Steijger P, Wessels LF, Jonkers J, van de Vijver MJ, and van Lohuizen M. **EZH2 and BMI1 inversely correlate with prognosis and TP53 mutation in breast cancer**. *Breast Cancer Res* 2008; 10(6): p. R109.
32. Varambally S, Dhanasekaran SM, Zhou M, Barrette TR, Kumar-Sinha C, Sanda MG, Ghosh D, Pienta KJ, Sewalt RG, Otte AP, Rubin MA, and Chinnaiyan AM. **The polycomb group protein EZH2 is involved in progression of prostate cancer**. *Nature* 2002; 419(6907): p. 624-9.

33. Holm K, Grabau D, Lovgren K, Aradottir S, Gruvberger-Saal S, Howlin J, Saal LH, Ethier SP, Bendahl PO, Stal O, Malmstrom P, Ferno M, Ryden L, Hegardt C, Borg A, and Ringner M. **Global H3K27 trimethylation and EZH2 abundance in breast tumor subtypes**. *Mol Oncol* 2012; 6(5): p. 494-506.
34. McGarvey KM, Greene E, Fahrner JA, Jenuwein T, and Baylin SB. **DNA methylation and complete transcriptional silencing of cancer genes persist after depletion of EZH2**. *Cancer Res* 2007; 67(11): p. 5097-102.
35. Ezhkova E, Pasolli HA, Parker JS, Stokes N, Su IH, Hannon G, Tarakhovsky A, and Fuchs E. **Ezh2 orchestrates gene expression for the stepwise differentiation of tissue-specific stem cells**. *Cell* 2009; 136(6): p. 1122-35.
36. Kunderfranco P, Mello-Grand M, Cangemi R, Pellini S, Mensah A, Albertini V, Malek A, Chiorino G, Catapano CV, and Carbone GM. **ETS transcription factors control transcription of EZH2 and epigenetic silencing of the tumor suppressor gene Nkx3.1 in prostate cancer**. *PLoS One* 2010; 5(5): p. e10547.
37. Lonergan PE and Tindall DJ. **Androgen receptor signaling in prostate cancer development and progression**. *J Carcinog* 2011; 10: p. 20.
38. Zhu ML and Kyprianou N. **Androgen receptor and growth factor signaling cross-talk in prostate cancer cells**. *Endocr Relat Cancer* 2008; 15(4): p. 841-9.
39. Hodgson MC, Shao LJ, Frolov A, Li R, Peterson LE, Ayala G, Ittmann MM, Weigel NL, and Agoulnik IU. **Decreased expression and androgen regulation of the tumor suppressor gene INPP4B in prostate cancer**. *Cancer Res* 2011; 71(2): p. 572-82.
40. Chen M, Pratt CP, Zeeman ME, Schultz N, Taylor BS, O'Neill A, Castillo-Martin M, Nowak DG, Naguib A, Grace DM, Murn J, Navin N, Atwal GS, Sander C, Gerald WL, Cordon-Cardo C, Newton AC, Carver BS, and Trotman LC. **Identification of PHLPP1 as a tumor suppressor reveals the role of feedback activation in PTEN-mutant prostate cancer progression**. *Cancer Cell* 2011; 20(2): p. 173-86.
41. Agoulnik IU, Hodgson MC, Bowden WA, and Ittmann MM. **INPP4B: the new kid on the PI3K block**. *Oncotarget* 2011; 2(4): p. 321-8.
42. Carver BS, Chapinski C, Wongvipat J, Hieronymus H, Chen Y, Chandarlapaty S, Arora VK, Le C, Koutcher J, Scher H, Scardino PT, Rosen N, and Sawyers CL. **Reciprocal feedback regulation of PI3K and androgen receptor signaling in PTEN-deficient prostate cancer**. *Cancer Cell* 2011; 19(5): p. 575-86.
43. Mulholland DJ, Tran LM, Li Y, Cai H, Morim A, Wang S, Plaisier S, Garraway IP, Huang J, Graeber TG, and Wu H. **Cell autonomous role of PTEN in regulating castration-resistant prostate cancer growth**. *Cancer Cell* 2011; 19(6): p. 792-804.
44. Thompson TC. **Turning reciprocal feedback regulation into combination therapy**. *Cancer Cell* 2011; 19(6): p. 697-9.
45. Lin HK, Hu YC, Lee DK, and Chang C. **Regulation of androgen receptor signaling by PTEN (phosphatase and tensin homolog deleted on chromosome 10) tumor suppressor through distinct mechanisms in prostate cancer cells**. *Mol Endocrinol* 2004; 18(10): p. 2409-23.
46. Schulz WA and Hatina J. **Epigenetics of prostate cancer: beyond DNA methylation**. *J Cell Mol Med* 2006; 10(1): p. 100-25.
47. Cooper CS and Foster CS. **Concepts of epigenetics in prostate cancer development**. *Br J Cancer* 2009; 100(2): p. 240-5.
48. Nakayama M, Bennett CJ, Hicks JL, Epstein JI, Platz EA, Nelson WG, and De Marzo AM. **Hypermethylation of the human glutathione S-transferase-pi gene (GSTP1) CpG island is present in a subset of proliferative inflammatory atrophy lesions but not in normal or hyperplastic epithelium of the prostate: a detailed study using laser-capture microdissection**. *Am J Pathol* 2003; 163(3): p. 923-33.
49. Florl AR, Steinhoff C, Muller M, Seifert HH, Hader C, Engers R, Ackermann R, and Schulz WA. **Coordinate hypermethylation at specific genes in prostate carcinoma precedes LINE-1 hypomethylation**. *Br J Cancer* 2004; 91(5): p. 985-94.

50. Schulz WA, Alexa A, Jung V, Hader C, Hoffmann MJ, Yamanaka M, Fritzsche S, Wlazlinski A, Muller M, Lengauer T, Engers R, Florl AR, Wullich B, and Rahnenfuhrer J. **Factor interaction analysis for chromosome 8 and DNA methylation alterations highlights innate immune response suppression and cytoskeletal changes in prostate cancer**. *Mol Cancer* 2007; 6: p. 14.
51. Goering W, Ribarska T, and Schulz WA. **Selective changes of retroelement expression in human prostate cancer**. *Carcinogenesis* 2011; 32(10): p. 1484-92.
52. Karanikolas BD, Figueiredo ML, and Wu L. **Polycomb group protein enhancer of zeste 2 is an oncogene that promotes the neoplastic transformation of a benign prostatic epithelial cell line**. *Mol Cancer Res* 2009; 7(9): p. 1456-65.
53. Ugolkov AV, Eisengart LJ, Luan C, and Yang XJ. **Expression analysis of putative stem cell markers in human benign and malignant prostate**. *Prostate* 2011; 71(1): p. 18-25.
54. Schlesinger Y, Straussman R, Keshet I, Farkash S, Hecht M, Zimmerman J, Eden E, Yakhini Z, Ben-Shushan E, Reubinoff BE, Bergman Y, Simon I, and Cedar H. **Polycomb-mediated methylation on Lys27 of histone H3 pre-marks genes for de novo methylation in cancer**. *Nat Genet* 2007; 39(2): p. 232-6.
55. Ko S, Ahn J, Song CS, Kim S, Knapczyk-Stwora K, and Chatterjee B. **Lysine methylation and functional modulation of androgen receptor by Set9 methyltransferase**. *Mol Endocrinol* 2011; 25(3): p. 433-44.
56. Xu K, Wu ZJ, Groner AC, He HH, Cai C, Lis RT, Wu X, Stack EC, Loda M, Liu T, Xu H, Cato L, Thornton JE, Gregory RI, Morrissey C, Vessella RL, Montironi R, Magi-Galluzzi C, Kantoff PW, Balk SP, Liu XS, and Brown M. **EZH2 oncogenic activity in castration-resistant prostate cancer cells is Polycomb-independent**. *Science* 2012; 338(6113): p. 1465-9.
57. Gaughan L, Stockley J, Wang N, McCracken SR, Treumann A, Armstrong K, Shaheen F, Watt K, McEwan IJ, Wang C, Pestell RG, and Robson CN. **Regulation of the androgen receptor by SET9-mediated methylation**. *Nucleic Acids Res* 2011; 39(4): p. 1266-79.
58. He A, Shen X, Ma Q, Cao J, von Gise A, Zhou P, Wang G, Marquez VE, Orkin SH, and Pu WT. **PRC2 directly methylates GATA4 and represses its transcriptional activity**. *Genes Dev* 2012; 26(1): p. 37-42.
59. Lee ST, Li Z, Wu Z, Aau M, Guan P, Karuturi RK, Liou YC, and Yu Q. **Context-specific regulation of NF-kappaB target gene expression by EZH2 in breast cancers**. *Mol Cell* 2011; 43(5): p. 798-810.
60. Shi B, Liang J, Yang X, Wang Y, Zhao Y, Wu H, Sun L, Zhang Y, Chen Y, Li R, Hong M, and Shang Y. **Integration of estrogen and Wnt signaling circuits by the polycomb group protein EZH2 in breast cancer cells**. *Mol Cell Biol* 2007; 27(14): p. 5105-19.
61. Broze GJ, Jr. and Girard TJ. **Tissue factor pathway inhibitor: structure-function**. *Front Biosci* 2012; 17: p. 262-80.
62. Ettelaie C, Li C, Collier ME, Pradier A, Frentzou GA, Wood CG, Chetter IC, McCollum PT, Bruckdorfer KR, and James NJ. **Differential functions of tissue factor in the trans-activation of cellular signalling pathways**. *Atherosclerosis* 2007; 194(1): p. 88-101.
63. Chen J, Bierhaus A, Schiekofer S, Andrassy M, Chen B, Stern DM, and Nawroth PP. **Tissue factor--a receptor involved in the control of cellular properties, including angiogenesis**. *Thromb Haemost* 2001; 86(1): p. 334-45.
64. Abdulkadir SA, Carvalhal GF, Kaleem Z, Kisiel W, Humphrey PA, Catalona WJ, and Milbrandt J. **Tissue factor expression and angiogenesis in human prostate carcinoma**. *Hum Pathol* 2000; 31(4): p. 443-7.
65. Versteeg HH, Schaffner F, Kerver M, Petersen HH, Ahamed J, Felding-Habermann B, Takada Y, Mueller BM, and Ruf W. **Inhibition of tissue factor signaling suppresses tumor growth**. *Blood* 2008; 111(1): p. 190-9.
66. Rak J, Milsom C, Magnus N, and Yu J. **Tissue factor in tumour progression**. *Best Pract Res Clin Haematol* 2009; 22(1): p. 71-83.
67. Bluff JE, Brown NJ, Reed MW, and Staton CA. **Tissue factor, angiogenesis and tumour progression**. *Breast Cancer Res* 2008; 10(2): p. 204.

68. Kaushal V, Mukunyadzi P, Siegel ER, Dennis RA, Johnson DE, and Kohli M. **Expression of tissue factor in prostate cancer correlates with malignant phenotype**. *Appl Immunohistochem Mol Morphol* 2008; 16(1): p. 1-6.
69. Akashi T, Furuya Y, Ohta S, and Fuse H. **Tissue factor expression and prognosis in patients with metastatic prostate cancer**. *Urology* 2003; 62(6): p. 1078-82.
70. Ohta S, Wada H, Nakazaki T, Maeda Y, Nobori T, Shiku H, Nakamura S, Nagakawa O, Furuya Y, and Fuse H. **Expression of tissue factor is associated with clinical features and angiogenesis in prostate cancer**. *Anticancer Res* 2002; 22(5): p. 2991-6.
71. Konduri SD, Tasiou A, Chandrasekar N, and Rao JS. **Overexpression of tissue factor pathway inhibitor-2 (TFPI-2), decreases the invasiveness of prostate cancer cells in vitro**. *Int J Oncol* 2001; 18(1): p. 127-31.
72. Guo H, Lin Y, Zhang H, Liu J, Zhang N, Li Y, Kong D, Tang Q, and Ma D. **Tissue factor pathway inhibitor-2 was repressed by CpG hypermethylation through inhibition of KLF6 binding in highly invasive breast cancer cells**. *BMC Mol Biol* 2007; 8: p. 110.
73. Hibi K, Goto T, Kitamura YH, Yokomizo K, Sakuraba K, Shirahata A, Mizukami H, Saito M, Ishibashi K, Kigawa G, Nemoto H, and Sanada Y. **Methylation of TFPI2 gene is frequently detected in advanced well-differentiated colorectal cancer**. *Anticancer Res* 2010; 30(4): p. 1205-7.
74. Rao CN, Segawa T, Navari JR, Xu L, Srivastava S, Moul JW, and Phillips B. **Methylation of TFPI-2 gene is not the sole cause of its silencing**. *Int J Oncol* 2003; 22(4): p. 843-8.
75. Sato N, Parker AR, Fukushima N, Miyagi Y, Iacobuzio-Donahue CA, Eshleman JR, and Goggins M. **Epigenetic inactivation of TFPI-2 as a common mechanism associated with growth and invasion of pancreatic ductal adenocarcinoma**. *Oncogene* 2005; 24(5): p. 850-8.
76. Takada H, Wakabayashi N, Dohi O, Yasui K, Sakakura C, Mitsufuji S, Taniwaki M, and Yoshikawa T. **Tissue factor pathway inhibitor 2 (TFPI2) is frequently silenced by aberrant promoter hypermethylation in gastric cancer**. *Cancer Genet Cytogenet* 2010; 197(1): p. 16-24.
77. Morison IM, Ramsay JP, and Spencer HG. **A census of mammalian imprinting**. *Trends Genet* 2005; 21(8): p. 457-65.
78. Li Y and Sasaki H. **Genomic imprinting in mammals: its life cycle, molecular mechanisms and reprogramming**. *Cell Res* 2011; 21(3): p. 466-73.
79. Ferguson-Smith AC. **Genomic imprinting: the emergence of an epigenetic paradigm**. *Nat Rev Genet* 2011; 12(8): p. 565-75.
80. Bartolomei MS and Ferguson-Smith AC. **Mammalian genomic imprinting**. *Cold Spring Harb Perspect Biol* 2011; 3(7).
81. John RM and Lefebvre L. **Developmental regulation of somatic imprints**. *Differentiation* 2011; 81(5): p. 270-80.
82. Strogantsev R and Ferguson-Smith AC. **Proteins involved in establishment and maintenance of imprinted methylation marks**. *Brief Funct Genomics* 2012; 11(3): p. 227-39.
83. Singh P, Wu X, Lee DH, Li AX, Rauch TA, Pfeifer GP, Mann JR, and Szabo PE. **Chromosome-wide analysis of parental allele-specific chromatin and DNA methylation**. *Mol Cell Biol* 2011; 31(8): p. 1757-70.
84. Kacem S and Feil R. **Chromatin mechanisms in genomic imprinting**. *Mamm Genome* 2009; 20(9-10): p. 544-56.
85. Ciccone DN and Chen T. **Histone lysine methylation in genomic imprinting**. *Epigenetics* 2009; 4(4): p. 216-20.
86. Murrell A. **Setting up and maintaining differential insulators and boundaries for genomic imprinting**. *Biochem Cell Biol* 2011; 89(5): p. 469-78.
87. Banerjee S, Smallwood A, Lamond S, Campbell S, and Nargund G. **Igf2/H19 imprinting control region (ICR): an insulator or a position-dependent silencer?** *ScientificWorldJournal* 2001; 1: p. 218-24.

88. Singh P, Lee DH, and Szabo PE. **More than insulator: multiple roles of CTCF at the H19-Igf2 imprinted domain**. *Front Genet* 2012; 3: p. 214.
89. Pauler FM, Barlow DP, and Hudson QJ. **Mechanisms of long range silencing by imprinted macro non-coding RNAs**. *Curr Opin Genet Dev* 2012; 22(3): p. 283-9.
90. Pauler FM, Koerner MV, and Barlow DP. **Silencing by imprinted noncoding RNAs: is transcription the answer?** *Trends Genet* 2007; 23(6): p. 284-92.
91. Peters J and Robson JE. **Imprinted noncoding RNAs**. *Mamm Genome* 2008; 19(7-8): p. 493-502.
92. Radford EJ, Ferron SR, and Ferguson-Smith AC. **Genomic imprinting as an adaptative model of developmental plasticity**. *FEBS Lett* 2011; 585(13): p. 2059-66.
93. Edwards CA, Rens W, Clarke O, Mungall AJ, Hore T, Graves JA, Dunham I, Ferguson-Smith AC, and Ferguson-Smith MA. **The evolution of imprinting: chromosomal mapping of orthologues of mammalian imprinted domains in monotreme and marsupial mammals**. *BMC Evol Biol* 2007; 7: p. 157.
94. Renfree MB, Papenfuss AT, Shaw G, and Pask AJ. **Eggs, embryos and the evolution of imprinting: insights from the platypus genome**. *Reprod Fertil Dev* 2009; 21(8): p. 935-42.
95. Renfree MB, Hore TA, Shaw G, Graves JA, and Pask AJ. **Evolution of genomic imprinting: insights from marsupials and monotremes**. *Annu Rev Genomics Hum Genet* 2009; 10: p. 241-62.
96. Wolf JB and Hager R. **A maternal-offspring coadaptation theory for the evolution of genomic imprinting**. *PLoS Biol* 2006; 4(12): p. e380.
97. Diplas AI, Lambertini L, Lee MJ, Sperling R, Lee YL, Wetmur J, and Chen J. **Differential expression of imprinted genes in normal and IUGR human placentas**. *Epigenetics* 2009; 4(4): p. 235-40.
98. McMinn J, Wei M, Schupf N, Cusmai J, Johnson EB, Smith AC, Weksberg R, Thaker HM, and Tycko B. **Unbalanced placental expression of imprinted genes in human intrauterine growth restriction**. *Placenta* 2006; 27(6-7): p. 540-9.
99. Frost JM and Moore GE. **The importance of imprinting in the human placenta**. *PLoS Genet* 2010; 6(7): p. e1001015.
100. Bressan FF, De Bem TH, Perecin F, Lopes FL, Ambrosio CE, Meirelles FV, and Miglino MA. **Unearthing the roles of imprinted genes in the placenta**. *Placenta* 2009; 30(10): p. 823-34.
101. Hamed M, Ismael S, Paulsen M, and Helms V. **Cellular functions of genetically imprinted genes in human and mouse as annotated in the gene ontology**. *PLoS One* 2012; 7(11): p. e50285.
102. Abu-Amero S, Monk D, Apostolidou S, Stanier P, and Moore G. **Imprinted genes and their role in human fetal growth**. *Cytogenet Genome Res* 2006; 113(1-4): p. 262-70.
103. Frontera M, Dickins B, Plagge A, and Kelsey G. **Imprinted genes, postnatal adaptations and enduring effects on energy homeostasis**. *Adv Exp Med Biol* 2008; 626: p. 41-61.
104. Ishida M and Moore GE. **The role of imprinted genes in humans**. *Mol Aspects Med* 2012.
105. Ivanova E and Kelsey G. **Imprinted genes and hypothalamic function**. *J Mol Endocrinol* 2011; 47(2): p. R67-74.
106. Reik W, Davies K, Dean W, Kelsey G, and Constancia M. **Imprinted genes and the coordination of fetal and postnatal growth in mammals**. *Novartis Found Symp* 2001; 237: p. 19-31; discussion 31-42.
107. Tycko B and Morison IM. **Physiological functions of imprinted genes**. *J Cell Physiol* 2002; 192(3): p. 245-58.
108. Weinstein LS, Xie T, Qasem A, Wang J, and Chen M. **The role of GNAS and other imprinted genes in the development of obesity**. *Int J Obes (Lond)* 2010; 34(1): p. 6-17.
109. Wilkinson LS, Davies W, and Isles AR. **Genomic imprinting effects on brain development and function**. *Nat Rev Neurosci* 2007; 8(11): p. 832-43.
110. Davies W, Isles AR, Humby T, and Wilkinson LS. **What are imprinted genes doing in the brain?** *Adv Exp Med Biol* 2008; 626: p. 62-70.

111. Davies W, Lynn PM, Relkovic D, and Wilkinson LS. **Imprinted genes and neuroendocrine function**. *Front Neuroendocrinol* 2008; 29(3): p. 413-27.
112. Ubeda F and Gardner A. **A model for genomic imprinting in the social brain: adults**. *Evolution* 2011; 65(2): p. 462-75.
113. Prickett AR and Oakey RJ. **A survey of tissue-specific genomic imprinting in mammals**. *Mol Genet Genomics* 2012; 287(8): p. 621-30.
114. Dekel B, Metsuyanim S, Schmidt-Ott KM, Fridman E, Jacob-Hirsch J, Simon A, Pinthus J, Mor Y, Barasch J, Amariglio N, Reisner Y, Kaminski N, and Rechavi G. **Multiple imprinted and stemness genes provide a link between normal and tumor progenitor cells of the developing human kidney**. *Cancer Res* 2006; 66(12): p. 6040-9.
115. Wu Q, Kawahara M, and Kono T. **Synergistic role of Igf2 and Dlk1 in fetal liver development and hematopoiesis in bi-maternal mice**. *J Reprod Dev* 2008; 54(3): p. 177-82.
116. Zacharek SJ, Fillmore CM, Lau AN, Gludish DW, Chou A, Ho JW, Zamponi R, Gazit R, Bock C, Jager N, Smith ZD, Kim TM, Saunders AH, Wong J, Lee JH, Roach RR, Rossi DJ, Meissner A, Gimelbrant AA, Park PJ, and Kim CF. **Lung stem cell self-renewal relies on BMI1-dependent control of expression at imprinted loci**. *Cell Stem Cell* 2011; 9(3): p. 272-81.
117. Sul HS. **Minireview: Pref-1: role in adipogenesis and mesenchymal cell fate**. *Mol Endocrinol* 2009; 23(11): p. 1717-25.
118. Yan Z, Choi S, Liu X, Zhang M, Schageman JJ, Lee SY, Hart R, Lin L, Thurmond FA, and Williams RS. **Highly coordinated gene regulation in mouse skeletal muscle regeneration**. *J Biol Chem* 2003; 278(10): p. 8826-36.
119. Berg JS, Lin KK, Sonnet C, Boles NC, Weksberg DC, Nguyen H, Holt LJ, Rickwood D, Daly RJ, and Goodell MA. **Imprinted genes that regulate early mammalian growth are coexpressed in somatic stem cells**. *PLoS One* 2011; 6(10): p. e26410.
120. Kubota Y, Osawa M, Jakt LM, Yoshikawa K, and Nishikawa S. **Necdin restricts proliferation of hematopoietic stem cells during hematopoietic regeneration**. *Blood* 2009; 114(20): p. 4383-92.
121. Besson V, Smeriglio P, Wegener A, Relaix F, Nait Oumesmar B, Sassoon DA, and Marazzi G. **PW1 gene/paternally expressed gene 3 (PW1/Peg3) identifies multiple adult stem and progenitor cell populations**. *Proc Natl Acad Sci U S A* 2011; 108(28): p. 11470-5.
122. Valente T, Junyent F, and Auladell C. **Zac1 is expressed in progenitor/stem cells of the neuroectoderm and mesoderm during embryogenesis: differential phenotype of the Zac1-expressing cells during development**. *Dev Dyn* 2005; 233(2): p. 667-79.
123. Lui JC, Finkielstain GP, Barnes KM, and Baron J. **An imprinted gene network that controls mammalian somatic growth is down-regulated during postnatal growth deceleration in multiple organs**. *Am J Physiol Regul Integr Comp Physiol* 2008; 295(1): p. R189-96.
124. Delaval K, Wagschal A, and Feil R. **Epigenetic deregulation of imprinting in congenital diseases of aberrant growth**. *Bioessays* 2006; 28(5): p. 453-9.
125. Weinstein LS. **The role of tissue-specific imprinting as a source of phenotypic heterogeneity in human disease**. *Biol Psychiatry* 2001; 50(12): p. 927-31.
126. Jelinic P and Shaw P. **Loss of imprinting and cancer**. *J Pathol* 2007; 211(3): p. 261-8.
127. Butler MG. **Genomic imprinting disorders in humans: a mini-review**. *J Assist Reprod Genet* 2009; 26(9-10): p. 477-86.
128. Uribe-Lewis S, Woodfine K, Stojic L, and Murrell A. **Molecular mechanisms of genomic imprinting and clinical implications for cancer**. *Expert Rev Mol Med* 2011; 13: p. e2.
129. Ito Y, Koessler T, Ibrahim AE, Rai S, Vowler SL, Abu-Amero S, Silva AL, Maia AT, Huddleston JE, Uribe-Lewis S, Woodfine K, Jagodic M, Nativio R, Dunning A, Moore G, Klenova E, Bingham S, Pharoah PD, Brenton JD, Beck S, Sandhu MS, and Murrell A. **Somatically acquired hypomethylation of IGF2 in breast and colorectal cancer**. *Hum Mol Genet* 2008; 17(17): p. 2633-43.
130. Chao W and D'Amore PA. **IGF2: epigenetic regulation and role in development and disease**. *Cytokine Growth Factor Rev* 2008; 19(2): p. 111-20.

131. Timp W, Levchenko A, and Feinberg AP. **A new link between epigenetic progenitor lesions in cancer and the dynamics of signal transduction**. *Cell Cycle* 2009; 8(3): p. 383-90.
132. Gao N, Zhang Z, Jiang BH, and Shi X. **Role of PI3K/AKT/mTOR signaling in the cell cycle progression of human prostate cancer**. *Biochem Biophys Res Commun* 2003; 310(4): p. 1124-32.
133. Murrell A, Ito Y, Verde G, Huddleston J, Woodfine K, Silengo MC, Spreafico F, Perotti D, De Crescenzo A, Sparago A, Cerrato F, and Riccio A. **Distinct methylation changes at the IGF2-H19 locus in congenital growth disorders and cancer**. *PLoS One* 2008; 3(3): p. e1849.
134. Xu W, Fan H, He X, Zhang J, and Xie W. **LOI of IGF2 is associated with esophageal cancer and linked to methylation status of IGF2 DMR**. *J Exp Clin Cancer Res* 2006; 25(4): p. 543-7.
135. Fu VX, Dobosy JR, Desotelle JA, Almassi N, Ewald JA, Srinivasan R, Berres M, Svaren J, Weindruch R, and Jarrard DF. **Aging and cancer-related loss of insulin-like growth factor 2 imprinting in the mouse and human prostate**. *Cancer Res* 2008; 68(16): p. 6797-802.
136. Nakagawa H, Chadwick RB, Peltomaki P, Plass C, Nakamura Y, and de La Chapelle A. **Loss of imprinting of the insulin-like growth factor II gene occurs by biallelic methylation in a core region of H19-associated CTCF-binding sites in colorectal cancer**. *Proc Natl Acad Sci U S A* 2001; 98(2): p. 591-6.
137. Zhao R, DeCoteau JF, Geyer CR, Gao M, Cui H, and Casson AG. **Loss of imprinting of the insulin-like growth factor II (IGF2) gene in esophageal normal and adenocarcinoma tissues**. *Carcinogenesis* 2009; 30(12): p. 2117-22.
138. Mori M, Inoue H, Shiraishi T, Mimori K, Shibuta K, Nakashima H, Mafune K, Tanaka Y, Ueo H, Barnard GF, Sugimachi K, and Akiyoshi T. **Relaxation of insulin-like growth factor 2 gene imprinting in esophageal cancer**. *Int J Cancer* 1996; 68(4): p. 441-6.
139. Woodson K, Flood A, Green L, Tangrea JA, Hanson J, Cash B, Schatzkin A, and Schoenfeld P. **Loss of insulin-like growth factor-II imprinting and the presence of screen-detected colorectal adenomas in women**. *J Natl Cancer Inst* 2004; 96(5): p. 407-10.
140. Cruz-Correa M, Cui H, Giardiello FM, Powe NR, Hylind L, Robinson A, Hutcheon DF, Kafonek DR, Brandenburg S, Wu Y, He X, and Feinberg AP. **Loss of imprinting of insulin growth factor II gene: a potential heritable biomarker for colon neoplasia predisposition**. *Gastroenterology* 2004; 126(4): p. 964-70.
141. Sasaki J, Konishi F, Kawamura YJ, Kai T, Takata O, and Tsukamoto T. **Clinicopathological characteristics of colorectal cancers with loss of imprinting of insulin-like growth factor 2**. *Int J Cancer* 2006; 119(1): p. 80-3.
142. Cui H. **Loss of imprinting of IGF2 as an epigenetic marker for the risk of human cancer**. *Dis Markers* 2007; 23(1-2): p. 105-12.
143. Murphy SK, Huang Z, Wen Y, Spillman MA, Whitaker RS, Simel LR, Nichols TD, Marks JR, and Berchuck A. **Frequent IGF2/H19 domain epigenetic alterations and elevated IGF2 expression in epithelial ovarian cancer**. *Mol Cancer Res* 2006; 4(4): p. 283-92.
144. Bhusari S, Yang B, Kueck J, Huang W, and Jarrard DF. **Insulin-like growth factor-2 (IGF2) loss of imprinting marks a field defect within human prostates containing cancer**. *Prostate* 2011; 71(15): p. 1621-30.
145. Paradowska A, Fenic I, Konrad L, Sturm K, Wagenlehner F, Weidner W, and Steger K. **Aberrant epigenetic modifications in the CTCF binding domain of the IGF2/H19 gene in prostate cancer compared with benign prostate hyperplasia**. *Int J Oncol* 2009; 35(1): p. 87-96.
146. Kaneda A, Wang CJ, Cheong R, Timp W, Onyango P, Wen B, Iacobuzio-Donahue CA, Ohlsson R, Andraos R, Pearson MA, Sharov AA, Longo DL, Ko MS, Levchenko A, and Feinberg AP. **Enhanced sensitivity to IGF-II signaling links loss of imprinting of IGF2 to increased cell proliferation and tumor risk**. *Proc Natl Acad Sci U S A* 2007; 104(52): p. 20926-31.

147. Vu TH, Nguyen AH, and Hoffman AR. **Loss of IGF2 imprinting is associated with abrogation of long-range intrachromosomal interactions in human cancer cells**. *Hum Mol Genet* 2010; 19(5): p. 901-19.
148. Pateras IS, Apostolopoulou K, Niforou K, Kotsinas A, and Gorgoulis VG. **p57KIP2: "Kip"ing the cell under control**. *Mol Cancer Res* 2009; 7(12): p. 1902-19.
149. Schwarze SR, Shi Y, Fu VX, Watson PA, and Jarrard DF. **Role of cyclin-dependent kinase inhibitors in the growth arrest at senescence in human prostate epithelial and uroepithelial cells**. *Oncogene* 2001; 20(57): p. 8184-92.
150. Jin RJ, Lho Y, Wang Y, Ao M, Revelo MP, Hayward SW, Wills ML, Logan SK, Zhang P, and Matusik RJ. **Down-regulation of p57Kip2 induces prostate cancer in the mouse**. *Cancer Res* 2008; 68(10): p. 3601-8.
151. Guo H, Tian T, Nan K, and Wang W. **p57: A multifunctional protein in cancer (Review)**. *Int J Oncol* 2010; 36(6): p. 1321-9.
152. Borriello A, Caldarelli I, Bencivenga D, Criscuolo M, Cucciolla V, Tramontano A, Oliva A, Perrotta S, and Della Ragione F. **p57(Kip2) and cancer: time for a critical appraisal**. *Mol Cancer Res* 2011; 9(10): p. 1269-84.
153. Li Y, Nagai H, Ohno T, Yuge M, Hatano S, Ito E, Mori N, Saito H, and Kinoshita T. **Aberrant DNA methylation of p57(KIP2) gene in the promoter region in lymphoid malignancies of B-cell phenotype**. *Blood* 2002; 100(7): p. 2572-7.
154. Shen L, Toyota M, Kondo Y, Obata T, Daniel S, Pierce S, Imai K, Kantarjian HM, Issa JP, and Garcia-Manero G. **Aberrant DNA methylation of p57KIP2 identifies a cell-cycle regulatory pathway with prognostic impact in adult acute lymphocytic leukemia**. *Blood* 2003; 101(10): p. 4131-6.
155. Soejima H, Nakagawachi T, Zhao W, Higashimoto K, Urano T, Matsukura S, Kitajima Y, Takeuchi M, Nakayama M, Oshimura M, Miyazaki K, Joh K, and Mukai T. **Silencing of imprinted CDKN1C gene expression is associated with loss of CpG and histone H3 lysine 9 methylation at DMR-LIT1 in esophageal cancer**. *Oncogene* 2004; 23(25): p. 4380-8.
156. Kikuchi T, Toyota M, Itoh F, Suzuki H, Obata T, Yamamoto H, Kakiuchi H, Kusano M, Issa JP, Tokino T, and Imai K. **Inactivation of p57KIP2 by regional promoter hypermethylation and histone deacetylation in human tumors**. *Oncogene* 2002; 21(17): p. 2741-9.
157. Lodygin D, Epanchintsev A, Menssen A, Diebold J, and Hermeking H. **Functional epigenomics identifies genes frequently silenced in prostate cancer**. *Cancer Res* 2005; 65(10): p. 4218-27.
158. Pateras IS, Apostolopoulou K, Koutsami M, Evangelou K, Tsantoulis P, Liloglou T, Nikolaidis G, Sigala F, Kittas C, Field JK, Kotsinas A, and Gorgoulis VG. **Downregulation of the KIP family members p27(KIP1) and p57(KIP2) by SKP2 and the role of methylation in p57(KIP2) inactivation in nonsmall cell lung cancer**. *Int J Cancer* 2006; 119(11): p. 2546-56.
159. Kanduri C. **Kcnq1ot1: a chromatin regulatory RNA**. *Semin Cell Dev Biol* 2011; 22(4): p. 343-50.
160. Diaz-Meyer N, Day CD, Khatod K, Maher ER, Cooper W, Reik W, Junien C, Graham G, Algar E, Der Kaloustian VM, and Higgins MJ. **Silencing of CDKN1C (p57KIP2) is associated with hypomethylation at KvDMR1 in Beckwith-Wiedemann syndrome**. *J Med Genet* 2003; 40(11): p. 797-801.
161. Nakano S, Murakami K, Meguro M, Soejima H, Higashimoto K, Urano T, Kugoh H, Mukai T, Ikeguchi M, and Oshimura M. **Expression profile of LIT1/KCNQ1OT1 and epigenetic status at the KvDMR1 in colorectal cancers**. *Cancer Sci* 2006; 97(11): p. 1147-54.
162. Thakur N, Tiwari VK, Thomassin H, Pandey RR, Kanduri M, Gondor A, Grange T, Ohlsson R, and Kanduri C. **An antisense RNA regulates the bidirectional silencing property of the Kcnq1 imprinting control region**. *Mol Cell Biol* 2004; 24(18): p. 7855-62.
163. Hoffmann MJ, Florl AR, Seifert HH, and Schulz WA. **Multiple mechanisms downregulate CDKN1C in human bladder cancer**. *Int J Cancer* 2005; 114(3): p. 406-13.

164. Schwienbacher C, Gramantieri L, Scelfo R, Veronese A, Calin GA, Bolondi L, Croce CM, Barbanti-Brodano G, and Negrini M. **Gain of imprinting at chromosome 11p15: A pathogenetic mechanism identified in human hepatocarcinomas**. *Proc Natl Acad Sci U S A* 2000; 97(10): p. 5445-9.
165. Diaz-Meyer N, Yang Y, Sait SN, Maher ER, and Higgins MJ. **Alternative mechanisms associated with silencing of CDKN1C in Beckwith-Wiedemann syndrome**. *J Med Genet* 2005; 42(8): p. 648-55.
166. Yang X, Karuturi RK, Sun F, Aau M, Yu K, Shao R, Miller LD, Tan PB, and Yu Q. **CDKN1C (p57) is a direct target of EZH2 and suppressed by multiple epigenetic mechanisms in breast cancer cells**. *PLoS One* 2009; 4(4): p. e5011.
167. Gabory A, Ripoche MA, Le Digarcher A, Watrin F, Ziyyat A, Forne T, Jammes H, Ainscough JF, Surani MA, Journot L, and Dandolo L. **H19 acts as a trans regulator of the imprinted gene network controlling growth in mice**. *Development* 2009; 136(20): p. 3413-21.
168. Varrault A, Gueydan C, Delalbre A, Bellmann A, Houssami S, Aknin C, Severac D, Chotard L, Kahli M, Le Digarcher A, Pavlidis P, and Journot L. **Zac1 regulates an imprinted gene network critically involved in the control of embryonic growth**. *Dev Cell* 2006; 11(5): p. 711-22.
169. Charalambous M, da Rocha ST, and Ferguson-Smith AC. **Genomic imprinting, growth control and the allocation of nutritional resources: consequences for postnatal life**. *Curr Opin Endocrinol Diabetes Obes* 2007; 14(1): p. 3-12.
170. Ribarska T, Bastian KM, Koch A, and Schulz WA. **Specific changes in the expression of imprinted genes in prostate cancer--implications for cancer progression and epigenetic regulation**. *Asian J Androl* 2012; 14(3): p. 436-50.
171. Varrault A, Ciani E, Apiou F, Bilanges B, Hoffmann A, Pantaloni C, Bockaert J, Spengler D, and Journot L. **hZAC encodes a zinc finger protein with antiproliferative properties and maps to a chromosomal region frequently lost in cancer**. *Proc Natl Acad Sci U S A* 1998; 95(15): p. 8835-40.
172. Abdollahi A, Pisarcik D, Roberts D, Weinstein J, Cairns P, and Hamilton TC. **LOT1 (PLAGL1/ZAC1), the candidate tumor suppressor gene at chromosome 6q24-25, is epigenetically regulated in cancer**. *J Biol Chem* 2003; 278(8): p. 6041-9.
173. Lemeta S, Salmenkivi K, Pylkkanen L, Sainio M, Saarikoski ST, Arola J, Heikkila P, Haglund C, Husgafvel-Pursiainen K, and Bohling T. **Frequent loss of heterozygosity at 6q in pheochromocytoma**. *Hum Pathol* 2006; 37(6): p. 749-54.
174. Cvetkovic D, Pisarcik D, Lee C, Hamilton TC, and Abdollahi A. **Altered expression and loss of heterozygosity of the LOT1 gene in ovarian cancer**. *Gynecol Oncol* 2004; 95(3): p. 449-55.
175. Hoffmann A, Ciani E, Boeckardt J, Holsboer F, Journot L, and Spengler D. **Transcriptional activities of the zinc finger protein Zac are differentially controlled by DNA binding**. *Mol Cell Biol* 2003; 23(3): p. 988-1003.
176. Kamiya M, Judson H, Okazaki Y, Kusakabe M, Muramatsu M, Takada S, Takagi N, Arima T, Wake N, Kamimura K, Satomura K, Hermann R, Bonthron DT, and Hayashizaki Y. **The cell cycle control gene ZAC/PLAGL1 is imprinted--a strong candidate gene for transient neonatal diabetes**. *Hum Mol Genet* 2000; 9(3): p. 453-60.
177. Ciani E, Hoffmann A, Schmidt P, Journot L, and Spengler D. **Induction of the PAC1-R (PACAP-type I receptor) gene by p53 and Zac**. *Brain Res Mol Brain Res* 1999; 69(2): p. 290-4.
178. Czubryt MP, Lamoureux L, Ramjiawan A, Abrenica B, Jangamreddy J, and Swan K. **Regulation of cardiomyocyte Glut4 expression by ZAC1**. *J Biol Chem* 2010; 285(22): p. 16942-50.
179. Hoffmann A and Spengler D. **A new coactivator function for Zac1's C2H2 zinc finger DNA-binding domain in selectively controlling PCAF activity**. *Mol Cell Biol* 2008; 28(19): p. 6078-93.

180. Wang WM, Liu ST, Huang SM, Lin WS, Chen SG, and Chang YL. **Zac1 functional interactions mediate AP-1 transcriptional activity**. *Biochim Biophys Acta* 2011; 1813(12): p. 2050-60.
181. Chou WY, Ho CL, Tseng ML, Liu ST, Yen LC, and Huang SM. **Human Spot 14 protein is a p53-dependent transcriptional coactivator via the recruitment of thyroid receptor and Zac1**. *Int J Biochem Cell Biol* 2008; 40(9): p. 1826-34.
182. Huang SM, Schonthal AH, and Stallcup MR. **Enhancement of p53-dependent gene activation by the transcriptional coactivator Zac1**. *Oncogene* 2001; 20(17): p. 2134-43.
183. Huang SM and Stallcup MR. **Mouse Zac1, a transcriptional coactivator and repressor for nuclear receptors**. *Mol Cell Biol* 2000; 20(5): p. 1855-67.
184. Valleley EM, Cordery SF, and Bonthron DT. **Tissue-specific imprinting of the ZAC/PLAGL1 tumour suppressor gene results from variable utilization of monoallelic and biallelic promoters**. *Hum Mol Genet* 2007; 16(8): p. 972-81.
185. Bilanges B, Varrault A, Mazumdar A, Pantaloni C, Hoffmann A, Bockaert J, Spengler D, and Journot L. **Alternative splicing of the imprinted candidate tumor suppressor gene ZAC regulates its antiproliferative and DNA binding activities**. *Oncogene* 2001; 20(10): p. 1246-53.
186. Monk D, Wagschal A, Arnaud P, Muller PS, Parker-Katiraee L, Bourc'his D, Scherer SW, Feil R, Stanier P, and Moore GE. **Comparative analysis of human chromosome 7q21 and mouse proximal chromosome 6 reveals a placental-specific imprinted gene, TFPI2/Tfpi2, which requires EHMT2 and EED for allelic-silencing**. *Genome Res* 2008; 18(8): p. 1270-81.
187. Steiner FA, Hong JA, Fischette MR, Beer DG, Guo ZS, Chen GA, Weiser TS, Kassis ES, Nguyen DM, Lee S, Trepel JB, and Schrump DS. **Sequential 5-Aza 2'-deoxycytidine/depsipeptide FK228 treatment induces tissue factor pathway inhibitor 2 (TFPI-2) expression in cancer cells**. *Oncogene* 2005; 24(14): p. 2386-97.
188. Hibi K, Goto T, Shirahata A, Saito M, Kigawa G, Nemoto H, and Sanada Y. **Methylation of TFPI2 no longer detected in the serum DNA of colorectal cancer patients after curative surgery**. *Anticancer Res* 2012; 32(3): p. 787-90.
189. Gabory A, Jammes H, and Dandolo L. **The H19 locus: role of an imprinted non-coding RNA in growth and development**. *Bioessays* 2010; 32(6): p. 473-80.
190. Rubio-Briones J, Fernandez-Serra A, Calatrava A, Garcia-Casado Z, Rubio L, Bonillo MA, Iborra I, Solsona E, and Lopez-Guerrero JA. **Clinical implications of TMPRSS2-ERG gene fusion expression in patients with prostate cancer treated with radical prostatectomy**. *J Urol* 2010; 183(5): p. 2054-61.
191. Bismar TA, Dolph M, Teng LH, Liu S, and Donnelly B. **ERG protein expression reflects hormonal treatment response and is associated with Gleason score and prostate cancer specific mortality**. *Eur J Cancer* 2012; 48(4): p. 538-46.
192. Nam RK, Sugar L, Wang Z, Yang W, Kitching R, Klotz LH, Venkateswaran V, Narod SA, and Seth A. **Expression of TMPRSS2:ERG gene fusion in prostate cancer cells is an important prognostic factor for cancer progression**. *Cancer Biol Ther* 2007; 6(1): p. 40-5.
193. Vire E, Brenner C, Deplus R, Blanchon L, Fraga M, Didelot C, Morey L, Van Eynde A, Bernard D, Vanderwinden JM, Bollen M, Esteller M, Di Croce L, de Launoit Y, and Fuks F. **The Polycomb group protein EZH2 directly controls DNA methylation**. *Nature* 2006; 439(7078): p. 871-4.
194. Gao F, Shi L, Russin J, Zeng L, Chang X, He S, Chen TC, Giannotta SL, Weisenberger DJ, Zada G, Mack WJ, and Wang K. **DNA methylation in the malignant transformation of meningiomas**. *PLoS One* 2013; 8(1): p. e54114.
195. Sandhu KS, Shi C, Sjolinder M, Zhao Z, Gondor A, Liu L, Tiwari VK, Guibert S, Emilsson L, Imreh MP, and Ohlsson R. **Nonallelic transvection of multiple imprinted loci is organized by the H19 imprinting control region during germline development**. *Genes Dev* 2009; 23(22): p. 2598-603.

196. Strohmeyer DM, Berger AP, Moore DH, 2nd, Bartsch G, Klocker H, Carroll PR, Loening SA, and Jensen RH. **Genetic aberrations in prostate carcinoma detected by comparative genomic hybridization and microsatellite analysis: association with progression and angiogenesis**. *Prostate* 2004; 59(1): p. 43-58.
197. Dong H, Zhang H, Liang J, Yan H, Chen Y, Shen Y, Kong Y, Wang S, Zhao G, and Jin W. **Digital karyotyping reveals probable target genes at 7q21.3 locus in hepatocellular carcinoma**. *BMC Med Genomics* 2011; 4: p. 60.
198. Jia HL, Ye QH, Qin LX, Budhu A, Forgues M, Chen Y, Liu YK, Sun HC, Wang L, Lu HZ, Shen F, Tang ZY, and Wang XW. **Gene expression profiling reveals potential biomarkers of human hepatocellular carcinoma**. *Clin Cancer Res* 2007; 13(4): p. 1133-9.
199. Nakao K, Shibusawa M, Tsunoda A, Yoshizawa H, Murakami M, Kusano M, Uesugi N, and Sasaki K. **Genetic changes in primary colorectal cancer by comparative genomic hybridization**. *Surg Today* 1998; 28(5): p. 567-9.
200. Bourque DK, Avila L, Penaherrera M, von Dadelszen P, and Robinson WP. **Decreased placental methylation at the H19/IGF2 imprinting control region is associated with normotensive intrauterine growth restriction but not preeclampsia**. *Placenta* 2010; 31(3): p. 197-202.
201. Zhao Z, Tavoosidana G, Sjolinder M, Gondor A, Mariano P, Wang S, Kanduri C, Lezcano M, Sandhu KS, Singh U, Pant V, Tiwari V, Kurukuti S, and Ohlsson R. **Circular chromosome conformation capture (4C) uncovers extensive networks of epigenetically regulated intra- and interchromosomal interactions**. *Nat Genet* 2006; 38(11): p. 1341-7.
202. Mackay DJ, Coupe AM, Shield JP, Storr JN, Temple IK, and Robinson DO. **Relaxation of imprinted expression of ZAC and HYMAI in a patient with transient neonatal diabetes mellitus**. *Hum Genet* 2002; 110(2): p. 139-44.
203. Mackay DJ, Callaway JL, Marks SM, White HE, Acerini CL, Boonen SE, Dayanikli P, Firth HV, Goodship JA, Haemers AP, Hahnemann JM, Kordonouri O, Masoud AF, Oestergaard E, Storr J, Ellard S, Hattersley AT, Robinson DO, and Temple IK. **Hypomethylation of multiple imprinted loci in individuals with transient neonatal diabetes is associated with mutations in ZFP57**. *Nat Genet* 2008; 40(8): p. 949-51.
204. Axlund SD, Lambert JR, and Nordeen SK. **HOXC8 inhibits androgen receptor signaling in human prostate cancer cells by inhibiting SRC-3 recruitment to direct androgen target genes**. *Mol Cancer Res* 2010; 8(12): p. 1643-55.
205. McCabe CD, Spyropoulos DD, Martin D, and Moreno CS. **Genome-wide analysis of the homeobox C6 transcriptional network in prostate cancer**. *Cancer Res* 2008; 68(6): p. 1988-96.
206. Lei H, Juan AH, Kim MS, and Ruddle FH. **Identification of a Hoxc8-regulated transcriptional network in mouse embryo fibroblast cells**. *Proc Natl Acad Sci U S A* 2006; 103(27): p. 10305-9.
207. Fan T, Hagan JP, Kozlov SV, Stewart CL, and Muegge K. **Lsh controls silencing of the imprinted Cdkn1c gene**. *Development* 2005; 132(4): p. 635-44.
208. Kondo M, Matsuoka S, Uchida K, Osada H, Nagatake M, Takagi K, Harper JW, Takahashi T, and Elledge SJ. **Selective maternal-allele loss in human lung cancers of the maternally expressed p57KIP2 gene at 11p15.5**. *Oncogene* 1996; 12(6): p. 1365-8.
209. Rodriguez BA, Weng YI, Liu TM, Zuo T, Hsu PY, Lin CH, Cheng AL, Cui H, Yan PS, and Huang TH. **Estrogen-mediated epigenetic repression of the imprinted gene cyclin-dependent kinase inhibitor 1C in breast cancer cells**. *Carcinogenesis* 2011; 32(6): p. 812-21.
210. McCabe MT, Ott HM, Ganji G, Korenchuk S, Thompson C, Van Aller GS, Liu Y, Graves AP, Della Pietra A, 3rd, Diaz E, LaFrance LV, Mellinger M, Duquenne C, Tian X, Kruger RG, McHugh CF, Brandt M, Miller WH, Dhanak D, Verma SK, Tummino PJ, and Creasy CL. **EZH2 inhibition as a therapeutic strategy for lymphoma with EZH2-activating mutations**. *Nature* 2012; 492(7427): p. 108-12.

211. Qi W, Chan H, Teng L, Li L, Chuai S, Zhang R, Zeng J, Li M, Fan H, Lin Y, Gu J, Ardayfio O, Zhang JH, Yan X, Fang J, Mi Y, Zhang M, Zhou T, Feng G, Chen Z, Li G, Yang T, Zhao K, Liu X, Yu Z, Lu CX, Atadja P, and Li E. **Selective inhibition of Ezh2 by a small molecule inhibitor blocks tumor cells proliferation**. *Proc Natl Acad Sci U S A* 2012; 109(52): p. 21360-5.
212. Crea F, Paolicchi E, Marquez VE, and Danesi R. **Polycomb genes and cancer: time for clinical application?** *Crit Rev Oncol Hematol* 2012; 83(2): p. 184-93.
213. Anwar SL, Krech T, Hasemeier B, Schipper E, Schweitzer N, Vogel A, Kreipe H, and Lehmann U. **Loss of Imprinting and Allelic Switching at the DLK1-MEG3 Locus in Human Hepatocellular Carcinoma**. *PLoS One* 2012; 7(11): p. e49462.
214. Gejman R, Batista DL, Zhong Y, Zhou Y, Zhang X, Swearingen B, Stratakis CA, Hedley-Whyte ET, and Klibanski A. **Selective loss of MEG3 expression and intergenic differentially methylated region hypermethylation in the MEG3/DLK1 locus in human clinically nonfunctioning pituitary adenomas**. *J Clin Endocrinol Metab* 2008; 93(10): p. 4119-25.
215. Cruz-Correa M, Zhao R, Oviedo M, Bernabe RD, Lacourt M, Cardona A, Lopez-Enriquez R, Wexner S, Cuffari C, Hylind L, Platz E, Cui H, Feinberg AP, and Giardiello FM. **Temporal stability and age-related prevalence of loss of imprinting of the insulin-like growth factor-2 gene**. *Epigenetics* 2009; 4(2): p. 114-8.
216. Woodfine K, Huddleston JE, and Murrell A. **Quantitative analysis of DNA methylation at all human imprinted regions reveals preservation of epigenetic stability in adult somatic tissue**. *Epigenetics Chromatin* 2011; 4(1): p. 1.
217. Wood AJ, Roberts RG, Monk D, Moore GE, Schulz R, and Oakey RJ. **A screen for retrotransposed imprinted genes reveals an association between X chromosome homology and maternal germ-line methylation**. *PLoS Genet* 2007; 3(2): p. e20.
218. Bernstein BE, Mikkelsen TS, Xie X, Kamal M, Huebert DJ, Cuff J, Fry B, Meissner A, Wernig M, Plath K, Jaenisch R, Wagschal A, Feil R, Schreiber SL, and Lander ES. **A bivalent chromatin structure marks key developmental genes in embryonic stem cells**. *Cell* 2006; 125(2): p. 315-26.
219. Mikkelsen TS, Ku M, Jaffe DB, Issac B, Lieberman E, Giannoukos G, Alvarez P, Brockman W, Kim TK, Koche RP, Lee W, Mendenhall E, O'Donovan A, Presser A, Russ C, Xie X, Meissner A, Wernig M, Jaenisch R, Nusbaum C, Lander ES, and Bernstein BE. **Genome-wide maps of chromatin state in pluripotent and lineage-committed cells**. *Nature* 2007; 448(7153): p. 553-60.
220. Zhao J, Ohsumi TK, Kung JT, Ogawa Y, Grau DJ, Sarma K, Song JJ, Kingston RE, Borowsky M, and Lee JT. **Genome-wide identification of polycomb-associated RNAs by RIP-seq**. *Mol Cell* 2010; 40(6): p. 939-53.
221. Saxena A and Carninci P. **Long non-coding RNA modifies chromatin: epigenetic silencing by long non-coding RNAs**. *Bioessays* 2011; 33(11): p. 830-9.
222. Schoenfelder S, Sexton T, Chakalova L, Cope NF, Horton A, Andrews S, Kurukuti S, Mitchell JA, Umlauf D, Dimitrova DS, Eskiw CH, Luo Y, Wei CL, Ruan Y, Bieker JJ, and Fraser P. **Preferential associations between co-regulated genes reveal a transcriptional interactome in erythroid cells**. *Nat Genet* 2010; 42(1): p. 53-61.
223. Horike S, Mitsuya K, Meguro M, Kotobuki N, Kashiwagi A, Notsu T, Schulz TC, Shirayoshi Y, and Oshimura M. **Targeted disruption of the human LIT1 locus defines a putative imprinting control element playing an essential role in Beckwith-Wiedemann syndrome**. *Hum Mol Genet* 2000; 9(14): p. 2075-83.
224. Grandjean V, Smith J, Schofield PN, and Ferguson-Smith AC. **Increased IGF-II protein affects p57kip2 expression in vivo and in vitro: implications for Beckwith-Wiedemann syndrome**. *Proc Natl Acad Sci U S A* 2000; 97(10): p. 5279-84.
225. Yang F, Bi J, Xue X, Zheng L, Zhi K, Hua J, and Fang G. **Up-regulated long non-coding RNA H19 contributes to proliferation of gastric cancer cells**. *FEBS J* 2012; 279(17): p. 3159-65.

226. Relaix F, Wei X, Li W, Pan J, Lin Y, Bowtell DD, Sassoon DA, and Wu X. **Pw1/Peg3 is a potential cell death mediator and cooperates with Siah1a in p53-mediated apoptosis**. *Proc Natl Acad Sci U S A* 2000; 97(5): p. 2105-10.
227. Liu PY, Chan JY, Lin HC, Wang SL, Liu ST, Ho CL, Chang LC, and Huang SM. **Modulation of the cyclin-dependent kinase inhibitor p21(WAF1/Cip1) gene by Zac1 through the antagonistic regulators p53 and histone deacetylase 1 in HeLa Cells**. *Mol Cancer Res* 2008; 6(7): p. 1204-14.
228. Hasegawa K and Yoshikawa K. **Necdin regulates p53 acetylation via Sirtuin1 to modulate DNA damage response in cortical neurons**. *J Neurosci* 2008; 28(35): p. 8772-84.
229. Agell L, Hernandez S, de Muga S, Lorente JA, Juanpere N, Esgueva R, Serrano S, Gelabert A, and Lloreta J. **KLF6 and TP53 mutations are a rare event in prostate cancer: distinguishing between Taq polymerase artifacts and true mutations**. *Mod Pathol* 2008; 21(12): p. 1470-8.
230. Schlomm T, Iwers L, Kirstein P, Jessen B, Kollermann J, Minner S, Passow-Drolet A, Mirlacher M, Milde-Langosch K, Graefen M, Haese A, Steuber T, Simon R, Huland H, Sauter G, and Erbersdobler A. **Clinical significance of p53 alterations in surgically treated prostate cancers**. *Mod Pathol* 2008; 21(11): p. 1371-8.
231. Griewe GL, Dean RC, Zhang W, Young D, Sesterhenn IA, Shanmugam N, McLeod DG, Moul JW, and Srivastava S. **p53 Immunostaining guided laser capture microdissection (p53-LCM) defines the presence of p53 gene mutations in focal regions of primary prostate cancer positive for p53 protein**. *Prostate Cancer Prostatic Dis* 2003; 6(4): p. 281-5.
232. Zuo T, Liu TM, Lan X, Weng YI, Shen R, Gu F, Huang YW, Liyanarachchi S, Deatherage DE, Hsu PY, Taslim C, Ramaswamy B, Shapiro CL, Lin HJ, Cheng AS, Jin VX, and Huang TH. **Epigenetic silencing mediated through activated PI3K/AKT signaling in breast cancer**. *Cancer Res* 2011; 71(5): p. 1752-62.
233. Nacerddine K, Beaudry JB, Ginjala V, Westerman B, Mattiroli F, Song JY, van der Poel H, Ponz OB, Pritchard C, Cornelissen-Steijger P, Zevenhoven J, Tanger E, Sixma TK, Ganesan S, and van Lohuizen M. **Akt-mediated phosphorylation of Bmi1 modulates its oncogenic potential, E3 ligase activity, and DNA damage repair activity in mouse prostate cancer**. *J Clin Invest* 2012; 122(5): p. 1920-32.
234. Hsu PY, Hsu HK, Singer GA, Yan PS, Rodriguez BA, Liu JC, Weng YI, Deatherage DE, Chen Z, Pereira JS, Lopez R, Russo J, Wang Q, Lamartiniere CA, Nephew KP, and Huang TH. **Estrogen-mediated epigenetic repression of large chromosomal regions through DNA looping**. *Genome Res* 2010; 20(6): p. 733-44.
235. Leu YW, Yan PS, Fan M, Jin VX, Liu JC, Curran EM, Welshons WV, Wei SH, Davuluri RV, Plass C, Nephew KP, and Huang TH. **Loss of estrogen receptor signaling triggers epigenetic silencing of downstream targets in breast cancer**. *Cancer Res* 2004; 64(22): p. 8184-92.
236. Ip WK, Lai PB, Wong NL, Sy SM, Beheshti B, Squire JA, and Wong N. **Identification of PEG10 as a progression related biomarker for hepatocellular carcinoma**. *Cancer Lett* 2007; 250(2): p. 284-91.
237. Tsuji K, Yasui K, Gen Y, Endo M, Dohi O, Zen K, Mitsuyoshi H, Minami M, Itoh Y, Taniwaki M, Tanaka S, Arii S, Okanoue T, and Yoshikawa T. **PEG10 is a probable target for the amplification at 7q21 detected in hepatocellular carcinoma**. *Cancer Genet Cytogenet* 2010; 198(2): p. 118-25.
238. Luk JM, Burchard J, Zhang C, Liu AM, Wong KF, Shek FH, Lee NP, Fan ST, Poon RT, Ivanovska I, Philippar U, Cleary MA, Buser CA, Shaw PM, Lee CN, Tenen DG, Dai H, and Mao M. **DLK1-DIO3 genomic imprinted microRNA cluster at 14q32.2 defines a stemlike subtype of hepatocellular carcinoma associated with poor survival**. *J Biol Chem* 2011; 286(35): p. 30706-13.
239. Braconi C, Kogure T, Valeri N, Huang N, Nuovo G, Costinean S, Negrini M, Miotto E, Croce CM, and Patel T. **microRNA-29 can regulate expression of the long non-coding RNA gene MEG3 in hepatocellular cancer**. *Oncogene* 2011; 30(47): p. 4750-6.

240. Wang P, Ren Z, and Sun P. **Overexpression of the long non-coding RNA MEG3 impairs in vitro glioma cell proliferation**. *J Cell Biochem* 2012; 113(6): p. 1868-74.
241. Zhang X, Zhou Y, Mehta KR, Danila DC, Scolavino S, Johnson SR, and Klibanski A. **A pituitary-derived MEG3 isoform functions as a growth suppressor in tumor cells**. *J Clin Endocrinol Metab* 2003; 88(11): p. 5119-26.
242. Zhou Y, Zhong Y, Wang Y, Zhang X, Batista DL, Gejman R, Ansell PJ, Zhao J, Weng C, and Klibanski A. **Activation of p53 by MEG3 non-coding RNA**. *J Biol Chem* 2007; 282(34): p. 24731-42.
243. Astuti D, Latif F, Wagner K, Gentle D, Cooper WN, Catchpoole D, Grundy R, Ferguson-Smith AC, and Maher ER. **Epigenetic alteration at the DLK1-GTL2 imprinted domain in human neoplasia: analysis of neuroblastoma, phaeochromocytoma and Wilms' tumour**. *Br J Cancer* 2005; 92(8): p. 1574-80.
244. Fujiwara K, Hasegawa K, Ohkumo T, Miyoshi H, Tseng YH, and Yoshikawa K. **Necdin controls proliferation of white adipocyte progenitor cells**. *PLoS One* 2012; 7(1): p. e30948.
245. Cypess AM, Zhang H, Schulz TJ, Huang TL, Espinoza DO, Kristiansen K, Unterman TG, and Tseng YH. **Insulin/IGF-I regulation of necdin and brown adipocyte differentiation via CREB- and FoxO1-associated pathways**. *Endocrinology* 2011; 152(10): p. 3680-9.
246. Asai T, Liu Y, Di Giandomenico S, Bae N, Ndiaye-Lobry D, Deblasio A, Menendez S, Antipin Y, Reva B, Wevrick R, and Nimer SD. **Necdin, a p53 target gene, regulates the quiescence and response to genotoxic stress of hematopoietic stem/progenitor cells**. *Blood* 2012; 120(8): p. 1601-12.
247. Pessina P, Conti V, Tonlorenzi R, Touvier T, Meneveri R, Cossu G, and Brunelli S. **Necdin enhances muscle reconstitution of dystrophic muscle by vessel-associated progenitors, by promoting cell survival and myogenic differentiation**. *Cell Death Differ* 2012; 19(5): p. 827-38.
248. Sciorati C, Touvier T, Buono R, Pessina P, Francois S, Perrotta C, Meneveri R, Clementi E, and Brunelli S. **Necdin is expressed in cachectic skeletal muscle to protect fibers from tumor-induced wasting**. *J Cell Sci* 2009; 122(Pt 8): p. 1119-25.
249. Ingraham CA, Wertalik L, and Schor NF. **Necdin and neurotrophin receptors: interactors of relevance for neuronal resistance to oxidant stress**. *Pediatr Res* 2011; 69(4): p. 279-84.
250. Kurita M, Kuwajima T, Nishimura I, and Yoshikawa K. **Necdin downregulates CDC2 expression to attenuate neuronal apoptosis**. *J Neurosci* 2006; 26(46): p. 12003-13.
251. Andrieu D, Watrin F, Niinobe M, Yoshikawa K, Muscatelli F, and Fernandez PA. **Expression of the Prader-Willi gene Necdin during mouse nervous system development correlates with neuronal differentiation and p75NTR expression**. *Gene Expr Patterns* 2003; 3(6): p. 761-5.
252. Francois S, D'Orlando C, Fatone T, Touvier T, Pessina P, Meneveri R, and Brunelli S. **Necdin enhances myoblasts survival by facilitating the degradation of the mediator of apoptosis CCAR1/CARP1**. *PLoS One* 2012; 7(8): p. e43335.
253. Chapman EJ and Knowles MA. **Necdin: a multi functional protein with potential tumor suppressor role?** *Mol Carcinog* 2009; 48(11): p. 975-81.
254. Vlachos P and Joseph B. **The Cdk inhibitor p57(Kip2) controls LIM-kinase 1 activity and regulates actin cytoskeleton dynamics**. *Oncogene* 2009; 28(47): p. 4175-88.
255. Yokoo T, Toyoshima H, Miura M, Wang Y, Iida KT, Suzuki H, Sone H, Shimano H, Gotoda T, Nishimori S, Tanaka K, and Yamada N. **p57Kip2 regulates actin dynamics by binding and translocating LIM-kinase 1 to the nucleus**. *J Biol Chem* 2003; 278(52): p. 52919-23.
256. Kavanagh E and Joseph B. **The hallmarks of CDKN1C (p57, KIP2) in cancer**. *Biochim Biophys Acta* 2011; 1816(1): p. 50-6.
257. Berteaux N, Lottin S, Monte D, Pinte S, Quatannens B, Coll J, Hondermarck H, Curgy JJ, Dugimont T, and Adriaenssens E. **H19 mRNA-like noncoding RNA promotes breast cancer cell proliferation through positive control by E2F1**. *J Biol Chem* 2005; 280(33): p. 29625-36.

258. Berteaux N, Aptel N, Cathala G, Genton C, Coll J, Daccache A, Spruyt N, Hondermarck H, Dugimont T, Curgy JJ, Forne T, and Adriaenssens E. **A novel H19 antisense RNA overexpressed in breast cancer contributes to paternal IGF2 expression**. *Mol Cell Biol* 2008; 28(22): p. 6731-45.
259. Lottin S, Adriaenssens E, Dupressoir T, Berteaux N, Montpellier C, Coll J, Dugimont T, and Curgy JJ. **Overexpression of an ectopic H19 gene enhances the tumorigenic properties of breast cancer cells**. *Carcinogenesis* 2002; 23(11): p. 1885-95.
260. Yoshimizu T, Miroglio A, Ripoche MA, Gabory A, Vernucci M, Riccio A, Colnot S, Godard C, Terris B, Jammes H, and Dandolo L. **The H19 locus acts in vivo as a tumor suppressor**. *Proc Natl Acad Sci U S A* 2008; 105(34): p. 12417-22.
261. Gao ZH, Suppola S, Liu J, Heikkila P, Janne J, and Voutilainen R. **Association of H19 promoter methylation with the expression of H19 and IGF-II genes in adrenocortical tumors**. *J Clin Endocrinol Metab* 2002; 87(3): p. 1170-6.
262. Spengler D, Villalba M, Hoffmann A, Pantaloni C, Houssami S, Bockaert J, and Journot L. **Regulation of apoptosis and cell cycle arrest by Zac1, a novel zinc finger protein expressed in the pituitary gland and the brain**. *EMBO J* 1997; 16(10): p. 2814-25.
263. Vilela C and McCarthy JE. **Regulation of fungal gene expression via short open reading frames in the mRNA 5'untranslated region**. *Mol Microbiol* 2003; 49(4): p. 859-67.
264. Meijer HA and Thomas AA. **Control of eukaryotic protein synthesis by upstream open reading frames in the 5'-untranslated region of an mRNA**. *Biochem J* 2002; 367(Pt 1): p. 1-11.
265. Kochetov AV, Ischenko IV, Vorobiev DG, Kel AE, Babenko VN, Kisselev LL, and Kolchanov NA. **Eukaryotic mRNAs encoding abundant and scarce proteins are statistically dissimilar in many structural features**. *FEBS Lett* 1998; 440(3): p. 351-5.
266. Amanso AM, Debbas V, and Laurindo FR. **Proteasome inhibition represses unfolded protein response and Nox4, sensitizing vascular cells to endoplasmic reticulum stress-induced death**. *PLoS One* 2011; 6(1): p. e14591.
267. Mazroui R, Di Marco S, Kaufman RJ, and Gallouzi IE. **Inhibition of the ubiquitin-proteasome system induces stress granule formation**. *Mol Biol Cell* 2007; 18(7): p. 2603-18.
268. Park HS, Jun do Y, Han CR, Woo HJ, and Kim YH. **Proteasome inhibitor MG132-induced apoptosis via ER stress-mediated apoptotic pathway and its potentiation by protein tyrosine kinase p56lck in human Jurkat T cells**. *Biochem Pharmacol* 2011; 82(9): p. 1110-25.
269. Komar AA and Hatzoglou M. **Cellular IRES-mediated translation: the war of ITAFs in pathophysiological states**. *Cell Cycle* 2011; 10(2): p. 229-40.
270. Zimmermann J, Erdmann D, Lalande I, Grossenbacher R, Noorani M, and Furst P. **Proteasome inhibitor induced gene expression profiles reveal overexpression of transcriptional regulators ATF3, GADD153 and MAD1**. *Oncogene* 2000; 19(25): p. 2913-20.
271. Gareau C, Fournier MJ, Filion C, Coudert L, Martel D, Labelle Y, and Mazroui R. **p21(WAF1/CIP1) upregulation through the stress granule-associated protein CUGBP1 confers resistance to bortezomib-mediated apoptosis**. *PLoS One* 2011; 6(5): p. e20254.
272. Laroia G, Sarkar B, and Schneider RJ. **Ubiquitin-dependent mechanism regulates rapid turnover of AU-rich cytokine mRNAs**. *Proc Natl Acad Sci U S A* 2002; 99(4): p. 1842-6.
273. Kedersha N, Stoecklin G, Ayodele M, Yacono P, Lykke-Andersen J, Fritzler MJ, Scheuner D, Kaufman RJ, Golan DE, and Anderson P. **Stress granules and processing bodies are dynamically linked sites of mRNP remodeling**. *J Cell Biol* 2005; 169(6): p. 871-84.
274. Oliveira CC and McCarthy JE. **The relationship between eukaryotic translation and mRNA stability. A short upstream open reading frame strongly inhibits translational initiation and greatly accelerates mRNA degradation in the yeast Saccharomyces cerevisiae**. *J Biol Chem* 1995; 270(15): p. 8936-43.

275. Royo F, Paz N, Espinosa L, McQueen PG, Vellon L, and Parada LA. **Spatial link between nucleoli and expression of the Zac1 gene**. *Chromosoma* 2009; 118(6): p. 711-22.
276. Iglesias-Platas I, Martin-Trujillo A, Cirillo D, Court F, Guillaumet-Adkins A, Camprubi C, Bourc'his D, Hata K, Feil R, Tartaglia G, Arnaud P, and Monk D. **Characterization of novel paternal ncRNAs at the Plagl1 locus, including Hymai, predicted to interact with regulators of active chromatin**. *PLoS One* 2012; 7(6): p. e38907.
277. Arima T, Kamikihara T, Hayashida T, Kato K, Inoue T, Shirayoshi Y, Oshimura M, Soejima H, Mukai T, and Wake N. **ZAC, LIT1 (KCNQ1OT1) and p57KIP2 (CDKN1C) are in an imprinted gene network that may play a role in Beckwith-Wiedemann syndrome**. *Nucleic Acids Res* 2005; 33(8): p. 2650-60.
278. Liu PY, Hsieh TY, Liu ST, Chang YL, Lin WS, Wang WM, and Huang SM. **Zac1, an Sp1-like protein, regulates human p21(WAF1/Cip1) gene expression in HeLa cells**. *Exp Cell Res* 2011; 317(20): p. 2925-37.
279. Hoffmann A, Barz T, and Spengler D. **Multitasking C2H2 zinc fingers link Zac DNA binding to coordinated regulation of p300-histone acetyltransferase activity**. *Mol Cell Biol* 2006; 26(14): p. 5544-57.
280. Starostina NG and Kipreos ET. **Multiple degradation pathways regulate versatile CIP/KIP CDK inhibitors**. *Trends Cell Biol* 2012; 22(1): p. 33-41.
281. Blagosklonny MV, Wu GS, Omura S, and el-Deiry WS. **Proteasome-dependent regulation of p21WAF1/CIP1 expression**. *Biochem Biophys Res Commun* 1996; 227(2): p. 564-9.
282. Gartel AL, Najmabadi F, Goufman E, and Tyner AL. **A role for E2F1 in Ras activation of p21(WAF1/CIP1) transcription**. *Oncogene* 2000; 19(7): p. 961-4.
283. Lagger G, Doetzlhofer A, Schuettengruber B, Haidweger E, Simboeck E, Tischler J, Chiocca S, Suske G, Rotheneder H, Wintersberger E, and Seiser C. **The tumor suppressor p53 and histone deacetylase 1 are antagonistic regulators of the cyclin-dependent kinase inhibitor p21/WAF1/CIP1 gene**. *Mol Cell Biol* 2003; 23(8): p. 2669-79.
284. Ocker M and Schneider-Stock R. **Histone deacetylase inhibitors: signalling towards p21cip1/waf1**. *Int J Biochem Cell Biol* 2007; 39(7-8): p. 1367-74.
285. Kim HJ, Park YI, and Dong MS. **Comparison of prostate cancer cell lines for androgen receptor-mediated reporter gene assays**. *Toxicol In Vitro* 2006; 20(7): p. 1159-67.
286. Wang H, Sun D, Ji P, Mohler J, and Zhu L. **An AR-Skp2 pathway for proliferation of androgen-dependent prostate-cancer cells**. *J Cell Sci* 2008; 121(Pt 15): p. 2578-87.
287. Agoulnik IU and Weigel NL. **Androgen receptor action in hormone-dependent and recurrent prostate cancer**. *J Cell Biochem* 2006; 99(2): p. 362-72.
288. Lin B, Wang J, Hong X, Yan X, Hwang D, Cho JH, Yi D, Utleg AG, Fang X, Schones DE, Zhao K, Omenn GS, and Hood L. **Integrated expression profiling and ChIP-seq analyses of the growth inhibition response program of the androgen receptor**. *PLoS One* 2009; 4(8): p. e6589.

Appendix 1. Expression of imprinted genes in benign and cancerous prostate tissues

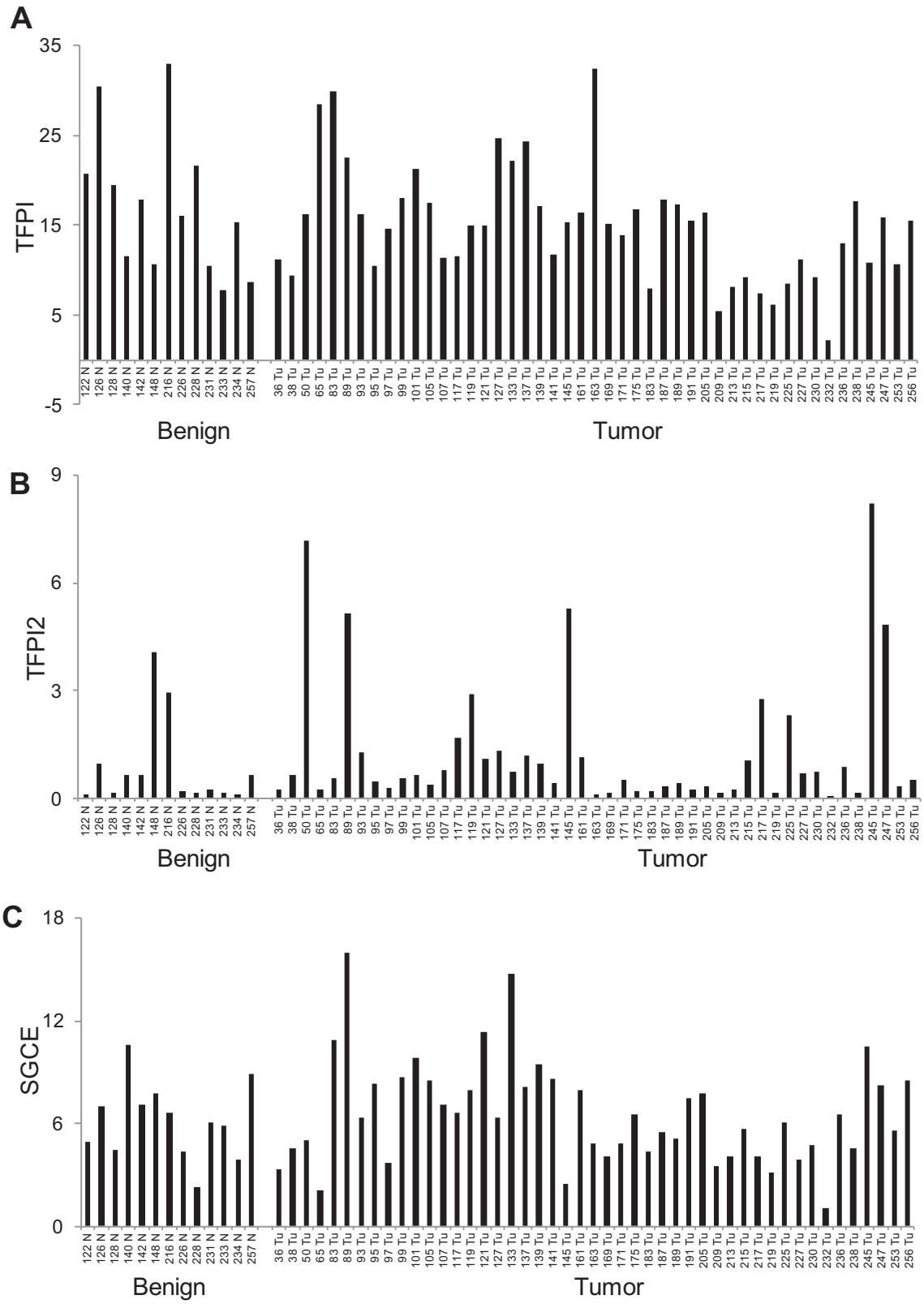

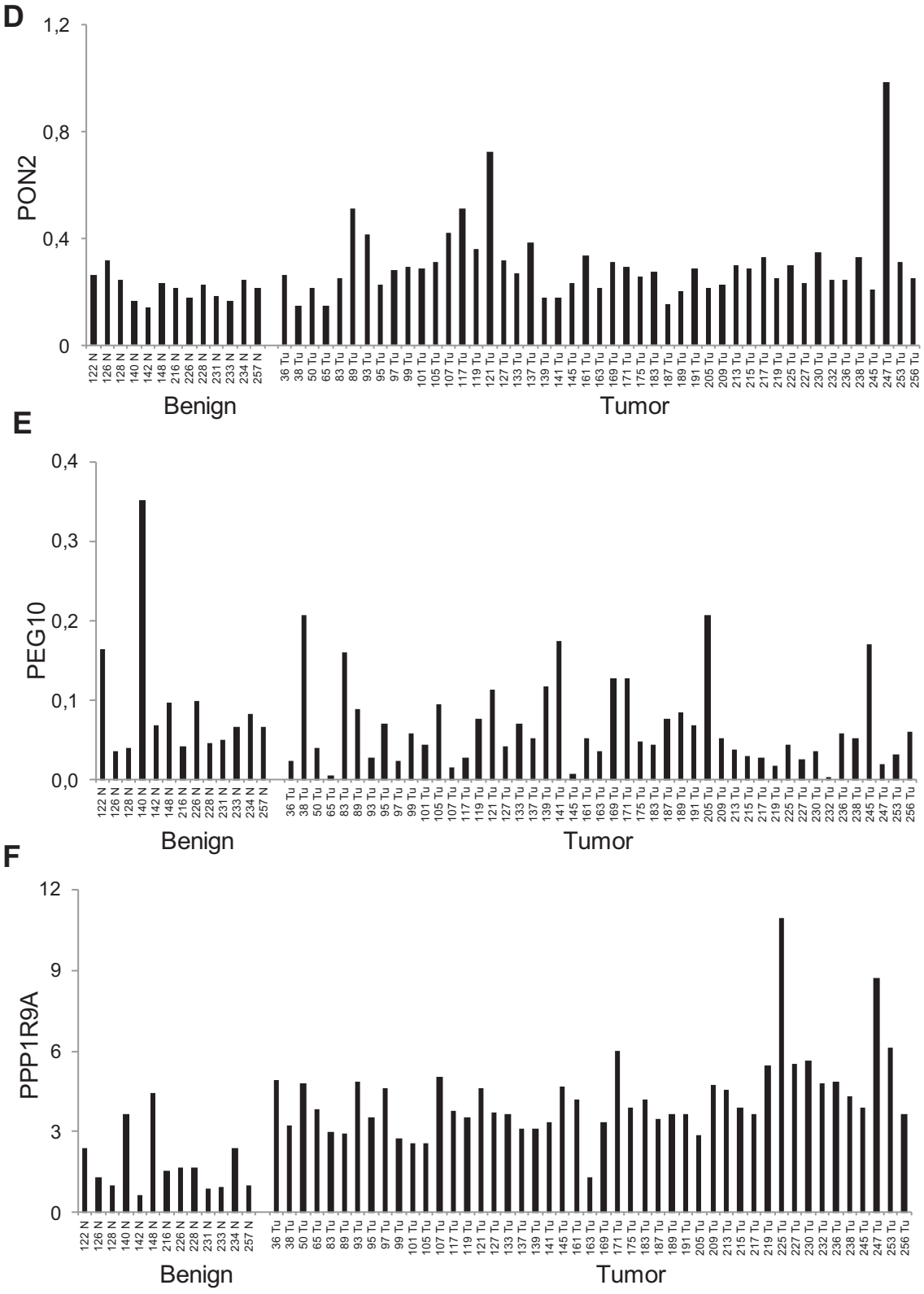
D
PON2
1,2
0,8
0,4
0
Benign
Tumor
E
PEG10
0,4
0,3
0,2
0,1
0,0
Benign
Tumor
F
PPP1R9A
12
9
6
3
0
Benign
Tumor

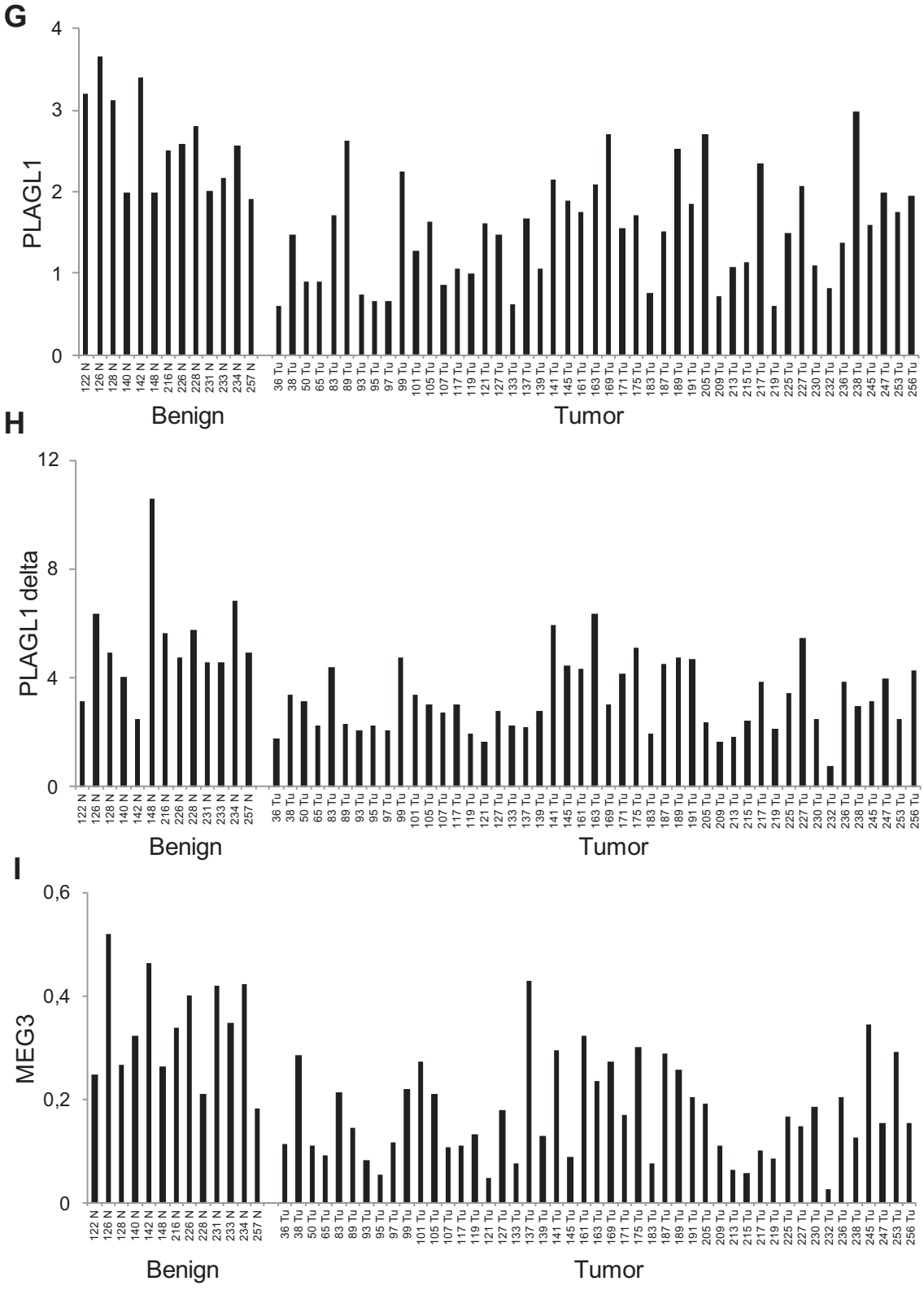
G
PLAGL1
4
3
2
1
0
122 N 126 N 128 N 140 N 142 N 148 N 216 N 226 N 228 N 231 N 233 N 234 N 257 N
36 Tu 38 Tu 50 Tu 65 Tu 83 Tu 89 Tu 93 Tu 95 Tu 97 Tu 99 Tu 101 Tu 105 Tu 107 Tu 117 Tu 119 Tu 121 Tu 127 Tu 133 Tu 137 Tu 139 Tu 141 Tu 145 Tu 161 Tu 163 Tu 169 Tu 171 Tu 175 Tu 183 Tu 187 Tu 189 Tu 191 Tu 205 Tu 209 Tu 213 Tu 215 Tu 217 Tu 219 Tu 225 Tu 227 Tu 230 Tu 232 Tu 236 Tu 238 Tu 245 Tu 247 Tu 253 Tu 256 Tu
Benign
Tumor
H
PLAGL1 delta
12
8
4
0
122 N 126 N 128 N 140 N 142 N 148 N 216 N 226 N 228 N 231 N 233 N 234 N 257 N
36 Tu 38 Tu 50 Tu 65 Tu 83 Tu 89 Tu 93 Tu 95 Tu 97 Tu 99 Tu 101 Tu 105 Tu 107 Tu 117 Tu 119 Tu 121 Tu 127 Tu 133 Tu 137 Tu 139 Tu 141 Tu 145 Tu 161 Tu 163 Tu 169 Tu 171 Tu 175 Tu 183 Tu 187 Tu 189 Tu 191 Tu 205 Tu 209 Tu 213 Tu 215 Tu 217 Tu 219 Tu 225 Tu 227 Tu 230 Tu 232 Tu 236 Tu 238 Tu 245 Tu 247 Tu 253 Tu 256 Tu
Benign
Tumor
I
MEG3
0,6
0,4
0,2
0
122 N 126 N 128 N 140 N 142 N 148 N 216 N 226 N 228 N 231 N 233 N 234 N 257 N
36 Tu 38 Tu 50 Tu 65 Tu 83 Tu 89 Tu 93 Tu 95 Tu 97 Tu 99 Tu 101 Tu 105 Tu 107 Tu 117 Tu 119 Tu 121 Tu 127 Tu 133 Tu 137 Tu 139 Tu 141 Tu 145 Tu 161 Tu 163 Tu 169 Tu 171 Tu 175 Tu 183 Tu 187 Tu 189 Tu 191 Tu 205 Tu 209 Tu 213 Tu 215 Tu 217 Tu 219 Tu 225 Tu 227 Tu 230 Tu 232 Tu 236 Tu 238 Tu 245 Tu 247 Tu 253 Tu 256 Tu
Benign
Tumor

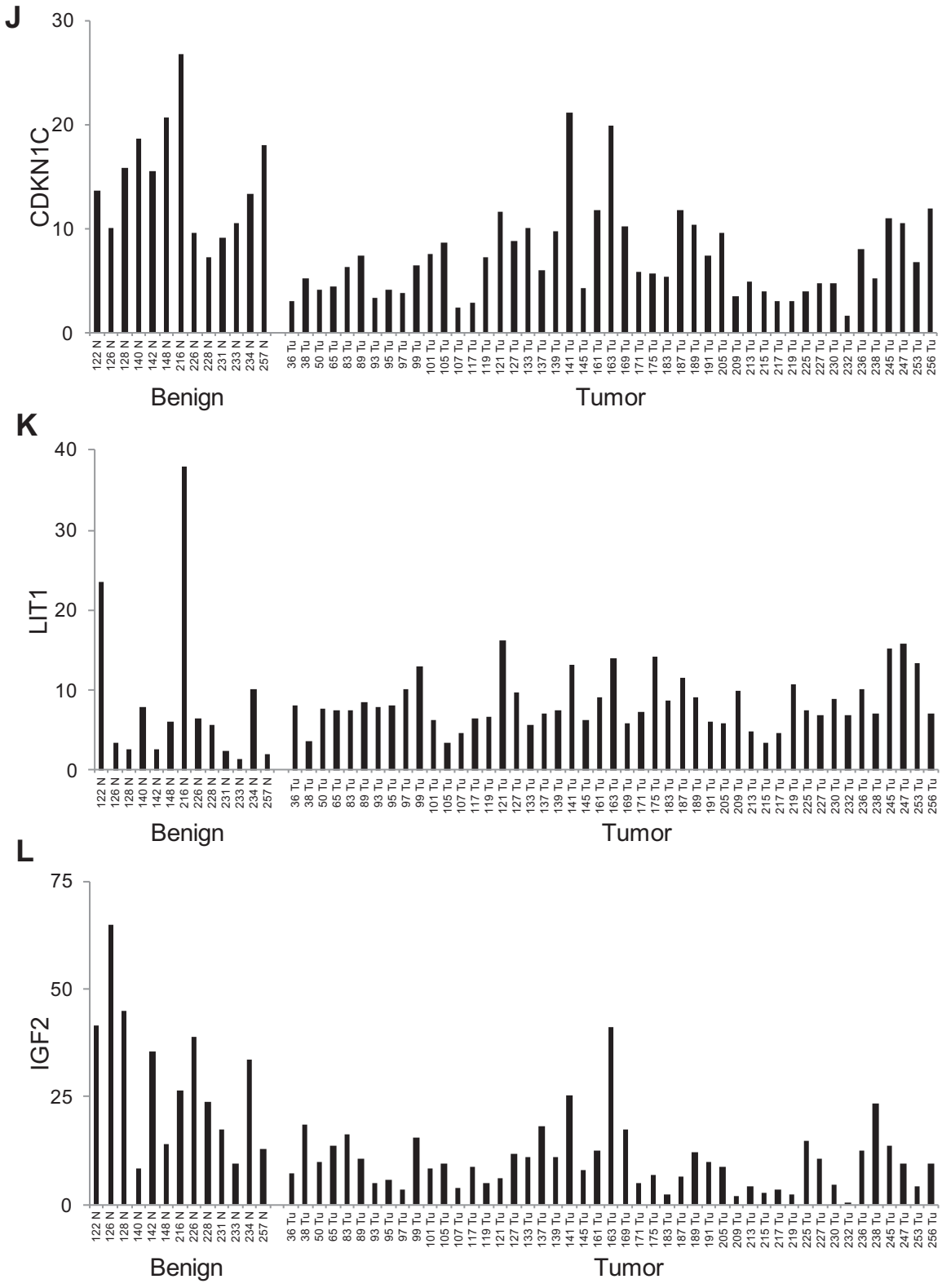
J
CDKN1C
30
20
10
0
122 N 126 N 128 N 140 N 142 N 148 N 216 N 226 N 228 N 231 N 233 N 234 N 257 N
36 Tu 38 Tu 50 Tu 65 Tu 83 Tu 89 Tu 93 Tu 95 Tu 97 Tu 99 Tu 101 Tu 105 Tu 107 Tu 117 Tu 119 Tu 121 Tu 127 Tu 133 Tu 137 Tu 139 Tu 141 Tu 145 Tu 161 Tu 163 Tu 169 Tu 171 Tu 175 Tu 183 Tu 187 Tu 189 Tu 191 Tu 205 Tu 209 Tu 213 Tu 215 Tu 217 Tu 219 Tu 225 Tu 227 Tu 230 Tu 232 Tu 236 Tu 238 Tu 245 Tu 247 Tu 253 Tu 256 Tu
Benign
Tumor
K
LIT1
40
30
20
10
0
Benign
Tumor
L
IGF2
75
50
25
0
Benign
Tumor

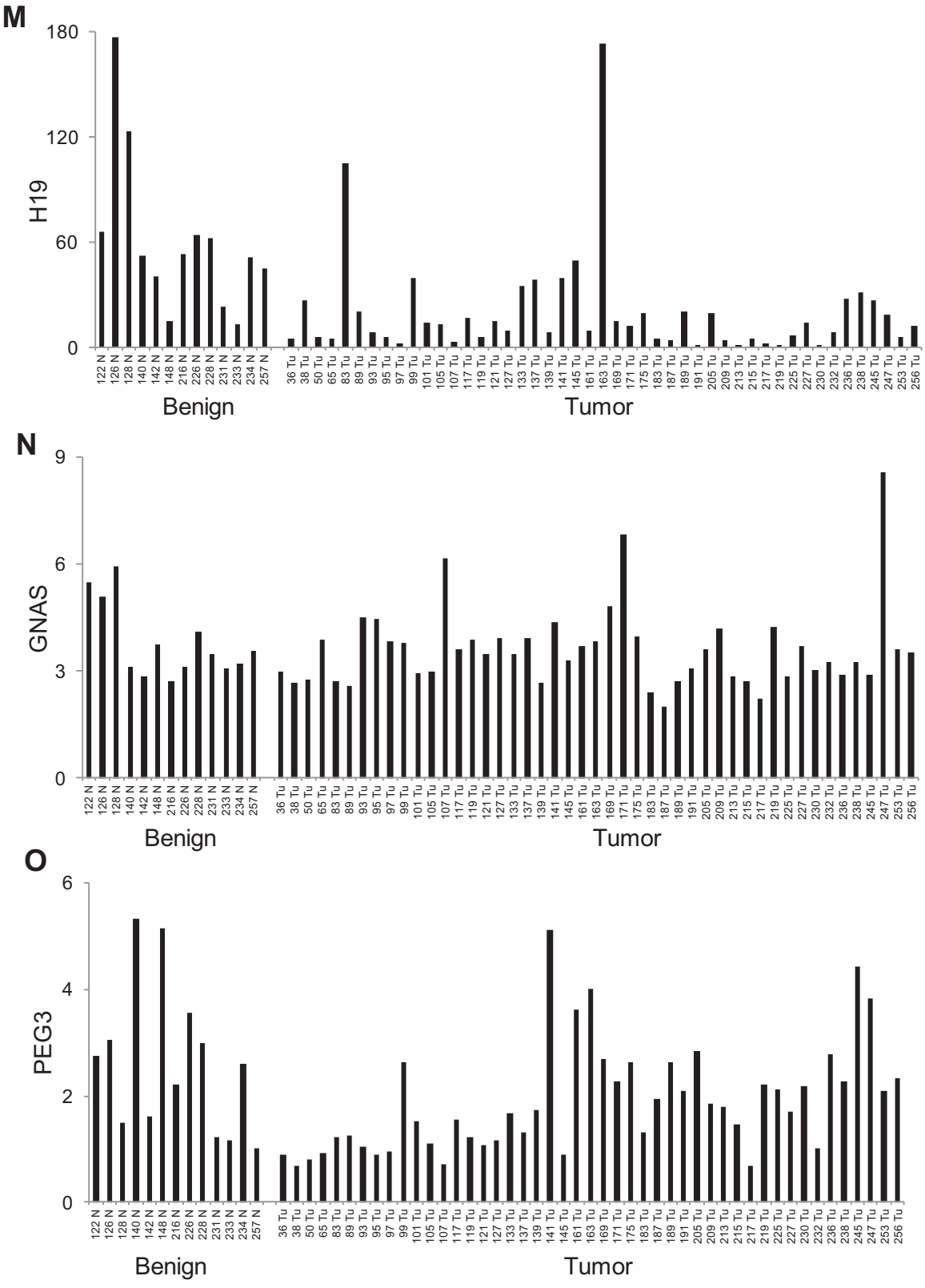
M
H19
180
120
60
0
122 N 126 N 128 N 140 N 142 N 148 N 216 N 226 N 228 N 231 N 233 N 234 N 257 N
36 Tu 38 Tu 50 Tu 65 Tu 83 Tu 89 Tu 93 Tu 95 Tu 97 Tu 99 Tu 101 Tu 105 Tu 107 Tu 117 Tu 119 Tu 121 Tu 127 Tu 133 Tu 137 Tu 139 Tu 141 Tu 145 Tu 161 Tu 163 Tu 169 Tu 171 Tu 175 Tu 183 Tu 187 Tu 189 Tu 191 Tu 205 Tu 209 Tu 213 Tu 215 Tu 217 Tu 219 Tu 225 Tu 227 Tu 230 Tu 232 Tu 236 Tu 238 Tu 245 Tu 247 Tu 253 Tu 256 Tu
Benign
Tumor
N
GNAS
9
6
3
0
122 N 126 N 128 N 140 N 142 N 148 N 216 N 226 N 228 N 231 N 233 N 234 N 257 N
36 Tu 38 Tu 50 Tu 65 Tu 83 Tu 89 Tu 93 Tu 95 Tu 97 Tu 99 Tu 101 Tu 105 Tu 107 Tu 117 Tu 119 Tu 121 Tu 127 Tu 133 Tu 137 Tu 139 Tu 141 Tu 145 Tu 161 Tu 163 Tu 169 Tu 171 Tu 175 Tu 183 Tu 187 Tu 189 Tu 191 Tu 205 Tu 209 Tu 213 Tu 215 Tu 217 Tu 219 Tu 225 Tu 227 Tu 230 Tu 232 Tu 236 Tu 238 Tu 245 Tu 247 Tu 253 Tu 256 Tu
Benign
Tumor
O
PEG3
6
4
2
0
122 N 126 N 128 N 140 N 142 N 148 N 216 N 226 N 228 N 231 N 233 N 234 N 257 N
36 Tu 38 Tu 50 Tu 65 Tu 83 Tu 89 Tu 93 Tu 95 Tu 97 Tu 99 Tu 101 Tu 105 Tu 107 Tu 117 Tu 119 Tu 121 Tu 127 Tu 133 Tu 137 Tu 139 Tu 141 Tu 145 Tu 161 Tu 163 Tu 169 Tu 171 Tu 175 Tu 183 Tu 187 Tu 189 Tu 191 Tu 205 Tu 209 Tu 213 Tu 215 Tu 217 Tu 219 Tu 225 Tu 227 Tu 230 Tu 232 Tu 236 Tu 238 Tu 245 Tu 247 Tu 253 Tu 256 Tu
Benign
Tumor

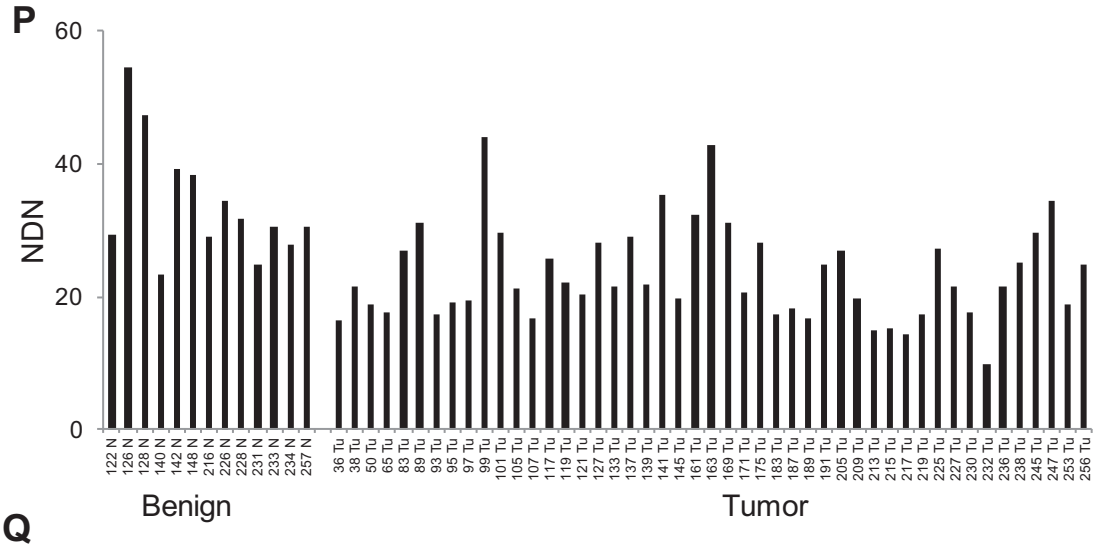
P
NDN
60
40
20
0
122 N 126 N 128 N 140 N 142 N 148 N 216 N 226 N 228 N 231 N 233 N 234 N 257 N
36 Tu 38 Tu 50 Tu 65 Tu 83 Tu 89 Tu 93 Tu 95 Tu 97 Tu 99 Tu 101 Tu 105 Tu 107 Tu 117 Tu 119 Tu 121 Tu 127 Tu 133 Tu 137 Tu 139 Tu 141 Tu 145 Tu 161 Tu 163 Tu 169 Tu 171 Tu 175 Tu 183 Tu 187 Tu 189 Tu 191 Tu 205 Tu 209 Tu 213 Tu 215 Tu 217 Tu 219 Tu 225 Tu 227 Tu 230 Tu 232 Tu 236 Tu 238 Tu 245 Tu 247 Tu 253 Tu 256 Tu
Benign
Tumor

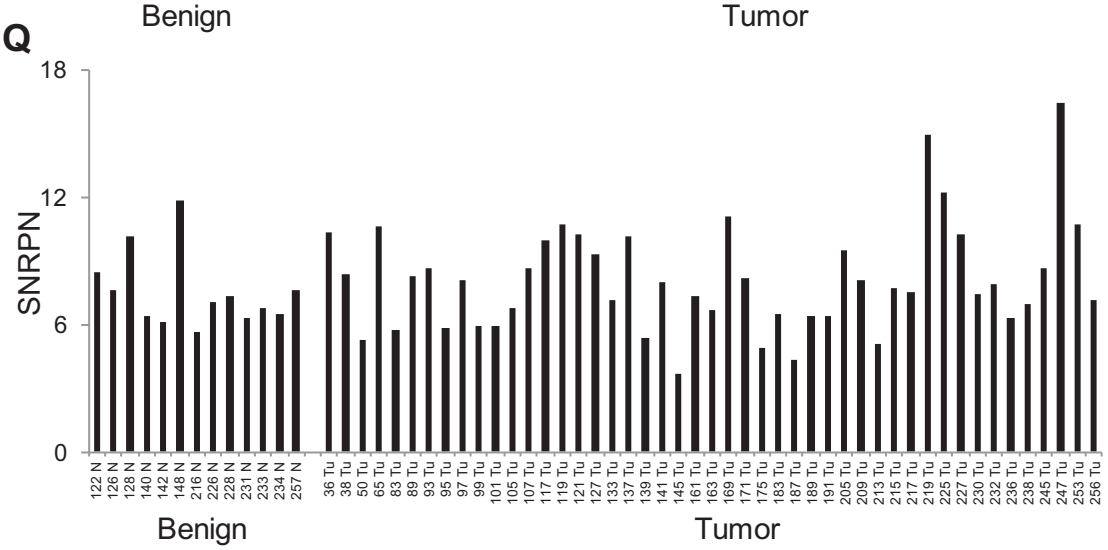
Q
SNRPN
18
12
6
0
122 N 126 N 128 N 140 N 142 N 148 N 216 N 226 N 228 N 231 N 233 N 234 N 257 N
36 Tu 38 Tu 50 Tu 65 Tu 83 Tu 89 Tu 93 Tu 95 Tu 97 Tu 99 Tu 101 Tu 105 Tu 107 Tu 117 Tu 119 Tu 121 Tu 127 Tu 133 Tu 137 Tu 139 Tu 141 Tu 145 Tu 161 Tu 163 Tu 169 Tu 171 Tu 175 Tu 183 Tu 187 Tu 189 Tu 191 Tu 205 Tu 209 Tu 213 Tu 215 Tu 217 Tu 219 Tu 225 Tu 227 Tu 230 Tu 232 Tu 236 Tu 238 Tu 245 Tu 247 Tu 253 Tu 256 Tu
Benign
Tumor

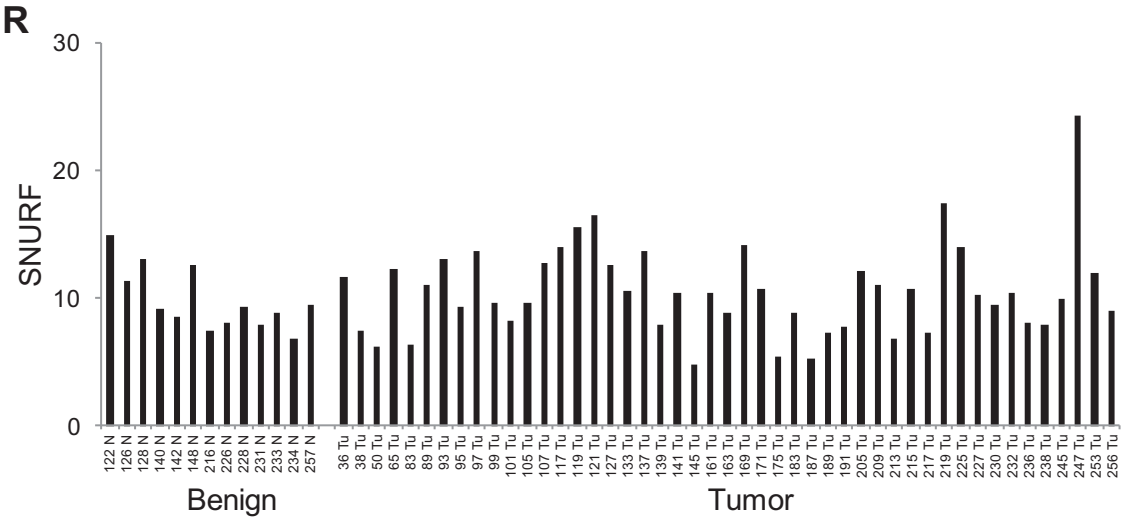
R
SNURF
30
20
10
0
122 N 126 N 128 N 140 N 142 N 148 N 216 N 226 N 228 N 231 N 233 N 234 N 257 N
36 Tu 38 Tu 50 Tu 65 Tu 83 Tu 89 Tu 93 Tu 95 Tu 97 Tu 99 Tu 101 Tu 105 Tu 107 Tu 117 Tu 119 Tu 121 Tu 127 Tu 133 Tu 137 Tu 139 Tu 141 Tu 145 Tu 161 Tu 163 Tu 169 Tu 171 Tu 175 Tu 183 Tu 187 Tu 189 Tu 191 Tu 205 Tu 209 Tu 213 Tu 215 Tu 217 Tu 219 Tu 225 Tu 227 Tu 230 Tu 232 Tu 236 Tu 238 Tu 245 Tu 247 Tu 253 Tu 256 Tu
Benign
Tumor

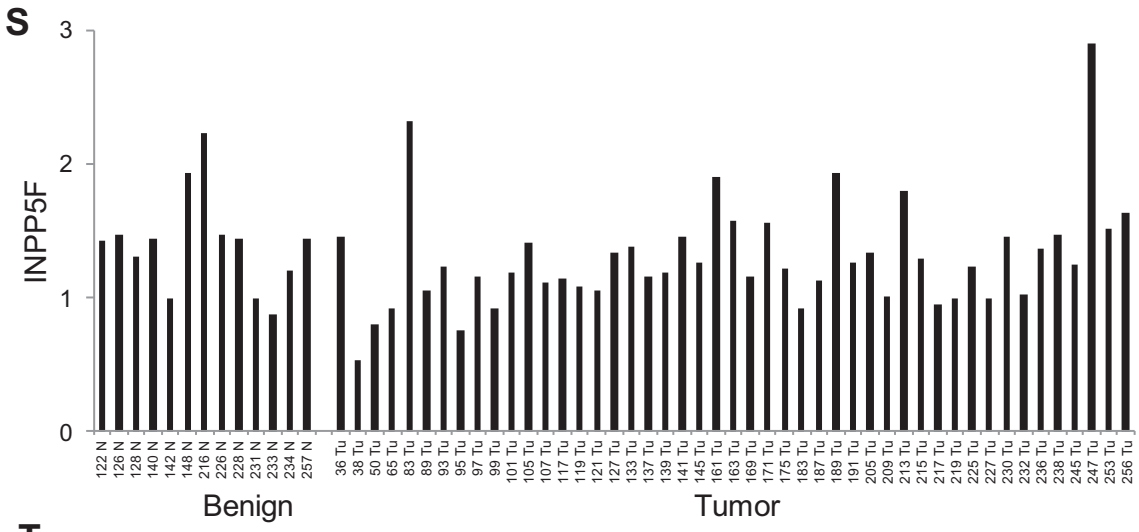
S
INPP5F
3
2
1
0
122 N 126 N 128 N 140 N 142 N 148 N 216 N 226 N 228 N 231 N 233 N 234 N 257 N
36 Tu 38 Tu 50 Tu 65 Tu 83 Tu 89 Tu 93 Tu 95 Tu 97 Tu 99 Tu 101 Tu 105 Tu 107 Tu 117 Tu 119 Tu 121 Tu 127 Tu 133 Tu 137 Tu 139 Tu 141 Tu 145 Tu 161 Tu 163 Tu 169 Tu 171 Tu 175 Tu 183 Tu 187 Tu 189 Tu 191 Tu 205 Tu 209 Tu 213 Tu 215 Tu 217 Tu 219 Tu 225 Tu 227 Tu 230 Tu 232 Tu 236 Tu 238 Tu 245 Tu 247 Tu 253 Tu 256 Tu
Benign
Tumor

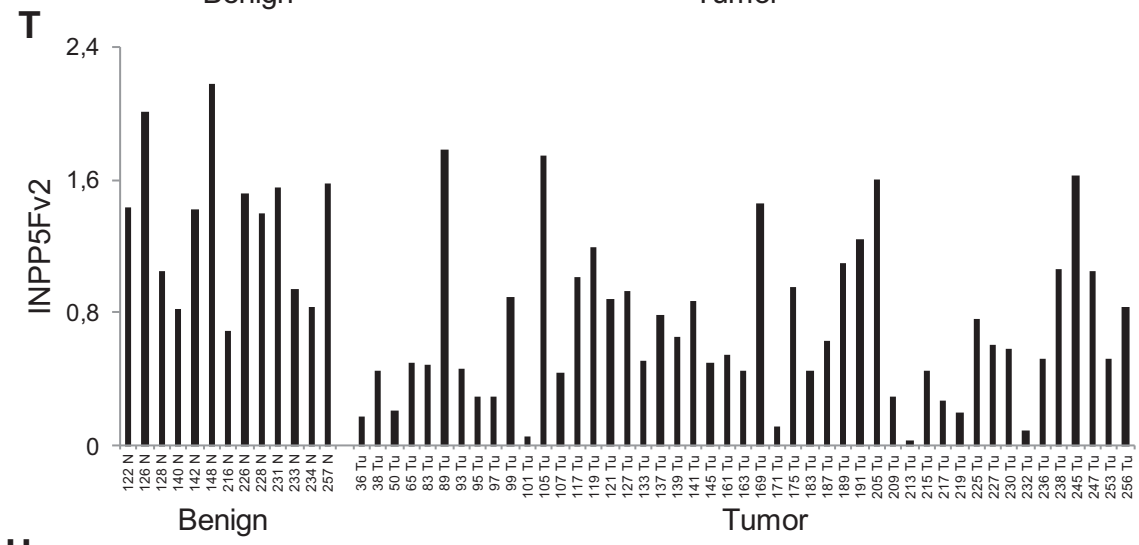
T
INPP5Fv2
2,4
1,6
0,8
0
122 N 126 N 128 N 140 N 142 N 148 N 216 N 226 N 228 N 231 N 233 N 234 N 257 N
36 Tu 38 Tu 50 Tu 65 Tu 83 Tu 89 Tu 93 Tu 95 Tu 97 Tu 99 Tu 101 Tu 105 Tu 107 Tu 117 Tu 119 Tu 121 Tu 127 Tu 133 Tu 137 Tu 139 Tu 141 Tu 145 Tu 161 Tu 163 Tu 169 Tu 171 Tu 175 Tu 183 Tu 187 Tu 189 Tu 191 Tu 205 Tu 209 Tu 213 Tu 215 Tu 217 Tu 219 Tu 225 Tu 227 Tu 230 Tu 232 Tu 236 Tu 238 Tu 245 Tu 247 Tu 253 Tu 256 Tu
Benign
Tumor

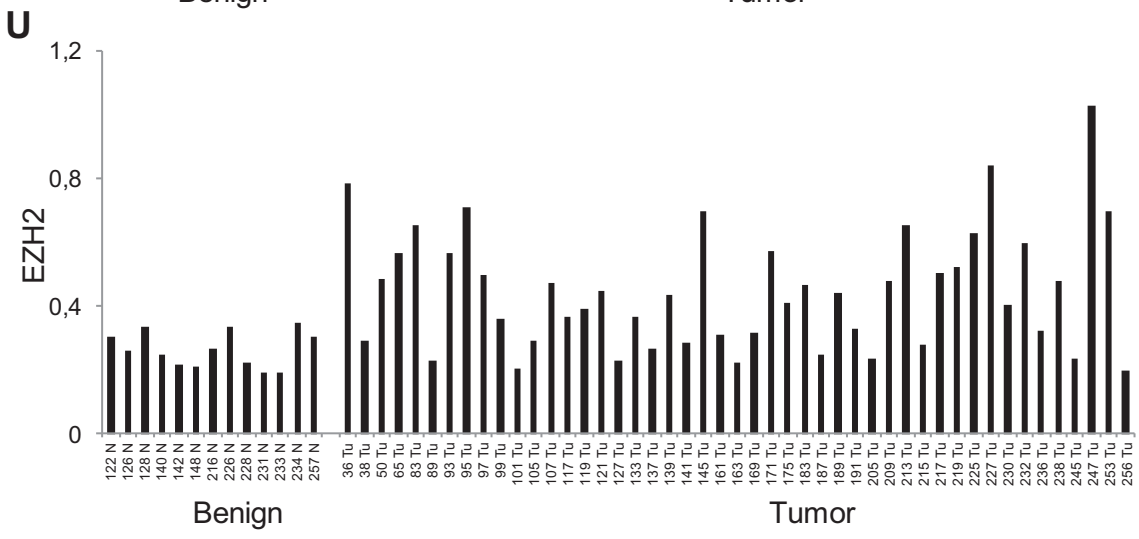
U
EZH2
1,2
0,8
0,4
0
122 N 126 N 128 N 140 N 142 N 148 N 216 N 226 N 228 N 231 N 233 N 234 N 257 N
36 Tu 38 Tu 50 Tu 65 Tu 83 Tu 89 Tu 93 Tu 95 Tu 97 Tu 99 Tu 101 Tu 105 Tu 107 Tu 117 Tu 119 Tu 121 Tu 127 Tu 133 Tu 137 Tu 139 Tu 141 Tu 145 Tu 161 Tu 163 Tu 169 Tu 171 Tu 175 Tu 183 Tu 187 Tu 189 Tu 191 Tu 205 Tu 209 Tu 213 Tu 215 Tu 217 Tu 219 Tu 225 Tu 227 Tu 230 Tu 232 Tu 236 Tu 238 Tu 245 Tu 247 Tu 253 Tu 256 Tu
Benign
Tumor

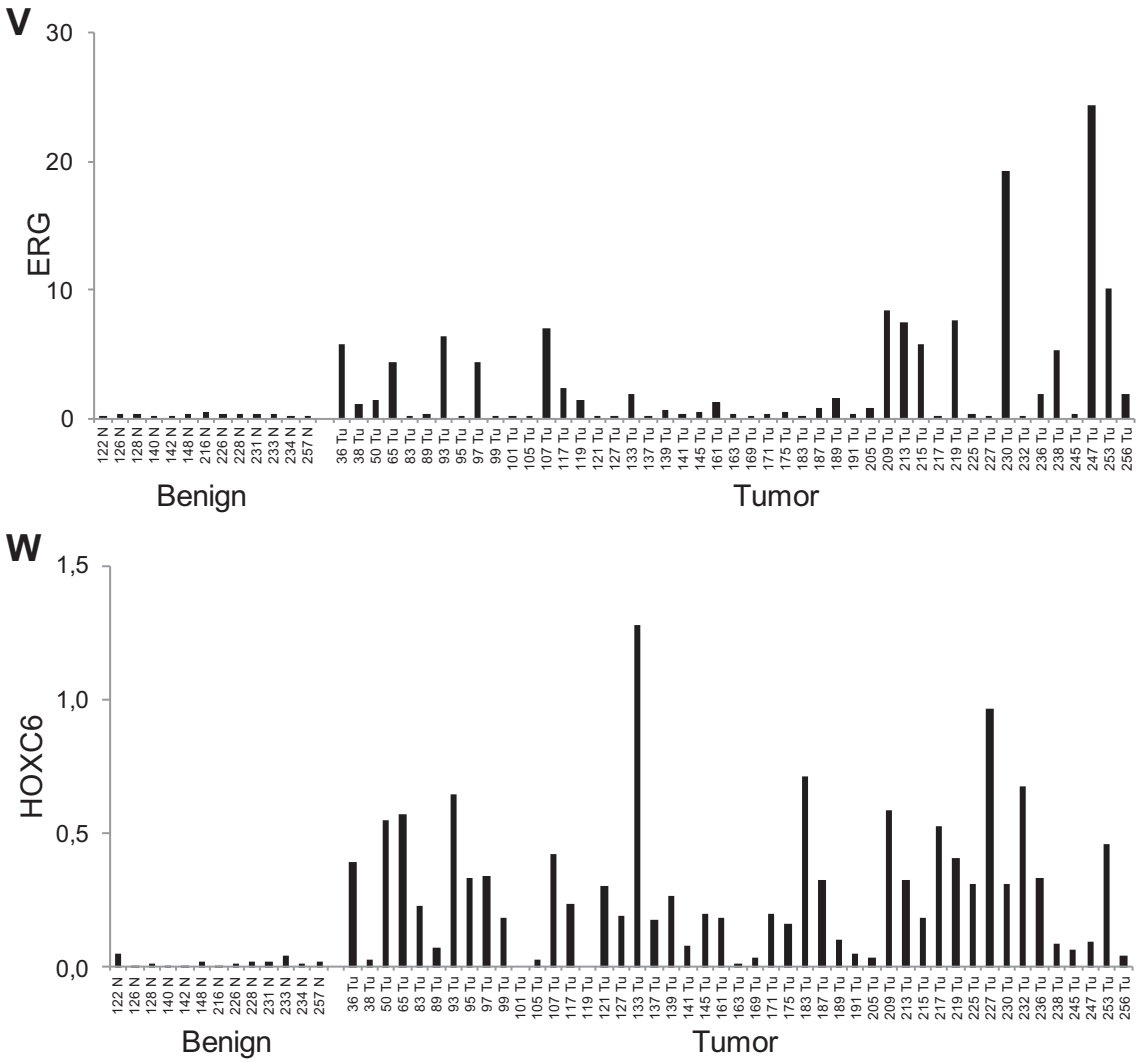

Messenger RNA expression of the indicated genes relative to *TBP* in 47 prostate carcinoma and 13 benign prostate tissue samples measured by qRT-PCR.

Appendix 2. Location of regions analyzed by bisulfite pyrosequencing

7q21 DMR chr7: 94,284,600- 94,284,681

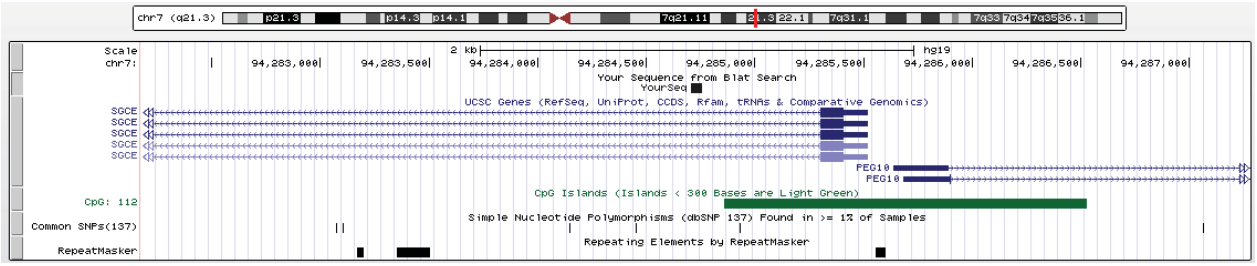

KvDMR chr11: 2,721,592-2,721,680

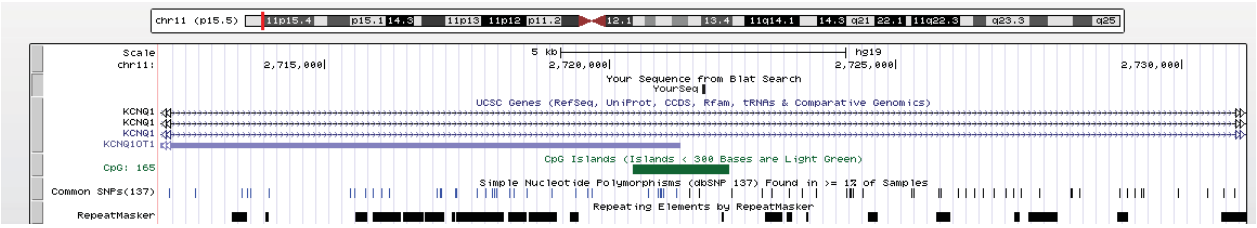

CDKN1C promoter excerpt chr11: 2,907,633-2,907,750

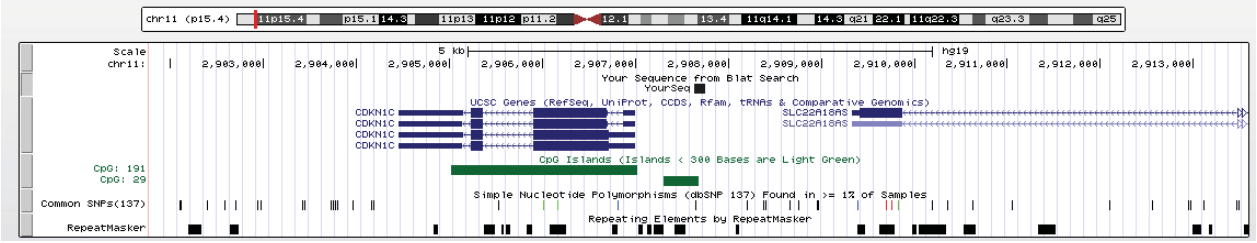

PLAGL1 DMR chr6: 144,329,726-144,329,987

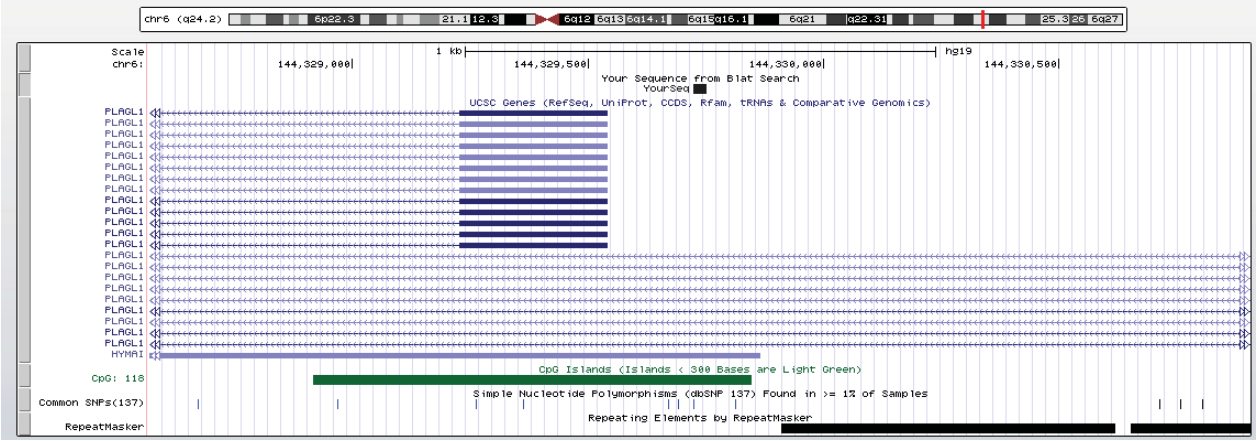

MEG3 DMR chr3: 101,290,923-101,291,134

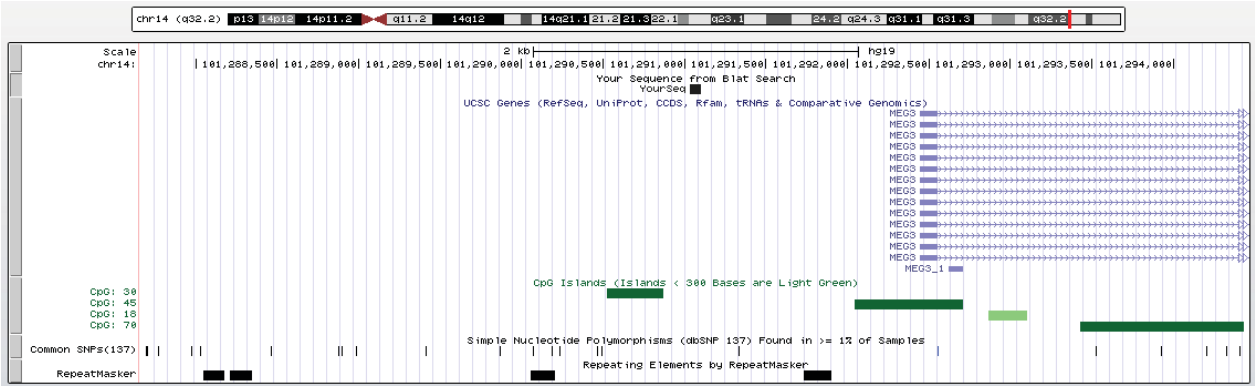

The pictures were obtained from UCSC gene browser.

Appendix 3. CpG methylation of selected imprinted genes in prostate benign and cancer tissues

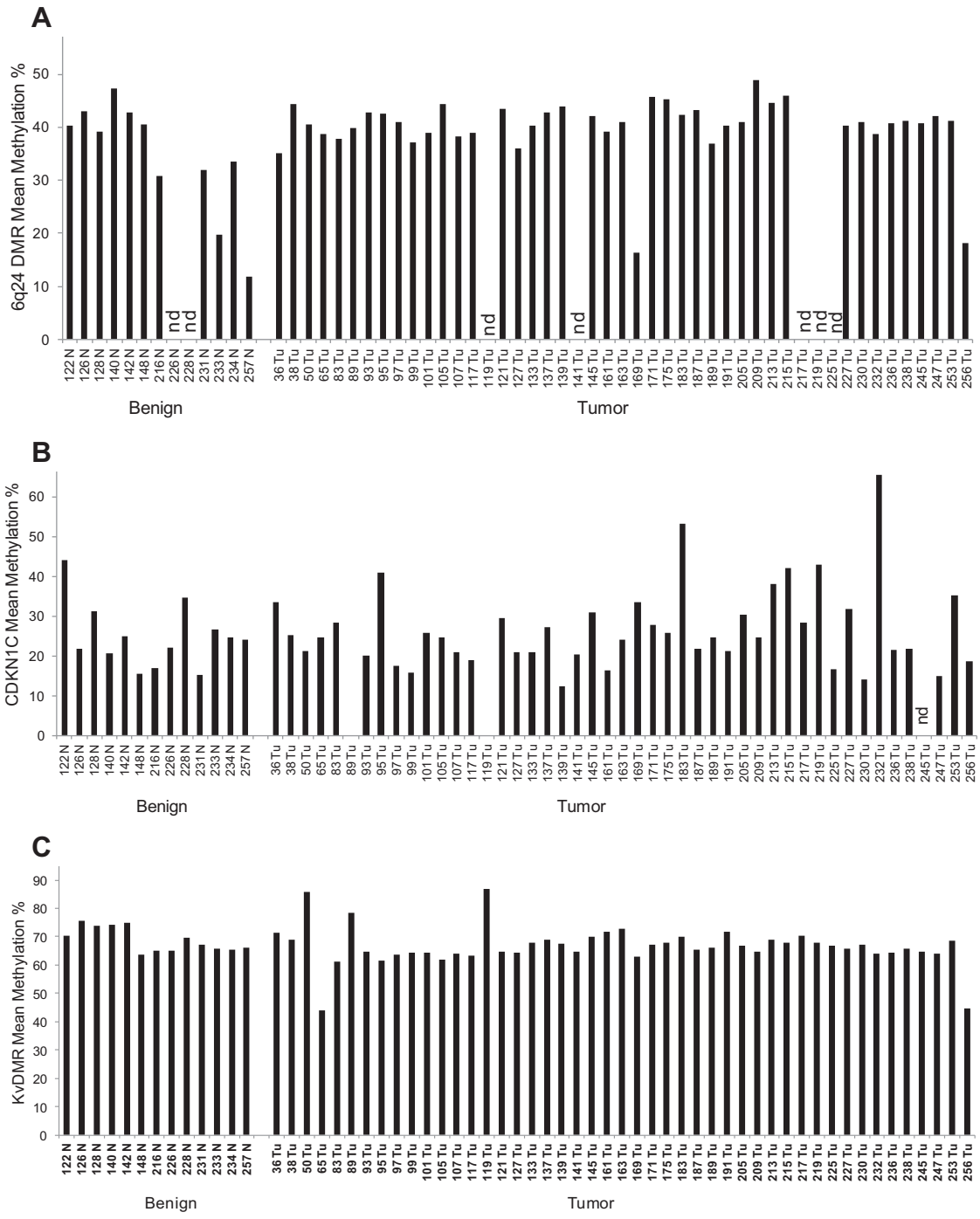

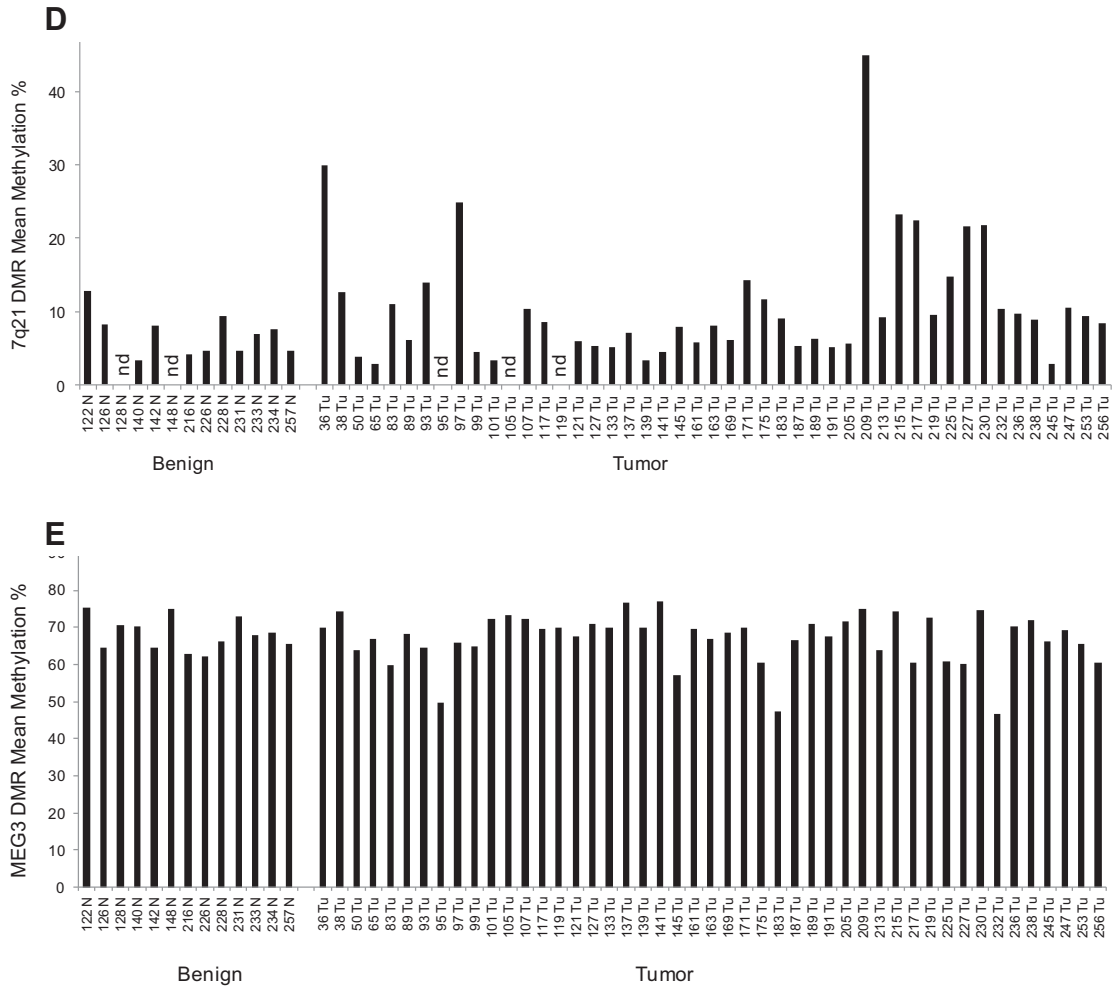

Mean methylation (%) of several CpG positions in the indicated regions in benign and carcinoma prostate tissues, obtained by bisulfite pyrosequencing.

Appendix 4. ZAC1 transcripts and cDNA sequences contained in ZAC1 expression plasmids

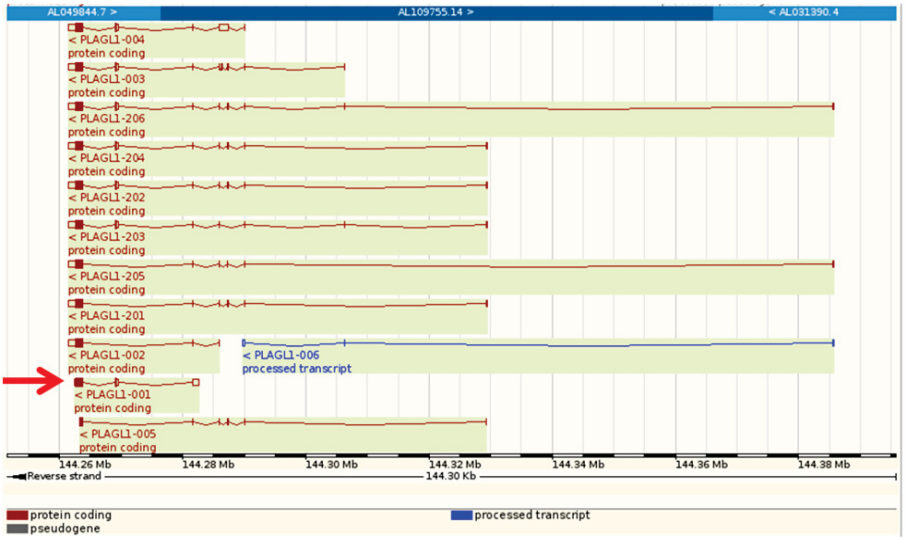

Fig.1. ZAC1 transcript variants included in the Ensembl database. The transcript variant corresponding to the ZAC1 cDNA in the pBS.hZAC1 plasmid obtained from A.Varrault is PLAGL1-001, transcript ID ENST00000367571 (see red arrow), coding for a 463-amino acid- long ZAC1 protein.

AGCCTCCGGACTCTAGCGTTTAAACTTAAGCTTGATATCGAATTCcggttctttcaattcagaatttgttttaggttctgttattg
catagatttgcatacctgttttATGgtattttaatactgttggttttaaaaaataccatttcctctgagtgctgttctgaatatattATGtaagcaatt
ttgtgtgttctttttttttccacttgcataaagcaggggaaaagttgagagtttttcttaatccagttgcaagtaggacaaaggatATGagtgtttaa
agatcatctattaaaATGcATGaaaaaacactagaaaatctcctgtgcacatcgccagtcgtgtgtgtgctctagaagtgaagttcagggggt
aacataATGgaggaATGttttcctagcttcattccctgacgATGtacaaggtctcttctcacaggtttgaatcttcagacaaacttctgggagg
actcggtccctgcctcgcagcagATGttccctgtcactcagtagccaatccgggggacccaggacATGccccagctatagtgATGcagattac
ctttctgctcctgaatcgcacctgtgcctcagactttctcccctcagcttgagactgcATGtaaactgggATGtgtgaaagcaggaagcaaagct
agtgacagctgagaggtccATGtctgggtagaaccaggcccacgATGctgcctctcccgtggtctggagttcagctgcagggactctgctgatt
ggcccagcaccatcgttctgtttgtgcttaaATGgcacagcatttggtcagcacatctgaaaaggaaggtgtgagaagcaaagccc**ATG**GCC
ACGTTCCCCTGCCAGTTATGTGGCAAGACGTTCCTCACCCTGGAGAAGTTCACGATTCACAATTATTCCCACTCC
AGGGAGCGGCCGTACAAGTGTGTGCAGCCTGACTGTGGCAAAGCCTTTGTTTCCAGATATAAATTG**ATG**AGGC
AT**ATG**GCTACCCATTCTCCCCAGAAATCTCACCAGTGTGCTCACTGTGAGAAGACGTTCAACCGGAAAGACCAC
CTGAAAAACCACCTCCAGACCCACGACCCCAACAAA**ATG**GCCTTTGGGTGTGAGGAGTGTGGGAAGAAGTAC
AACACC**ATG**CTGGGCTATAAGAGGCACCTGGCCCTCC**ATG**CGGCCAGCAGTGGGGACCTCACCTGTGGGGTC
TGTGCCCTGGAGCTAGGGAGCACCGAGGTGCTACTGGACCACCTCAAAGCCC**ATG**CGGAAGAGAAGCCCCCT
AGCGGAACCAAGGAAAAGAAGCACCAGTGCGACCACTGTGAAAG**ATG**CTTCTACACCCGGAAGG**ATG**TGCG
ACGCCACCTGGTGGTCCACACAGG**ATG**CAAGGACTTCCTGTGCCAGTTCTGTGCCCAGAGATTTGGGCGCAAG
GATCACCTCACCCGGCATACCAAGAAGACCCACTCACAGGAGCTG**ATG**AAAGAGAGCTTGCAGACCGGAGAC
CTTCTGAGCACCTTCCACACCATCTCGCCTTCATTCCAACTGAAGGCTGCTGCCTTGCCTCCTTTCCCTTTAGGAG
CTTCTGCCCAGAACGGGCTTGCAAGTAGCTTGCCAGCTGAGGTCCATAGCCTCACCCTCAGTCCCCCAGAACAA
GCCGCCCAGCCT**ATG**CAGCCGCTGCCAGAGTCCCTGGCCTCCCTCCACCCCTCGGTATCCCCTGGCTCTCCTCC
GCCACCCCTTCCCAATCACAAGTACAACACCACTTCTACCTCATACTCCCCACTTGCAAGCCTGCCCCTCAAAGC
AGATACTAAAGGTTTTTGCAATATCAGTTTGTTTGAGGACTTGCCTCTGCAAGAGCCTCAGTCACCTCAAAAGC
TCAACCCAGGTTTTGATCTGGCTAAGGGAA**ATG**CTGGTAAAGTAAACCTGCCCAAGGAGCTGCCTGCAG**ATG**C
TGTGAACCTAACAATACCTGCCTCTCTGGACCTGTCCCCCCTGTTGGGCTTCTGGCAGCTGCCCCCTCCTGCTAC
CCAAAATACCTTTGGGAATAGCACTCTTGCCCTGGGGCCTGGGGAATCTTTGCCCCACAGGTTAAGCTGTCTGG
GGCAGCAGCAGCAAGAACCCCCACTTGCC**ATG**GGCACTGTGAGCCTGGGCCAGCTCCCCCTGCCCCCCATCCC
TC**ATG**TGTTCTCAGCTGGCACTGGCTCTGCCATCCTGCCTCATTTCCATC**ATG**CATTCAGAtaattgatttttaaagtgt
atttttcgtattctggaagATGttttaagaagcattttaaATGtcagttacaatATGagaaagatttggaaaacgagactgggactATGgctt
attcagtgATGactggcttgagATGataagaGAATTCCTGCAGCCCGGGGGATCCACTAGTTCTAGAGCGGCCGCTCGA
GTCTAGAGGGCCCGTTTAAACCCGCTGATCAGCCTCGACTGTGC

Fig. 2. Excerpt of the DNA sequence of the pcDNA4/TO.ZAC.VA plasmid containing the ZAC.VA cDNA insert. The 5'- and 3'-UTRs are denoted in lower case letters, with exception of potential ORF start ATGs which are in upper case letters. Coding sequences are highlighted yellow and ATGs are bolded. *HindIII* and *NotI* restriction sites of insert integration are highlighted in pink.

Fig. 3. Excerpt of the DNA sequence of the pcDNA4/TO.ZAC.DS plasmid containing ZAC.DS cDNA insert. The coding sequence is highlighted in yellow. The original transcription start site TSS (ATG) is mutated (red letters) and new TSS (ATG) at position -24 is in bold lettes. Restriction sites *BamHI* and *EcoRV* of insert integration are highlighted in pink.

AGCCTCCGGACTCTAGCGTTTAAACTTAAGCTCCTTTGTTTCCAGATATAAATTG**ATG**AGGCAT**ATG**GCTACC
CATTCTCCCCAGAAATCTCACCAGTGTGCTCACTGTGAGAAGACGTTCAACCGGAAAGACCACCTGAAAAACC
ACCTCCAGACCCACGACCCCAACAAA**ATG**GCCTTTGGGTGTGAGGAGTGTGGGAAGAAGTACAACACC**ATG**C
TGGGCTATAAGAGGCACCTGGCCCTCC**ATG**CGGCCAGCAGTGGGGACCTCACCTGTGGGGTCTGTGCCCTGG
AGCTAGGGAGCACCGAGGTGCTACTGGACCACCTCAAAGCCC**ATG**CGGAAGAGAAGCCCCCTAGCGGAACCA
AGGAAAAGAAGCACCAGTGCGACCACTGTGAAAG**ATG**CTTCTACACCCGGAAGG**ATG**TGCGACGCCACCTGG
TGGTCCACACAGG**ATG**CAAGGACTTCCTGTGCCAGTTCTGTGCCCAGAGATTTGGGCGCAAGGATCACCTCAC
CCGGCATACCAAGAAGACCCACTCACAGGAGCTG**ATG**AAAGAGAGCTTGCAGACCGGAGACCTTCTGAGCAC
CTTCCACACCATCTCGCCTTCATTCCAACTGAAGGCTGCTGCCTTGCCTCCTTTCCCTTTAGGAGCTTCTGCCCAG
AACGGGCTTGCAAGTAGCTTGCCAGCTGAGGTCCATAGCCTCACCCTCAGTCCCCCAGAACAAGCCGCCCAGC
CT**ATG**CAGCCGCTGCCAGAGTCCCTGGCCTCCCTCCACCCCTCGGTATCCCCTGGCTCTCCTCCGCCACCCCTTC
CCAATCACAAGTACAACACCACTTCTACCTCATACTCCCCACTTGCAAGCCTGCCCCTCAAAGCAGATACTAAAG
GTTTTTGCAATATCAGTTTGTTTGAGGACTTGCCTCTGCAAGAGCCTCAGTCACCTCAAAAGCTCAACCCAGGTT
TTGATCTGGCTAAGGGAA**ATG**CTGGTAAAGTAAACCTGCCCAAGGAGCTGCCTGCAG**ATG**CTGTGAACCTAAC
AATACCTGCCTCTCTGGACCTGTCCCCCCTGTTGGGCTTCTGGCAGCTGCCCCCTCCTGCTACCCAAAATACCTT
TGGGAATAGCACTCTTGCCCTGGGGCCTGGGGAATCTTTGCCCCACAGGTTAAGCTGTCTGGGGCAGCAGCAG
CAAGAACCCCCACTTGCC**ATG**GGCACTGTGAGCCTGGGCCAGCTCCCCCTGCCCCCCATCCCTC**ATG**TGTTCTC
AGCTGGCACTGGCTCTGCCATCCTGCCTCATTTCCATC**ATG**CATTCAGAtaattgatttttaaagtgtatttttcgtattctgga
agATGttttaagaagcattttaaATGtcagttacaatATGagaaagatttggaaaacgagactgggactATGgcttattcagtgATGactg
gcttgagATGataagaGAATTCCTGCAGCCCGGGGGATCCACTAGTTCTAGAGCGGCCGCTCGAGTCTAGAGGGC

Fig. 4. Excerpt of the DNA sequence of the pcDNA4/TO.ZAC.delta plasmid containing ZACdelta cDNA insert. Coding sequences include the cDNA sequence from the second protein-coding exon together with a small stretch of cDNA from the first protein-coding exon of ZAC1 are in upper case letters and highlighted in yellow. The 3' UTRs is denoted in lower case letters. ATGs are bolded and in upper case. The transcription start site (ATG) of the second protein-coding exon is denoted by a bigger ATG. Another potential in frame TSS (ATG) upstream and of it, if utilized, can code for 3 more amino acids to the original protein form coded by the ZAC1.delta splice isoform. Restriction sites *HindIII* (disrupted upon cloning) and *EcoRV* of insert integration are highlighted in pink.

Appendix 5: Predicted IRES sequences in ZAC1 5'-UTR

RegRNA database search:

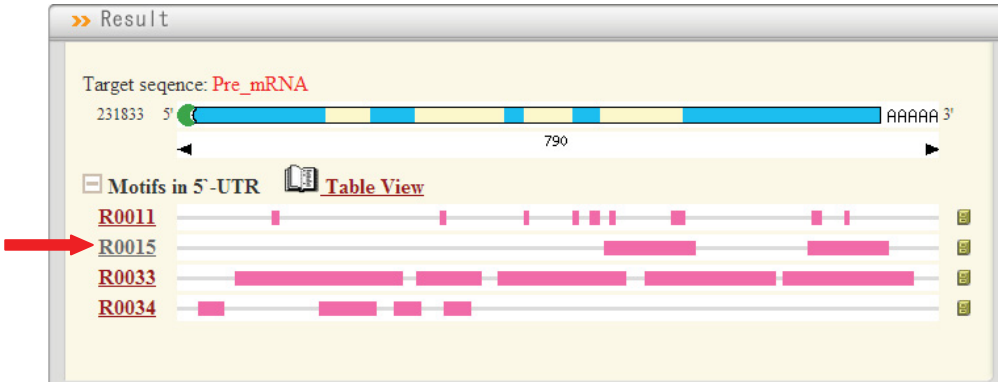

Target Sequence	>hZAC1 5'-UTR ttctttcaattcagaatttgttttaggttctgttattgcatagatttgcatacctgttttATGgtattttaatactgttg gttttaaaaaataccatttcctctgagtgctgttctgaatatattATGtaagcaattttgtgtgttctttttttttccact tgcataaagcaggggaaaagttgagagtttttcttaatccagttgcaagtaggacaaaggatATGagtgtttaaagatca tctattaaaATGcATGaaaaaacactagaaaatctcctgtgcacatcgccagtcgtgtgtgtgctctagaagtgaagttc agggggtaacataATGgaggaATGttttcctagcttcattccctgacgATGtacaaggtctcttctcacaggtttgaatc ttcagacaaacttctgggaggactcggtccctgcctcgcagcagATGttccctgtcactcagtag ccaatccgggggac ccaggacATGccccagctatagtgATGcagattacctttctgctcctgaatcgcacctgtgcctcagactttctcccctc agcttgagactgcATGtaaactgggATGtgtgaaagcaggaagcaaagctagtgacagctgagaggtccATGtctgggta gaaccaggcccacgATGctgcctctcccgtggtctggagttcagctgcagggactctgctgattggcccagcaccatcgt tctgtttgtgcttaaATGgcacagcatttggtcagcacatctgaaaaggaaggtgtgagaagcaaagccc

No.	RegRNA ID	Location	Len	Sequence	View	Profile
2	R0015	655~737	83	tgctgcctctcccgtggtctggagttcagc tgcagggactctgctgattggcccagcacc atcgttctgtttgtgcttaaatg		
		445~533	89	tctgc.tgcgaggcagggaccgagtcctcc cagaagtttgtctgaagattcaaacctgtg agaagagaccttgtacatcgtcagggaatg		
		445~533	89	tctgctgcgaggcagggaccgagtcctccc agaagtttgtctgaagattcaaacctgtga gaagagaccttgtacatcgtcagggaatg		
		445~533	89	tctgctgcgagg.cagggaccgagtcctcc cagaagtttgtctgaagattcaaacctgtg agaagagaccttgtacatcgtcagggaatg		
		445~533	89	tctgct.gcgaggcagggaccgagtcctcc cagaagtttgtctgaagattcaaacctgtg agaagagaccttgtacatcgtcagggaatg		
		445~533	89	tctgctgcgagg.cagggaccgagtcctcc cagaagtttgtctgaagattcaaacctgtg .agaagagaccttgtacatcgtcagggaat g		
		447~537	91	catctgctgcgaggcagggaccgagtcctc ccagaagtttgtctgaagattcaaacctgt g.agaagagaccttgtacatcgtcagggaa tg		
		447~537	91	catctgctgcgaggcagggaccgagtcctc ccagaagtttgtctgaagattcaaacctgt gagaagagaccttgtacatcgtcagggaat g		
		447~537	91	catctgctgcgagg.cagggaccgagtcct cccagaagtttgtctgaagattcaaacctg tg.agaagagaccttgtacatcgtcaggga atg		

IRESite database search:

Sequences producing significant alignments:

ODC1 IRES- gctgcagggact
NDST1 IRES- ctctgctgattg
HAP4 IRES- tttttttccac
FGF1A IRES -ttctgggaggac

>5'-UTR from ZAC.VA
ttctttcaattcagaatttgttttaggttctgttattgcatagatttgcatacctgttttATGgtattttaatactgttggttttaaaaaatac
catttcctctgagtgctgttctgaatatattATGtaagcaattttgtgtgttctttttttccacttgcataaagcaggggaaaagttga
gagtttttcttaatccagttgcaagtaggacaaaggatATGagtgtttaaagatcatctattaaaATGcATGaaaaaacac
tagaaaatctcctgtgcacatcgccagtcgtgtgtgtgctctagaagtgaagttcagggggtaacataATGgaggaATGttt
tcctagcttcattccctgacgATGtacaaggtctcttctcacaggtttgaatcttcagacaaacttctgggaggactcggtccctg
cctcgcagcagATGttccctgtcactcagtagccaatccgggggacccaggacATGccccagctatagtgATGcagat
taccttttctgctcctgaatcgcacctgtgcctcagactttctcccctcagcttgagactgcATGtaaactgggATGtgtgaaag
caggaagcaaagctagtgacagctgagaggtccATGtctgggtagaaccaggcccacgATGctgcctctcccgtggtct
ggagttcagctgcagggactctgctgattggcccagcaccatcgttctgtttgtgcttaaATGgcacagcatttggtcagcaca
tctgaaaaggaaggtgtgagaagcaaagccc

Declaration

„I declare under penalty of perjury, that the thesis has been created by me independently and without undue outside assistance in compliance with the "Principles of Good Scientific Practice at the Heinrich-Heine-University of Dusseldorf.""

I further certify that I have tried either at the Heinrich-Heine-University Dusseldorf yet another university to submit this dissertation. Likewise, I've made no less successful promotion attempts.

Düsseldorf, March 2013

Acknowledgements

Firstly, I want to thank Prof. Dr. Wolfgang Schulz for his demanding yet patient and caring guidance and encouragement that led to the realization of my ideas in this project. I sincerely thank him for the numerous weekends he spent correcting thousands of pages of manuscripts, stipend proposals and the many versions of this thesis, for his efforts to keep me in the lab, for writing the grant proposal that enabled my further research on imprinted genes, as well as for his strategic and active help that brought several publications of my work to fruition. I could always rely on his useful advice and want to thank him for his correctness and his honest and good-hearted manner towards me and the other students.

My gratitude for his patience and straightforward support goes to my second supervisor Prof. Dr. Martin Beye. I furthermore want to thank the Wilhelm-Sander Foundation for supporting this project and Prof. Dr. Jörg Rahnenführer for his expert statistical analyses that greatly assisted our hypotheses and decisions making.

I owe a very special thanks to Christiane Hader for her regular valuable professional support in the everyday lab work. Thank you for the friendship and encouragement, the inspiring coffee-break conversations and the bike tours in the beautiful Düsseldorf countryside that helped me clear my mind.

I want to acknowledge the useful and constructive recommendations from Dr. Wolfgang Göring, Dr. Michele Hoffmann and Dr. Annemarie Koch who helped me write the thesis in a more ‘to the point’ way. Dr. Wolfgang Göring also performed for me most of the pyrosequencing measurements and I could always rely on his friendly help with computer, cloning, and other problems, thank you for being such a cool guy.

I am deeply grateful to Klaus-Marius Bastian, Mark Ingenwerth and Michael Kloth for their help with *in silico* analyses, statistics, graphs, and all kinds of stuff physicians do better than biologists. I also want to thank the colleagues from the urological clinic, especially Dr. Günter Niegisch and Dr. Christian Arsov, for their assistance with the tissue- and database.

My heartily gratitude to all of my colleagues from the lab, especially Annemarie and Jenny, for their strong cooperation and involvement in the team, for their assistance and good advices on experiments, presentations, manuscripts, and for the friendly and pleasant atmosphere they created. I enjoyed very much our girls’ evenings and cooking parties, thank you for your friendship and support.

Last but not least, I owe my deepest gratitude to my family and all my friends, the Ludi Mladi and my former colleagues from the Uhrberg research group. Thank you for your unconditional support and understanding when I could not be there. Your belief in me gave me the strength and motivation to keep moving forward in good and hard times.